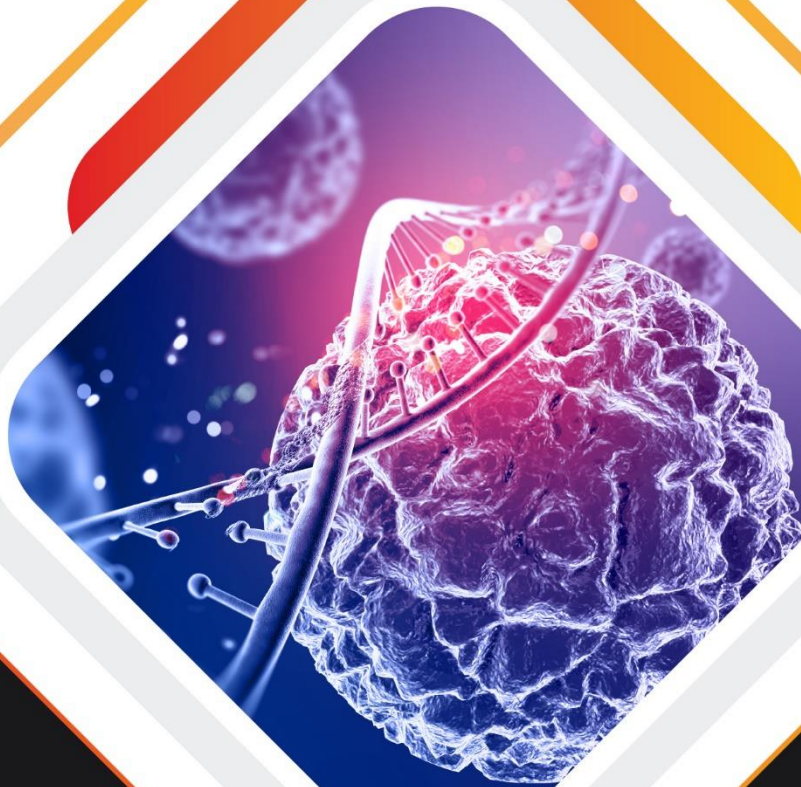


15th NATIONAL AND 1st INTERNATIONAL CONGRESS OF HISTOLOGY AND EMBRYOLOGY

THEP niche²⁰²²



FULL TEXT BOOK

FULL TEXT BOOK



EDITOR
Prof. Dr. Gamze TANRIOVER

2022

**15th NATIONAL – 1st INTERNATIONAL CONGRESS OF HISTOLOGY AND EMBRYOLOGY
26-28 MAY 2022 TURKEY**

This book is subject to copyright. All copyrights reserved. None of this publication may be stored, reproduced or broadcast in any form, including electronic, mechanical, reprographic or photographic, without the prior written permission of the publisher.

Personal contributions in this publication and any liabilities arising therefrom are the responsibility of the authors. The publisher is not responsible for any possible damages as a result of the content obtained from this publication.

info@nichecongress.com
www.nichecongress.com



**15th NATIONAL – 1st INTERNATIONAL CONGRESS OF HISTOLOGY AND EMBRYOLOGY
26-28 MAY 2022 TURKEY**

ORGANIZING COMMITTEE

PRESIDENT OF CONGRESS

Prof. Dr. Gamze TANRIOVER

Akdeniz University Faculty of Medicine Department of Histology and Embryology

CONGRESS ORGANISATION COMMITTEE

Prof. Dr. Gamze TANRIOVER

Akdeniz University Faculty of Medicine Department of Histology and Embryology

Prof. Dr. Altug YAVASOGLU

Ege University Faculty of Medicine Department of Histology and Embryology

Prof. Dr. Alev Gurol BAYRAKTAROGLU

Ankara University Faculty of Veterinary Medicine Department of Histology and Embryology

Prof. Dr. Selcuk TUNIK

Dicle University Faculty of Medicine Department of Histology and Embryology

Assoc. Prof. Dr. Kanat GULLE

Süleyman Demirel University Faculty of Medicine Department of Histology and Embryology

Assoc. Prof. Dr. Ferda Topal CELIKKAN

Ankara University Faculty of Medicine Department of Histology and Embryology

Assoc. Prof. Dr. Leman SENCAR

Çukurova University Faculty of Medicine Department of Histology and Embryology

Asst. Prof. Dr. Hilal NAKKAS

Ankara Yıldırım Beyazıt University Faculty of Medicine Department of Histology and Embryology

Asst. Prof. Dr. Esra OZKOCER

Gazi University Faculty of Medicine Department of Histology and Embryology

SCIENTIFIC COMMITTEE OF THE CONGRESS

Prof. Dr. A. Cevik TUFAN

Ankara Yıldırım Beyazıt University, Faculty of Medicine, Department of Histology and Embryology, Turkey

Prof. Dr. Alistair WAREN (*invited speaker*)

Nottingham University, Faculty of Medicine & Health Sciences, Department of Anatomy, England

Prof. Dr. Alp CAN (*invited speaker*)

Ankara University, Faculty of Medicine, Department of Histology and Embryology, Turkey

Prof. Dr. Aydın GIRGIN

Bingöl University, Faculty of Veterinary Medicine, Department of Histology and Embryology

Prof. Dr. Bayram YILMAZ (*invited speaker*)

Yeditepe University, Faculty of Medicine, Department of Physiology, Turkey

Prof. Dr. Candan OZOGUL

Girne University, Faculty of Medicine, Department of Histology and Embryology, Turkey

Prof. Dr. Cem KORKMAZ

University of Health Sciences, Gülhane Faculty of Medicine, Department of Histology and Embryology, Turkey

SCIENTIFIC COMMITTEE OF THE CONGRESS

Prof. Dr. Ciler CELIK OZENCI (invited speaker)

Koç University, Faculty of Medicine, Department of Histology and Embryology, Turkey

Prof. Dr. Ebru KARADAG SARI

Kafkas University, Faculty of Veterinary Medicine, Department of Histology and Embryology, Turkey

Prof. Dr. Emel KOPTAGEL

Yüksek İhtisas University, Faculty of Medicine, Department of Histology and Embryology, Turkey

Prof. Dr. Emel ULUPINAR (invited speaker)

Eskisehir Osmangazi University, Faculty of Medicine, Department of Anatomy, Turkey

Prof. Dr. Engin ULUKAYA (invited speaker)

Istinye University, Faculty of Medicine, Department of Biochemistry, Turkey

Prof. Dr. Engin YENILMEZ (invited speaker)

Karadeniz Technical University, Faculty of Medicine, Department of Histology and Embryology, Turkey

Prof. Dr. Fevziye Figen KAYMAZ

Istinye University, Faculty of Medicine, Department of Histology and Embryology, Turkey

Prof. Dr. Giuseppe MUSUMECI (invited speaker)

Catania University, Biomedical and Biotechnological Sciences, Italy

Prof. Dr. Gulcin ABBAN METE

Pamukkale University, Faculty of Medicine, Department of Histology and Embryology, Turkey

SCIENTIFIC COMMITTEE OF THE CONGRESS

Prof. Dr. Gülperi OKTEM (invited speaker)

Ege University, Faculty of Medicine, Department of Histology and Embryology, Turkey

Prof. Dr. H. Seda VATANSEVER

Manisa Celal Bayar University, Faculty of Medicine, Department of Histology and Embryology, Turkey

Prof. Dr. Hüseyin AKTUG (invited speaker)

Ege University, Faculty of Medicine, Department of Histology and Embryology, Turkey

Prof. Dr. Kemal ERGIN

Aydın Adnan Menderes University, Faculty of Medicine, Department of Histology and Embryology, Turkey

Prof. Dr. Melda YARDIMOGLU YILMAZ

Kocaeli University, Faculty of Medicine, Department of Histology and Embryology, Turkey

Prof. Dr. Meltem KURUS

İzmir Kâtip Çelebi University, Faculty of Medicine, Department of Histology and Embryology, Turkey

Prof. Dr. Meltem OZGUNER (invited speaker)

Ankara Yıldırım Beyazıt University, Faculty of Medicine, Department of Histology and Embryology, Turkey

Prof. Dr. Nureddin CENGİZ

Bandırma Onyedi Eylül University, Faculty of Medicine, Department of Histology and Embryology, Turkey

Prof. Dr. Oya EVIRGEN

Ankara University, Faculty of Medicine, Department of Histology and Embryology, Turkey

SCIENTIFIC COMMITTEE OF THE CONGRESS

Prof. Dr. Pergin ATILLA

Hacettepe University, Faculty of Medicine, Department of Histology and Embryology, Turkey

Prof. Dr. Petek KORKUSUZ (invited speaker)

Hacettepe University, Faculty of Medicine, Department of Histology and Embryology, Turkey

Prof. Dr. Sait POLAT

Çukurova University, Faculty of Medicine, Department of Histology and Embryology, Turkey

Prof. Dr. Selen AKYOL BAHCECI

İzmir Kâtip Çelebi University, Faculty of Medicine, Department of Histology and Embryology, Turkey

Prof. Dr. Sema TIMURKAAN

Fırat University, Faculty of Medicine, Department of Histology and Embryology, Turkey

Prof. Dr. Serap ARBAK (invited speaker)

Acıbadem Mehmet Ali Aydınlar University, Faculty of Medicine, Department of Histology and Embryology, Turkey

Prof. Dr. Sevda MUFTUOGLU

Hacettepe University, Faculty of Medicine, Department of Histology and Embryology, Turkey

Prof. Dr. Sevinc INAN

İzmir Ekonomi Üniversitesi University, Faculty of Medicine, Department of Histology and Embryology, Turkey

Prof. Dr. Shafiq KHAN (invited speaker)

Clark Atlanta University, Center for Cancer Research and Therapeutic Development, United States of America

SCIENTIFIC COMMITTEE OF THE CONGRESS

Prof. Dr. Tunc AKKOC (invited speaker)

*Marmara University, Faculty of Sport Sciences, Department of Sports and Health Sciences,
Turkey*

Prof. Dr. Unal USLU

*İstanbul Medeniyet University, Faculty of Medicine, Department of Histology and
Embryology, Turkey*

Prof. Dr. Yeter TOPCU TARLADACALISIR

Trakya University, Faculty of Medicine, Department of Histology and Embryology, Turkey

Prof. Dr. Yiğit UYANIKGIL

Ege University, Faculty of Medicine, Department of Histology and Embryology, Turkey

Prof. Dr. Yusuf NERGİZ

Dicle University, Faculty of Medicine, Department of Histology and Embryology, Turkey

Assoc. Prof. Dr. Adem KARA

*Erzurum Technical University, Faculty of Sciences, Department of Molecular Biology and
Genetics, Turkey*

Assoc. Prof. Dr. Aylin YABA UCAR

Yeditepe University, Faculty of Medicine, Department of Histology and Embryology, Turkey

Assoc. Prof. Dr. Basak BUYUK

*İzmir Demokrasi University, Faculty of Medicine, Department of Histology and Embryology,
Turkey*

Assoc. Prof. Dr. Derya KARABULUT

Erciyes University, Faculty of Medicine, Department of Histology and Embryology, Turkey

SCIENTIFIC COMMITTEE OF THE CONGRESS

Assoc. Prof. Dr. Fikret GEVREK

Tokat Gaziosmanpaşa University, Faculty of Medicine, Department of Histology and Embryology, Turkey

Assoc. Prof. Dr. Gözde ERKANLI SENTÜRK

İstanbul University, Faculty of Medicine, Department of Histology and Embryology, Turkey

Assoc. Prof. Dr. HÜLYA ELBE

Muğla Sıtkı Koçman University, Faculty of Medicine, Department of Histology and Embryology, Turkey

Assoc. Prof. Dr. Nuray ACAR AYDEMİR

Akdeniz University, Faculty of Medicine, Department of Histology and Embryology, Turkey

Assoc. Prof. Dr. Özlem Tugce CILINGIR KAYA

Marmara University, Faculty of Medicine, Department of Histology and Embryology, Turkey

Assoc. Prof. Dr. Pelin ERGUVEN

University of Health Sciences, International Hamidiye Faculty of Medicine, Department of Histology and Embryology, Turkey

Assoc. Prof. Dr. Sinan OZKAVUKCU (invited speaker)

Dundee University, Faculty of Medicine, Turkey

Assoc. Prof. Dr. Tarık OZBOLAT (invited speaker)

Penn State University, Engineering Science and Mechanics Department, United States of America

Assoc. Prof. Dr. Tolga MERCANTEPE

Recep Tayyip Erdoğan University, Faculty of Medicine, Department of Histology and Embryology, Turkey

SCIENTIFIC COMMITTEE OF THE CONGRESS

Assoc. Prof. Dr. Tuba DEMIRCI

Atatürk University, Faculty of Medicine, Department of Histology and Embryology, Turkey

Assoc. Prof. Dr. Tugba KOTIL

İstanbul University, Faculty of Medicine, Department of Histology and Embryology, Turkey

Assoc. Prof. Dr. Züleyha DOĞANYIGIT

*Yozgat Bozok University, Faculty of Medicine, Department of Histology and Embryology,
Turkey*

Assoc. Prof. Dr. Züleyha ERIŞGIN

Giresun University, Faculty of Medicine, Department of Histology and Embryology, Turkey

Asst. Prof. Dr. Alev CUMBUL

Yeditepe University, Faculty of Medicine, Department of Histology and Embryology, Turkey

Asst. Prof. Dr. Ammad Ahmad FAROOQI (invited speaker)

Institute of Biomedical and Genetic Engineering (IBGE), Molecular Oncology, Pakistan

Asst. Prof. Dr. Elif GELENLI DOLANBAY

*İstanbul Medeniyet University, Faculty of Medicine, Department of Histology and
Embryology, Turkey*

Asst. Prof. Dr. Fatma FIRAT

*Afyonkarahisar University of Health Sciences University, Faculty of Medicine, Department of
Histology and Embryology, Turkey*

Asst. Prof. Dr. Isil AYDEMİR

*Niğde Ömer Halisdemir University, Faculty of Medicine, Department of Histology and
Embryology, Turkey*

SCIENTIFIC COMMITTEE OF THE CONGRESS

Asst. Prof. Dr. Ismail CAN

Kafkas University, Faculty of Medicine, Department of Histology and Embryology, Turkey

Asst. Prof. Dr. Murat SERKANT UNAL

Pamukkale University, Faculty of Medicine, Department of Histology and Ebriology, Turkey

Asst. Prof. Dr. Nazlı ÇİL

*Pamukkale University, Faculty of Medicine, Department of Histology and Embryology,
Turkey*

Asst. Prof. Dr. Özlem OZBEY UNLU

Akdeniz University, Faculty of Medicine, Department of Histology and Embryology, Turkey

Asst. Prof. Dr. Selim ZIRH

*Erzincan Binali Yıldırım University, Faculty of Medicine, Department of Histology and
Embryology, Turkey*

Asst. Prof. Dr. Semin GEDIKLI

*Atatürk University, Faculty of Veterinary Medicine, Department of Histology and
Embryology, Turkey*

Asst. Prof. Dr. Sercin KARAHUSEYINOGLU (invited speaker)

Koç University, Faculty of Medicine, Department of Histology and Embryology, Turkey

Dr. Hakan COSKUN (invited speaker)

*Harvard Medical School, Department of Cardiology Boston Children's Hospital, United
States of America*

Dr. Vedrana Filic MILETA (invited speaker)

Ruđer Bošković Institute, Division of Molecular Biology, Croatia

*Members of the Organisation Committee are also members of the Scientific Committee.

CONGRESS SCIENTIFIC SECRETARIAT

Assoc. Prof. Dr. Ferda Topal CELIKKAN

Ankara University Faculty of Medicine Department of Histology and Embryology

CONGRESS ORGANISATION

[Atlax Organization](#)



WELCOME TO NICHE 2022

Dear Members of the Turkish Histology and Embryology Family,

The 15th National – 1st International Congress of Histology and Embryology (NICHE 2022) will be held online by the **Turkish Histology and Embryology Society** between 26-28 May 2022. It is our great pleasure to invite you to our congress.

Despite our extreme efforts as the 16th Term Administrative Board of the Turkish Histology and Embryology Society to hold this congress face-to-face, our congress, will be online due to the progression of COVID- 19 pandemic and economic situations in Turkey.

In addition to the conferences of valuable researchers who have a word in their fields, our congress, where the results of current research will be shared, and experts from abroad will be invited, will be held with your valuable participation. We are excited to meet you at our congress even on the screen.

At the 15th National – 1st International Congress of Histology and Embryology, we will be very closely involved in developmental biology, molecular biology and cell biology, stem cells, cellular therapies, regenerative and reconstructive medicine, assisted reproduction techniques, tumor biology, biomedical engineering, biotechnology, bioinformatics and neuroscience. It is aimed to create a scientific environment with multidisciplinary contributions on current issues of interest.

I invite you to the **15th National – 1st International Congress of Histology and Embryology**, which we are sure will be enriched scientifically with your participation and the knowledge and experience you will share.

With my best regards.

Prof. Dr. Gamze TANRIOVER

President of Congress

CONTENTS

KOLİSTİNE BAĞLI KARACİĞER HASARINA KARŞI MEZENKİMAL KÖK HÜCRELERİN ETKİSİ	17
MESENCHYMAL STEM CELLS INDUCE IN VITRO SPERMATOGENESIS ON INDIRECT AIR-LIQUID INTERPHASE PLATFORM	26
TOPICAL INTRANASAL INSULIN ENHANCES THE HEALING OF NASAL MUCOSA	31
ARID3A AND ARID3B DIRECTLY REGULATES LNCRNAS MALAT1 AND NORAD İN NSCLC	36
INVESTIGATION OF THE EFFECTS OF IMATINIB USE ON THE OVARY IN THE EARLY PRENATAL PERIOD	40
THE EFFECTS OF THE USE OF BOUIN AND FORMALDEHYDE FIXATIVES IN TESTICULAR TISSUE ON HISTOPATHOLOGICAL EVALUATION IN ROUTINE AND IMMUNOHISTOCHEMICAL STAINING	49
EPİDİDİMAL BEYAZ YAĞ DOKUSUNUN <i>IN VITRO</i> SPERMATOGENEZ ÜZERİNE ETKİSİNİN İKİ FARKLI KÜLTÜR PLATFORMUNDA KARŞILAŞTIRILMASI	56
ARE TESTICULAR STROMAL CELLS A VALUABLE RESOURCE THAT HAS BEEN OVERLOOKED UNTIL NOW?.....	64
TAKROLİMUS NEFROTOKSİSİTESİNİN DEĞERLENDİRMESİ İÇİN ÜÇ BOYUTLU BÖBREK PROKSİMAL TÜBÜL MODELİNİN GELİŞTİRİLMESİ	71
IVF LABORATUVARINDA OOSİT MAYOZ MEKİĞİ DEĞERLENDİRMESİNİN İNFERTİLİTE TEDAVİ BAŞARISINDAKİ YERİ.....	76
PRODUCTION OF A 3-DIMENSIONAL ARTIFICIAL STOMACH MODEL WITH ALONG MUCUS LAYER.....	83
3D BIOPRINTING, CELL CULTURE AND HISTOLOGICAL EVALUATION OF 3D PRINTED SKIN TISSUE ENGINEERING PRODUCTS FOR REGENERATIVE MEDICINE APPLICATION	88
BIOINK DESIGN, BIOPRINTING OF 3D BONE MODEL, AND <i>IN VITRO</i> ANALYSIS	94
ASPALATHUS LİNERAİS (ROOİBOS) EKSTRAKTININ SIÇAN TESTİS DOKUSUNDA AKUT DÖNEMDE MELAMİNİN OLUŞTURDUĞU HASAR ÜZERİNE KORUYUCU ETKİSİNİN İNCELENMESİ	104
YENİ TASARLANMIŞ PORÖZ TİTANYUM DENTAL İMPLANTLARIN OSTEOİNTEGRASYON VE KEMİK OLUŞUMUNA ETKİSİNİN ARAŞTIRILMASI	116
IVF İŞLEMLERİNDE TOPLANAN OOSİTLERDEKİ ANOMALİLERİN TEDAVİ SONUÇLARINA ETKİSİ	122
KEMİK TÜMÖRLERİNDE KANNABİNOİDLERİN RESEPTÖR ARACILI ANTİPROLİFERATİF VE APOPTOTİK ETKİLERİNİN ARAŞTIRILMASI	128
EVALUATION OF SEMEN PARAMETERS AND SPERM MORPHOLOGY IN INDIVIDUALS WITH DIFFERENT BODY MASS INDEX (BMI).....	138

PHOENIXIN-14 IMMUNOREACTIVITY IN RAT KIDNEY TISSUE 155

THREE-DIMENSIONAL MODELLING OF HASSALL'S CORPUSCLES..... 159

THE ROLE OF CYTOKINES IN THE EFFECT OF CHRONOLOGICAL AGE ON OVARIAN RESERVE; COMPARISON OF CYTOKINE CONCENTRATIONS IN FOLLICULAR FLUID AND OVARIAN RESERVES IN IVF CYCLES OF WOMEN OVER AND UNDER 35 YEARS OF AGE 164

INVESTIGATION OF WOUND HEALING POTENTIALS OF PINE BARK EXTRACTS AND DEVELOPMENT OF GEL FORMULATION..... 174

ALLOGENEIC BONE MARROW MESENCHYMAL STEM CELL-DERIVED EXOSOMES AMELIORATE HYPOXIC ACUTE TUBULAR INJURY IN HUMAN PROXIMAL TUBULE-ON-A-CHIP WITHIN A PRECISE TREATMENT WINDOW 179



KOLİSTİNE BAĞLI KARACİĞER HASARINA KARŞI MEZENKİMAL KÖK HÜCRELERİN ETKİSİ

Özlem ÖZ GERGIN¹, Özge CENGİZ MAT², Demet BOLAT², Burçin GÖNEN³

¹Erciyes Üniversitesi Tıp Fakültesi Anesteziyoloji ve Reanimasyon AD, Kayseri, Türkiye,
oozgergin@erciyes.edu.tr

²Erciyes Üniversitesi Tıp Fakültesi Histoloji Embriyoloji AD, Kayseri, Türkiye,
ozgemat@erciyes.edu.tr, demetbolat92@hotmail.com

³Erciyes Üniversitesi Genom ve Kök Hücre Merkezi, Kayseri, Türkiye,
zeynepburcin@erciyes.edu.tr

Özet: Kolistin, çoklu ilaca dirençli gram-negatif bakteriyel enfeksiyonlara karşı tedavi için kullanılan bir glikopeptid antibiyotiktir. Mezenkimal kök hücreler (MSC) ise, birçok hastalıkta terapötik araçlar olarak kapsamlı bir şekilde çalışılmaktadır. Bu hücreler, nispeten kolay genişletilebildikleri gibi, güçlü anti-inflamatuar, immünomodülatör ve pro-anjiyojenik etkilere sahip oldukları ve bağışıklık sistemini uyarma riski düşük olduğundan dolayı tedavi için özellikle dikkat çekicidir. Bu çalışmada Kolistin'in karaciğerde oluşturacağı toksisiteye karşı mezenkimal kök hücrelerin olası koruyucu etkisinin belirlenmesi amaçlanmıştır. Çalışmada 40 adet wistar albino dişi sıçan her grupta 10 adet olacak şekilde; kontrol, kolistin (36 mg/kgi.p), MSC (1×10^6 100 μ l/rat i.v), MSC (1×10^6 100 μ l/rat i.v) + kolistin (36 mg/kg i.p) gruplarına ayrıldı. Deney sonunda, karaciğer dokuları eksize edildi ve rutin histolojik doku takibi basamaklarından geçirilerek parafine gömüldü. Hazırlanan parafin bloklardan alınan 5 μ m kalınlığındaki kesitler histopatolojik değerlendirme için Hematoksilen&Eozin ve Masson trikrom ile boyanarak ışık mikroskopunda incelendi. TNF- α ve PCNA ekspresyonları immünohistokimya metodu ile incelenmiştir. Işık mikroskopik bulgulara göre, kontrol grubuna ait karaciğer dokularının normal histolojik bir görünümüne sahip olduğu gözlemlendi. Ana karaciğer hücreleri olan hepatositler, lobül içinde ışınsal olarak düzenlenmişti. Kolistin grubuna ait karaciğer bölümlerinde, lökosit infiltrasyonu, hepatosit hücrelerinde hasar ve hemoraji gibi dejeneratif değişiklikler görülmüştür. Bu görünüm, kolistine maruz kalmanın sıçan karaciğerinde ciddi hasara neden olduğunu göstermektedir. Kolistin grubu karaciğer dokusunda TNF- α ve PCNA ekspresyon yoğunlukları, diğer gruplar ile karşılaştırıldığında anlamlı farklılık gösterdi. MSC+kolistin grubunda ise, kolistinin neden olduğu karaciğer hasarında MSC'nin koruyucu rolünü göstermiştir. Bu bulgular, MSC'nin kolistinin neden olduğu karaciğer hasarını önlemek ve kolistin kaynaklı karaciğer

fonksiyonunu iyileştirmek için uygun bir farmasötik müdahale olabileceğini düşündürmektedir.

Anahtar Kelimeler: Karaciğer, Kolistin, MSC, PCNA

EFFECT OF MESENCHIMAL STEM CELLS AGAINST COLISTINE DUE TO LIVER DAMAGE

Abstract: Colistin is a laboratory glycopeptide model for study. Mesenchymal rooting (MSC), on the other hand, is worked in some way as intermediaries here. As such, they are anti-inflammatory, immunomodulatory and immunomodulatory, easily eroded. Countermezen is a possible possibility, as will be established in the results of Colistin in this study. In the study, there will be 40 wistar albinos, 10 in body size; control, colistin (36 mg/kg i.p), MSC (1×10^6 100 μ l/rat i.v), MSC (1×10^6 100 μ l/rat i.v) + colistin (36 mg/kg i.p) were separated. At the end of the experiment, the results and histological tissues excised from the routine tissues can be passed through paraffin. The paraffin sections taken from the prepared blocks were stained with Hemaat for histopathological evaluation and examined under a light microscope. TNF- α PCNA expression is followed and applied by immunohistochemistry method. According to the light microscopy, it was observed that the tissues of the control examination had a normal histological characteristic. The hosts, which have good training controls, are radially vehicles in hepatocytes. It is estimated what the colistin belongs to. These views are intended to make predictions about adverse exposure. Expressions of TNF- α and PCNA in teams of colistin groups, demonstrations for purposes related to other groups. In MSC+colistin application, MSC's services are used when colistin is not good. It is true that MS colistin is not true.

Keywords: Liver, Colistin, MSC, PCNA

1.GİRİŞ

"Polymyxin B" olarak da bilinen Kolistin, dirençli gram negatif bakteriyel enfeksiyonların tedavisinde önemli rol oynayan antimikrobiyal bir ajandır (1). Antibiyotiğe dirençli mikroorganizmaların neden olduğu enfeksiyonlara karşı en etkili antibiyotiklerden biridir (2). Bununla birlikte, terapötik dozlarda bile yüksek nefrotoksisite insidansı, bakteriyel enfeksiyonun yönetiminde kolistinin kullanımına karşı önemli bir engel teşkil eder (3). Kolistin kullanımını sınırlayan en yaygın yan etkiler nefrotoksisite ve nörotoksisitedir. Her iki yan etki de doza bağımlıdır ve geri dönüşümlüdür. Kalıcı böbrek hasarı nadiren görülmüştür

(4). Farklı yayınlanmış çalışmalarda kolistine bağı nefrotoksisite insidansının %20 ila %76 arasında değiştiği bulunmuştur (5). Bu nefrotoksik etkinin altında yatan mekanizmaları netleştirmek için birkaç çalışma yapılmıştır. Çoğu sonuçlar, reaktif oksijen türlerinin (ROS) neden olduğu oksidatif hasarın ve apoptozun etkilenmesinin, kolistin kaynaklı böbrek hasarının patogeneğinde suçlandığını göstermiştir (6). Ayrıca kolistin, inflamatuvar süreçlerde yer alan farklı aracılardan ekspresyonunu arttırdığı, anti-inflamatuvar aracılardan aktivitesini inhibe ettiği ve ardından böbrek dokularına verilen hasarın şiddetlendiği kanıtlanmıştır (7).

Çeşitli kök hücre türleri arasında mezenkimal kök hücreler (MSC'ler) oldukça umut verici bir terapötik seçenektir, çünkü MSC'lerin kendini yenileme, farklılaşma ve immünomodülasyon gibi özellikleri vardır. Ayrıca, kemik iliği, akciğer, yağ, karaciğer, kordon kanı, amniyotik sıvı, plasenta ve göbek kordonu dahil olmak üzere geniş dağılımları nedeniyle MSC'ler kolayca izole edilebilir (8,9).

Kolistin böbrek ve beyin üzerindeki yan etkilerini birçok çalışma bildirmiş olsada, kolistin karaciğer üzerindeki etkilerine dair bilimsel çalışmalar sınırlıdır. Bu çalışma, kolistin karaciğer üzerindeki potansiyel toksisitesini ve Msc'nin kolistin toksisitesi üzerindeki etkisini araştırmayı amaçlamıştır

2. MATERYAL VE METOD

Çalışma, Erciyes Üniversitesi Hayvan Deneyleri Yerel Etik Kurul Başkanlığı'nın onayı alındıktan sonra etik kurallara uygun olarak gerçekleştirildi. Deneyde kullanılan hayvanlar Erciyes Üniversitesi Deneysel Araştırmalar Uygulama ve Araştırma Merkezinden (DEKAM) temin edildi. Toplam 40 adet Wistar albino cinsi dişi sıçan çalışmaya dahil edildi ve rastgele 4 gruba ayrıldı (Tablo 2.1).

Tablo 2.1: Deney Gruplarının Oluşturulması

Gruplar	Uygulanan madde ve uygulama şekli
Kontrol	1 ml sf i.p.
Kolistin	36 mg/kg i.p (7 gün)
MSC	1x10 ⁶ 100µl/rat i.v (tek doz)
Kolistin + MSC	36 mg/kg i.p + 1x10 ⁶ 100µl/rat i.v (7 gün kolistin uygulamasının)

	ardından son kolistin enjeksiyonundan yarım saat sonra MSC uygulanan grup)
--	--

Deneyin tamamlanmasının ardından sıçanlar etik kurallara uygun bir şekilde dekapite edilerek karaciğer dokuları eksize edilip %10'luk formaldehit solüsyonu içerisinde tespit edildi. Rutin histolojik doku takibi basamaklarının ardından parafine gömüldü. Elde edilen parafin bloklardan 5µm kalınlığında kesitler alınarak Hematoksilen&Eosin ve Masson Trikrom ile boyanarak ışık mikroskobu (Olympus BX51, Tokyo, Japan) altında incelendi.

2.1. İmmünohistokimya boyama yöntemi

TNF- α ve PCNA primer antikorlarının karaciğer dokularındaki lokalizasyonlarını ve ekspresyon seviyelerini göstermek amacıyla tüm deney gruplarına immunohistokimyasal boyama metodu uygulandı ve ışık mikroskobunda incelendi. Her gruptaki deneğe ait dokulardan alınan kesitlerden 5 farklı alan ölçüme dâhil edildi ve tüm gruplar için TNF- α ortalama immunoreaktivite yoğunluğu hesaplandı. Ayrıca çekirdek ve sitoplazması pozitif boyanan PCNA hücreleri sayıldı. Tüm immunohistokimyasal analizler X40 büyütmede, Image J software programı kullanılarak gerçekleştirildi ve elde edilen sonuçlar kaydedildi.

2.2. İstatistiksel Analiz

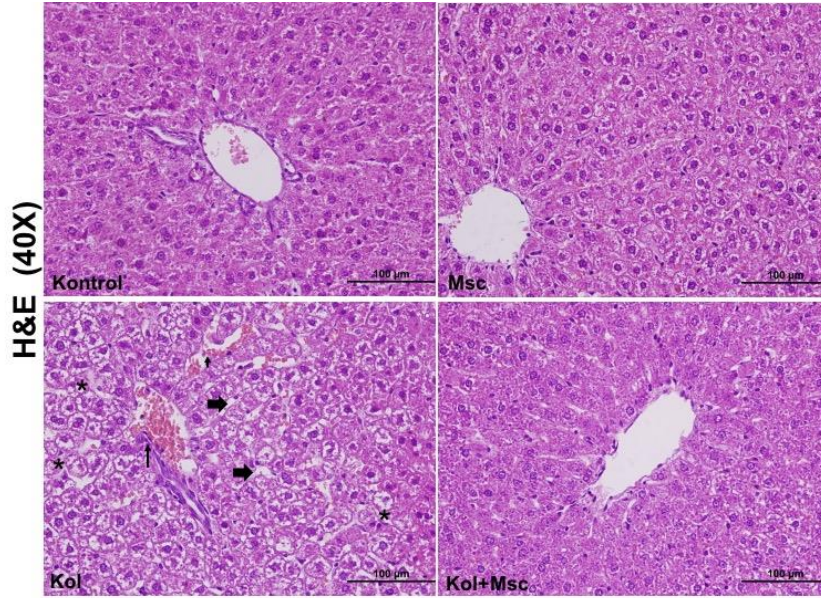
Tüm veriler, ortalama \pm SEM (ortalamanın standart hatası) olarak ifade edildi ve GraphPad Prism yazılımı sürüm 9.0 (GraphPad Inc., San Diego, CA) kullanılarak analiz edildi. Kontrol ve deney fareleri arasındaki farklılıkların istatistiksel önemi, Bonferroni analizi ile tek yönlü ANOVA ile değerlendirildi. İki'den fazla grup arasındaki karşılaştırmalarda Kruskal wallis testleri kullanıldı. Çoğul karşılaştırmalar için Dunn testi uygulandı. P-değerleri <0.05 istatistiksel olarak anlamlı kabul edildi.

3. BULGULAR

3.1. Işık Mikroskobik Bulgular

Kol ve Msc uygulanan gruplarda karaciğer dokusu üzerine histopatolojisini belirlemek için H&E tekniği ile boyanmış preparatları kullandık. Her grubun histolojik sonuçları Şekil 3.1'de gösterilmiştir. Kontrol grubundaki hayvanlardan alınan karaciğer dokusunun genel mimarisi, düzenli olarak yerleşim gösteren karaciğer lobüllerinden ve merkezden periferine ışınal uzanan sinüzoid kordonlarından oluşmaktaydı. Sadece Msc uygulanan gruba ait karaciğer dokusu

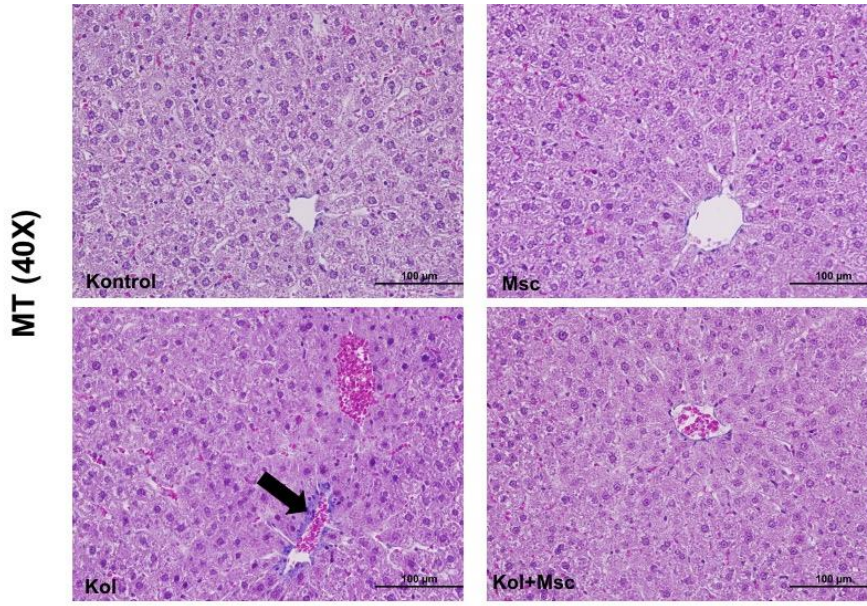
kesitleri kontrol grubuna benzer histolojik özellik sergiledi. Kol grubuna ait kesitler incelendiğinde, kontrol grubuna göre hepatositlerde vakuolizasyon, sinüzoid dilatasyon ve hemoraji gibi patolojik bulgular gözlemlendi. İlginç bir şekilde, Kol+Msc grubu sadece Kol uygulanan gruba kıyasla daha sağlıklı bir histolojik görünüm sergiledi.



Şekil 3.1. Tüm deney gruplarına ait H&E ile boyanan histolojik görüntüler.

Kalın ok: Sinüzoidlerde dilatasyon, **İnce ok;** Hemoraji *; Hepatositlerde vakuolizasyon

Damar çevrelerinde bağ dokusu yapısını incelemek için tüm deney gruplarına ait preparatlar Masson trikrom ile boyandı. Karaciğerde bulunan her lobülün köşelerinde yer alan portal alanlara komşu duvar bağ dokusu yapısının kontrol grubunda normal histolojik görünümde olduğunu sadece Msc uygulanan grubun kontrole yakın görünüm sergilediği belirlendi. Kol uygulanan grupta ise bazı portal alanlarda fibroze rastlandı. Ancak grubun tüm örnekleri incelendiğinde genel olarak artmış bir fibrozis durumu bulunmamaktaydı (Şekil 3.2).



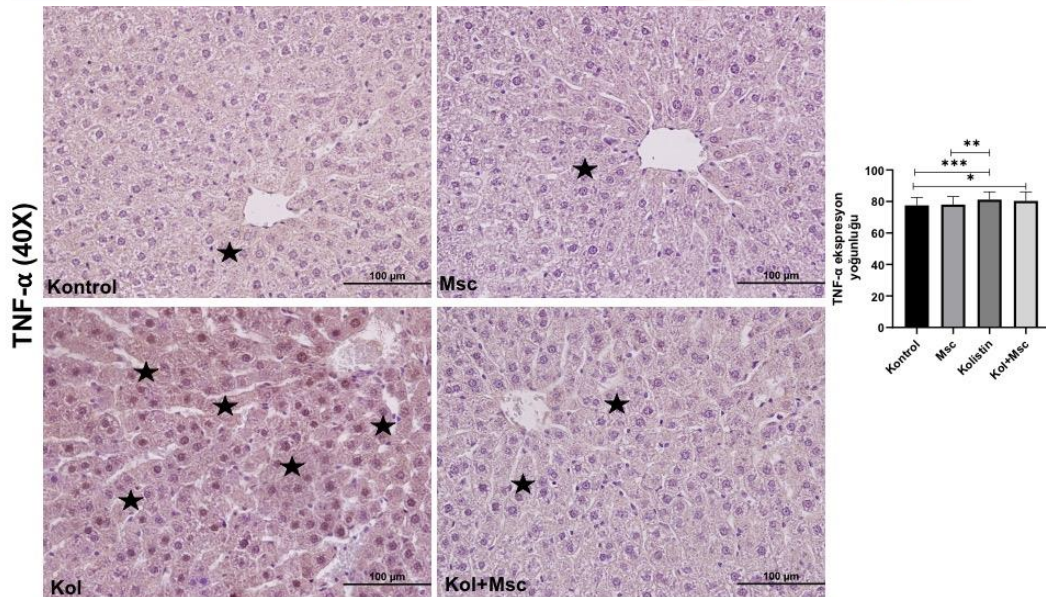
Şekil 3.2. Tüm deney gruplarına ait MT ile boyanmış preparatlar.

Kalın ok: Fibrozis

3.2. İmmünohistokimyasal Bulgular

3.2.1. TNF- α

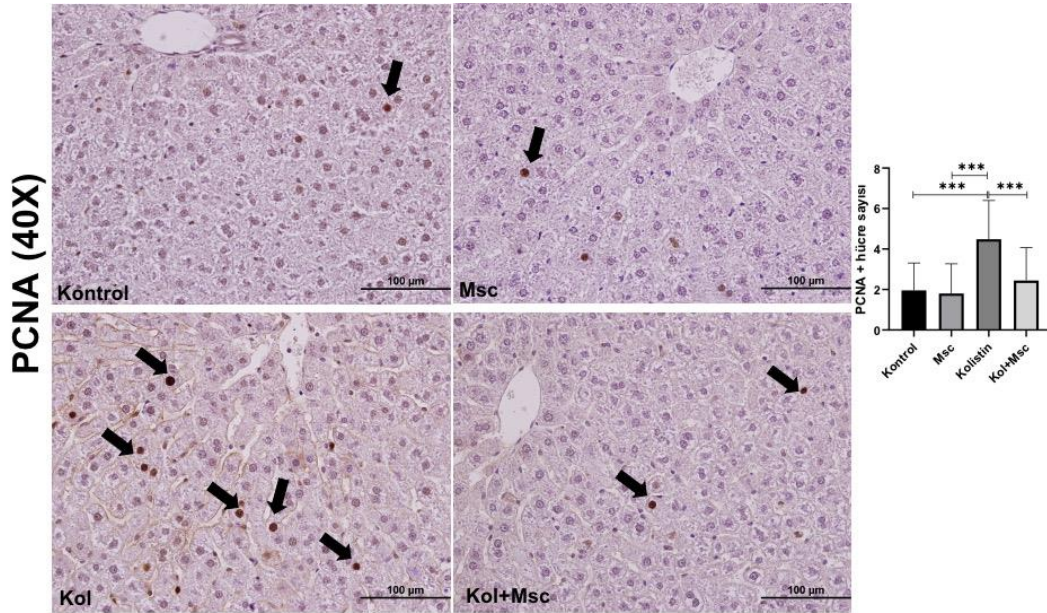
TNF- α primer antikoruyla boyanan karaciğer dokusu kesitlerinde, kontrol grubuna göre Kol uygulanan grupta istatistiksel olarak anlamlı düzeyde bir artış gözlemlendi ($p < 0.001$). TNF- α immünreaktivite yoğunluğunun en az olduğu grup kontrol iken, en yoğun grup Kol olarak belirlendi (Şekil 3.3).



Şekil 3.3. Deney gruplarına ait karaciğer kesitlerinde TNF- α ekspresyonu, immunohistokimyasal boyama görüntüleri, (X40), ★ ; TNF- α ekspresyonu, **Grafik**; Tüm deney gruplarına ait TNF- α immünreaktivite yoğunluklarının istatistiksel analizi

3.2.2. PCNA

PCNA, normal hücre siklusu sırasında sentezlenen ve hücre siklusunu düzenleyen bir protein olarak bilinmektedir. PCNA ekspresyonu düzensiz hücre proliferasyonunun göstergesi olarak kullanılabilir. Bu çalışmada karaciğer dokularında meydana gelen düzensiz hücre proliferasyonunu göstermek amacıyla PCNA primer antikoruyla boyama yapıldı. Kontrol grubuna en yakın Msc grubu olarak gözlenirken, sadece Kol uygulanan grupta PCNA pozitif hücre sayısında istatistiksel olarak anlamlı derecede bir artış gözlemlendi ($p < 0.001$). Kol+Msc'nin birlikte uygulandığı grupta ise sadece Kol grubuna göre anlamlı derecede azalma görüldü (Şekil 3.4).



Şekil 3.4. Deney gruplarına ait karaciğer kesitlerinde PCNA immunohistokimyasal boyama görüntüleri, (X40), **Kalın ok**; Pozitif hücreler, **Grafik**; Tüm deney gruplarına ait PCNA pozitif hücre sayısının istatistiksel analizi

4. TARTIŞMA, SONUÇ

Kolistin, nefrotoksisite ve nörotoksisite nedeniyle kullanılmaktan uzak durulan, çoklu ilaca dirençli mikroorganizmalara bağlı enfeksiyonların özellikle yoğun bakım hastalarında

görülmeye başlamasıyla tekrar kullanıma girmiş önemli bir ajandır (10). Bununla birlikte, hayvan modellerinde bildirilen kolistin tedavisi ile ilişkili histolojik anormalliklerin değerlendirilmesi, klinik ortamda yapılamasa da kolistin nefrotoksisitesini belirlenmesinde önemli rol oynamaktadır. 7 gün boyunca kolistin ile tedavi edilen sıçan böbreklerinde epitel hücre vakuolizasyonu, tübüler dilatasyon ve tübüler epitel hücre nekrozu görüldüğü bildirilmiştir (11). Luan ve ark., (12); farklı dozlarda uyguladığı kolistin karaciğerde hasara neden olduğunu ve hücre infiltrasyonunun meydana geldiğini vurgulamışlardır. Portal alanlarında şiddetli histopatolojik değişiklikler ve sinüzoidal tıkanıklıklar gösterilmiştir. Bu çalışma yapılan çalışmalarla benzer bir şekilde Kol'un karaciğerde hasara yol açtığını özellikle hepatositlerde vakuolizasyona ve sinüzoid dilatasyonlara sebep olduğunu ortaya koymuştur. Ayrıca Kol gruplarının histolojik görünümünde hemoraji ve fibrozis gibi patolojik bulgular yer almaktadır. Msc'ler bu hasarı iyileştirmeye yönelik etki göstermiştir.

İnflamasyon, doku ve organın mikrobiyal patojenler, toksik hücrel bileşenler veya irritanlar gibi zararlı uyarılara maruz kalmasının bir sonucu olarak ortaya çıkar (13). İnflamatuar yanıtta sıklıkla TNF- α , IL-6, ve interlökin-1 β (IL-1 β) gibi aşırı proinflamatuar sitokin üretimi eşlik eder (14). TNF- α güçlü bir proinflamatuar sitokindir ve inflammatuar doku hasarının önemli bir aracısıdır (15). Bu çalışmada Kol verilen grupta TNF- α düzeyinin yüksek olduğu görülmüştür.

PCNA, normal hücre siklusu sırasında sentezlenir ve hücre siklusunu düzenleyici bir protein olarak bilinmektedir (16,17). PCNA nükleotid eksizyonu tamir mekanizmasında rol oynamakta ve böylece siklusta olmayan DNA'sı hasarlanmış hücrelerde de ekspresyonu bulunmaktadır (18,19). PCNA'nın immünohistokimyasal olarak saptanması hem aktif DNA replikasyonunu hem de karsinogenezis ile sonuçlanan DNA hasarını göstermektedir. PCNA ekspresyonu aynı zamanda düzensiz hücre proliferasyonunun göstergesi olarak kullanılmaktadır (20). Bu çalışmada Kol uygulanan grupta PCNA pozitif hücre sayısında artış gözlenmiştir. Kol+ Msc grubunda ise bu artışın önemli ölçüde azaldığı görülmüştür.

H&E ile boyanan kesitlerde, tüm diğer deney gruplarına göre Kol uygulanan gruba ait karaciğer dokularında normal histolojik yapının bozulduğu hepatosit hücrelerinde hasar ve hemoraji gibi patolojik bulguların varlığı gözlemlendi. Bu sonuçlar Kol'un hepatotoksisite etkisini gösteren bulgulardan biridir. Masson trikrom ile boyanan kesitlerde, tüm diğer deney gruplarına göre Kol uygulanan gruba ait karaciğer dokularında fibrozis gözlemlendi. Ayrıca Kol, TNF- α immünreaktivitelerinde ve PCNA pozitif hücre sayısında ise artışa neden olarak karaciğerde hasara yol açmıştır.

Çalışmamızdan elde edilen histolojik ve immunohistokimyasal sonuçlara göre, Msc'nin Kol'un neden olduğu karaciğer hasarını iyileştirmek için uygun bir farmasötik müdahale olabileceğini düşündürmektedir.

5. KAYNAKÇA

1. Arslan, BY, Arslan, F, Erkalp, K, et al. (2016). Luteolin ameliorates colistin-induced nephrotoxicity in the rat models. *Ren Fail*, 38, 1735–1740.
2. Gharaibeh, MH, Shatnawi, SQ (2019). An overview of colistin resistance, mobilized colistin resistance genes dissemination, global responses, and the alternatives to colistin: a review. *Vet World*, 12, 1735–1746.
3. Inci, A, Toker, MK, Bicer, IG, et al. (2018). Determination of colistin-related nephrotoxicity and risk factors in intensive care unit. *North Clin Istanb*, 5, 120–124.
4. Falagas, ME, Fragoulis, KN, Kasiakou, SK, Sermaidis, GJ, Michalopoulos, A (2005). Nephrotoxicity of intravenous colistin: a prospective evaluation. *Int J Antimicrob Agents*, 26(6), 504–507.
5. Ordooei, JA, Shokouhi, S, Sahraei, Z (2015). A review on colistin nephrotoxicity. *Eur J Clin Pharmacol*, 71(7), 801–810.
6. Gai, Z, Samodelov, SL, Kullak-Ublick, GA, et al. (2019). Molecular mechanisms of colistin-induced nephrotoxicity. *Molecules*, 24, 653.
7. Edrees, NE, Galal, AAA, Abdel Monaem, AR, et al. (2018). Curcumin alleviates colistin-induced nephrotoxicity and neurotoxicity in rats via attenuation of oxidative stress, inflammation, and apoptosis. *Chem Biol Interact*, 294, 56–64.
8. Kwon, A, Kim, Y, Kim, M, Kim, J, Choi, H, Jekarl, DW, Lee, S, Kim, JM, Shin, JC, Park, IY (2016). Tissue-specific Differentiation Potency of Mesenchymal Stromal Cells from Perinatal Tissues. *Sci Rep*, 6, 23544.
9. Li, L, Chen, X, Wang, WE, Zeng, C (2016). How to Improve the Survival of Transplanted Mesenchymal Stem Cell in Ischemic Heart? *Stem Cells Int*, 9682757.
10. Nation, RL, Li, J, Cars, O, Couet, W, Dudley, MN, Kaye, KS (2015). Frame work for optimisation of the clinical use of colistin and polymyxin B: the Prato polymyxin consensus. *Lancet Infect Dis*, 15, 225–34.
11. Ghilissi, Z, Hakim, A, Mnif, H, Ayadi, FM, Zeghal, K, Rebai, T, Sahnoun, Z (2013). Evaluation of colistin nephrotoxicity administered at different doses in therat model. *Renal Failure*, 35, 1130–1135.
12. Luan, YH, Zhao, JJ, Han, HF, Shen, JZ, Tang, SS, Cheng, LL (2021). Toxicologic effect and transcriptome analysis for short-term orally dosed enrofloxacin combined with two veterinary antimicrobials on rat liver. *Ecotoxicol Environ Saf*, 220, 10.
13. Turner, MD, Nedjai, B, Hurst, T, Pennington, DJ (2014). Cytokines and chemokines: at the crossroads of cell signalling and inflammatory disease *Biochim. Biophys Acta Mol Cell Res*, 1843, 2563-2582.
14. Keirstead, ND, Wagoner, MP, Bentley, P (2014). Early prediction of polymyxin induced nephrotoxicity with next-generation urinary kidney injury biomarkers. *Toxicol Sci*, 137(2), 278-91.
15. Edrees, NE, Galal, AAA, Abdel Monaem, AR, Beheiry, RR, Metwally, MMM (2018). Curcumin alleviates colistin-induced nephrotoxicity and neurotoxicity in rats via attenuation of oxidative stress, inflammation and apoptosis. *Chem Biol Interact*, 294, 56-64.
16. Ogata, K, Kurki, P, Celic, J (1986). Monoclonal antibodies to a nuclear protein associated DNA replication. *Exp Cell Res*, 168, 476-86.
17. Iachino, C, Katsikoyiannis, N, Dallera, F (1995). Assessment of proliferating cell nuclear antigen (PCNA) immunoreactivity in carcinomas. *Pathologica*, 87, 56-8.
18. Jaskulski, D, Gatti, C, Travali, S, Calabretta, B, Baserga, R (1998). Regulation of the proliferating cell nuclear antigen cyclin and thymidine kinase m RNA levels by growth factors. *J Biol Chem*, 263, 101-7.
19. Scott, RJ, Hall, PA, Haldane, JS et al (1999). A comparison of immunohistochemical markers of cell proliferating with experimentally determined growth fraction. *J Pathol*, 165, 173.
20. Andre, F, Fiazzì, K, Culline, S, Droz, JP, Gatineau, M, Takahashi, Y, Oudard, S, Theadore, C (2000). Peritoneal carcinomatosis in germ cell tumor: relations with retroperitoneal lymph node dissection. *Am J Clin Oncol*, 23(5), 460-2.

MESENCHYMAL STEM CELLS INDUCE IN VITRO SPERMATOGENESIS ON INDIRECT AIR-LIQUID INTERPHASE PLATFORM

Selin ÖNEN^{1,2}, Sevil KÖSE³, Nilgün YERSAL⁴, Petek KORKUSUZ⁵

¹ Hacettepe University, Graduate School of Health Sciences, Department of Stem Cell Sciences, Ankara, Turkey, selinonen@hacettepe.edu.tr

² Atilim University, Faculty of Medicine, Department of Medical Biology, Ankara, Turkey, selin.onen@atilim.edu.tr

³ Atilim University, Department of Nutrition and Dietetics, Faculty of Health Sciences, Ankara, Turkey, sevil.kose@atilim.edu.tr

⁴ Gaziosmanpaşa University, Faculty of Medicine, Department of Histology and Embryology, Tokat, Turkey, nilgun.yersal@gop.edu.tr

⁵ Hacettepe University, Department of Histology and Embryology, Faculty of Medicine, Ankara, Turkey, petek@hacettepe.edu.tr

Abstract: Chemo-radiotherapy applications result in permanent infertility in half of the male pediatric cancer survivors. Spermatogonial stem cells (SSC) constitute the only option for fertility before puberty. The rationale of the study is that bone marrow-derived mesenchymal stem cells (BM-MSC) have similar embryonic origin and gene expression profile with Sertoli cells responsible for the self-renewal, maintenance, proliferation, and differentiation of SSCs. The aim of this study is to evaluate the inductive effect of BM-MSCs on in vitro spermatogenesis and cellular viability of neonatal C57BL/6 mice testes on ALI setup. Isolated mouse BM-MSCs were characterized, and constituted indirect ALI set up was maintained for 7 to 42 days. Single-cell suspension from testicular tissue was prepared; differentiating spermatogonia and cellular viability were evaluated by using c-Kit and Ki-67 flow cytometric and immunohistochemical analyses. Quantification of ID4(+) SSCs, Scp3(+) spermatocytes, Acr(+) round spermatids and Ki67(+) proliferative cells has also done by immunohistochemistry. The percentage of c-Kit labeled and germ cell viability in co-culture group was higher than the control at day 42 ($p < 0.05$). The number of ID4(+) SSCs, Scp3(+) spermatocytes, Acr(+) round spermatids and Ki(+) proliferative germ cells on days 7-42 ($p < 0.05$). The results demonstrated that the new BM-MSC contributed co-culture system led to the maintenance of germ cell pool and differentiation for 42 days in vitro. Addition of BM-MSCs to ALI co-culture system provide a promising tool for a personalized cellular therapy platform for preservation of fertility in childhood cancer survivors by initiation of spermatogenesis in immature testis strips in vitro.

Keywords: Male infertility, spermatogonial stem cell, mesenchymal stem cell, germ cell, in vitro spermatogenesis

INTRODUCTION

Chemo-radiotherapy applications in childhood cancers cause permanent infertility in 46% of male patients as a result of spermatogenesis not continuing due to the deterioration of the spermatogonial stem cell (SSC) microenvironment in the testicles [1]. Childhood cancers, which make up 0.5% - 4.6% of total cancers in the world, generally progress with low mortality (70% in Turkey, 85% long-term survival in high-income countries) but high morbidity by resulting in infertility [2, 3]. In order for these patients to have children of their own, cryopreservation is performed by taking tissue from the testicles before cancer treatment, and a small number of SSCs that can be preserved by thawing the frozen tissue pieces are expected to enter spermatogenesis and form sperm after injection into the testis [4]. However, since the SSC microenvironment cannot be established with the methods used, fertility cannot be achieved in the vast majority of patients in this way. In order for these patients to have biological children naturally in the future, an effective system has not yet been developed in which the culture conditions of the testicular tissues taken before chemo/radiotherapy will protect the three-dimensional microenvironment, the SSC pool will be expanded and the loss of spermatogenic serial cells will be minimized. It is important that the testicular microenvironment is preserved and returned to the patient in the long term, as it can provide a permanent solution to male infertility due to childhood cancer treatment.

Preservation of the testicular stem cell microenvironment (niche) is essential in order to maintain the vitality and number of healthy SSCs in childhood before cancer treatment and to ensure spermatogenetic differentiation. Mesenchymal stem cells are multipotent, somatic, adult stem cells that can be easily obtained from sources such as bone marrow, adipose tissue, and placenta. They have antiapoptotic, proliferative and immune regulatory effects in their microenvironment [5, 6].

Although data on limited differentiation capacity of MSCs into germ cells have been presented in some studies in the literature [7, 8], in general, in damage models performed with *in vitro* culture conditions and *in vivo* application of busulfan, a chemotherapeutic. Bone marrow derived mesenchymal stem cells (BMMSC) share some of their secretomes and their embryonic origin with Sertoli cells which are the main modulators of spermatogenesis [9]. In addition, it has been suggested that Sertoli cells may be a kind of BM-MS-like cell by means of paracrine factors and differentiation process [10]. Thus, we aimed to evaluate the

inductive effect of BM-MSCs on *in vitro* spermatogenesis and cellular viability of neonatal C57BL/6 mice testes on ALI set up.

METHOD

The animal experiments were approved by Hacettepe University Animal Experiments Local Ethical Board (#52338575-96). Isolated mouse BM-MSCs were characterized at passage 3, and the indirect ALI set up was constituted with transwell inserts. The dissected and decapsulated testicular strips were cultured for 7 to 42 days. Then, single cell suspension from testicular tissue was prepared; differentiating spermatogonia and cellular viability were evaluated by using c-Kit and Ki-67 antibodies, respectively, and quantitated by using flow cytometric analysis (ACEA, Novocyte, Novoexpress). Quantification of ID4(+) SSCs, Scp3(+) spermatocytes, Acr(+) round spermatids and Ki67(+) proliferative cells has also done by immunohistochemistry (Leica, LASv3). Since the data was normally distributed, one-way ANOVA was used in statistical analysis.

FINDINGS

The isolated BM-MSCs were characterized of passage 3 (Fig. 1A) by surface antigens (Fig. 1B), adipogenic (Fig. 1C) and osteogenic (Fig. 1D) differentiation capacity; and used for further experiments in study for culture for 7 to 42 days (Fig. 2A).

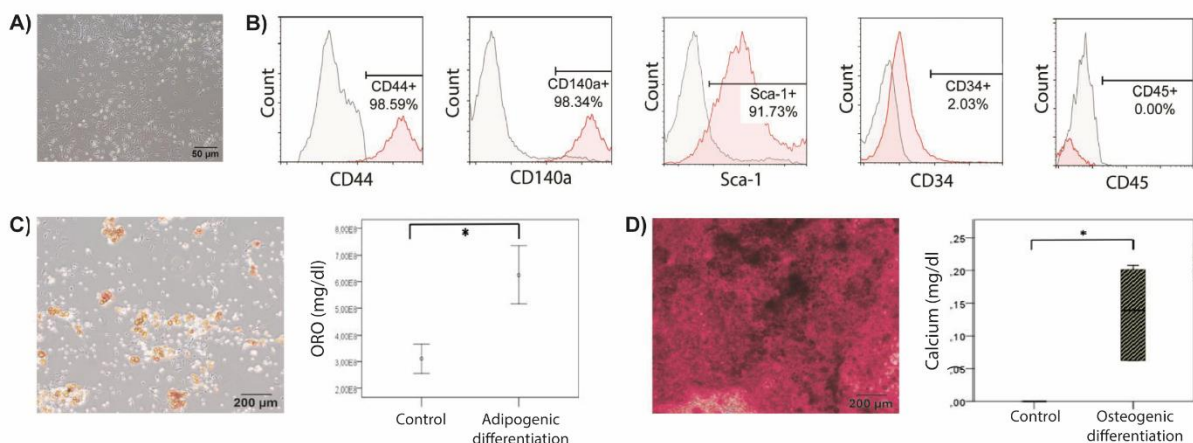


Figure 1. (A) Isolated BM-MSCs has adherent and spindle shape characteristic. (B) Cells expressed MSC surface antigens which are CD44, CD140a, Sca-1, while not expressing hematopoietic markers that are CD34, CD45. They were differentiated through (C) adipogenic and (D) osteogenic directions (* $p < 0.01$). strips to the culture systems in both control and co-culture plates are accepted as day 0.

The percentage of c-Kit labeled (Fig. 2B, $p < 0.05$) and germ cell viability (Fig. 2C, $p < 0.05$) in co-culture group was higher than the control at day 42. The number of ID4(+) SSCs (Fig. 2D, $p < 0.05$), Oct4(+) differentiating spermatogonia (Fig. 2E, $p < 0.05$), Scp3(+) spermatocytes (Fig. 2F, $p < 0.05$), Acr(+), round spermatids (Fig. 2G, $p < 0.05$) and Ki67(+) proliferative germ cells (Fig. 2H, $p < 0.05$) on days 7-42. The results demonstrated that the new BM-MSC contributed co-culture system led to maintenance of germ cell pool and differentiation for 42 days *in vitro*.

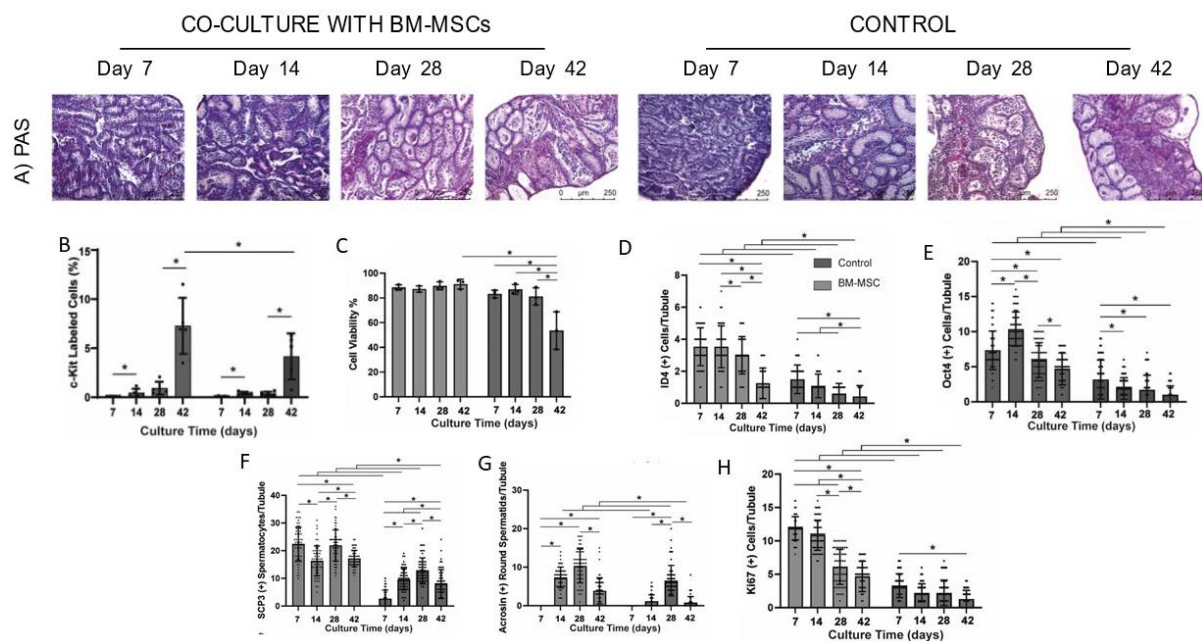


Figure 2. Prepubertal mice testes cultured for 7 to 42 days *in vitro* (A) with and without BM-MSCs. The difference in (B) c-Kit(+) differentiating spermatogonia, (C) cell viability percentage, (D) ID4(+) SSCs, Oct4(+) differentiating germ cells, Scp3(+) spermatocytes, Acrosin(+) spermatids and Ki67(+) proliferative germ cells in BM-MSC co-culture and control groups are illustrated by bar graphs (n=6 testes, 300 tubules, H&E, 200x).

DISCUSSION, CONCLUSION

Our study revealed that BM-MSCs promotes the maintenance of ID4(+) SSCs, Oct4(+) and c-Kit(+) differentiating spermatogonia, Ki67(+) proliferative germ cells, Scp3(+) spermatocytes, Acrosin(+) spermatids and cell viability during 42 day-long *in vitro* testicular culture.

Monsefi et al demonstrated the inductive effect of BM-MSCs on increase of tubular and luminal area in sterile rats by intratesticular injection [11]. By our study, we revealed the induction in tubular and luminal area with BM-MSCs by using ALI technique in mice,

similarly. It is also demonstrated that intratesticular injection of MSCs increases the number of spermatogonia expression of *germline specific markers in vivo* [12]. Likewise, we demonstrated that BM-MSCs rises the the cells which are immune reactive for germ cell specific markers, ID4, Scp3, Acrosin *in vitro*.

Addition of BM-MSCs to ALI co-culture system provide a promising tool for a personalized cellular therapy platform for preservation of fertility in childhood cancer survivors by initiation of spermatogenesis in immature testis strips *in vitro*.

ACKNOWLEDGEMENT

Hacettepe University Scientific Research Projects Coordination Unit funded the study (#TYL-2018-17531).

REFERENCES

1. Wasilewski-Masker, K., et al., Male infertility in long-term survivors of pediatric cancer: a report from the childhood cancer survivor study. *J Cancer Surviv*, 2014. 8(3): p. 437-47.
2. Hudson, M.M., Reproductive outcomes for survivors of childhood cancer. *Obstet Gynecol*, 2010. 116(5): p. 1171-83.
3. Kutluk, M.T. and A. Yesilipek, Pediatric cancer registry Turkey: 2009-2016 (TPOG & TPHD). *Journal of Clinical Oncology*, 2017. 35(15_suppl): p. e22015-e22015.
4. Onofre, J., et al., Cryopreservation of testicular tissue or testicular cell suspensions: a pivotal step in fertility preservation. *Hum Reprod Update*, 2016. 22(6): p. 744-761.
5. Kankilic, B., et al., Mesenchymal Stem Cells and Nano-Bioceramics for Bone Regeneration. *Curr Stem Cell Res Ther*, 2016. 11(6): p. 487-493.
6. Kose, S., et al., Human bone marrow mesenchymal stem cells secrete endocannabinoids that stimulate in vitro hematopoietic stem cell migration effectively comparable to beta-adrenergic stimulation. *Exp Hematol*, 2018. 57: p. 30-41 e1.
7. Ghaem Maghami, R., T. Mirzapour, and A. Bayrami, Differentiation of mesenchymal stem cells to germ-like cells under induction of Sertoli cell-conditioned medium and retinoic acid. *Andrologia*, 2018. 50(3).
8. Salem, M., et al., Germ cell differentiation of bone marrow mesenchymal stem cells. *Andrologia*, 2019. 51(4): p. e13229.
9. Hsiao, C.-H., et al., Local injection of mesenchymal stem cells protects testicular torsion-induced germ cell injury. *Stem Cell Research & Therapy*, 2015. 6(1): p. 113.
10. Gong, D., et al., Are Sertoli cells a kind of mesenchymal stem cells? *Am J Transl Res*, 2017. 9(3): p. 1067-1074.
11. Monsefi, M., et al., Mesenchymal stem cells repair germinal cells of seminiferous tubules of sterile rats. *Iran J Reprod Med*, 2013. 11(7): p. 537-44.
12. Yang, R.-F., et al., Enhancement of mouse germ cell-associated genes expression by injection of human umbilical cord mesenchymal stem cells into the testis of chemical-induced azoospermic mice. *Asian journal of andrology*, 2014. 16(5): p. 698-704.

TOPICAL INTRANASAL INSULIN ENHANCES THE HEALING OF NASAL MUCOSA

Çağrı KÜLEKÇİ¹, Serdar ÖZER¹, Selin ÖNEN^{2,3}, Petek KORKUSUZ⁴

¹ Hacettepe University, Faculty of Medicine, Department of Otolaryngology, Ankara, Turkey,
cagrikulekci@hacettepe.edu.tr, serdaro@hacettepe.edu.tr

² Hacettepe University, Graduate School of Health Sciences, Department of Stem Cell Sciences, Ankara, Turkey,
selinonen@hacettepe.edu.tr

³ Atilim University, Faculty of Medicine, Department of Medical Biology, Ankara, Turkey,
selin.onen@atilim.edu.tr

⁴ Hacettepe University, Faculty of Medicine, Department of Histology and Embryology, Ankara, Turkey,
petek@hacettepe.edu.tr

Abstract: *Sinonasal surgeries are one of the most performed group of ear, nose, throat surgical procedures. The post-operative wound care mainly consists of nasal irrigations, lubrication of nasal mucosa. It is important to improve the post-operative wound healing both in surgical and public health perspective. The rationale of this study is that the topical insulin promotes healing of acute tympanic membrane, according to various in vivo and in vitro human and animal studies. The hypothesis is that the topical intranasal insulin application may enhance the healing of nasal mucosa. Left nasal mucosa of Wistar rats has removed via curette. Then, rats were applied regular insulin diluted with 0.9 % physiological serum, while saline was used as control group. On days 5, 10, and 15, ciliated cell loss, inflammation, edema, goblet cell loss, defect length and defect area were quantitated on Masson Trichrome stained sections. On day 5, the reduction of defect size was 56% in insulin group vs 21% in saline group ($p<0.05$). On day 10, reduction was 79% in insulin group vs 62% in saline group ($p<0.05$). On day 15, groups treated with insulin had complete closure vs 37% full closure in saline group ($p<0.05$). Both inflammation and edema were decreased and less apparent at insulin group on day 15 ($p<0.05$). Those preliminary data present a foundation for further studies that focus on mechanism of action of insulin on nasal wound healing process for possible clinical application.*

Keywords: Wound Healing, Nasal Mucosa, Insulin

INTRODUCTION

A properly functioning sinonasal unit contains healthy mucosa. Sinonasal surgeries are one of the most performed applications of ENT surgical procedures [1]. For sinonasal wound care, lubrication of the nasal mucosa in post-operative care and application of occlusive material during surgery are current practices in medicine.

Because of the population undergoing surgical procedures, any measure that improves post-operative wound healing and outcome is an invaluable tool for both surgery and public health. Various human and animal studies have shown that the use of topical insulin is effective in healing and skin healing in decubitus ulcers [2-6]. *In vitro* studies examined the pathways that lead to the enhanced metabolic and proliferative effects of topical insulin and concluded that insulin both increased the migration of existing basal cells and induced proliferation of both keratinocytes and fibroblasts [7].

Few animal studies have examined the effect of topical insulin on acute tympanic membrane healing [8, 9]. The aim of this study is to evaluate the inductive effect of topical intranasal insulin application on the healing process of the nasal mucosa.

METHOD

The animal experiments were approved by Kobay Laboratories Animal Experimentation Local Ethics Committee (323/2018). Left nasal mucosa of 48 Wistar rats 10-12 weeks old, weighing between 250-300 grams has been removed via 1.9 mm curette. Then, 24 of rats were applied 1 cc of 5 IU/ml regular insulin diluted with 0.9 % physiological serum, while the other 24 were treated with 1 cc of 0.9 % saline 3 times a day as control group. On days 5, 10, and 15, the animals were sacrificed and histomorphometric evaluation was performed by scoring the ciliated cell loss, inflammation, edema, goblet cell loss, defect length, and defect area was quantitated on Masson Trichrome stained sections (Leica, LASv3).

FINDINGS

The ciliated cell loss was similar in both groups on days 5 (Fig. 1A, B, Fig. 2A, n.s.), 10 (Fig. 1C, D, Fig. 2A, n.s.), and 15 (Fig. 1E, F, Fig. 2A, n.s.). The insulin group showed a lower inflammation and edema score at wound edges on days 5 (Fig. 1A, B, Fig. 2B, C, $p < 0.05$), 10 (Fig. 1C, D, Fig. 2B, C, n.s.) and 15 (Fig. 1E, F, Fig. 2B, C, $p < 0.05$). STI parameter was similar in both groups, and ETI parameter was higher in the insulin group when compared to control on days 5 ($p < 0.05$), 10 ($p < 0.05$), and 15 (n.s.) (Fig. 2D, E). Goblet cell loss was similar in both groups on days 5 to 15 (Fig. 1 and 2F, n.s.). Defect area and length declined with insulin application when compared to saline-applied control on days 5 (Fig. 1A, 1B, Fig. 2G, H, $p < 0.05$), 10 (Fig. 1C, 1D, Fig. 2G, H, $p < 0.05$, n.s., respectively) and 15 (Fig. 1E, 1F, Fig. 2G, H, $p < 0.05$).

Macroscopically, there was no incidence of infection and mucosal synechia. On day 5, the reduction of defect size was 56% in the insulin group vs 21% in the saline group (Fig. 1A, B, Fig. 2, $p=0.006$).

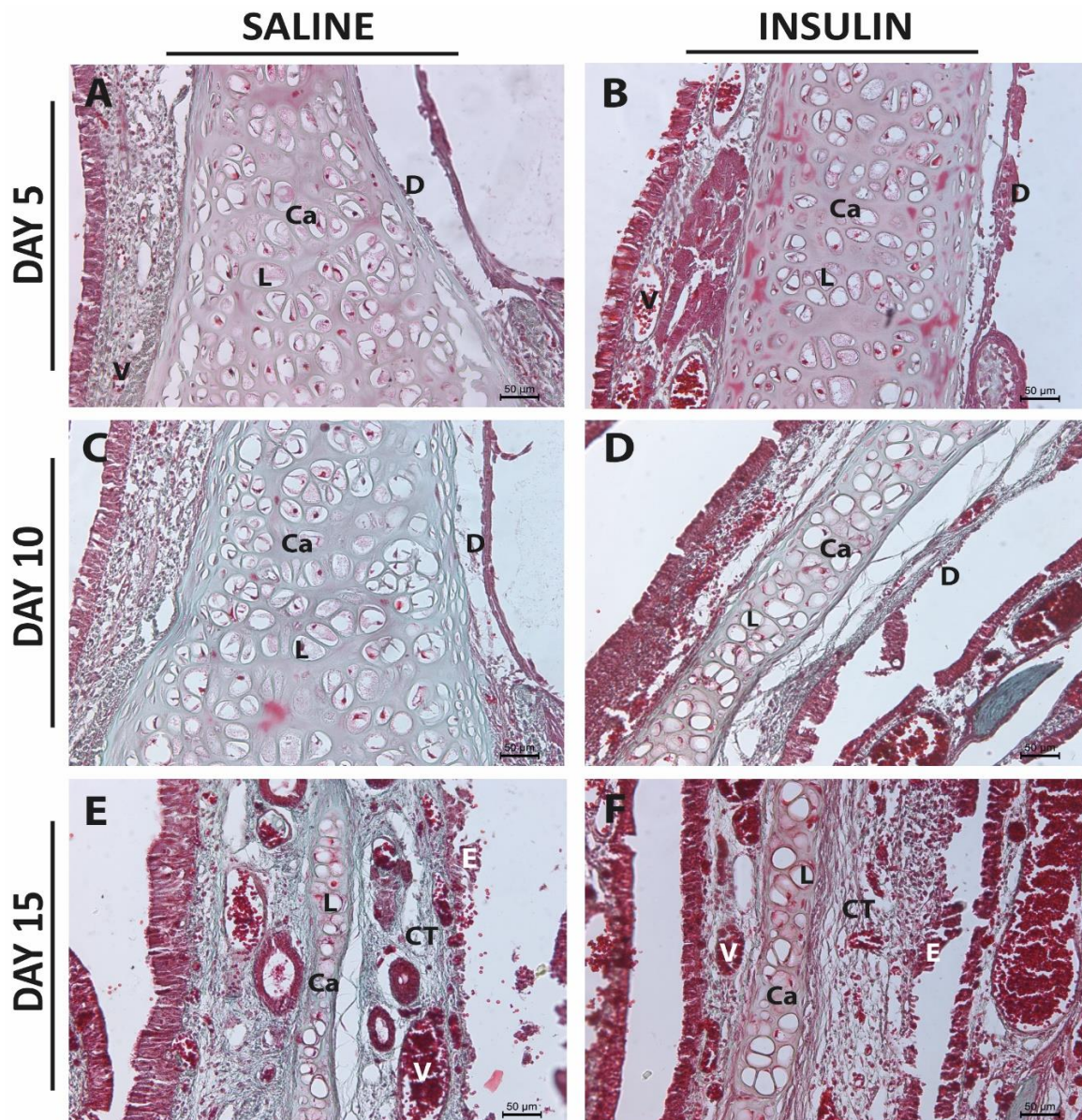


Figure 1. On the left and the right column, the micrographs of saline and insulin groups are shown respectively for days 5, 10 and 15. (A, B) the cartilage lack of mucosa is remarkable on day 5. The connective tissue is rich in collagen fibers (green) and blood vessels in (D) in insulin applied group when compared to (C) control on day 10. (E, F) Epithelization is completed on day 15. (D: Defect, Ca: Cartilage, CT: Connective Tissue, V: Vessel, L: Lacuna. Masson Trichrome, x200.)

On day 10, the reduction was 79% in the insulin group vs 62% in the saline group (Fig. 1C, D, Fig. 2, $p<0.05$). On day 15, groups treated with insulin had complete closure vs 37% full closure in the saline group (100% vs 92% epithelial defect reduction, $p<0.05$). Both

inflammation and edema were decreased and less apparent at the insulin group on day 15 (Fig. 1E, F, Fig. 2, $p < 0.05$).

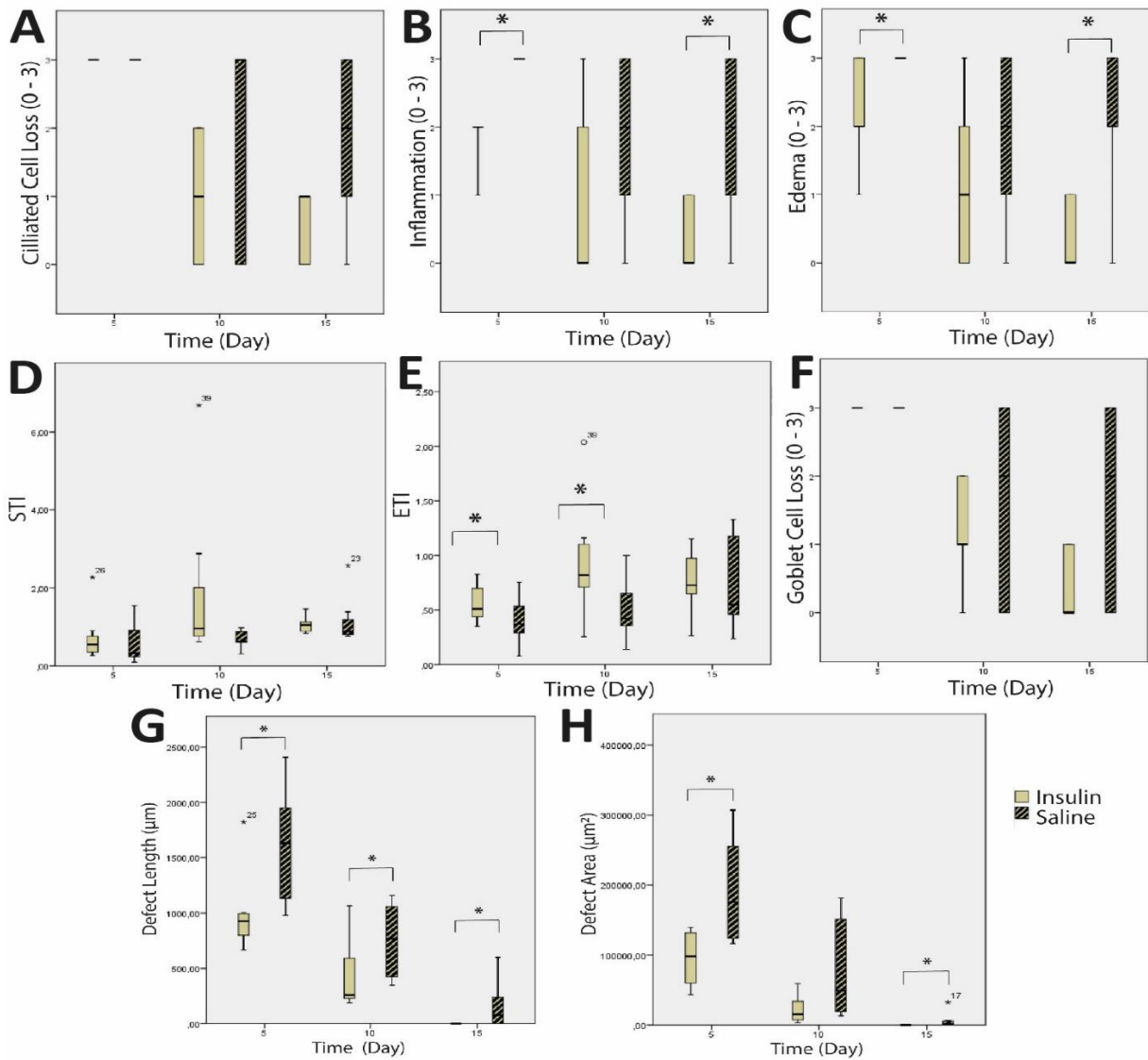


Figure 2. Box-plot graphs are showing the median, minimum and maximum values for (A) the ciliated cell loss, (B) inflammation, (C) edema, (D) STI, (E) ETI and (F) goblet cell loss (G) defect length and (H) defect area on days 5, 10 and 15 in insulin and saline applied groups (* $p < 0.05$).

DISCUSSION, CONCLUSION

Sinonasal surgeries are frequently performed in the clinic and are applied especially to the younger population. The speed of recovery after surgery is important for individuals to be able to breathe smoothly after the surgery and return to their routines. This study showed that topical intranasal insulin administration can be a suitable and effective agent for accelerating sinonasal wound healing and improving the process.

In the literature, limited local effects and systemic side effects were observed in subcutaneous insulin wound healing studies, therefore a topical insulin application was preferred. Various clinical trials have demonstrated the effectiveness of topical insulin on skin wounds [2, 4-6, 10, 11]. Our results of defect closure rate demonstrate enhancement of the healing process in nasal mucosa on days 5 and 15. The defect length is significantly lower in the insulin group compared to the control and our finding is consistent with literature by means of the effect of insulin on the wound healing process [4, 10].

In this study, it was determined that topical intranasal insulin increased the healing rate and closure of nasal mucosal wounds during 15 days of application in rats, and decreased inflammation and edema during the recovery period. Further studies focusing also on the mechanism of action with different doses of insulin may be beneficial before human use of intranasal insulin. This study can be used as a basis for studies examining nasal mucosal healing.

REFERENCES

1. Manoukian, P.D., et al., Recent trends in utilization of procedures in otolaryngology-head and neck surgery. *Laryngoscope*, 1997. 107(4): p. 472-7.
2. Van Ort, S.R. and R.M. Gerber, Topical application of insulin in the treatment of decubitus ulcers: a pilot study. *Nurs Res*, 1976. 25(1): p. 9-12.
3. Hanam, S.R., C.E. Singleton, and W. Rudek, The effect of topical insulin on infected cutaneous ulcerations in diabetic and nondiabetic mice. *J Foot Surg*, 1983. 22(4): p. 298-301.
4. Greenway, S.E., L.E. Filler, and F.L. Greenway, Topical insulin in wound healing: a randomised, double-blind, placebo-controlled trial. *J Wound Care*, 1999. 8(10): p. 526-8.
5. Wilson, J., et al., A role for topical insulin in the management problematic surgical wounds. *The Annals of The Royal College of Surgeons of England*, 2008. 90(2): p. 160-160.
6. Rezvani, O., et al., A randomized, double-blind, placebo-controlled trial to determine the effects of topical insulin on wound healing. *Ostomy Wound Manage*, 2009. 55(8): p. 22-8.
7. Lima, M.H., et al., Topical insulin accelerates wound healing in diabetes by enhancing the AKT and ERK pathways: a double-blind placebo-controlled clinical trial. *PLoS One*, 2012. 7(5): p. e36974.
8. Eken, M., et al., The effect of topical insulin application on the healing of acute tympanic membrane perforations: a histopathologic study. *Eur Arch Otorhinolaryngol*, 2007. 264(9): p. 999-1002.
9. Araujo, M.M., et al., The topical use of insulin accelerates the healing of traumatic tympanic membrane perforations. *Laryngoscope*, 2016. 126(1): p. 156-62.
10. Belfield, W.O., S. Golinsky, and M.D. Compton, The use of insulin in open-wound healing. *Vet Med Small Anim Clin*, 1970. 65(5): p. 455-60.
11. Chen, X., Y. Liu, and X. Zhang, Topical insulin application improves healing by regulating the wound inflammatory response. *Wound Repair Regen*, 2012. 20(3): p. 425-34.

**ARID3A AND ARID3B DIRECTLY REGULATES LNCRNAS MALAT1 AND
NORAD IN NSCLC**

**Şedin NASUH¹, Sibel Oğuzkan BALCI¹, Ibrahim BOZGEYİK², Masa-Aki IKEDA³,
Khandakar A. S. M. SAADAT¹**

¹Gaziantep University, Faculty of Medicine, Medical Biology Department, Gaziantep, Turkey;
shadden.nssh@gmail.com.

¹Gaziantep University, Faculty of Medicine, Medical Biology Department, Gaziantep, Turkey;
oguzkan@gaziantep.edu.tr.

²Adiyaman University, Faculty of Medicine, Medical Biology Department, Adiyaman, Turkey;
i.bozgeyik@gmail.com.

³Tokyo Medical and Dental University, Graduate School of Medical and Dental Sciences, Section of Molecular
Craniofacial Embryology, Tokyo, Japan; mikeda.emb@tmd.ac.jp.

¹Gaziantep University, Faculty of Medicine, Medical Biology Department, Gaziantep, Turkey;
shameensaadat@gantep.edu.tr.

Abstract: Lung cancer is the leading cause of cancer-related deaths with poor prognosis. Early diagnosis and effective treatment strategies are keys for survival efforts. Non-small cell lung cancer (NSCLC) accounts for approximately 85% of all lung cancers. Long non-coding RNAs (lncRNAs) play vital roles in many biological processes. Their dysregulation causes carcinogenesis and may influence the pathways that might be crucial therapeutic targets in various types of cancers. Dysregulation of lncRNAs metastasis associated lung adenocarcinoma transcript 1 (MALAT1) and non-coding RNA activated by DNA damage (NORAD) leads to the neoplastic initiation, progression, metastasis, tumor angiogenesis, chemoresistance and genomic instability in NSCLC. Both MALAT1 and NORAD are important for cell cycle progression as they directly regulate the expression of the transcription factor E2F1. The expression of p53 target genes is also affected by MALAT1 by repressing p53 promoter activity followed by cell cycle progression, and NORAD is indirectly regulated by p53. The AT-rich interaction domain (ARID) family of DNA-binding proteins, especially ARID3A and ARID3B are involved in various biological processes, including cell proliferation, differentiation, and development. ARID3A and ARID3B play important roles in E2F-dependent transcription and are transcriptional targets of p53. The pivotal function in promoting either cellular proliferation by pRb-E2F or growth arrest by p53 pathways implies a tight and finely tuned regulation. Both ARID3A, ARID3B and lncRNAs MALAT1, NORAD are involved in pRb-E2F and p53 pathways. In this study, we tried to find probable interactive and functional connectivity among ARID3A, ARID3B, lncRNAs MALAT1 and NORAD in NSCLC.

Keywords: *ARID3A, ARID3B, MALAT1, NORAD, Non-small-cell lung carcinoma*

1. INTRODUCTION:

1.1. Lung cancer:

Lung cancer is the leading cause of cancer-related deaths with poor prognosis. Early diagnosis and effective treatment strategies are keys for survival efforts. Non-small cell lung cancer (NSCLC) accounts for approximately 85% of all lung cancers (1).

1.2. Non-small cell lung cancer (NSCLC):

NSCLC is any type of epithelial lung cancer other than small cell lung cancer (SCLC). The most common types of NSCLC are squamous cell carcinoma, large cell carcinoma, and adenocarcinoma, but there are several other types that occur less frequently, and all types can occur in unusual histological variants. It is estimated that 130,180 deaths (68,820 men and 61,360 women) from this disease will occur in the United States last year. In 2020, an estimated 1,796,144 people died worldwide from the disease. For people with localized NSCLC, which means the cancer has not spread outside the lung, the overall 5-year survival rate is 63%. For regional NSCLC, which means the cancer has spread outside of the lung to nearby lymph nodes, the 5-year survival rate is about 35% (1).

1.3. ARID3 family members:

The ARID3 family consists of three closely related proteins (2):

- ARID3A/DRIL1/E2FBP1/Bright
- ARID3B/DRIL2/BDP
- ARID3C/Bright-like

1.4. ARID3A/ARID3B & E2F relationship:

T98G cells, and suppressed tumor cell growth. ARID3A and ARID3B play distinct and overlapping roles in E2F-dependent transcription by directly binding to the E2F target genes. The E2F dysregulation caused by ARID3A and ARID3B overexpression, which may have a significant influence on the progression of tumorigenesis (3).

1.5. Long non-coding RNAs (lncRNAs):

Long noncoding RNAs (lncRNAs) refer to a group of noncoding RNAs (ncRNAs) that has a transcript of more than 200 nucleotides in length in eukaryotic cells. The lncRNAs play vital

roles in many biological processes. They regulate gene expression at epigenetic, transcriptional, and post-transcriptional levels by multiple action modes. Their dysregulation causes carcinogenesis and may influence the pathways that might be crucial therapeutic targets in various types of cancers (4).

1.6. MALAT 1 (metastasis associated lung adenocarcinoma transcript 1):

MALAT 1 (metastasis associated lung adenocarcinoma transcript 1) is a long non-coding RNA, which is highly conserved amongst mammals and highly expressed in the nucleus. MALAT1 was identified in multiple types of physiological processes, such as alternative splicing, nuclear organization, epigenetic modulating of gene expression. And a number of evidences indicate that MALAT1 also closely relate to various pathological processes, ranging from diabetes complications to cancers (5).

1.7. NORAD (Non-coding RNA activated by DNA damage):

Noncoding RNA activated by DNA damage (NORAD) is a newly identified long non-coding RNA (lncRNA). NORAD is unique among lncRNAs because it is highly conserved, abundantly expressed, upregulated upon DNA damage, and maintains chromosomal stability in human cells (6).

1.8. MALAT1 and NORAD in p53 pathway:

It was also reported that the expression of p53 target genes is affected by MALAT1 by repressing p53 promoter activity followed by cell cycle progression, and NORAD is indirectly regulated by p53 (7).

2. MATERIALS & METHODS:

Overexpression of ARID3A and ARID3B was achieved using recombinant expression plasmids. As a NSCLC cell line model A549 cells were used. After successful overexpression of ARID3A and ARID3B, their effect on lncRNAs MALAT1 and NORAD were investigated using Real-time quantitative reverse transcription-PCR. Fold change analysis of MALAT1 and NORAD were done using $2^{(-\Delta\Delta Ct)}$ method. Resulting findings were statistically evaluated using GraphPad Prism 8 and paired t test was applied.

3. RESULTS:

As a result, it was found that the expression of MALAT1 and NORAD was increased 8.3-fold and 9.7-fold, respectively, in lung cancer cells overexpressing ARID3A. In addition, the expression of MALAT1 and NORAD was found to be increased 3.4-fold and 3-fold,

respectively, in lung cancer cells overexpressing ARID3B compared with the control group. These results were found to be statistically significant.

4. CONCLUSION:

Our results indicate that ARID3A and ARID3B regulates MALAT1 and NORAD in NSCLC. We show here that activities of MALAT1 and NORAD were significantly increased after overexpressing ARID3A and ARID3B. To conclude, we can say that ARID3A and ARID3B might have significant roles in the oncogenic activity of MALAT1 and NORAD in NSCLC. Thus, ARID3A and ARID3B can be used as a therapeutic target in NSCLC as they directly control the expression of MALAT1 and NORAD.

5. REFERENCES:

- (1) Yang YR, Zang SZ, Zhong CL, et al. (2014) Increased expression of the lncRNA PVT1 promotes tumorigenesis in non-small cell lung cancer. *International Journal of Clinical and Experimental Pathology* 7(10): 6929–6935.
- (2) Pratama, E. et al., *Biochem Biophys Res Commun*, 2015. 468:p.248-54.
- (3) Saadat, K. A., S. M., et al., *International Journal of Oncology* 58.4 (2021): 12.
- (4) Z. Cao *et al.*, “The roles of long non-coding RNAs in lung cancer,” *J Cancer*, vol. 13, no.1, pp. 174–183, 2022, doi: 10.7150/jca.65031.
- (5) Yoshimoto R, Mayeda A, Yoshida M, Nakagawa S. MALAT1 long non-coding RNA in cancer. *Biochim Biophys Acta*. 2016;1859(1):192–9.
- (6) Lee S, Kopp F, Chang TC, Sataluri A, Chen B, Sivakumar S, et al. Noncoding RNA NORAD Regulates Genomic Stability by Sequestering PUMILIO Proteins. *Cell* (2016) 164:69–80. doi: 10.1016/j.cell.2015.12.017.
- (7) Zhang A, Zhou N, Huang J, Liu Q, Fukuda K, Ma D, Lu Z, Bai C, Watabe K and Mo YY: The human long non-coding RNA-RoR is a p53 repressor in response to DNA damage. *Cell Res* 23: 340-350, 2013.

INVESTIGATION OF THE EFFECTS OF IMATINIB USE ON THE OVARY IN THE EARLY PRENATAL PERIOD

Zehra TOPAL SUZAN¹, Mehtap ATAĞ², Levent TÜMKAYA³

¹Recep Tayyip Erdoğan Üniversitesi, Tıp Fakültesi, Histoloji ve Embriyoloji AD, Rize, TÜRKİYE,
zehratal@gmail.com

²Recep Tayyip Erdoğan Üniversitesi, Tıp Fakültesi, Tıbbi Biyokimya AD, Rize, TÜRKİYE,
mehtap.atak@erdogan.edu.tr

³Recep Tayyip Erdoğan Üniversitesi, Tıp Fakültesi, Histoloji ve Embriyoloji AD, Rize, TÜRKİYE,
levent.tumkaya@erdogan.edu.tr

Özet: İmatinib tedavisi sırasında beklenmeyen gebeliklerin klinikte karşılaşılması sonucu, erken embriyonal dönemdeki maruziyetin yetişkin yaşamındaki dişi üreme sağlığına etkilerini incelemek amacıyla bu çalışma tasarlanmıştır. On iki adet Sprague Dawley dişi sıçan rastgele dört gruba ayrıldı; östrus evresinde olduğu belirlenen dişi sıçanlar koitus sonrası sperm görülen sıçanlar gebe kabul edildi. Gruplar; kontrol grubu (tedavi uygulanmadı), İma-20 (20 mg/kg), İma-40 (40 mg/kg), İma-60 (60 mg/kg) olarak belirlendi. Embriyonik 1. günde (E1)-E8 günlerinde gruplara tek doz imatinib uygulandı. Yavru dişi sıçanlar postnatal 80. günde sakrifiye edildi. Ovaryum dokuları histopatolojik ve biyokimyasal analizlerle incelendi. Kontrol grubunun ovaryum dokularının normal histolojik yapıları sahip olduğu gözlemlendi. Kontrol grubuna göre İma-40 ve İma-60 gruplarında medullar ödemde artış olduğu; inflamasyon skorunun ise tüm gruplarda arttığı görüldü. Dejeneratif folikül skorlamasında İma-20 ve İma-40 gruplarında anlamlı artış tespit edildi. İlaç grupları arasında apoptotik hücrelerde değişiklik gözlenmedi. Yapılan ölçümlerde TBARS seviyelerinin kontrol grubu ile karşılaştırıldığında İma-20 ve İma-40 gruplarında arttığı gösterildi. TT düzeylerinin kontrol grubuna göre tüm ilaç gruplarında arttığı; ilaç grupları kendi aralarında karşılaştırıldığında İma-60 grubunun TT düzeylerinin İma-20 ve İma-40 gruplarına göre azaldığı belirlendi. Embriyonik dönemde imatinib kaynaklı maruziyetin ovaryumda histopatolojik dejeneratif bulgulara neden olduğu ve oksidatif stres oluşturduğu belirlendi. İlaç grupları arasındaki bu değişimin farklı yöntemlerle incelenmesi ve daha fazla çalışmalarla desteklenmesi önerilmektedir.

Abstract: This study to examine the effects of early embryonal exposure on female reproductive health in adult life to result in unexpected pregnancies during in-clinic imatinib treatment. Twelve Sprague Dawley female rats were divided randomly into four groups; Female rats determined to be in the estrus stage were mated with male rats. Groups; control group (no treatment was administered), İma-20 (20 mg/kg), İma-40 (40 mg/kg), İma-60 (60

mg/kg). After a post-coital vaginal wash in the female rats was accepted on embryonic day 1 (E1) and single doses were administered imatinib to the groups E1-E8 days. The offspring of female rats were sacrificed on the 80th postnatal day. Ovarian tissues were analyzed by histopathological and biochemical analysis. Observed ovarian tissues of the control group to have normal histological structures. Compared to the control group, medullary edema increased in the ima-40 and ima-60 groups; the inflammation score increased in all groups. Determined significant increase in Ima-20 and Ima-40 groups in degenerative follicle scoring. No change in apoptotic cells was observed in the drug groups. Compared with the control group; increase in TBARS levels in the Ima-20 and Ima-40 groups. TT levels increased in all groups and drug groups were compared with each other, determined that the TT levels of the Ima-60 group decreased compared to the Ima-20 and Ima-40 groups. Determined imatinib-induced exposure in the embryonic period caused histopathological degenerative findings in the ovaries and oxidative stress occurred. Recommended supporting this change between drug groups by investigating different studies and examining different methods.

Keywords: Early, imatinib, ovary, prenatal rat.

INTRODUCTION

Triosine kinases are a group of enzymes that transfer a phosphate from the nucleotide triphosphate to the hydroxyl group and cause changes in protein conformation (1). These are involved in processes such as growth, differentiation, and apoptosis in the biological system (2). Triosine kinases and their receptors function reported in the ovary and their inhibitions may be functionally effective in this organ (3). Imatinib is a triosine kinase inhibitor (TKI) used in the treatment of chronic myeloid leukemia (CML), Philadelphia chromosome (+) ALL, and gastrointestinal tumors (4). In the literature, there are studies showing the toxicity of imatinib in different organs such as the heart, liver and skin (5, 6, 7). Imatinib is an inhibitor of triosine kinases platelet-derived growth factor receptors (PDGFR) and stem-cell factor (c-kit); and play a role in spermatogenesis and oogenesis in both male and female reproductive systems during the embryonal period (8). In previous studies, different TKIs have a negative effect on the ovulation process (9) and inhibit some signaling pathways in the ovary (10).

Various growth factors involved in ovarian function such as folliculogenesis, luteogenesis, oogenesis, proliferation, and apoptosis (11). C-kit and kit ligand (KL) in the ovary play

important role in stages such as primordial follicle, formation of antrum structure, and meiotic maturation (12). Addition, PDGF effective in the transition of the primordial follicle to the primary follicle with some signaling factors (13). PDGF inhibition, changes in follicular development, formation of more atretic follicles, and ovarian apoptosis were observed (14).

MATERIAL-METHOD

Animal experiment: The rats used in the study procured and housed, practices carried out at RTUE Experimental Animals Application and Research Center. Fifteen Sprague-Dawley adult mother rats and 32 baby females used in the study. Vaginal washing with PBS was applied to determine the regular oestrus stages of mother rats and epithelial cells examined in smear and smear preparation. In female rats, which determined in the estrus stage, those with sperm detected after coitus considered embryonic 1st day. Mother rats randomly divided into four groups; control, Ima-20, Ima-40, and Ima-60.

Preparation and administration of the drug: Imatinib (Imavec, Koçak Farma, Turkey) administered to rats was dissolved in sterile distilled water daily and injected intraperitoneally (i.p.) at the specified dosages. Mother rats in the control group were not injected; Embryonic 1-8 to Ima-20 (20mg/kg/day), Ima-40 (40mg/kg/day) and Ima-60 (60mg/kg/day) groups. The single daily dose of imatinib i.p. injected. Newborn female rats were sacrificed under anesthesia on the postnatal 80th day without any treatment.

Histopathological analyzes: The ovaries of young female rats were removed and fixed in 10% formaldehyde, dehydrated in alcohol series (Merck GmbH, Darmstadt, Germany), and embedded in paraffin blocks after xylene (Merck GmbH, Darmstadt, Germany) steps. In a rotary microtome (Leica, RM2525, Germany) in our research laboratory, 4-5 μ m thick sections stained with hematoxylin Harris hematoxylin, Merck GmbH, Darmstadt, Germany) and eosin Eosin G, Merck GmbH, Darmstadt, Germany (H&E) and Olympus DP72 camera. Histopathological evaluation and histopathological damage evaluation score (Table 1) performed in 10 randomly selected areas under the Olympus trinocular BX51 TF (Olympus, Tokyo, Japan) light microscope with attachment (Olympus, Tokyo, Japan).

Table 1 Histopathological damage evaluation score (15 ,16).

Findings	Score
< 25	1
\geq 25	2

≥ 50	3
≥ 75	4

The terminal deoxynucleotide transferase dUTP nick end labeling (TUNEL) method:

After deparaffinization, xylene, and dehydration procedures, ovarian sections apply following the TUNEL Assay Kit - HRP-DAB (ab206386, Abcam, USA) brand kit protocol. Counterstained ovaries with methyl green after DAB chromogen incubation.

Biochemical analyzes:

TBARS Evaluation: Ohkawa et al. (17) method used to measure TBARS levels in ovarian tissues to determine oxidative damage. Samples that appeared pink after incubation were pipetted into 96-well plates and read at 532 nm in the spectrophotometer. Analysis results determine as $\mu\text{mol/g}$ wet tissue.

TT Evaluation: TT levels in homogenized ovarian tissues determined by the method described by Ellman (18). The sulfhydryl groups reduced by 5,5'-dithiobis 2-nitrobenzoic acid read in the spectrophotometer at a wavelength of 412 nm, the results given as $\mu\text{mol/g}$ wet tissue.

RESULTS

Histopatological Results

Examination of the control group had normal histological structures in the ovarian tissues (Figure 1); semi-quantitative analysis scores were in the range of 0-1 (Table 2). Ima-40 and Ima-60 groups observed swelling and loss of the cytoplasm of the cells belonging to the medulla region. Compared to the control group, medullary edema increased in the Ima-40 ($p=0.022$) and Ima-60 groups ($p=0.001$) (Table 2). The inflammation score increased in all groups compared to the control group ($p<0.05$) (Figure 1, Table 2). The degenerative follicle score is analyzed and determined a significant increase in Ima-20 ($p=0.021$) and Ima-40 ($p=0.007$) groups in degenerative follicle scoring (Figure 1, Table 2). There was no difference between drug groups in the apoptosis examination. (Figure 2, Table 3).

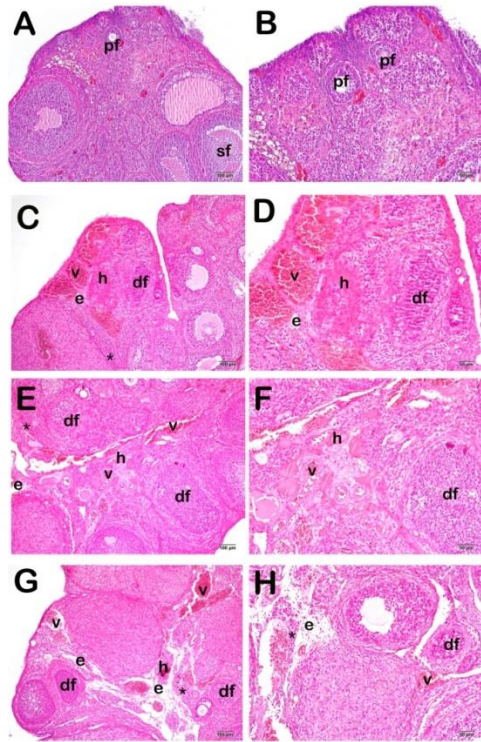
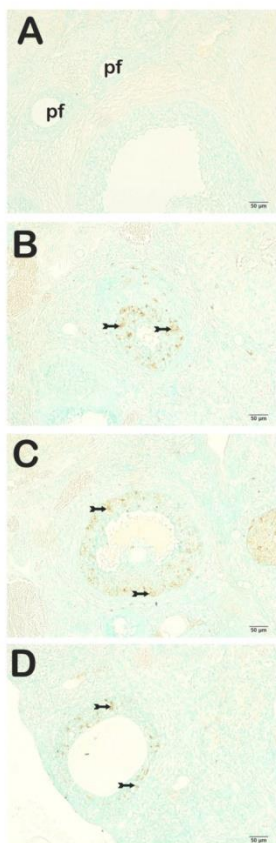


Figure 1. Representative light microscopic picture of sections of ovarian tissue stained with H&E. **A(x10)-B(x20):** Control group. **C(x10)-D(x20):** Ima-20 group. **E(x10)-F(x20):** Ima-40 group. **G(x10)-H(x20):** Ima-60 group. Degenerative follicles (df), vascular congestion (vc), hemorrhagic areas (h), edematous areas (e) and infiltrative (asterix).



chne²⁰₂₂

Figure 2. Representative light microscopic picture of sections of ovarian tissue stained with TUNEL methods. **A(x20):** Control group. **B(x20):** Ima-20 group. **C(x20):** Ima-40 group. **D(x20):** Ima-60 group. Preantral follicles (pf), immunopositivity preantral follicles (tailed arrow).

Table 2 Semi-quantitative Analysis Results (Median-25%-75% interquartile range).

Groups	Vascular Congestion	Hemorrhage	Medullar edema	Inflammation	Degenerative Follicles
Control	1(0-1)	0.5(0-1)	0.5(0-1)	0(0-0)	0.5(0-1)
Ima-20	3.5(3-4)	1(1-1)	1(1-1)	2(2-2) ^a	2(1-2) ^d
Ima-40	3.5(2-4)	1(1-1)	2.5(2-3) ^a	2.5(2-3) ^c	2(2-2) ^e
Ima-60	3(3-3)	1(1-2)	2(2-2) ^b	2(2-2) ^b	1.5(1-2)

^a*p*=0.022; versus to Control group,
^b*p*=0.001; versus to Control group,
^c*p*=0.000; versus to Control group,
^d*p*=0.021; versus to Control group,
^e*p*=0.007; versus to Control group,
 Kruskal Wallis/Tamhane T2 test

Table 3. TUNEL positivitiy score (median-(25%-75% interquartile range)).

Group	TUNEL Positivity Score
Control	0(0-1)
Ima-20	2.5(2-3) ^a
Ima-40	2.5(2-3) ^a
Ima-60	2(2-3) ^a

^a*p*=0.000; versus to Control group.
 Kruskal Wallis/Tamhane T2 test

Biochemical Results

Compared with the control group; increase in TBARS levels in the Ima-20 and Ima-40 groups (*p*<0.05) (Table 4). In addition, TT levels increased in all groups (*p*<0.05) (Table 4). When

the drug groups were compared with each other, it was determined that the TT levels of the Ima-60 group decreased compared to the Ima-20 and Ima-40 groups ($p < 0.05$) (Table 4).

Table 4. Biochemical Results

Groups	TT ($\mu\text{mol/wet tissue}$)	TBARS ($\mu\text{mol/wet tissue}$)
Control	2,69 \pm 0,28 a*b**	0,56 \pm 0,18 a**
Ima-20	5,62 \pm 0,56	0,80 \pm 0,12
Ima-40	6,50 \pm 0,68	0,82 \pm 0,08
Ima-60	4,05 \pm 1,22 c*	0,61 \pm 0,20

*: $p < 0,001$ ve **: $p < 0,05$
a: Control group versus Ima-20 and Ima-40 groups
b: Control group versus Ima-60 group
c: Ima-60 group versus Ima-20 and Ima-40 groups
ANOVA tests

DISCUSSION

There are concerns about the adverse effects of TKI use on the ovary. Studies in the literature on the toxic effects of different TKIs on the ovary. Bernard et al. (9) stated that sunitinib (TKI) causes a decrease number of corpora lutea and Anti-Müllerian hormone levels in the ovary, but does not show any change in the number of primordial and developing follicles. Total number of follicles in the ovaries administered nilotinib of female rats decrease, follicles are cause irregularity in the ovarian placement (19).

Long-term use of imatinib in adulthood reported causes ovarian failure (20). In another study in mice, that the use of imatinib decreases the egg reserve by causing a decrease in the number of primordial follicles and an increase in the number of developing follicles in the ovary, as well as having negative effects in terms of embryonal development and fertility (21). While there are studies on the use of imatinib in the adult period, there are limited studies in the embryonal or prenatal period. Imatinib exposure causes histopathological and biochemical changes testicular tissue in the male reproductive system on prenatal period (22). Imatinib delays follicle formation and inhibits primodial follicle activation in female individuals in the postnatal period (23). Histopathological evaluations determined medullary edema in the Ima-40 and Ima-60 groups; swelling cells, loss of cytoplasm. Inflammation findings determine in all drug groups. In addition, an increase in degenerative follicles observed in Ima-20 and Ima-40 groups.

Imatinib causes oxidative damage by increasing ROS in organs; reported to reduce GSH levels (6, 24). This study observed that TBARS levels increased in the Ima-20 and Ima-40 groups of imatinib, causing oxidative stress, while an increase in TT levels observed. Thiol an organic component containing –SH groups in its structure and play an important role in preventing oxidative stress and proteins with amino acids containing these groups are the first target of ROS (25). Based on this information, we think that imatinib causes oxidative stress in the ovarian tissue and may increase thiol levels depending on this stress.

Women protected against the potential teratogenicity of this drug with contraception during imatinib treatment (26). More studies are needed to reduce the teratogenic effects by discontinuing TKIs before pregnancy even longer-term studies should be planned for epigenetic risks that may occur in the baby after discontinuation of use (27).

CONCLUSION

Imatinib exposure may cause histopathological findings and oxidative stress in the ovary during the embryonic period. More research is needed to establish teratogenic effects during imatinib therapy.

REFERENCES

1. Katopodis, P., Chudasama, D., Wander, G., Sales, L., Kumar, J., Pandhal, M., Anikin, V., Chatterjee, J., Hall, M., Karteris, E. (2019). Kinase Inhibitors and Ovarian Cancer. *Cancers (Basel)* 11(9):1357. doi: 10.3390/cancers11091357.
2. Iqbal, N., Iqbal N. (2014). Imatinib: A Breakthrough of Targeted Therapy in Cancer. *Chemother Res Pract.* 2014:357027. doi: 10.1155/2014/357027.
3. Alesi, L.R., Amy L. Winship, A.L., Hutt K. J. (2021). Evaluating the impacts of emerging cancer therapies on ovarian function. *Current Opinion in Endocrine and Metabolic Research* 18:15–28.
4. Iram, H., Iram, F., Husain, A. (2016). A Review on Imatinib: A wonder drug in Oncology. *Adv. Biomed. Pharma.* 3(4), 227-244.
5. Herman, E.H., Knapton, A., Rosen, E., Thompson, K., Rosenzweig, B., Estis, J., Agee, S., Lu, Q.A., Todd, J.A., Lipshultz, S., Hasinoff, B., Zhang J. (2011). A Multifaceted Evaluation of Imatinib-induced Cardiotoxicity in the Rat. *Toxicologic Pathology* 39: 1091-1106.
6. Al-Rasheed, N.M., El-Masry, T.A., Tousson, E., Hassan, H.M., Al-Ghadeer, A. (2017). Protective Potential of Grape Seed Proanthocyanidins Extract against Glivec (Imatinib Mesylate) Induced Liver Toxicity and Oxidative Stress in Male Rats. *Annual Research & Review in Biology* 20(6): 1-9.
7. Tsao, A.S., Kantarjian, H., Cortes, J., O'Brien, S., Talpaz, M. (2003). Imatinib Mesylate Causes Hypopigmentation in the Skin. *CANCER* 98 (11): 2483-2487.
8. Carlier, P., Bernard, N., Lagarce, L., Dautriche, A., Be'ne', J., Sam-Lai, N.F., Eftekhari P. (2017). Pregnancy outcome among partners of male patients receiving imatinib, dasatinib or nilotinib in chronic myeloid leukemia: reports collected by the French network pharmacovigilance centers. *Arch Gynecol Obstet* 295:269–271.
9. Bernard, V., Bouilly, J., Kramer P., Carré, N., Schlumberger, M., Visser, J.A., Young, J., Nadine Binart N. (2016). The Tyrosine Kinase Inhibitor Sunitinib Affects Ovulation but Not Ovarian Reserve in Mouse: A Preclinical Study. *PLoS ONE* 11(4): e0152872. doi:10.1371/journal.pone.0152872.
10. Liao, Q., Feng, X., Li, X., Chen, G., Chen, J., Yang, B., Li, K., Ai, J. (2020). Lapatinib-induced inhibition of ovarian function is counteracted by the STAT3 pathway both in vivo and in vitro. *ONCOLOGY REPORTS* 44: 1127-1135.
11. Sirotkin A.V. (2011). Growth Factors Controlling Ovarian Functions. *J. Cell. Physiol.* 226: 2222–2225.

12. Hutt, K.J., McLaughlin, E.A., Holland, M.K. (2006). Kit ligand and c-Kit have diverse roles during mammalian oogenesis and folliculogenesis. *Molecular Human Reproduction* 12(2): 61–69.
13. Nilsson, E.E., Detzel, C., Skinner, M.K. (2006). Platelet-derived growth factor modulates the primordial to primary follicle transition. *Reproduction* 131:1007–1015.
14. Pascuali, N., Scotti, L., Abramovich, D., Irusta, G., Di Pietro, M., Bas, D., Tesone, M., Parborell, F. (2015). Inhibition of platelet-derived growth factor (PDGF) receptor affects follicular development and ovarian proliferation, apoptosis and angiogenesis in prepubertal eCG-treated rats. *Molecular and Cellular Endocrinology* 412: 148–158.
15. Topcu, A., Balik, G., Atak, M., Mercantepe, T., Uydu, H.A., Tumkaya, L. (2019). An investigation of the effects of metformin on ovarian ischemia-reperfusion injury in rats. *European Journal of Pharmacology* 865:172790.
16. Nevin Sağsöz, N., Kisa, Ü., Apan, A (2002). Ischaemia–reperfusion injury of rat ovary and the effects of vitamin C, mannitol and verapamil. *Human Reproduction* 17(11): 2972–2976.
17. Ohkawa, H., Ohishi, N., Yagi, K. (1979). Assay for lipid peroxides in animal tissues by thiobarbituric acid reaction. *Anal Biochem* 95: 351–358.
18. Ellman, G.L. (1959). Tissue sulfhydryl groups. *Arch Biochem Biophys* 82: 70–77.
19. Seval, G. C., Özkavukçu, S., Seval, M., Aylı, M (2016). Gonadotoxic Effects of Nilotinib in Chronic Myeloid Leukemia Treatment Dose in a Mouse Model. *Turk J Hematol* 34: 137-142.
20. Christopoulos, C., Dimakopoulou, V., Rotas, E (2008). Primary Ovarian Insufficiency Associated with Imatinib Therapy. *N Engl J Med*. 358(10):1079-80. doi: 10.1056/NEJMc0707841.
21. Salem, W., Ho, J.R., Woo, I., Ingles, S.A., Chung, K., Paulson, R.J., McGinnis, L.K. (2020). Long-term imatinib diminishes ovarian reserve and impacts embryo quality. *J Assist Reprod Genet* 37:1459–1466.
22. Suzan, Z.T., Tumkaya, L., Mercantepe, T., Atak, M., Uydu, H.A (2021). The effect of imatinib administered in the prenatal period on testis development in rats. *Hum Exp Toxicol*. 40(4):634-648.
23. Asadi-Azarbaijani, B., Santos, R.R., Jahnukainen, K., Braber, S., Duursen, M.B.M., Toppari, J., Saugstad, O.D., Nurmio, M., Oskam, I.C. (2017). Developmental effects of imatinib mesylate on follicle assembly and early activation of primordial follicle pool in postnatal rat ovary. *Reproductive Biology* 17: 25–33.
24. Mansour, H.H., El kiki, S.M., Ibrahim, A.B., Omran, M.M. (2021). Effect of L-carnitine on cardiotoxicity and apoptosis induced by imatinib through PDGF/ PPAR γ /MAPK pathways. *Archives of Biochemistry and Biophysics* 704: 108866.
25. Kundi, H., Ates, I., Kiziltunc, E., Cetin, M., Cicekcioglu, H., Neselioglu, S., Erel, O., Ornek, E (2015). A novel oxidative stress marker in acute myocardial infarction; thiol/ disulphide homeostasis. *American Journal of Emergency Medicine* 33: 1567–1571.
26. Hensley, M.L., Ford, J.M. (2003). Imatinib Treatment: Specific Issues Related to Safety, Fertility, and Pregnancy. *Seminars in Hematology*, 40(2 Suppl 2):21-5.
27. Rambhatla, A., Strug, M.R., De Paredes, J.G., Munoz, M.I.C., Thakur, M. (2021). Fertility considerations in targeted biologic therapy with tyrosine kinase inhibitors: a review. *J Assist Reprod Genet* 38(8):1897-1908.

THE EFFECTS OF THE USE OF BOUIN AND FORMALDEHYDE FIXATIVES IN TESTICULAR TISSUE ON HISTOPATHOLOGICAL EVALUATION IN ROUTINE AND IMMUNOHISTOCHEMICAL STAINING

Zehra TOPAL SUZAN¹, Levent TMKAAYA², Tolga MERCANTEPE³, Tuęba ELİK
SAMANCI⁴

¹Recep Tayyip Erdoğan Üniversitesi, Tıp Fakltesi, Histoloji ve Embriyoloji AD, Rize, TRKİYE,
zehratorall@gmail.com

²Recep Tayyip Erdoğan Üniversitesi, Tıp Fakltesi, Histoloji ve Embriyoloji AD, Rize, TRKİYE,
levent.tumkaya@erdogan.edu.tr

³Recep Tayyip Erdoğan Üniversitesi, Tıp Fakltesi, Histoloji ve Embriyoloji AD, Rize, TRKİYE,
tolga.mercantepe@erdogan.edu.tr

⁴Recep Tayyip Erdoğan Üniversitesi, Tıp Fakltesi, Histoloji ve Embriyoloji AD, Rize, TRKİYE,
tugba.celik@erdogan.edu.tr

zet: alıřma, testis fiksasyonunda kullanılan formaldehit ve Bouin solsyonlarının histopatolojik, immnohistokimyasal bulgu sonularını karřılařtırmayı amalamaktadır. Testis dokuları %10 formaldehit ieren solsyon ve Bouin solsyonu ile tespit edilerek iki grup halinde incelendi ve H&E, Masson Goldner ve anti-kaspaz-3 ile boyandı. Histopatolojik analizler yapıldı ve immno-pozitif hcreler deęerlendirildi. Bouin grubunda H&E boyanan kesitlerde seminifer tbl yapısının btnlę, germ hcreleri ve testis dokularındaki hcre sınırları, primer spermatositlerin kromatin yapıları ve spermatid hcrelerinin grnrlęnin korunduęu grld. Ayrıca interstisyel alan, vaskler yapılar ve hcre btnlę morfolojik olarak normaldi. Formaldehit ile fikse edilen grupta seminifer tbldeki germ hcreleri ve interstisyel alandaki hcrelerin kromatin yapısı ve interstisyel alan btnlęnin normal olduęu izlendi. Ancak hcrelerin eozinofilik boyandıęı ve germ hcrelerinin btnlęnin daha zayıf olduęu; seminifer tbllerde hafif bzlme tespit edildi. Masson Goldner Trichrom boyamada formaldehit grubundaki kesitlerde germ hcreleri ve Leydig hcreleri soluk renkli, baę dokusu hcreleri ise parlak kırmızı boyandı. Bouin grubundaki germ hcreleri, Leydig hcreleri ve baę dokusu parlak kırmızıya boyandı. İmmnohistokimyasal incelemede anti-kaspaz 3 antikoru boyamada formaldehit grubu, Bouin grubuna kıyasla germ hcrelerinde daha yoęun pozitivite gsterildi. Her iki fiksatorn de farklı boyamalarda pozitivite yoęunluęu, kromatin yapısının grnrlę, hcre-doku btnlęnin korunması gibi eřitli avantajları olduęu ve alıřmalarda her iki fiksatorn de kullanılmasının morfolojik yapıların gsterilmesinde faydalı olacaęı gnerilmektedir.

Anahtar Kelimeler: Testis, formaldehit, Bouin, fiksasyon, histopatoloji.

Abstract: Study aims to compare the results of histopathological, immunohistochemical findings of formaldehyde and Bouin solutions used in testis fixation. Testicular tissues were

fixed in 10% formaldehyde-containing solution and Bouin's solution and analyzed in two groups and stained with H&E, Masson Goldner, and anti-caspase-3. The use for analysis histopathological and immuno-positive cells evaluation. H&E staining of the Bouin group preserved, the integrity of the seminiferous tubule structure, germ cells, and cell borders in testicular tissues, chromatin structures of primary spermatocytes, and visibility of spermatid cells. Additionally, the interstitial area, vascular structures, and cell integrity are morphologically normal. In the group fixed with formaldehyde, germ cells in the seminiferous tubule and chromatin structure cells in the interstitial area and interstitial area integrity were normal. However, determining the cells were stained eosinophilic and the integrity of the germ cells was weaker and detected mild shrinkage of the tubules. Germ cells and Leydig cells were stained in pale color by Masson Goldner staining of the sections in the formaldehyde group, while the cells of the connective tissue were stained bright red. In the Bouin group, germ cells, Leydig cells, and connective tissue were stained bright red. In the immunohistochemical examination, anti-caspase 3 antibody staining showed that the formaldehyde group was more intensely positive in germ cells compared to the Bouin group. Both fixators have various advantages such as positivity density in different staining, visibility of chromatin structure, preservation of cell-tissue integrity, and using both fixators in studies will be beneficial in demonstrating morphological structures.

Keywords: *Testis, formaldehyde, Bouin, fixation, histopathology.*

INTRODUCTION

Formaldehyde and Bouin solutions are commonly used for the fixation of testicular tissue in laboratories. Although the fixation of Bouin solution shows good results in the detection of lesions in the testis, it is not seen as a suitable fixator in the fixation of other tissues due to the difficulty in removing picric acid from the tissue (1). Liang et al. showed that after testis fixation of Bouin and neutralized buffer 4% formaldehyde solutions in monkey, mouse, and rat species, testosterone was immuno-labeled in bouin-fixed tissues, but labeling was negative in tissues fixed with neutralized buffer 4% formaldehyde (2).

MATERIAL AND METHOD

Histological analysis

Sprague Dawley (225-260 g) adult male rats were divided into two groups in the study. Two different fixators Bouin, and formaldehyde, were used for the fixation of testis tissues. The determined first group was the formaldehyde group and the second group was the Bouin

group. In the formaldehyde group, fixed tissues in a solution containing 10% formalin (Merck GmbH, Darmstadt, Germany). In the Bouin group, the fixed tissues in a liquid containing formaldehyde, acetic acid (Merck GmbH, Darmstadt, Germany), picric acid (Sigma-Aldrich, USA). Testicular tissue in 70% ethanol, and as a result, removed picric acid from the tissue. Testicles were embedded in paraffin blocks after dehydration (Merck GmbH, Darmstadt, Germany) and xylene (Merck GmbH, Darmstadt, Germany).

The 4-5 μm thickness sections with a microtome (Leica, RM2525, Germany) from the tissues embedded in the paraffin blocks. Sections were stained with hematoxylin (Harris hematoxylin, Merck GmbH, Darmstadt, Germany) and eosin (Eosin G, Merck GmbH, Darmstadt, Germany) (H&E), Masson-Goldner (Masson-Goldner staining kit, Merck GmbH, Darmstadt, Germany).

Immunohistochemical staining protocol

Mouse and Rabbit Specific HRP / DAB (ABC) Detection IHC Kit (ab64264, Abcam, USA) kit were used for immunohistochemical staining. It was taken on a positively charged slide (Patolab, PRC). After the deparaffinization and dehydration stages of the tissues; hydrogen peroxide block, antigen retrieval, protein block, incubation with anti-caspase-3 antibody (ab4051, Abcam, USA) (according to the manufacturer's recommendation), Biotinylated Goat Anti-Polyvalent, Streptavidin Peroxidase, DAB Chromogen, counterstaining with hematoxylin, dehydration and after xylene treatments covered with entellan medium.

RESULTS

Examined H&E staining testis tissues in the Bouin group, we observed that the seminiferous tubule structure and integrity between germ cells and cell borders were well preserved. Determine chromatin structures of primary spermatocyte and spermatid cells were visible in Bouin-fixed tissues. Evaluating interstitial area, vascular structures, and cell integrity as morphologically normal (Figure 1). Observed with fixed with formaldehyde group, germ cells in the seminiferous tubule and chromatin structures of the cells in the interstitial area, and the integrity of the interstitial area was normal. Formaldehyde fixed group compare to the Bouin group the cells staining eosinophilically and weaker in terms of the integrity of the germ cells in the tubule (Figure 1).

Masson Goldner staining sections of testes in the formaldehyde group observed the germ cells and Leydig cells stained in a paler color, but the connective tissue cells were stained bright red. Germ cells and Leydig cells and connective tissue stained bright red in the Bouin group

(Figure 2). Examining to anti-caspase 3 antibody staining sections determined that positive cells were prominent in the germ cells in the sections in the formaldehyde group compared to the Bouin group (Figure 3).

DISCUSSION

The fixation stage is one of the most important stages of the experiment, and a well-fixed tissue provides an objective aspect to the morphological examination. Different procedures have been used in laboratories from past to present. Different fixators such as immersion, NBF, Bouin, Helly's, Zenker, and formaldehyde are used in the fixation of testicular tissue (3, 1). Additional alcohol, glycerol, glacial acetic acid, and dimethyl sulfoxide (DMSO) solutions are used in fixators formed in different ratios (4). Fixation methods may vary according to the tissue type and attention should be paid to the pH, ambient temperature, and components used in the fixative (5).

Formaldehyde causes hyperosmolality in cells and causes condensation of the cytoplasm by its effect on membrane proteins (6). fixation of the testis with formaldehyde causes shrinkage in germinal and Sertoli cells and aggregation in the chromatin structure, although these artifacts are alleviated in tissues using Bouin's solution (3). The main reason for choosing a fixative other than formaldehyde solution in testis is that the seminiferous tubules are tightly arranged in the interstitial space and the integrity of the sensitive cells in the tubule is preserved (7). In our study, mild shrinkage of tubules was detected in the H&E-stained sections in the formaldehyde-fixed group, and this artifact was alleviated in the Bouin-fixed group.

While Bouin's solution provides a good opportunity for fixation of the testis, it is not suitable for use in other tissues due to its lack of fixation and the difficulty of removing picric acid from the tissue (1). Picric acid, which is the main component of Bouin, forms salts with basic proteins and causes proteins to precipitate and its diffusion into the tissue is slow, it protects glycogen structures well and some of the shrinkages it causes in cells are prevented by glacial acetic acid (8). In humans, the Bouin fixator is used for the examination of biopsy samples taken from infertile male patients (9). According to Bouine, modified Davidson's Fluid (mDF), which is a different fixative, has been shown to have the advantage of not containing picric acid and storing in 10% formaldehyde solution after 24-48 hours of fixation (10). This study determined that the visibility of intercellular borders and chromatin structures was clear in the morphological images of H&E stained sections in the Bouin-fixed group. In

immunohistochemical analyzes, the positivity was more intense in the groups fixed with formaldehyde compared to the sections fixed with Bouin of the tissues marked with caspase-3 antibodies.

Bouin and neutralized formaldehyde solutions were compared in different animal species, phosphate-buffered 4% formaldehyde solution provided insufficient morphology in testicular tissue in the histopathological examination; Bouin is more suitable for determining the immunohistochemical localization of testosterone in cynomolgus monkey, rat, and mice species (2). In the fixation of the testis, formaldehyde may cause shrinkage in cells and insufficient visibility of both cellular and nuclear structures; Although Bouin's solution provides improvement over formaldehyde, there are questions about the removal and safety of picric acid from the tissue (7).

As a result of these data, Bouin's fixative in routine staining, morphological examinations, and histopathological analyzes; formaldehyde fixative provides advantages in immunohistochemical analyzes and Masson Trichrome-Golder staining.

REFERENCES

1. Harleman, J.H., Nolte, T. (1997). Testicular Toxicity: Regulatory Guidelines—The End of Formaldehyde Fixation? *Toxicol Pathol.* 25(4):414-417.
2. Liang, J.H., Sankai, T., Yoshida, T., Yoshikawa, Y (2000). Comparison of the effects of two fixatives for immunolocalization of testosterone in the testes of the cynomolgus monkey, mouse and rat. *Exp Anim.* 49(4):301-4.
3. Chapin, R.E., Ross, M.D., Lamb, J.C. (1984). Immersion Fixation Methods for Glycol methacrylate embedded Testes. *Toxicol Pathol.* 12(3): 221-227.
4. Cabrera, N.C., Espinoza, J.R., Vargas-Jentzsch, P., Sandoval, P., Ramos, L.A., Aponte P.M. (2017). Alcohol-based solutions for bovine testicular tissue fixation. *Journal of Veterinary Diagnostic Investigation* 29(1) 91–99.
5. Dutta, D., Park, I., Mills, N.C (2012). Fixation Temperature Affects DNA Integrity in the Testis as Measured by the TUNEL Assay. *Toxicologic Pathology*, 40: 667-674.
6. Howroyd, P., Hoyle-Thacker, R., Lyght, O., Williams, D., Kleymenova, E. (2005). Morphology of the Fetal Rat Testis Preserved in Different Fixatives. *Toxicologic Pathology*, 33: 300–304.
7. Creasy, D.M. (2003). Evaluation of Testicular Toxicology: A Synopsis And Discussion Of The Recommendations Proposed by the Society of Toxicologic Pathology. *Birth Defects Research (Part B)* 68:4 08–415.
8. Tu, L., Yu, L., Zhang, H. (2011). Morphology of Rat Testis Preserved in Three Different Fixatives. *J Huazhong Univ Sci Technol [Med Sci]* 31(2):178-180.
9. Lellei, I., Magyar, E., Erdei, E. (2001). Histological Evaluation of Multiple Testicular Biopsies Helping Assisted Reproduction. *Pathol. Res. Pract.* 197: 727–733.
10. Latendresse, J.R., Warbritton, A.R., Jonassen, H., Creasy, D.M. (2002). Fixation of Testes and Eyes Using a Modified Davidson's Fluid: Comparison with Bouin's Fluid and Conventional Davidson's Fluid. *Toxicologic Pathology* 30(4): 524–533.

FIGURES

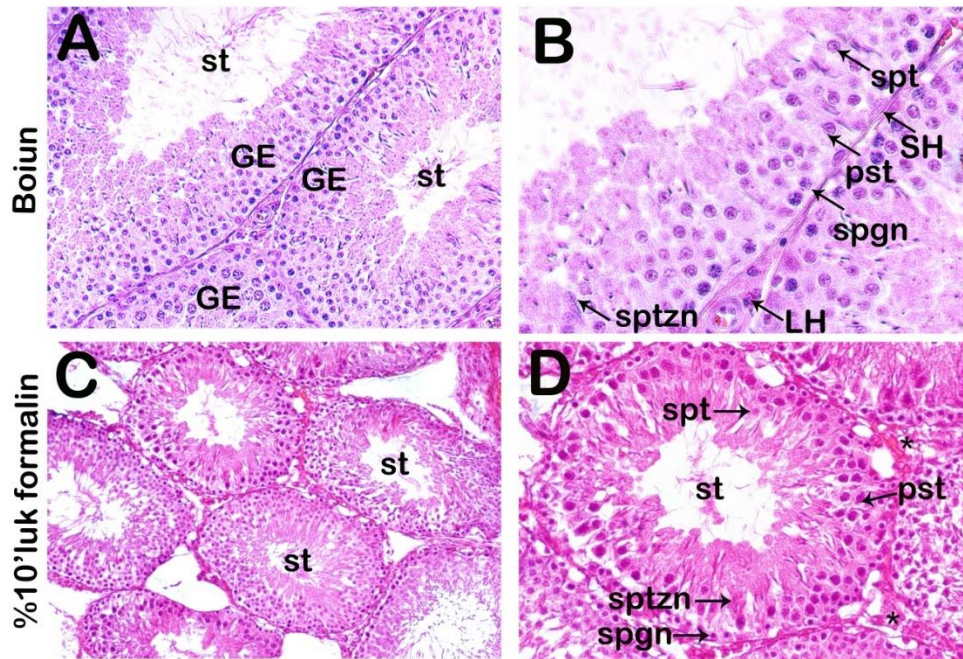


Figure 1. Representative light microscopic pictures of sections of testicular tissue. **A(x20)-B(x40), C(x20)-D(x40):** Seminiferous tubule (st). Germinal Epithelium (GE). Spermatogonia(spgn). Primary spermatocyte (pst), Spermatid (spt), Spermatozoon (sptzn). Sertoli Cell (SH), Leydig Cell (LH).

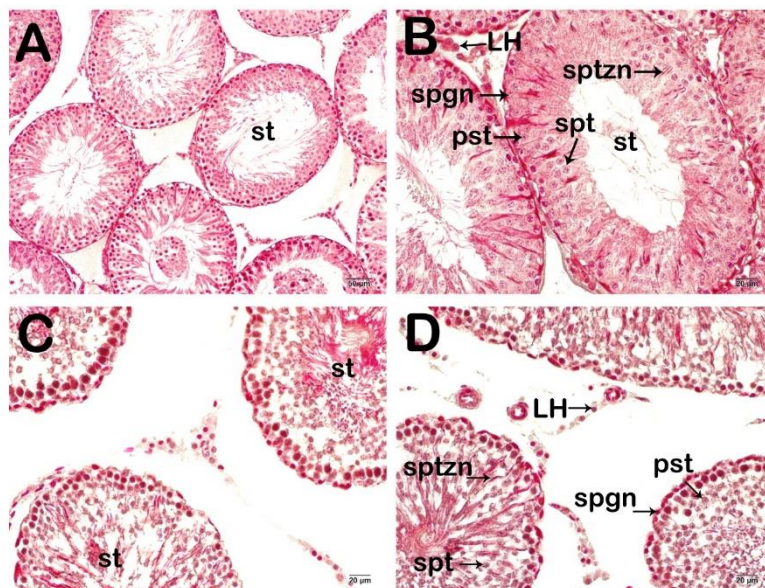


Figure 2. Representative light microscopic pictures of sections of testicular tissue. **A(x20)-B(x40), C(x20)-D(x40):** Seminiferous tubule (st). Germinal Epithelium (GE). Spermatogonia(spgn). Primary spermatocyte (pst), Spermatid (spt), Spermatozoon (sptzn). Sertoli Cell (SH), Leydig Cell (LH).

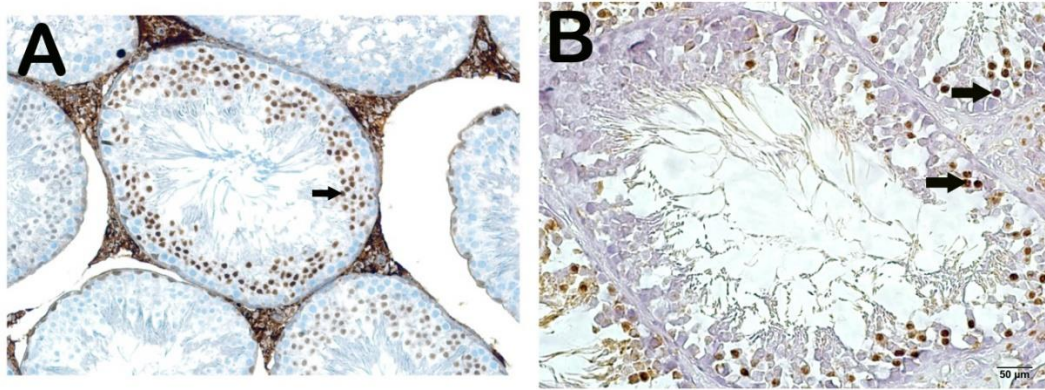


Figure 3. Representative light microscopic image of testicular tissue incubated with Caspase-3 primary antibody.

niche²⁰₂₂

**EPİDİDİMAL BEYAZ YAĞ DOKUSUNUN *IN VİTRO* SPERMATOGENEZ
ÜZERİNE ETKİSİNİN İKİ FARKLI KÜLTÜR PLATFORMUNDA
KARŞILAŞTIRILMASI**

**Oya Elif DALDAL¹, Nilgün YERSAL², Selin ÖNEN^{3,4}, Merve GİZER⁵, Petek
KORKUSUZ⁶**

¹ Hacettepe Üniversitesi Fen Bilimleri Enstitüsü Biyomühendislik Bölümü, Ankara, Türkiye, oedaldal@gmail.com

² Tokat Gaziosmanpaşa Üniversitesi Tıp Fakültesi Histoloji Ve Embriyoloji AbD, Ankara, Türkiye, nilgunyersal@gmail.com

³ Atılım Üniversitesi Sağlık Bilimleri Enstitüsü Tıbbi Biyoloji AbD, Ankara, Türkiye, onenselin@gmail.com

⁴ Hacettepe Üniversitesi Sağlık Bilimleri Enstitüsü Kök Hücre Bilimleri AbD, Ankara, Türkiye, onenselin@gmail.com

⁵ Hacettepe Üniversitesi Sağlık Bilimleri Enstitüsü Kök Hücre Bilimleri AbD, Ankara, Türkiye, gizermerve@gmail.com

⁶ Hacettepe Üniversitesi Tıp Fakültesi Histoloji Ve Embriyoloji, Ankara, Türkiye, petekorkusuz68@gmail.com

Özet: Çocukluk çağı kanser hastalarında uygulanan tedaviler testis germ hücreleri ve mikroçevresine hasar vererek hastaların %46'sının infertil olmasına neden olmaktadır. Epididimal beyaz yağ dokusunun (EBYD) spermatogenez için gerekli olan faktörleri ürettiği ve uzaklaştırıldığında spermatogenezin inhibe olduğu bilinmektedir. Yenidoğan fare testisleri, üç boyutlu hava sıvı interfaz (HSİ) ve U plak (UP) teknikleri ile kültüre edildiğinde EBYD'nin in vitro spermatogenezini destekleyeceği varsayılmıştır. Bu çalışmada EBYD ile desteklenen testislerin in vitro koşullarda UP ve HSİ kültür teknikleri ile kültürü sonucunda spermatogonyal kök hücre (SKH) havuzunun korunması ve sperm elde edilmesi amaçlanmıştır. Üç boyutlu HSİ ve UP teknikleri ile sinjeneik C57BL/6 fare yetişkin EBYD uygulanan yenidoğan testis kültür ve kokültürlerinde EBYD'nin, 1, 3, 4 ve 6. haftalarda in vitro spermatogenezine etkisi histomorfometrik ve immünohistokimyasal olarak değerlendirilmiştir. Seminifer tübül epitel alanı, tüm HSİ kültür platformlarında 3. haftaya kadar artmış ($p=0,0001$) sonra sabit olarak gözlenirken, tüm UP kültür platformlarında 1. haftadan 6. haftaya kadar değişiklik gözlenmemiştir. HSİ tekniğinin UP tekniğiyle karşılaştırıldığında SKH sayısı üzerinde 3. ve 6. haftalarda arttırıcı etkisi olduğu görülmüştür ($p<0,0001$). Epididimal beyaz yağ dokusu, HSİ kokültür platformlarında spermatid sayısını kontrol grubuna göre 3. ($p=0,0006$) ve 4. ($p=0,0203$) haftalarda anlamlı olarak arttırırken UP kokültür platformlarında spermatid sayısını arttırıcı etkisi gözlenmemiştir. Bu çalışma kapsamında EBYD'nin SKH havuzu ve in vitro spermatogenez üzerine HSİ tekniği ile olumlu etkisi ortaya konduğundan, çocukluk çağı kanser hastalarında sperm eldesini sağlayacak üç boyutlu testis organ kültürlerine iyi bir aday olabileceği değerlendirilmiştir.

Anahtar Kelimeler: Erkek İnfertilitesi, Organ Kültürü, In Vitro Spermatogenez

Abstract: Gonadotoxic treatments in childhood cancer patients damage the testicular germ cells and microenvironment, causing 46% of the patients to become infertile. It is known that epididymal white adipose tissue (EWAT) secretes the factors necessary for spermatogenesis and its surgical removal cause inhibition of spermatogenesis. We hypothesized that EWAT would support in vitro spermatogenesis when neonatal mouse testicles were cultured with three-dimensional air-fluid interphase (ALI) and U-plate (UP) techniques. In this study, it was aimed to protect the spermatogonial stem cell (SSC) pool and obtain sperm as a result of the culture of testes supported by EWAT with UP and ALI culture techniques in vitro. The effect of EWAT on in vitro spermatogenesis at 1, 3, 4 and 6 week time points was evaluated histomorphometrically and immunohistochemically in neonatal testicular cultures and cocultures in which syngeneic C57BL/6 mouse adult EWAT was applied with three-dimensional HSI and UP techniques. Seminiferous tubule epithelial area was observed to be constant after increasing ($p=0.0001$) up to 3 weeks in all ALI culture platforms, while no change was observed in UP culture platforms from week 1 to 6. When compared with the UP technique, the ALI technique had an increasing effect on the number of SSCs at the 3rd and 6th weeks ($p<0.0001$). While EWAT significantly increased the spermatid count in ALI coculture platforms at the 3rd ($p=0.0006$) and 4th ($p=0.0203$) weeks compared to the control group, no effect on increasing the spermatid count was observed in the UP coculture platforms. Since this study, showed the positive effect of EWAT on the SSCs and development in in vitro spermatogenesis with the ALI technique, it was evaluated that it could be a good alternative for 3D testicular organ cultures that will provide sperm retrieval in childhood cancer patients.

Keywords: Male Infertility, Organ Culture, In Vitro Spermatogenesis

Giriş

Çocukluk çağı kanser hastalarında uygulanan gonadotoksik tedaviler spermatogonyal kök hücreler ve mikroçevresine hasar vererek infertiliteye neden olmaktadır. İnfertilite vakalarının yaklaşık %50'si erkeklerde görülmekte olup, erkek infertilitesinin %46'sı gonadotoksik kanser tedavisi kaynaklı infertilitedir. Epididimal beyaz yağ dokusunun (EBYD) spermatogenez için gerekli olan endokrin ve parakrin sinyalleri ürettiği ve uzaklaştırıldığında spermatogenezin inhibe olduğu bilinmektedir (1). Yenidoğan fare testisleri, üç boyutlu hücre

kültürü teknikleri, hava sıvı interfaz (HSİ) ve U plak (UP) teknikleri ile kültüre edildiğinde EBYD'nin *in vitro* spermatogenezi destekleyeceği varsayılmıştır.

Yöntem

Üç boyutlu HSİ ve UP teknikleri ile yenidoğan C57BL/6 erkek fare testisleri ve sinjeneik yetişkin EBYD kültüre edilmiştir. Testis örnekleri 1, 3, 4 ve 6. hafta zaman noktalarında toplanarak *in vitro* spermatogenezin ilerlemesi gözlenmiştir. Histomorfometrik inceleme için Periyodik asit-Schiff boyaması yapılmış ve seminifer tübül epitel kalınlığı ile lümen alanı ölçülmüştür. İmmünohistokimyasal yöntem ile SKH belirteci ID4 ve spermatid belirteci Akrozin işaretlemesi yapılmış ve sayıları zamansal olarak değerlendirilmiştir.

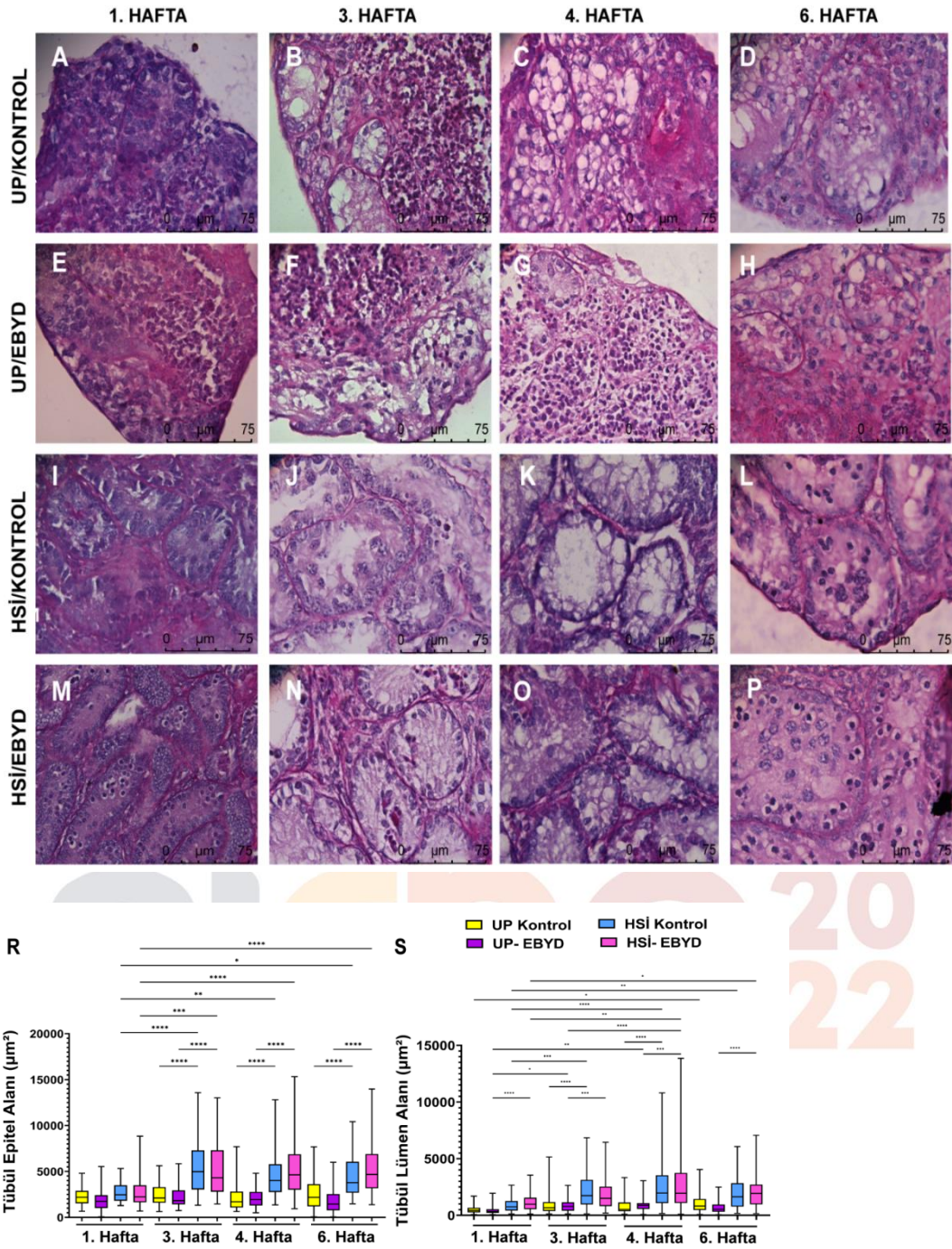
Hayvan deneyleri, Hacettepe Üniversitesi Hayvan Deneyleri Yerel Etik Kurulu'nun 23.09.2020 tarihli ve 52338575-128 sayılı izniyle gerçekleştirilmiştir.

Bu çalışma, Hacettepe Üniversitesi Bilimsel Araştırma Projeleri Koordinasyon Birimi, TSA-2021-18974 no'lu Kapsamlı Araştırma Projesi desteğiyle gerçekleştirilmiştir.

Bulgular

Yetişkin 2 aylık C57BL/6 erkek farelerden sinjeneik EBYD ve prepubertal 6 günlük erkek farelerden testis parçaları HSİ ve UP sistemlerinde 6 hafta kültüre edilmiştir.

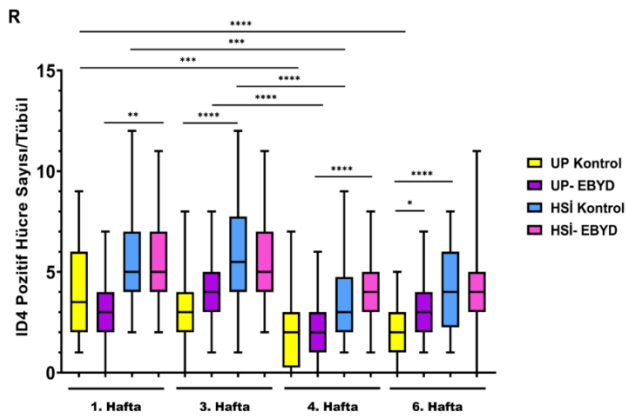
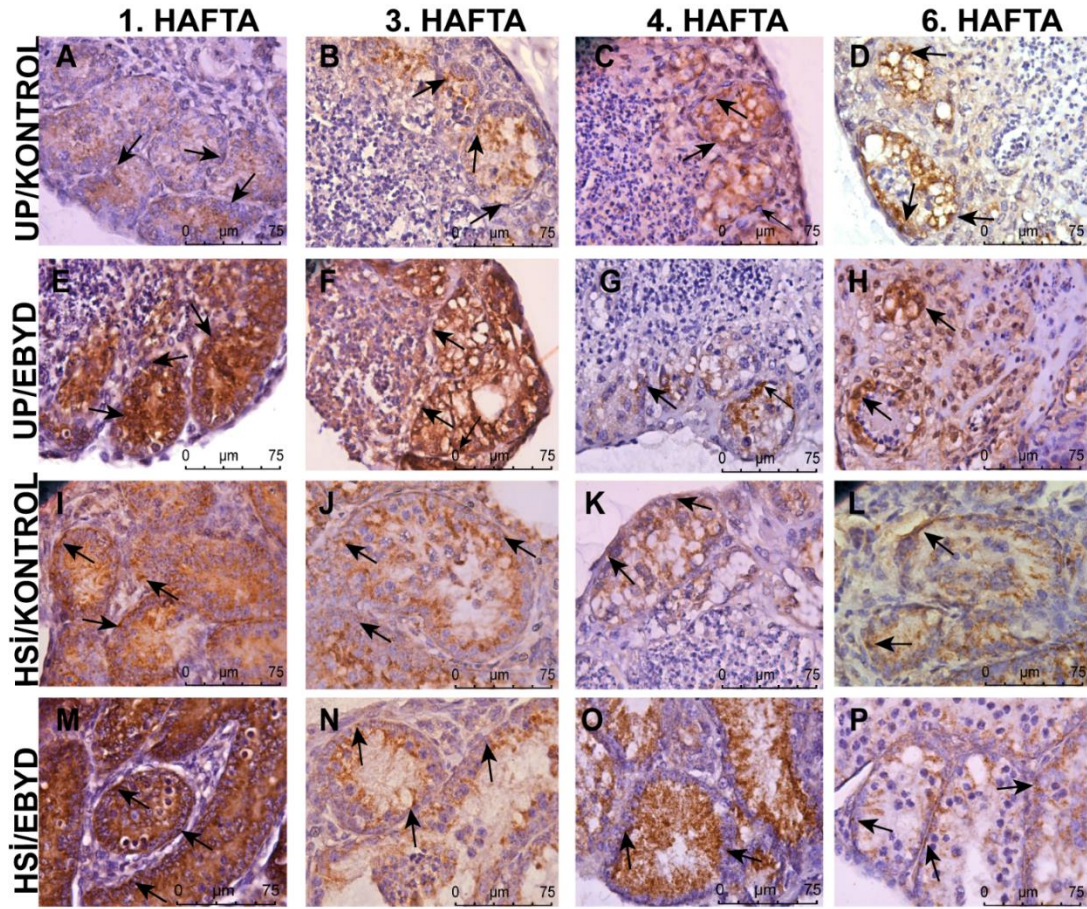
Hava sıvı interfaz kültür ve kokültür platformunda seminifer tübül epitel alanı 3. haftaya kadar artmış ($p=0,0001$) sonra sabit olarak gözlenirken, UP kültür ve kokültür platformlarında 1. haftadan 6. haftaya kadar değişiklik gözlenmemiştir. Bir ($p<0,0001$), üç ($p=0,0009$), dört ($p=0,0001$) ve altıncı ($p<0,0001$) haftalarda EBYD uygulanan HSİ kokültür platformunda seminifer tübül lümen alanı EBYD uygulanan UP kokültür platformuna göre anlamlı olarak artmıştır (Şekil 1).



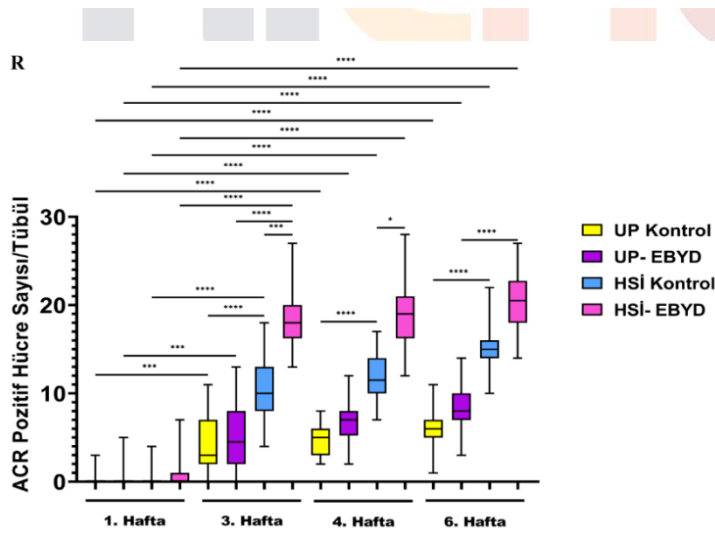
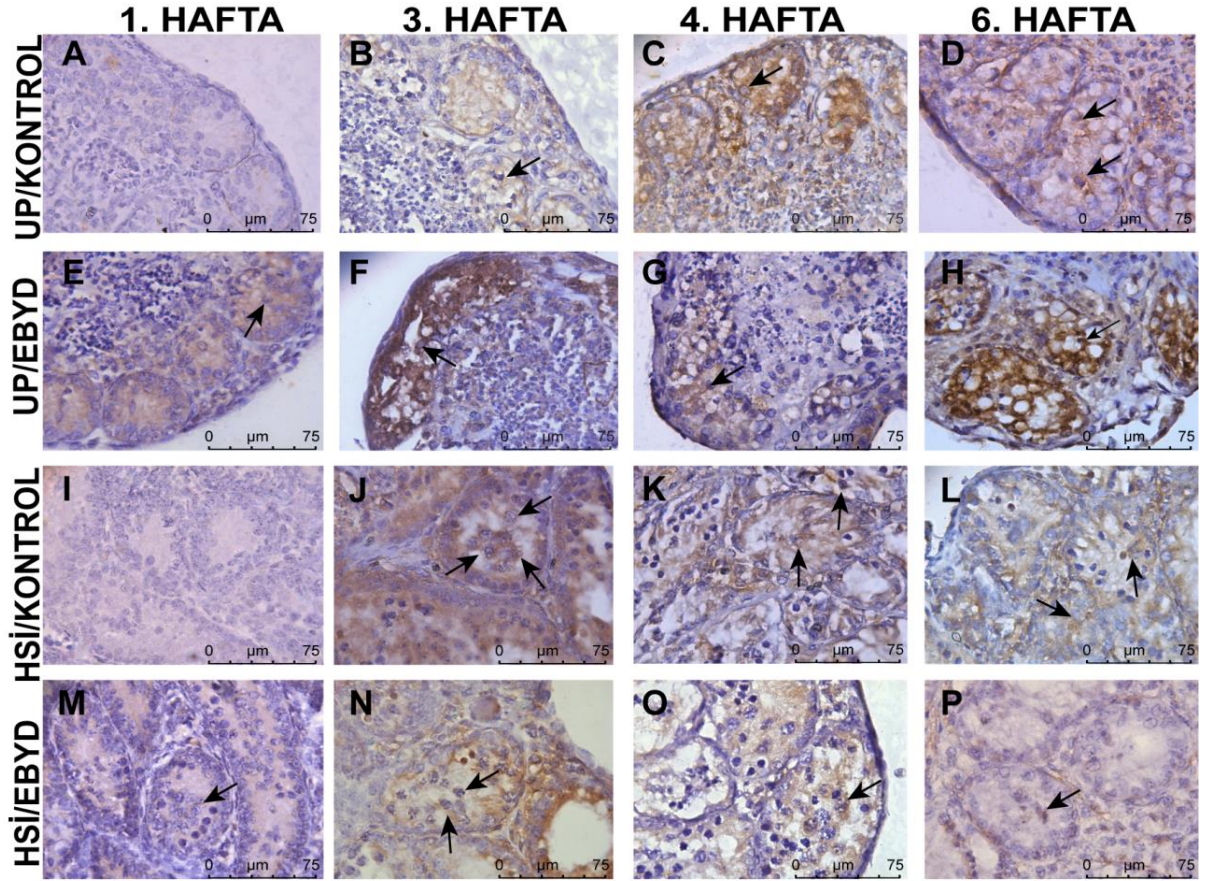
Şekil 1: Testis-EBYD kültür platformlarına ait mikrograflardır (A-P), PAS, x630.

Epididimal beyaz yağ dokusu, HSI kültür platformu ile uygulandığında ID4(+) SKH sayısını 6 hafta süreyle sabit tutmuş ve SKH havuzunu korumada katkı sağlamıştır. Epididimal beyaz yağ dokusu içeren HSI kültür platformu dışındaki tüm gruplarda ID4(+) SKH sayısı 4. haftada azalmış ve daha sonra sabit kalmıştır ($p < 0,0001$, Şekil 2). Tüm kültür ve kokültür platformlarında 1. haftadan 3. haftaya kadar olan ACR(+) spermatid sayıları artmış,

spermatogenez süreci SKH'lerden yuvarlak spermatid oluşumuna kadar ilerlemiştir. Epididimal beyaz yağ dokusu ile kültüre edilen testis parçaları, HSi kokültür platformu ile desteklendiğinde 3. ($p=0,0006$) ve 4. ($p=0,0203$) haftalarda ACR(+) spermatid sayısını kontrole göre arttırmıştır. Hava sıvı interfaz kültür platformunda, ACR(+) yuvarlak spermatid sayısının 3, 4 ve 6. haftalarda UP kültür platformuna göre daha fazla olduğu görülmüştür (Şekil 3).



Şekil 2: Testis-EBYD kokültür platformlarına ait mikrograflardır. ID4 ile immün işaretli SKH'ler ok ile gösterilmektedir (A-P), x630.



Şekil 3: Testis-EBYD kokültür platformlarına ait mikrograflardır. ACR ile immün işaretli spermatidler ok ile gösterilmektedir (A-P), x630.

Tartışma

Standart yöntem olarak kabul edilen agaroz temelli HSİ kültür platformu ile fare testisleri 1 mm³ boyutlarına getirilerek en az 42 gün kültüre edilmiştir (2-4). Bu süre farelerdeki bir spermatogenez döngüsünü kapsamaktadır.

Testis organoid kültürü için kullanılan UP kültür platformu (5) ile bu çalışmada literatürde ilk kez organ kültürü yapılmıştır. Seminifer tübül epitel alanının tübül lümen alanı ile birlikte artması, sertoli hücrelerinin olgunlaşması ile ilişkilendirilerek spermatogenezdeki ilerlemenin bir göstergesi olarak kabul edilmektedir (1, 6). ID4(+) SKH sayısının EBYD içeren HSİ kültür grubu dışında 4. haftada azalmış olması ID4'ün *A_{single}* spermatogonyaları işaretlemesi dolayısıyla daha seçici olmasıyla açıklanabilir (7, 8). İlk gözlem noktasından (1. hafta) itibaren ID4(+) SKH; 3. haftadan itibaren ACR(+) spermatidlerin görülmesi faredeki *in vivo* spermatogenezin zaman akışı ile uyumludur (9). Epididimal beyaz yağ dokusunun özellikle HSİ kültür platformlarında, 3. ve 4. haftalarda ACR(+) yuvarlak spermatid sayısını kontrole göre arttırmış olması organ kültüründe testis ve EBYD'nin fonksiyonel özelliklerinin HSİ kültür sisteminde UP kültür sistemine göre daha etkin sürdürüldüğünü ve postmayotik hücrelerin oluşumunda etkin rol oynadığı göstermiştir (10).

In vitro spermatogenez ile yuvarlak spermatidler tüm kültür platformlarında elde edilmiş olmakla birlikte elde edilen spermatidlerin genetik stabiliteleri ve fonksiyonel özellikleri test edilmelidir. Deney düzeneğinde spermatogenezini sağlayacak olan, başta testosteron olmak üzere, hormonlara ait inceleme yapılmamıştır. Diğer yandan 3. haftadan itibaren tüm deney gruplarında ACR(+) yuvarlak spermatidlerin görülmesi testosteron salgılandığının açık göstergesi olarak değerlendirilebilir.

Sonuç

Bu çalışma kapsamında tüm kültür platformlarında *in vitro* spermatogenez yuvarlak spermatid aşamasına kadar tamamlanmıştır. Germ hücre farklılaşması ve SKH havuzunun korunması bakımından karşılaştırıldığında EBYD ile desteklenen HSİ tekniğinin UP tekniğine göre daha başarılı olduğu, EBYD'nin seminifer tübüllerdeki SKH havuzunu 6 hafta süre ile koruduğu görülmüştür. Epididimal beyaz yağ dokusunun SKH havuzu ve *in vitro* spermatogenez üzerine HSİ tekniği ile olumlu etkisi ortaya konduğundan, çocukluk çağı kanser hastalarında sperm eldesini sağlayacak üç boyutlu testis organ kültürlerine iyi bir aday olabileceği saptanmıştır.

Kaynakça

1. Chu Y, Huddleston GG, Clancy AN, Harris RB, Bartness TJ. Epididymal fat is necessary for spermatogenesis, but not testosterone production or copulatory behavior. *Endocrinology*. 2010;151(12):5669-79.
2. Yokonishi T, Sato T, Komeya M, Katagiri K, Kubota Y, Nakabayashi K, et al. Offspring production with sperm grown in vitro from cryopreserved testis tissues. *Nat Commun*. 2014;5:4320.
3. Sato T, Katagiri K, Gohbara A, Inoue K, Ogonuki N, Ogura A, et al. In vitro production of functional sperm in cultured neonatal mouse testes. *Nature*. 2011;471(7339):504-7.
4. Komeya M, Kimura H, Nakamura H, Yokonishi T, Sato T, Kojima K, et al. Long-term ex vivo maintenance of testis tissues producing fertile sperm in a microfluidic device. *Sci Rep*. 2016;6:21472.
5. Pendergraft SS, Sadri-Ardekani H, Atala A, Bishop CE. Three-dimensional testicular organoid: a novel tool for the study of human spermatogenesis and gonadotoxicity in vitro. *Biol Reprod*. 2017;96(3):720-32.
6. Olawuyi TS, Ukwenya VO, Jimoh AGA, Akinola KB. Histomorphometric evaluation of seminiferous tubules and stereological assessment of germ cells in testes following administration of aqueous leaf-extract of *Lawsonia inermis* on aluminium-induced oxidative stress in adult Wistar rats. *JBRA Assist Reprod*. 2019;23(1):24-32.
7. Gholami K, Vermeulen M, Del Vento F, de Michele F, Giudice MG, Wyns C. The air-liquid interface culture of the mechanically isolated seminiferous tubules embedded in agarose or alginate improves in vitro spermatogenesis at the expense of attenuating their integrity. *In Vitro Cell Dev Biol Anim*. 2020;56(3):261-70.
8. Komeya M, Yamanaka H, Sanjo H, Yao M, Nakamura H, Kimura H, et al. In vitro spermatogenesis in two-dimensionally spread mouse testis tissues. *Reprod Med Biol*. 2019;18(4):362-9.
9. Margolin G, Khil PP, Kim J, Bellani MA, Camerini-Otero RD. Integrated transcriptome analysis of mouse spermatogenesis. *BMC Genomics*. 2014;15:39.
10. Reda A, Hou M, Winton TR, Chapin RE, Söder O, Stukenborg JB. In vitro differentiation of rat spermatogonia into round spermatids in tissue culture. *Mol Hum Reprod*. 2016;22(9):601-12.



ARE TESTICULAR STROMAL CELLS A VALUABLE RESOURCE THAT HAS BEEN OVERLOOKED UNTIL NOW?

Faruk ALTINBAŞAK^{1,2}, Gül YILDIRIM³, Murat Serkant ÜNAL⁴

¹Hitit University, Faculty of Medicine Department of Histology and Embryology, Corum, Turkey,
farukaltinbasak7@gmail.com

²Pamukkale University, Institute of Health Sciences Department of Histology and Embryology, Denizli, Turkey,
farukaltinbasak7@gmail.com

³Pamukkale University, Institute of Health Sciences Department of Stem Cells, Denizli, Turkey,
gulyldrmmm06@gmail.com

⁴Pamukkale University, Faculty of Medicine Department of Histology and Embryology, Denizli, Turkey,
serkantunal72@gmail.com

Abstract: Azoospermia, which is seen in 10-15% of male infertility today and constitutes 1% of the total male population, is the absence of sperm in the ejaculated semen. Mesenchymal stem cells are stromal-derived adult stem cells and multipotent. Having these properties makes them suitable for cell therapies. This study was carried out to isolate testicular stromal cells obtained from rats, to reproduce and characterize them in a culture medium. Testicular stromal cells (TSC) were isolated from the testis of two Wistar Albino rats and characterized with both morphologically and flow cytometry analysis by looking at mesenchymal stem cell markers. The findings showed that TSCs morphologically resemble fibroblasts and positive for mesenchymal stem cell markers CD54 and CD90 but negative for CD29. In addition to these findings, they expressed the hematopoietic stem cell marker CD45. In conclusion, testicular sperm extraction (TESE) material which is cryopreserved for infertility treatment or fertility preservation before anti-tumor treatment is a valuable source for spermatogonial stem cells and testicular stromal cells as well as spermatozoa. However spermatogonial stem cells and testicular stromal cells are not used in routine infertility treatment. Further research on these cells may bring different perspectives to the treatment of male infertility.

Keywords: Testis, Testicular Stromal Cells, Azoospermia, Male Infertility

1) Introduction

Infertility has recently become a global concern like well known as important global problems air pollution, climate change, and extinction of species. This disease, which can be caused by unhealthy nutrition as well as many genetic factors, can negatively affect the physical, psychological, and social life of the person (1).

Azoospermia, which is found in approximately 1% of the male population and 10-15% of patients with male infertility, is the absence of any sperm in the semen (2). The fact that azoospermia is a serious problem for male individuals causes research to focus on this issue.

Although surgical and hormonal treatments are generally more commonly used treatment methods, recent research in the field of stem cells has provided a new source of hope for infertility (3).

Mesenchymal stem cells (MSCs) are a heterogeneous cell population of stromal origin with self-renewal and differentiation potential, and these cells are morphologically similar to fibroblasts (4). A large number of bioactive molecules secreted by MSCs exert autocrine/paracrine effects that modulate the physiological processes of MSCs. The main reason why stromal cells are preferred as a treatment method is that they have these properties. MSCs are isolated from many tissues such as adipose tissue, bone marrow, cartilage, teeth, placenta, and amniotic membrane (5). MSCs have been quite difficult to identify because they have a heterogeneous population. That's why the International Society for Cellular Therapy (ISCT) has proposed 3 criteria for defining MSCs. These are;

1. Cells should adhere to plastic when maintained in standard culture conditions.
2. While MSCs express surface molecules such as CD105, CD90, and CD73, they should not express surface molecules such as CD14, CD19, CD34, and CD45.
3. Must have the capacity to differentiate into adipocytes, chondroblasts, and osteoblasts in vitro (6).

The testis is an organ located outside the body cavity and located within the scrotum. Testis consists of seminiferous tubules and interstitium (7). The seminiferous tubules contain spermatogenic stem cells that divide continuously to produce germ cells and Sertoli cells that support these stem cells, while the interstitium contains Leydig cells, peritubular myoid cells, macrophages, and vascular structures. At the stage of spermatogenesis, spermatogenic stem cells divide, mature, and differentiate into sperm in the seminiferous tubules (8).

Leydig cells regulate the functions of spermatogonial stem cells (SSC) by secreting insulin growth factor (IGF1) and colony-stimulating factor1 (CSF1). Macrophages provide proliferation (proliferation) and differentiation (differentiation) of SSC by secreting CSF1 and retinoic acid (RA). Vascular structures with secretions of CSF1 and endothelial growth factor (VEGF); peritubular myoid cells are effective in the self-renewal and proliferation of SSC with their secretion of neurotrophic factor (GDNF) and CSF1 originating from the glial cell line. Seminiferous tubule cells in the niche of the SSC contribute as intrinsic factors, while interstitium cells outside the niche play important roles for regulating the functions of the SSC as extrinsic factors (8).

This study was conducted to isolate and characterize testicular stromal cells in in vitro culture.

2) Materials and Methods

2.1) Animals

In our study, a total of 2 healthy, 20-day-old male Wistar Albino-type rats were used. During the experiment, rats were housed in separate cages in a quiet room, on a 12-hour light-dark cycle, with controlled ambient temperature (21 ± 3 °C) and ventilation (65-70%). The experimental animals were fed with pellet feed containing 21% protein and tap water as ad libitum. All animal procedures were approved by Pamukkale University Animal Experiments Ethics Committee.

2.2) Isolation of Testicular Stromal Cells

The testicles of 2 male Wistar Albino rats were excised. Removed testes were washed in Phosphate Buffered Saline (PBS) solution and washed in centrifuge tubes containing Dulbecco's Modified Eagle's Medium (DMEM), Fetal Bovine Serum (FBS), Penicillin-Streptomycin and brought to the laboratory under sterile conditions.

Testicular tissues were cut into the smallest pieces that could be separated in a petri dish containing the medium (DMEM; 50 U/ml penicillin, 50 µg/mL streptomycin, 10% FBS) with the help of pre-sterilized tissue scissors. 12 ml of DMEM was added to the testicular tissues, which were cut into small pieces, and placed in an incubator at 5% humidity and 37°C. At the end of the 12th day, the cells that became confluent (70-80%), were trypsinized (containing 0.25% trypsin) and the cells that adhered to the surface of the containers were removed. These cells were seeded in different flasks and their proliferation was examined by repeated passages.

2.3) Flow Cytometry Analysis of TSCs

Mesenchymal stem cell markers (CD29, CD54 and CD90) and hematopoietic surface markers (CD45) were used to identify undifferentiated TSCs by using Sysmex Cube 8 Model Flow cytometry device.

3) Results

3.1) TSC'lerin Kültürü

3.1) Culture of TSCs

In the examination performed with phase-contrast microscopy, it was observed that TSCs adhered to the culture dishes and their morphological appearance was similar to fibroblasts (Figure 1A and 1B).

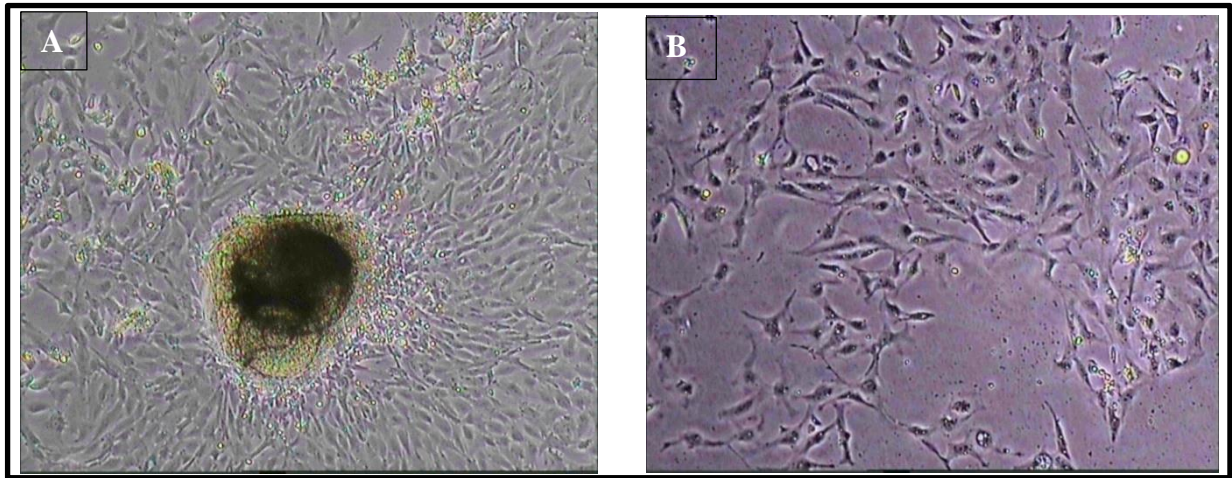


Figure 1) Morphology of TSCs produced from rat testis. A) TSCs migrating from testicular tissue. B) TSCs have a fibroblast-like morphology and appear adherent to flasks.

3.2) Flow Cytometry Results

In flow cytometry analysis, cells expressed CD54 and CD90, which are mesenchymal stem cell markers, but did not express CD29; It was determined that they expressed CD45, which is a hematopoietic stem cell marker.

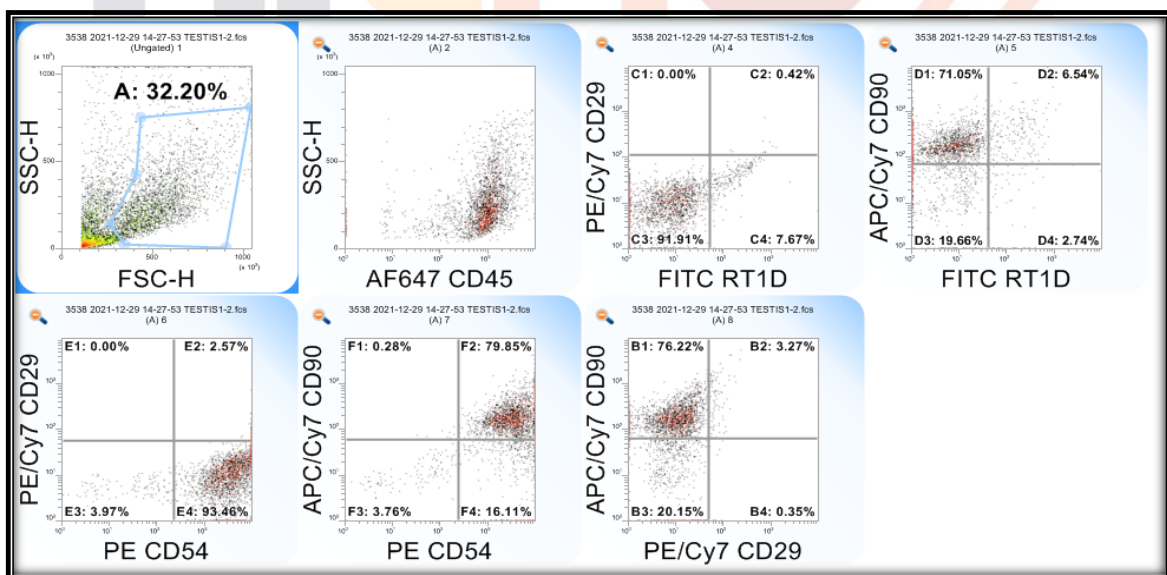


Figure 2) In TSCs with flow cytometry analysis; While it expressed CD54 and CD90, which are mesenchymal stem cell markers, it did not express CD29. It also expressed CD45, a hematopoietic stem cell marker, contrary to expectations.

4) Discussion

Infertility is a reproductive disorder which occur along with many diseases and affects the patient by psychologically, physically, socially, and economically. Azoospermia, one of these reproductive disorders, is defined as the absence of spermatozoa in the ejaculate and is found in approximately 10-20% of infertile men (9). Recent studies, especially in the field of stem cells, have become a new alternative method for the treatment of individuals with azoospermia (10). MSCs are a collection of self-renewing, multipotent, fibroblast-like stromal-derived adult stem cells. The fact that MSCs have both paracrine/autocrine effects and high differentiation capacity has been the biggest indicator of why they are a source of hope for infertility (11). The recent studies aimed to characterize the proliferation, expansion, and differentiation potentials of TSCs produced from different organisms in vitro to use TSCs in the pre-clinical setting (12).

In 2008, Kim et al. established a CD34 positive cell line called JK1, which they produced from mouse testicular stromal cells by the explant method. They reported that JK1 cells adhered to the culture dishes in their phase-contrast appearance and expressed CD34 in the flow cytometry analysis (13).

Ahmed et al. for the first time, they aimed to isolate testicular mesenchymal stromal cells (tMSC) produced from the testis from a mouse model by enzymatic method. They showed that the morphological structures of the tMSCs they produced were similar to fibroblasts and they expressed positive for CD44, CD73, and CD29 and negative for CD45 in the flow cytometry analysis (14).

Gonzalez et al. claimed that they isolated cells called gonadal stem cells (GSC) with mesenchymal stem cell (MSC) characteristics from the adult human testis. They showed that the enzymatically cultured GSCs had the same morphology as MSCs and that expression was positive for CD105, CD73, CD166, and negative for CD11b, CD19, CD34, CD45, and HLA-DR. They also reported that CD44, CD90, and STRO-1, which are expressed in MSCs, are expressed at high levels (15).

In 2014, Smith et al. identified a population of human testicular Thy1 cells containing MSCs. They showed that the cells cultured by the explant method adhere to the plastic and express mesenchymal markers such as CD105 and CD73, but not CD45 (16).

Chiara et al. aimed to show that the cell colonies isolated from human testicular biopsies are not derived from spermatogonial stem cells, on the contrary, are of mesenchymal origin. They

reported that these cells, which were analyzed by flow cytometry, were positive for CD73, CD90, and C105, and expression of CD14, CD34, and HLA-DR markers was negative (17).

As a result of the characterization of the testicular stromal cells isolated from the testicles of different experimental animals in the studies, it was stated that these cells were of mesenchymal character. When we looked at the flow cytometry analyzes, we observed that these cells were testicular stromal cells with mesenchymal characteristics. In the literature, there is different information about the characterization of testicular stromal cells and the markers used.

5) Conclusions

Cryopreservation of the cell suspension or testicular tissue pieces is preferred to preserve fertilization in patients who will undergo orchiectomy for a testicular tumor or any other reason. Then, by thawing these materials, the cryoprotectants are removed and the sperms can be used. In TESE (Testicular sperm extraction) operations, sperm are searched in the seminiferous tubules, ICSI (intracytoplasmic sperm injection) is performed when found, and the rest unused mature germ cells are frozen. However, valuable resources such as SSSs and TSCs, which are known to be in the TESE material, are not used. The fact that these cells are also frozen and using them later may bring different perspectives to research on the treatment of azoospermia patients, which is an important cause of male infertility.

6) References

- 1) Wu, J.X., Xia, T., She, L.P., Lin S., Luo, X.M. (2022). Stem Cell Therapies for Human Infertility: Advantages and Challenges, Cell Transplantation Volume 31: 1 –14.
- 2) Ünal, M.S., Özer M.C. (2019). Nonobstrüktif Azospermi Olgularında Yeni Yaklaşımlar, Med J SDU / SDÜ Tıp Fak Derg: 26(1):111-116
- 3) Baker, K., Sabanegh E. (2013). Obstructive Azoospermia: Reconstructive Techniques and Results. Clinics, 68(S1):61-73
- 4) Kadam, P., Saen, D.V., Goossens, E. (2017). Can Mesenchymal Stem Cells Improve Spermatogonial Stem Cell Transplantation Efficiency?, Andrology, 5, 2–9.
- 5) Rastegar, F., Shenaq, D., Huang, J., et al. (2010). Mesenchymal Stem Cells: Molecular Characteristics and Clinical Applications, World J Stem Cells 26; 2(4): 67-80.
- 6) Dominici, M., Blanc, K.L., Mueller, I., et al. (2006). Minimal Criteria for Defining Multipotent Mesenchymal Stromal Cells. The International Society For Cellular Therapy Position Statement, Cytotherapy; 8(4):315-7.
- 7) Ross, M.H, Pawlina W. (2001). *Histology: A Text and Atlas, with Correlated Cell and Molecular Biology*, Fifth Edition, Philadelphia, Lippincott Williams & Wilkins Wolters Kluwer Health, Inc.
- 8) Potter, S.J., DeFalco, T., (2017). Role of The Testis Interstitial Compartment in Spermatogonial Stem Cell Function, Reproduction; 153(4): R151–R162.
- 9) Altınbasak, F., Boz, İ. (2021). Mezenkimal Kök Hücrelerin Deneysel Azospermi Modellerinde Tedavi Edici Etkiler, 4th International Health Sciences and Life Congress, Full Text Book-2, (pp. 556-561), Burdur: University of Burdur Mehmet Akif Ersoy
- 10) Chang, Z., Zhu, H., Zhou, X., et al. (2021). Mesenchymal Stem Cells in Preclinical Infertility Cytotherapy: A Retrospective Review, Stem Cells International, 12 pages.
- 11) Qian, X.X., Liu, Y., Wang, H., Qi, N.M. (2020). Mesenchymal Stem Cells for the Treatment of Male Infertility, Zhonghua Nan Ke Xue;26(6):564-569.
- 12) Ghabriel, M., Amleh, A. (2019). The Testis: An Accessible Mesenchymal Stem Cells Source, Advances in Modern Oncology Research, 196.

- 13) Kim, J., Seandel, M., Falcatori, I., Wen, D., Rafii, S. (2008). CD34+ Testicular Stromal Cells Support Long-Term Expansion of Embryonic and Adult Stem and Progenitor Cells, *Stem Cells*; 26(10): 2516–2522.
- 14) Ahmed, M., Ghabriel, M., Amleh, A. (2017). Enrichment, Propagation, and Characterization of Mouse Testis-Derived Mesenchymal Stromal Cells, *Cellular Reprogramming*, Volume 19, Number 1.
- 15) Gonzalez, R., Griparic, L., Vargas, V., et al. (2009). A Putative Mesenchymal Stem Cells Population Isolated From Adult Human Testes, *Biochem Biophys Res Commun*;385(4):570-5.
- 16) Smith, J.F., Yango, P., Altman, E., et al. (2014). Testicular Niche Required for Human Spermatogonial Stem Cell Expansion, *Stem Cells Translational Medicine*; 3:1043–1054
- 17) Chiara, L.D., Famulari, E.S., Fagoonee, S., et al. (2018). Characterization of Human Mesenchymal Stem Cells Isolated from the Testis, *Stem Cells International*, 9 Pages.



TAKROLİMUS NEFROTOKSİSİTESİNİN DEĞERLENDİRMESİ İÇİN ÜÇ BOYUTLU BÖBREK PROKSİMAL TÜBÜL MODELİNİN GELİŞTİRİLMESİ

Nazlıhan GÜRBÜZ¹, Sefa Burak ÇAM², Fahriye Şeyda GÖKYER³, Pınar YILGÖR
HURİ³, Petek KORKUSUZ²

1. Hacettepe Üniversitesi, Fen Bilimleri Enstitüsü, Biyomühendislik Anabilim Dalı, 06800, Ankara, Türkiye,
nazlihan.gurbuz@hacettepe.edu.tr

2. Hacettepe Üniversitesi, Tıp Fakültesi, Histoloji ve Embriyoloji Anabilim Dalı, 06100, Ankara, Türkiye

3. Ankara Üniversitesi, Mühendislik Fakültesi, Biyomedikal Mühendisliği Bölümü, 06830, Ankara, Türkiye

Özet: Pek çok kanserojen madde, toksik çevresel ajan ve ilaçlara maruziyet nefrotoksisiteye neden olmaktadır. Klinikte kullanılan bir ilaç olan takrolimus, organ transplantasyonu sonrası allogreft reddini önemli derecede azaltmasına karşın, nefrotoksik etkileri klinik kullanımını zorlaştırmaktadır. Böbreğin işlevsel birimi olan nefronların toksik maddelere ilk önce maruz kalan ve duyarlı kısmı, çok sayıda mitokondriyona sahip ve özelleşmiş hücrelerden oluşan proksimal tübüldür. Proksimal tübül epitelinin özelleşmiş polarize yapısının in vitro iki boyutlu kültür yöntemlerinde modellenememesi ve in vivo çalışmalarda türe özgü farklılıklar nedeniyle üç boyutlu modellere ihtiyaç duyulmaktadır. Bu çalışmada üç boyutlu baskı ve döküm teknikleri ile in vitro koşullarda takrolimus nefrotoksisitesinin değerlendirilmesi için perfüze edilebilen bir insan proksimal tübül modeli oluşturulabileceği varsayılmıştır. Üç boyutlu proksimal tübül modelinin oluşturulması için üç boyutlu baskı yöntemi ile kalıp üretimi yapılmış ve kanalı çevreleyecek ekstrasellüler matriks için jelatin metakrilat kullanılarak döküm tekniği ile kanal oluşturulmuştur. Takrolimusun etkin dozunun belirlenmesi için insan kaynaklı böbrek proksimal tübül epitel hücrelerine (HK-2) 0.1, 1, 10, 100, 1000 µg/ml konsantrasyonlarda takrolimus uygulanıp gerçek zamanlı impedans temelli sitotoksisite analizi ile değerlendirilmiştir. Oluşturulan üç boyutlu proksimal tübül modelinde tutunmuş hücreler faz kontrast mikroskobu ile görüntülenmiştir. Gerçek zamanlı sitotoksisite analizinin sonucunda takrolimusun HK-2 hücreleri üzerindeki etkin dozu 48. saatte 44,69 µg/ml olarak bulunmuştur ($R^2= 0.98483$). Takrolimus, 48. saatte 0.1, 1, 10, 100, 1000 µg/ml konsantrasyonlarda kontrol grubuna göre anlamlı olarak hücre indeksini azaltmıştır (sırasıyla $p= 0.0043$, $p=0.0006$, $p<0.0001$, $p<0.0001$, $p<0.0001$). Takrolimusun proksimal tübül hücrelerindeki toksik dozu gerçek zamanlı olarak belirlenmiştir. Üç boyutlu mikrofizyolojik koşulları modelleyen bir kanal tasarlanmıştır.

Anahtar Kelimeler: Böbrek, Proksimal Tübül, Nefrotoksisite, Takrolimus, Üç Boyutlu Kültür

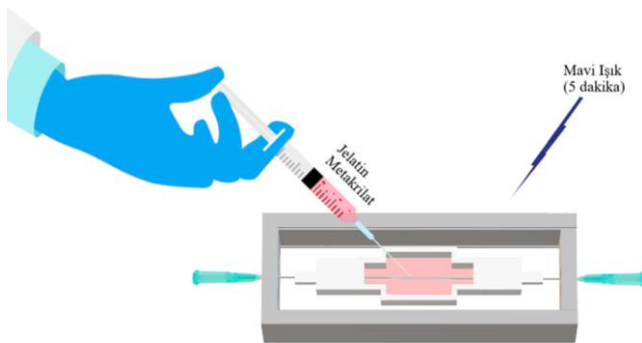
Giriş

Antibiyotikler ve antiviral ilaçlar, immünsüpresif ilaçlar, çeşitli çevresel kirletici ve ağır metal etken maddelerine akut veya kronik maruziyet nefrotoksisiteye yol açmaktadır. Akut takrolimus nefrotoksisitesi organ transplantasyonu sonrası immünsüpresif tedavisinde sıkça karşılaşılmakta ve klinik kullanımı zorlaştırmaktadır (1). Primer olarak proksimal tübül epitelini hedefleyen nefrotoksisitenin modellenmesinde iki boyutlu *in vitro* modeller mikro çevre, polarite, hücre-hücre etkileşimleri ve tübüler ultrafiltrat akışını sağlayamamakta bu nedenle üç boyutlu gerçekçi modellere ihtiyaç duyulmaktadır. Üç boyutlu baskı ve döküm teknikleri ile *in vitro* koşullarda takrolimus nefrotoksisitesinin değerlendirilmesi için perfüze edilebilen bir insan proksimal tübül modeli oluşturulabileceği varsayılmıştır.

Gereç ve Yöntem

Takrolimusun etkin dozunun belirlenmesi için, geniş doz aralığında (0.1, 1, 10, 100, 1000 µg/ml) takrolimus, insan kaynaklı proksimal tübül epitel hücrelerine (HK-2) uygulanmış, gerçek zamanlı impedans temelli sitotoksisite analizi ile değerlendirilmiştir. İlacın doz bağımlı gerçek zamanlı etki penceresi değerlendirilerek zaman bağımlı yarı-maksimum inhibitör konsantrasyonu (ID50) belirlenmiştir(2).

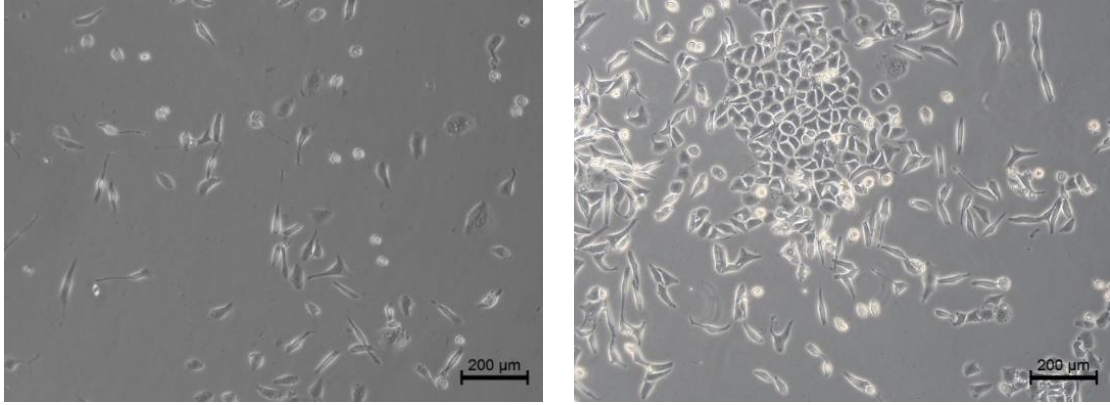
Üç boyutlu proksimal tübül modelinin oluşturulması için üç boyutlu baskı yöntemi ile kalıp üretimi yapılmış, kalıbın içerisinde enjektör uçları karşılıklı olarak birbiri içerisine geçirilmiştir. Kanalı çevreleyecek ekstrasellüler matriks için jelatin metakrilat(%16,5), kalıba dökülüp mavi ışık ile çapraz bağlanması tamamlandıktan sonra enjektör ucunun geri çekilmesi ile kanal oluşturulmuştur(Şekil1).



Şekil 1: Kanal üretiminin şematik çizimi Paint 3D uygulaması ile çizilmiştir.

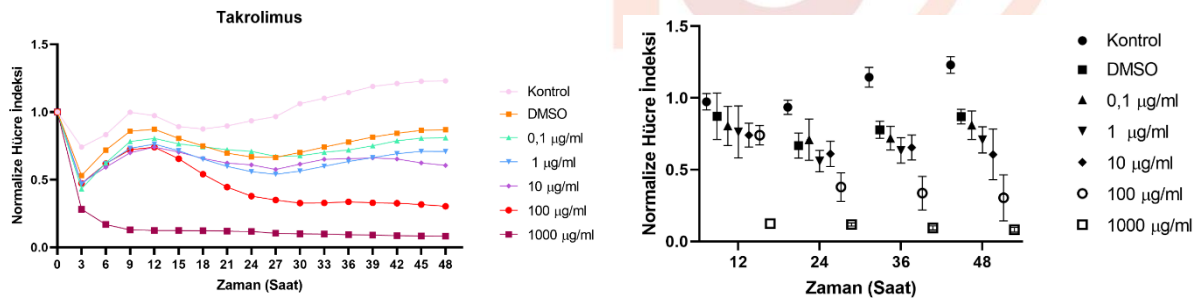
Bulgular

İnsan kaynaklı böbrek proksimal tübül epitel hücreleri kültür koşullarında uygun şekilde çoğaltılmış, invertte faz kontrast mikroskobu ile görüntülenmiştir. Hücrelerin ikinci ve altıncı gününe ait mikrografları elde edilmiş ve kültürün altıncı gününde karakteristik kaldırım taşı benzeri görünümde tutunarak gruplar yaptıkları gösterilmiştir (Şekil 2).



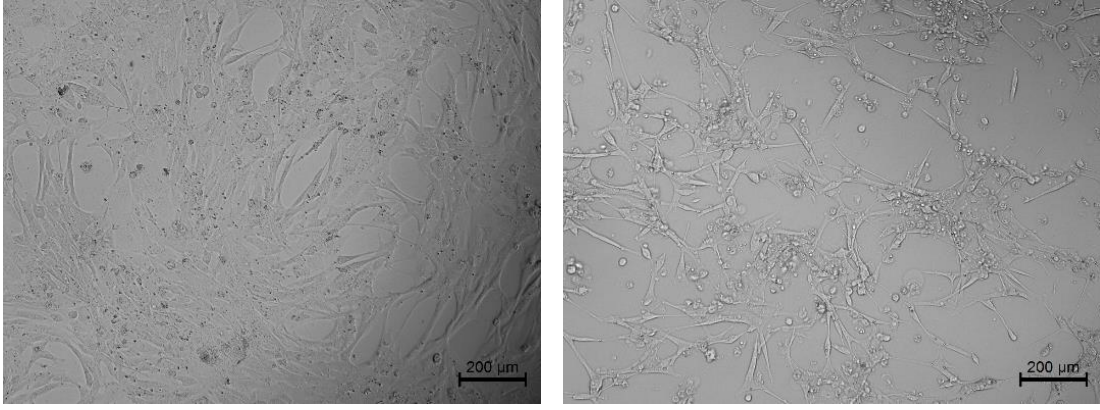
Şekil 2: İnsan kaynaklı proksimal tübül epitel hücrelerinin ikinci ve altıncı gününe ait mikrografları. X100

Takrolimus uygulamasından sonra 48 saate kadar hücre indeksi ölçülmüş ve ID50 değeri 44,69 µg/ml olarak bulunmuştur ($R^2=0.98483$). Takrolimus, 48. saatte 0.1, 1, 10, 100, 1000 µg/ml konsantrasyonlarda kontrol grubuna göre anlamlı olarak hücre indeksini azaltmıştır (Şekil3)(sırasıyla $p=0.0043$, $p=0.0006$, $p<0.0001$, $p<0.0001$, $p<0.0001$).



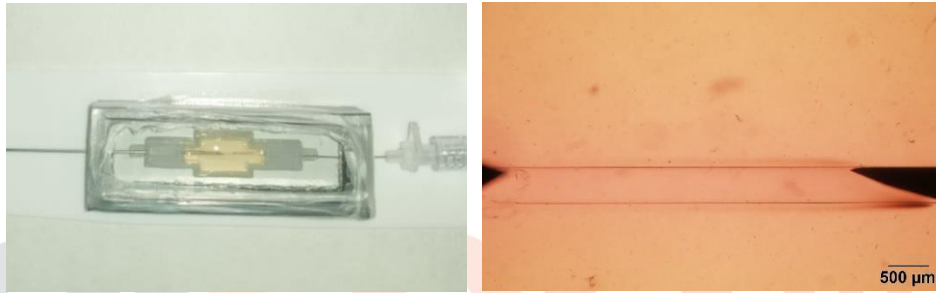
Şekil 3: Takrolimusun HK-2 hücrelerindeki sitotoksik etkisinin gerçek zamanlı değerlendirmesi ve 12- 48 saat aralığında normalize edilmiş hücre indeksinin Ortalama \pm Standart Hata grafiği

Etkin doz olarak belirlenen 44,69 µg/ml takrolimus, proksimal tübül epitel hücrelerine uygulandıktan 24 ve 48 saat sonra hücrelerde meydana gelen hasar invertte faz kontrast mikroskobu ile görüntülenmiştir (Şekil 4).



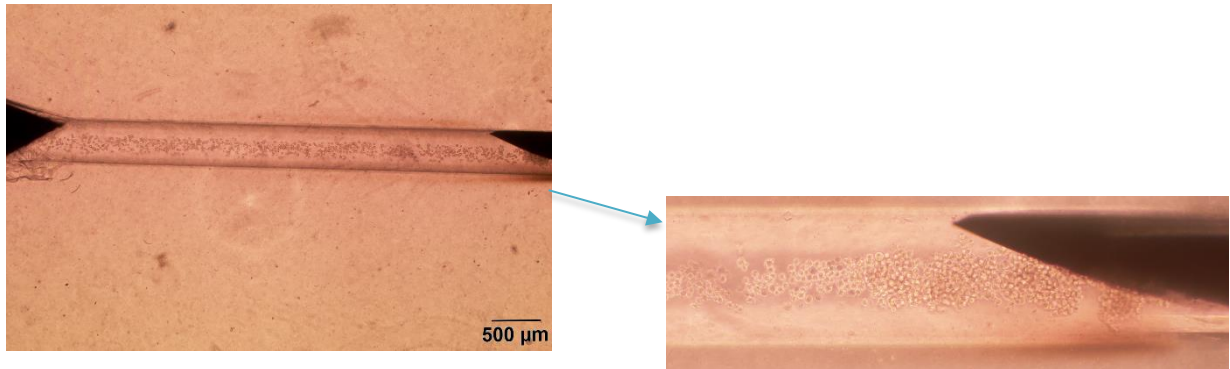
Şekil 4: İnsan kaynaklı proksimal tübül epitel hücrelerine 44,69 µg/ml takrolimus uygulandıktan 24 ve 48 saat sonra hücrelerde oluşan hasar görünmektedir. X100

Üç boyutlu baskı yöntemi ile üretilen kalıba enjektör uçları karşılıklı yerleştirilip jelatin metakrilat kalıba dökülüp çapraz bağlanması tamamlandıktan sonra iğne uçlarının geri çekilmesiyle kanal oluşturulmuş ve invertte faz kontrast mikroskopunda görüntülenmiştir (Şekil 5).



Şekil 5: Kanalın makroskopik ve mikroskopik(40x) görüntüsü.

Kanal içerisine proksimal tübül epitel hücrelerinin ekimi yapılmış ve gece boyu inkübasyona bırakılmıştır (Şekil 6). İnkübasyonun ardından şırınga pompası ile 1 µl/dk hızda besiyeri akışı başlatılmış ve kültüre edilmiştir.



Şekil 6: Kanal içerisinde proksimal tübül epitel hücrelerinin invertte faz kontrast mikrografı.x40

Sonuç

Takrolimusun proksimal tübül hücrelerindeki toksik dozu gerçek zamanlı olarak belirlendi. Üç boyutlu mikrofizyolojik koşulları modelleyen bir kanal tasarlanıp proksimal tübül epitel hücrelerinde nefrotoksitesinin değerlendirilmesi için uygun bir platform oluşturuldu.

Bu çalışma, Hacettepe Üniversitesi Bilimsel Araştırma Projeleri Koordinasyon Birimi tarafından TYL-2021-19632 numaralı Yüksek Lisans Tez Destek Projesi ile desteklenmiştir.

Kaynakça

1. Bentata Y. Tacrolimus: 20 years of use in adult kidney transplantation. What we should know about its nephrotoxicity. *Artificial organs*. 2020;44(2):140-52.
2. Yersal N, Köse S, Horzum U, Özkavukcu S, Orwig KE, Korkusuz P. Leptin promotes proliferation of neonatal mouse stem/progenitor spermatogonia. *Journal of Assisted Reproduction and Genetics*. 2020;37(11):2825-38.



IVF LABORATUVARINDA OOSİT MAYOZ MEKİĞİ DEĞERLENDİRMESİNİN İNFERTİLİTE TEDAVİ BAŞARISINDAKİ YERİ

**Dilşad ARISOY DEMİR¹, Kübra ÖZUNCA², Cem KORKMAZ³, Tanyeli
GÜNEYLİGİL KAZAZ⁴, Esin MUSLU BAL⁵, Halil OĞUZ⁵**

¹ Gaziantep Üniversitesi Tıp Fakültesi, Histoloji ve Embriyoloji AD, Gaziantep, Türkiye,
dr.dilsadarisoydemir@gmail.com

² Kübra ÖZUNCA, S.B.Ü. Gülhane Tıp Fakültesi, Histoloji ve Embriyoloji AD, Ankara, Türkiye,
rana94kubra.ozunca@gmail.com

³ Cem KORKMAZ, S.B.Ü. Gülhane Tıp Fakültesi, Histoloji ve Embriyoloji AD, ÜYTE Laboratuvar Sorumlusu,
Ankara, Türkiye, dr.cemkorkmaz@gmail.com

⁴ Tanyeli GÜNEYLİGİL KAZAZ, Gaziantep Üniversitesi Tıp Fakültesi, Biyoistatistik AD, Gaziantep, Türkiye,
tanyeliguneyligil@windowslive.com

⁵ Esin MUSLU BAL, Gülhane Eğitim ve Araştırma Hastanesi, Tüp Bebek Merkezi, Ankara, Türkiye,
esinmuslubal@gmail.com

⁵ Halil OĞUZ, Gülhane Eğitim ve Araştırma Hastanesi, Tüp Bebek Merkezi, Ankara, Türkiye,
hllogz14@gmail.com

Özet: Açıklanamayan infertilite olgularının arttığı IVF vakalarında noninvazif yöntemlerle oosit kalitesi değerlendirilmesi önemlidir. Çalışmamızda retrospektif olarak 2021 yılında infertilite nedeniyle Gülhane EAH ÜYTE Merkezi'ne başvuran hastaların verileri incelenmiştir. ICSI (Intra Cytoplasmic Sperm Injection) sırasında polarizasyon mikroskopi sistemi (PolScope) kullanılarak mayoz mekiği (MM) varlığı ve oositin I. Polar Body (PB)'sine göre konumu değerlendirilmiştir. PolScope eşliğinde ICSI yapılan 70 hastanın 341 ICSI uygulama sayısı için MM varlığı/yokluğu ve açılı konumları için yaşlar arası görülme yüzdesi, intrasitoplazmik (İS) ve ekstrasitoplazmik (ES) oosit anomalisi yüzdesi, fertilizasyon başarısı, embriyo kalitesi (EK) ve β -hCG(+)’liği değerlendirilmiştir. Yaşa göre MM varlığı/yokluğu/açılı konum yüzdesi değerlendirildiğinde her iki yaş grubu için aralarında istatistiksel anlamlı farklılık yoktur. MM varlığı/yokluğu/açılı konumda olması ile İS, ES, AY oosit gruplarında ve EK arasında istatistiksel anlamlı farklılık ve korelasyon saptanmamıştır. Benzer şekilde fertilizasyon ile MM değerlendirildiğinde MM olan ve açılı konumdaki oositlerle istatistiksel anlamlı farklılık yokken; MM olmayanların non fertilize/ölen yüzdesi arasında pozitif zayıf korelasyon vardır ($r=0,289$; $p=0,015$). MM ile yaş grupları arasında anlamlı farklılık olmasa da MM yokluğu fertilizasyon başarısını olumsuz etkilemektedir. MM varlığı/yokluğu/açılı konumda ile β -hCG(+)’liği arasında da istatistiksel olarak anlamlı farklılık olmamasına rağmen medyan (%25-75) değerleri sırasıyla 47,22(25 -66,66); 13,39(0 -50) ve 25(0 -55,55) olarak hesaplanmıştır. MM varlığında MM yokluğuna göre daha yüksek medyan değerleri oluşu örneklem sayısı artırıldığında β -hCG(+)’liği ile arasında istatistiksel anlamlılık oluşabileceğini öngörebilir. Sonuç olarak mayoz mekiği varlığının

değerlendirilmesi oosit seçimiyle fertilizasyon başarısının ve β -hCG(+)'liğinin öngörülmesinde belirleyici olabilir.

Anahtar Kelimeler: *Oosit mayoz mekiği, Polscope.*

1.GİRİŞ

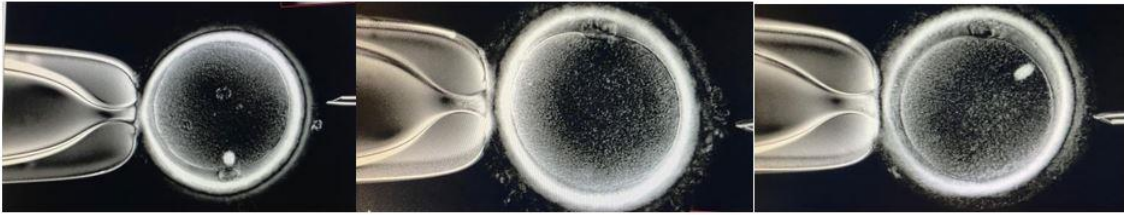
Açıklanamayan infertilite olgularının arttığı IVF vakalarında, sağlıklı gebelik için transfer edilecek embriyo seçimi büyük önem kazanmıştır. Embriyo kalitesinin noninvazif yöntemlerle belirlenmesi için geliştirilen teknikler de önemini her geçen gün attırmaktadır. Başarılı bir IVF tedavisi için toplanan oositlerin kalitesi belki de en önemli belirleyici faktör olabilir (1). Bu kapsamda embriyoda kromozomal aktarımın hatasız ve başarılı şekilde gerçekleşmesi için oosit değerlendirmesi önem arz etmektedir. Çünkü; oositte mayotik iğnin varlığı ve normal morfolojide oluşu kromozomların doğru düzenlenişini desteklerken, aksi durumlar mayotik bölünmede anöploidi gibi sonuçlara sebep olabilmektedir (2). Henüz aydınlatılmamış nedenlerle dişi gamet hücresi olan oositlerin özellikle ileri yaşlarda mayoz bölünme hatalarına daha duyarlı olduğu, bu nedenle anöploidi sıklığının arttığı ifade edilmiştir (3). Oositlerde mayotik iğ yapısı görüntülenenler ve görüntülenmeyenler karşılaştırıldığında mayotik iğ yapısı görüntülenen oositlerin fertilizasyon ve erken bölünme oranlarının daha yüksek olduğu, ayrıca transfer için tercih edildiklerinde de implantasyon ve gebelik oranlarının daha yüksek olduğu bildirilmiştir. Bu durumun oosit nükleer yapı olgunlaşması ile ilişkili olabileceği öne sürülmektedir (4). Bazı oositlerde yaş artışıyla mayotik iğ gözlenemeyebilir (5). Canlı oositlerde ışığın çift kırılma prensibine dayanarak mayotik iğnin görselleştirilebildiği PolScope ile ICSI'ye tabii tutulan oositlerin mayotik iğ analizleri yapılabilir (6). PolScope ile mikrotübül yapısındaki mayotik iğnin değerlendirilmesinde hem varlığı hem de yoğunluğu değerlendirilebilir (7). Oositlerde 1.PB konumu mayotik iğ için her zaman ön görücü olamayabilir(5). Bu nedenle IVF laboratuvarında ICSI (Intra Cytoplasmic Sperm Injection) yapılırken yaygın olarak kabul gören polar cismin saat 6 ya da 12 hizasına alınması uygulamasına (8) ek olarak polarize ışık altında mayoz mekiğinin görüntülenmesi daha güvenli olacaktır. Çünkü; mayotik iğnin tahmin edilemez konumu ICSI sırasında zarar görebilme ihtimalini de artırabilir (6, 9). Konfokal mikroskop ile mayotik iğ varlığı tespit edilemeyen oositlerin anormal mikrotübül organizasyonu ve anormal kromozom dizilimine sahip oldukları ortaya konmuştur. PolScope çalışmalarıyla canlı insan oositlerinden elde edilen iğ görüntüleri ile bu sonuçların benzer doğrultuda olduğu da gösterilmiştir. Bu nedenle ICSI öncesi PolScope ile mayotik iğ

değerlendirilmesinin kromozomal olarak normal olan oositlerin tahmin edilmesi için kullanılabileceği düşünülmektedir(10, 11).

Çalışmamızda IVF tedavi sürecinde laboratuvarında non invaziv oosit değerlendirme yöntemlerinden biri olan PolScope kullanımı ile, ICSI öncesi mayoz mekiği varlığı ve 1.polar cisme göre konumunun hastaların yaş, intra ve ekstrasitoplazmik oosit anomalileri ile ilişkisi ve fertilizasyon, embriyo kalitesi ve kimyasal gebelik sonuçlarına etkisini göstermeyi amaçlıyoruz.

3.YÖNTEM:

Çalışmamızda retrospektif olarak infertilite nedeniyle 2021 yılında Gülhane EAH ÜYTE Merkezi'ne başvuran hastaların verileri incelenmiştir. ICSI sırasında polarizasyon mikroskopi (PolScope) kullanılarak mayoz mekiği (MM) varlığı ve oositin 1.PB'sine göre konumu değerlendirilen hastalar çalışmaya dahil edilmiştir (Şekil 1). Erkek faktörü olan hastalar ve ICSI uygulanmayan Germinal Vezikül (GV) oositler çalışma dışı bırakılmıştır.



Şekil 1.: PolScope ile görüntüleme ile ICSI öncesi mayoz mekiği değerlendirme (Soldan sağa MM var/yok/açılı konumda)

Çalışmaya dahil olan hastalardan toplanmış olan oositlerde ICSI hazırlığı yapılarak cam tabanlı kültür kabında ışığın çift kırılma temeline dayanan bilgisayar destekli polarizasyon mikroskopi sistemi (PolScope) kullanılmış ve mayoz mekiği varlığı ile oositin 1. Polar Body (PB)'sine göre konumu değerlendirilmiştir. PolScope eşliğinde ICSI yapılan 70 hastanın toplam 341 oositinde MM varlığı/yokluğu ve konumları için yaş gruplarına göre görülme yüzdesi, intrasitoplazmik (İS) ve ekstrasitoplazmik (ES) oosit anomalisi yüzdesi (İS anomali granülasyon, vakuol, refraktil cisim, SER kümesi varlığı; ES anomali fragmente PB, geniş PVA ve PVA'da döküntü ve anomali olmayan AY grubu), fertilizasyon başarısı, embriyo kalitesi (EK) ve β hCG(+)'liği değerlendirilmiştir.

4.BULGULAR:

Çalışmamızda PolScope ile MM değerlendirilerek ICSI yapılan hastalarda fertilizasyon oranı % 90,32 (308/341) olarak saptanmıştır. Embriyo transferi yapılan hastalarda %50 (14/28) β hCG(+)’liği elde edilmiştir. Yaşa göre MM varlığı/yokluğu/ konum yüzdesi değerlendirildiğinde her iki yaş grubu için de istatistiksel anlamlı farklılık yoktur ($p=0,085$; $p=0,114$; $p=0,633$) (Tablo-1). MM varlığı/yokluğu/açılı konumda olması ile İS, ES, AY ve EK arasında istatistiksel anlamlı farklılık ve korelasyon saptanmamıştır. Benzer şekilde fertilizasyon ile MM değerlendirildiğinde MM olan ve açılı konumdaki oositlerle istatistiksel anlamlı farklılık yokken; MM olmayanların non-fertilize/ölen yüzdesi ile arasında pozitif zayıf korelasyon vardır ($r=0,289$; $p=0,015$) (Tablo-2). MM varlığı/yokluğu/açılı konumda olması ile β -hCG(+)’liği arasında da istatistiksel olarak anlamlı farklılık olmamasına rağmen medyan (%25-75) değerleri sırasıyla 47,22(25 -66,66); 13,39(0 -50) ve 25(0 -55,55) olarak hesaplanmıştır.

	<35 (n=41)	\geq 35 (n=29)	
	Medyan(%25- %75)	Medyan(%25- %75)	P
NORMAL MM	50 (28,57 -70)	33,33 (14,28 -50)	0,085
MM YOK	0 (0 -33,33)	16,66 (0 -55,55)	0,114
AÇILI MM	16,66 (0 -50)	18,18 (0 -66,66)	0,633

Tablo 1. : In Vitro Fertilizasyon Uygulamalarında Yaşa Göre Mayoz Mekiği Konumunun Değişimi. * $p<0,05$ düzeyinde anlamlı, Mann Whitney U Testi

		2 PN	1-3 PN	NON- FERTİLİZE/ ÖLEN
NORMAL MM	r	0,148	0,155	-0,128
	P	0,221	0,200	0,291
	N	70	70	70
MM YOK	r	-,0230	-0,011	0,289*

	P	0,055	0,930	0,015
	N	70	70	70
AÇILI MM	r	0,232	-0,056	-0,162
	P	0,053	0,644	0,180
	N	70	70	70

Tablo 2. : In Vitro Fertilizasyon Uygulamalarında Mayoz Mekiği ve Konumu (MM Var, Yok, Açılı) ile Fertilizasyon Başarısı Arasındaki İlişki. * $p < 0,05$ düzeyinde anlamlı, r: Spearman Rank Korelasyon Katsayısı

Sayısal değişkenlerin normal dağılıma uygunluğu Shapiro Wilk testi ile test edilmiştir. Normal dağılmayan değişkenlerin iki grupta karşılaştırılmasında Mann Whitney U testi, üç grupta karşılaştırılmasında Kruskal Wallis testi kullanılmıştır. Sayısal değişkenler arasındaki ilişkiler Spearman rank korelasyon katsayısı ile test edilmiştir. Analizlerde SPSS 22.0 Windows versiyon paket programı kullanılmıştır. $P < 0,05$ anlamlı kabul edilmiştir.

5.TARTIŞMA VE SONUÇ:

Henüz aydınlatılmamış nedenlerle dişi gamet hücresi olan oositlerin mayoz bölünme hatalarına daha duyarlı olduğu, bu nedenle anöploidi sıklığının arttığı ifade edilmiştir (3). Keefe ve ark. ile Wang ve ark. yaptıkları çalışmalarda konfokal mikroskop ile mayotik iğ varlığı tespit edilemeyen oositlerde anormal mikrotübül organizasyonu ve anormal kromozom dizilimine sahip olduklarını ve PolScope ile canlı insan oositlerinden elde edilen iğ görüntüleri ile sonuçların benzer doğrultuda olduğunu ortaya koymuşlardır. ICSI öncesi polarize mikroskop destekli sistemle mayotik iğ değerlendirilmesinin kromozomal olarak normal oositlerin tahmin edilmesi için kullanılabileceğini ifade etmişlerdir(10, 11). Çalışmamızda MM varlığı/yokluğu/açılı konumda olması ile İS, ES, AY ve EK arasında istatistiksel anlamlı farklılık ve korelasyon saptanmamıştır.

Liu ve ark. yaptıkları çalışmada maternal yaşın artmasıyla oosit yaşlanmasının doğurduğu iğ bütünlük kaybı ve açılanmasının tedavi sonuçlarını olumsuz yönde etkilediğini göstermişlerdir (12). Ayrıca yaşa bağlı oosit kalitesindeki düşüş ve mayotik hata oranındaki artış Bebbere ve ark. tarafından da raporlanmıştır(13). Çalışmamızda yaşa göre MM varlığı/yokluğu/ konum yüzdesi değerlendirildiğinde her iki yaş grubu için de istatistiksel anlamlı farklılık saptanmamıştır. ($p=0,085$; $p=0,114$; $p=0,633$). Yine de MM ile yaş grupları

arasında anlamlı farklılık olmasa da MM yokluğunun fertilizasyon başarısını olumsuz etkilediği gözlenmiştir.

Rienzi ve ark. tarafından yapılan çalışmada mayotik iğ ve 1.PB arasındaki açılanmanın fazla oluşu fertilizasyonu olumsuz yönde etkilemesine rağmen fertilizasyonun normal olduğu embriyolarda gelişim potansiyelleri üzerine olumsuz etki gözlenmemiştir. Ancak mayotik iğ konumu ile 1. PB (polar body) arası açının fertilizasyon anomali riskleri ile ilişkili olduğu bilinmektedir (6). Hatta in vitro ve in vivo olgunlaşmış insan oositlerinde yapılan çalışmada da 1.PB'ye göre mayotik iğ konumunun fertilizasyon oranlarını etkilediği gösterilmiştir(14). Çalışmamızda fertilizasyon ile MM değerlendirildiğinde MM olan ve açılı konumdaki oositlerle istatistiksel anlamlı farklılık yokken; MM olmayanların non-fertilize/ölen yüzdesi ile arasında pozitif zayıf korelasyon saptanmıştır. ($r=0,289$; $p=0,015$).

Mayoz mekikleri oositlerde kromozomların birbirine bağlanmasında görevli, ışığın çift kırılma özelliği ile polarize ışık mikroskobu ile görüntülenebilen mikrotübül yapılarıdır. Daha önceleri immun boyama ve transmisyon elektron mikroskobu gibi özel fiksasyon yöntemleri kullanımını gerektirmesinin ardından polarize ışık mikroskobu ile görüntülenebilmesi, IVF uygulamalarında noninvaziv bir oosit değerlendirme yöntemi olarak önemini korumaktadır(10). Yine de Woodward ve ark. tarafından yapılan çalışmada mayotik iğ konumunun fertilizasyon ve embriyo kalitesine etkisinin anlamlı olmadığı da raporlanmıştır. Hatta mayotik iğleri saat 3,4,8,9 gibi enjeksiyon düzlemine yakın oositlerde fertilizasyon ve embriyo kalitesinin yüksek oranları yaygın kullanılan uygulamayı da sorgulayıcı bir yaklaşımı desteklemektedir (15). Çalışmamızda da MM varlığı/yokluğu/açılı konumda bulunması ile β -hCG(+)'liği arasında da istatistiksel olarak anlamlı farklılık saptanmamıştır. Farklı bir bakış açısı olarak oositlerde mayotik iğ görüntülenmede Madaschi ark.'nın 1097 MII oosit ile yaptıkları çalışmada mayotik iğ görüntülenenler ve görüntülemeyenler karşılaştırıldığında mayotik iğ varlığında fertilizasyon ve erken bölünme oranlarının daha yüksek olduğu ayrıca transfer için tercih edildiklerinde implantasyon ve gebelik oranlarının da daha yüksek olduğu savunulmuştur (4). Madaschi ve ark. mayotik iğ değerlendirmenin fertilizasyon potansiyeli ve embriyo gelişiminin klinik sonuçlarının tahmini için önemli olabileceği, embriyo seçiminin oosit nükleer olgunluğu ile de ilişkili olduğu yönünde görüş bildirmişlerdir (4). Swiatecka ve ark. yaptıkları çalışmada da mayoz mekiği olan oositlerin gebelik oranları yüksek değerde olsalar da istatistiksel anlamlı farklılık saptanamamıştır ($p=0,471$) (16). Çalışmamızda MM varlığı/yokluğu/açılı konumda bulunması ile β -hCG(+)'liği arasında da istatistiksel olarak

anlamli farklılık olmamasına rağmen medyan (%25-75) deęerleri sırasıyla 47,22(25 -66,66); 13,39(0 -50) ve 25(0 -55,55) olarak hesaplanmıştır.

Sonuç olarak MM varlığında MM yokluęuna göre daha yüksek medyan deęerleri oluşu örneklem sayısı artırıldığında β -hCG(+)'lięi ile arasında istatistiksel anlamlılık oluşabileceğini öngörebilir. Ayrıca noninvazif olarak mayoz mekięi varlığının deęerlendirilmesi oosit seçimiyle fertilizasyon başarısının ve β -hCG(+)'lięinin öngörülmesinde belirleyici olabilir.

5.KAYNAKÇA

1. Sciorio R, Miranian D, Smith GD. Non-invasive oocyte quality assessment. *Biology of Reproduction*. 2022;106(2):274-90.
2. Shen Y, Betzendahl I, Tinneberg H-R, Eichenlaub-Ritter UJMRGT, Mutagenesis E. Enhanced polarizing microscopy as a new tool in aneuploidy research in oocytes. 2008;651(1-2):131-40.
3. Blengini CS, Schindler K. Acentriolar spindle assembly in mammalian female meiosis and the consequences of its perturbations on human reproduction. *Biology of Reproduction*. 2021;106(2):253-63.
4. Madaschi C, de Souza Bonetti TC, Braga DPdAF, Pasqualotto FF, Iaconelli Jr A, Borges Jr EJJF, et al. Spindle imaging: a marker for embryo development and implantation. 2008;90(1):194-8.
5. Konc J, Kanyó K, Cseh SJJoar, genetics. Visualization and examination of the meiotic spindle in human oocytes with polscope. 2004;21(10):349-53.
6. Rienzi L, Ubaldi F, Martinez F, Iacobelli M, Minasi M, Ferrero S, et al. Relationship between meiotic spindle location with regard to the polar body position and oocyte developmental potential after ICSI. 2003;18(6):1289-93.
7. Mandelbaum J, Anastasiou O, Levy R, Guérin J, De Larouziere V, Antoine JJEJoO, et al. Effects of cryopreservation on the meiotic spindle of human oocytes. 2004;113:S17-S23.
8. Silva CP, Kommineni K, Oldenbourg R, Keefe DLJF, sterility. The first polar body does not predict accurately the location of the metaphase II meiotic spindle in mammalian oocytes. 1999;71(4):719-21.
9. Korkmaz C, Cinar O, Akyol MJGE. The relationship between meiotic spindle imaging and outcome of intracytoplasmic sperm injection: a retrospective study. 2011;27(10):737-41.
10. Keefe D, Liu L, Wang W, Silva CJRbo. Imaging meiotic spindles by polarization light microscopy: principles and applications to IVF. 2003;7(1):24-9.
11. Wang W-H, Meng L, Hackett RJ, Oldenbourg R, Keefe DLJF, sterility. The spindle observation and its relationship with fertilization after intracytoplasmic sperm injection in living human oocytes. 2001;75(2):348-53.
12. Liu L, Keefe DL. Ageing-associated aberration in meiosis of oocytes from senescence-accelerated mice. *Human Reproduction*. 2002;17(10):2678-85.
13. Bebbere D, Coticchio G, Borini A, Ledda SJJAR, Genetics. Oocyte aging: looking beyond chromosome segregation errors. 2022:1-8.
14. Fang C, Tang M, Li T, Peng W-L, Zhou C-Q, Zhuang G-L, et al. Visualization of meiotic spindle and subsequent embryonic development in in vitro and in vivo matured human oocytes. 2007;24(11):547-51.
15. Woodward BJ, Montgomery SJ, Hartshorne GM, Campbell KH, Kennedy RJRbo. Spindle position assessment prior to ICSI does not benefit fertilization or early embryo quality. 2008;16(2):232-8.
16. Świątecka J, Anchim T, Leśniewska M, Wolczyński S, Bielawski T, Milewski RJGP. Oocyte zona pellucida and meiotic spindle birefringence as a biomarker of pregnancy rate outcome in IVF-ICSI treatment. 2014;85(4).

PRODUCTION OF A 3-DIMENSIONAL ARTIFICIAL STOMACH MODEL WITH ALONG MUCUS LAYER

**Selin URSAVAŞ¹, Aslı Nurşeval OYUNLU², Yağmur Ekin BOYOĞLU², Gülşah
TORKAY², Hakan DARICI¹**

1. Department of Histology and Embryology, Faculty of Medicine, Istinye University, Istanbul
2. Center for Stem Cell and Tissue Engineering Research & Practice, Istinye University, Istanbul

Özet: 3B kültür modelleri ve yapay organlar, geleneksel analiz yöntemlerinin yerini alabilecek yeni çalışma sistemleridir. Hayvan çalışmalarının zorluğu, maliyeti ve çoğu zaman insana uyumsuzluğunun yanı sıra insan çalışmalarındaki etik sınırlamalar, 3D kültür sistemlerini avantajlı hale getirmiştir. Ancak 3 boyutlu kültür çalışmaları arasında yapay mide dokusu çalışmaları çok azdır. Gastrit ve peptik ülser gibi yaygın mide hastalıklarını göz önünde bulundurarak, hastalık modellerine ve farmakolojik tedavi yöntemlerine temel oluşturmak için bu çalışmada doku iskeleleri ve 3 boyutlu kültür ile yapay bir mide mukozası ve mukus oluşturmayı amaçladık. İskele oluşturmak için Baseink™ ve gastrik lamina propria oluşumu için İnsan Fibroblastları ile Mezenkimal Kök Hücreler (MSC'ler) ve mide epiteli için İnsan Umbilikal Ven Endotel Hücreleri (HUVEC) kullandık. Nişasta, ksantan zamkı ve sığır serum albüminini (BSA) farklı oranlarda karıştırarak bulanık mide mukusunu taklit eden mukus elde ettik. Mide asidini taklit etmek için %30 HCl solüsyonu hazırladık. Sonuçlarımız, kontrol gruplarındaki hücrelerin yapay mide mukozası benzeri yapılar oluşturduğunu gösterdi. Mukusla kaplı örneklerin HCl ilavesinden sonra bozulmadığı gözlemlendi. Bunun aksine mukusla kaplanmayan örneklerde HCl ilave edildikten sonra hücre kaybına bağlı olarak yapay mide mukozası yapısında bozulma gözlemlendi. Çalışmamız, hücresel düzeyde yapay mide mukozasının oluşturulabileceğini ve bu modelin gelecekteki çalışmalara örnek teşkil edebileceğini, yanı sıra hastalık modellerinde kullanılabileceğini ortaya koydu.

Anahtar Kelimeler: MSC, HUVEC, 3D hücre kültürü, gastrik mukoza, yapay mide modeli.

Abstract: 3D culture models and artificial organs are new working systems that can replace traditional analysis methods. The difficulty, cost, and often incompatibility of animal studies, as well as ethical limitations in human studies, have made 3D culture systems advantageous. However, artificial stomach tissue studies are very few among 3D culture studies. Considering the common gastric diseases such as gastritis and peptic ulcer, we aimed to create an artificial gastric mucosa and mucus with tissue scaffolds and 3D culture in this study to form a basis for disease models and pharmacological treatment methods. We used

Baseink™ to create scaffold and Human Fibroblasts and Mesenchymal Stem Cells (MSCs) for the formation of gastric lamina propria and Human Umbilical Vein Endothelial Cells (HUVEC) for the gastric epithelia. By mixing starch, xanthan gum, and bovine serum albumin (BSA) in different ratios, we obtained mucus that mimics the cloudy gastric mucus. To mimic stomach acid, 30% HCl solution was prepared. Our results showed that cells in control groups constitute artificial gastric mucosa-like structures. It was observed that the samples covered with mucus did not deteriorate after the addition of HCl. On the contrary, after the addition of HCl in the samples not covered with mucus, deterioration in the structure of the artificial gastric mucosa was observed due to cell loss. Our study revealed that artificial gastric mucosa can be created at the cellular level and this model can serve as an example for future studies and can be used in disease models.

Keywords: MSC, HUVEC, 3D cell culture, gastric mucosa, artificial stomach model.

INTRODUCTION

The gastric glands produce the stomach's gastric juice, which partially digests the food transported from the esophagus. Surface mucous cells secrete the visible (cloudy) mucus to protect the gastric mucosa from the hydrochloric acid (HCl) of gastric juice thus providing a physiologic gastric mucosa barrier (1). Two of the most common stomach diseases are gastritis and peptic ulcer. Gastritis is inflammation of the gastric mucosa and peptic ulcer is an advanced state of gastritis that is characterized by obvious depth in the mucosa. The three most important causes of both diseases are Helicobacter pylori infection, non-steroidal anti-inflammatory drugs (NSAIDs) (and aspirin), and autoimmunity (2). Since animal studies were generally incompatible with humans, and human studies are limited due to ethical reasons, 3D culture models and artificial tissue pave the way for replacements for conventional analysis methods. In this regard, artificial stomach tissue studies are highly limited in number. In our study, we aimed to create an artificial gastric mucosa and mucus with tissue scaffolds and 3D culture.

MATERIAL-METHOD

We used the Human Fibroblasts and Mesenchymal Stem Cells (MSCs) for the formation of gastric lamina propria and Human Umbilical Vein Endothelial Cells (HUVEC) for the mimick of gastric epithelia. The tissue scaffold was prepared with Baseink™ and each vial was dissolved in 5 ml DMEM and autoclaved. Human fibroblasts and MSCs were added as 2

million cells per ml of the hydrogel and gels were crosslinked with calcium chloride (CaCl₂). After 48 hours of incubation with DMEM/F12 culture medium, non-adherent cells were removed with the medium. HUVECs were seeded at 3 million counts per well on top of the hydrogel and incubated for an additional 24 hours with DMEM/F12 culture medium. MSCs and HUVECs were also cultured in 2D conditions in wells as control. To mimic cloudy mucus, various combinations of starch, xanthan gum, and bovine serum albumin (BSA) were used to provide gel-like and viscous consistency of gastric mucus. DNA from banana fruits was isolated and added as a supporting polymer. Sodium bicarbonate was added to the samples to alkalize the medium. The media in the culture wells were withdrawn, and artificial mucus was added on top of the cells. No mucus was added to the control wells. Wells were covered with 1 ml of fresh media. To mimic stomach acid, 30% HCl solution was added in 3D wells. 2D cultures of HUVECs and MSCs without mucus were used as controls. Samples were cultured for 6-18 hours for analysis. At the end of the experiment, the live samples were examined under a fluorescent microscope and photographed.

RESULTS

HCl caused a drastic drop in media pH which was also observed via phenol red color change. Microscopic analyses showed that in 2D control groups, both human fibroblasts and MSCs had spindle-shaped morphology and HUVECs had epithelial-like morphology (Figure 1). We observed that in 3D control groups, human fibroblasts and MSCs residing in the deeper layer and HUVECs on the superficial layer together formed 3D artificial mucosa (Figure 2). When the groups were examined after the nuclei staining with DAPI, it was observed that the cells in the control group formed an artificial mucosa-like structure. The cellular extensions of the underlying MSCs and fibroblasts were covered with dense HUVECs on the surface, and it was observed that HUVECs formed a distinctly epithelial-like mucosal lining (Figure 3A). In the 3D wells without mucus after the addition of HCl, it was observed that the cells were damaged to a great extent, and accordingly, the cells were sparsely located. As a result of the loss of vitality of the cells in these wells, the integrity of the artificial mucosa-like structure that we created was disrupted (Figure 3B). We observed that the mucus-covered 3D wells contained intact cells. With DAPI staining, it was observed that the mucus layer on the cells protected the cells from HCl and the artificial mucosa-like structure was largely preserved. (Figure 3C).

CONCLUSION

Our results showed that 3D modeling gastric mucosa on a cellular level can provide a low-cost option for future disease modeling studies and pharmacological treatments of human gastric-related diseases.

REFERENCES

1. Ross, M. H., Pawlina, W. (2011). Histology: A Text and Atlas: With Correlated Cell and Molecular Biology. 7thEd. McGraw-Hill Education.
2. Bebb, J., James, M. W., Atherton, J. (2003). Gastritis and Peptic Ulcer. *Medicine*. 31(1):15-18.

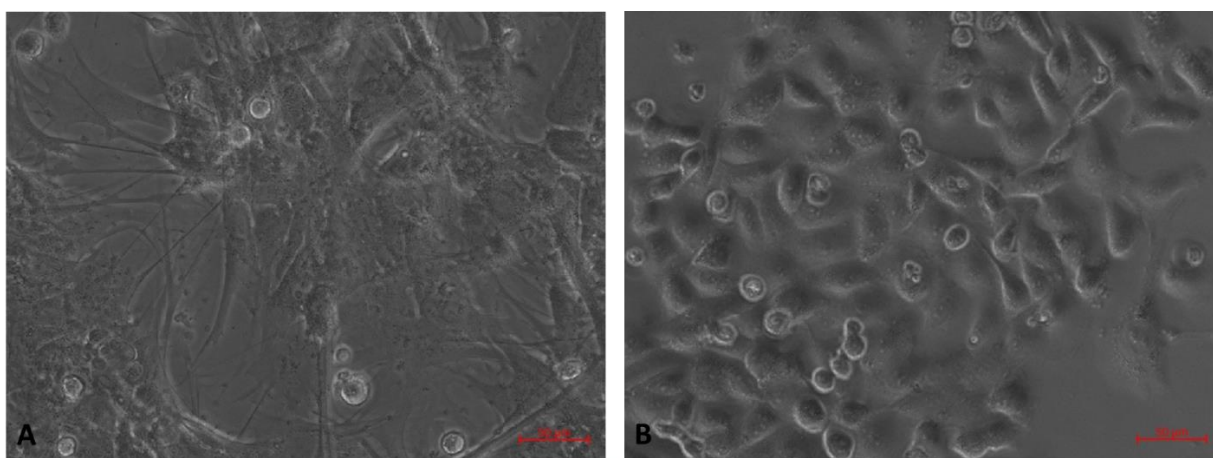


Figure 1. Control groups of MSCs and Fibroblasts (A) and HUVECs (B) in 2D culture.

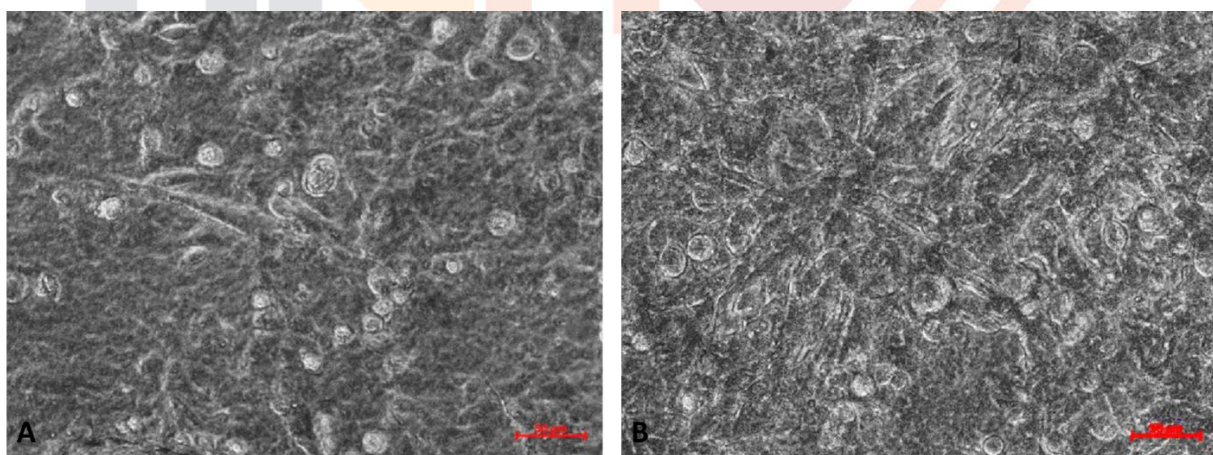


Figure 2. Control groups of 3D artificial gastric mucosa in 12 hours (A) and 24 hours (B).

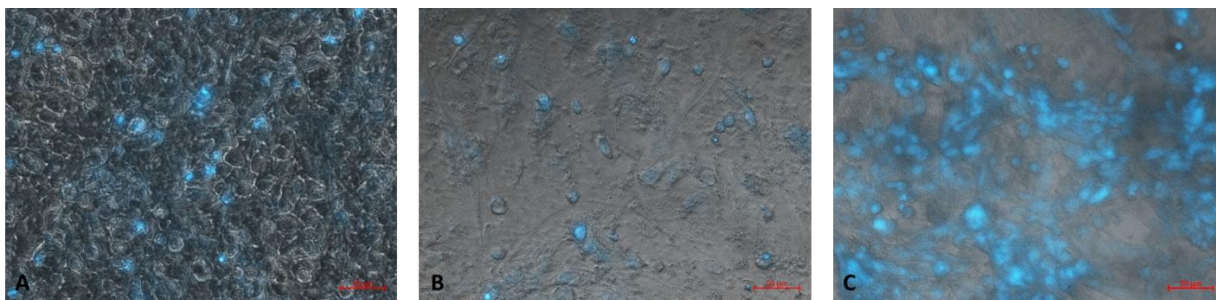


Figure 3. DAPI staining of control well in the 3D artificial gastric mucosa (A). DAPI staining of 3D well without mucus-covered and HCl solution added (B). DAPI staining of 3D well with mucus-covered and HCl solution added (C).

niche²⁰₂₂

3D BIOPRINTING, CELL CULTURE AND HISTOLOGICAL EVALUATION OF 3D PRINTED SKIN TISSUE ENGINEERING PRODUCTS FOR REGENERATIVE MEDICINE APPLICATION

Umut Doğu SEÇKİN¹, Özgün Selim GERMIYAN², Aylin ŞENDEMİR³, Yiğit
UYANIKGİL⁴

¹Ege University, Graduate School of Natural and Applied Sciences, Department of Bioengineering, Izmir,
Turkey, umutdoguseckin@gmail.com

²Ege University, Graduate School of Health Sciences, Department of Stem Cell, Izmir, Turkey,
ozgungermiyan@gmail.com

³Ege University, Faculty of Engineering, Department of Bioengineering, Izmir, Turkey,
aylin.sendemir@ege.edu.tr

⁴Ege University Faculty of Medicine, Department of Histology and Embryology, Izmir, Turkey,
yigit.uyanikgil@ege.edu.tr

Abstract: *In the field of bioengineering and tissue engineering, regenerative medicine provides the donor graft solution that allows tissue growth with free cell content. In addition, dermal matrix components offer cytokines and growth factors, while bioengineered skin tissues act as skin, protecting against fluid loss and contamination. In terms of skin tissue engineering, 3D bioprinting technique has the potential to be used especially in burn treatments and injuries in the military field. Different methods are used to ensure the solidification of the polymer, the most important of which is to ensure the solidification of the tissue in the desired time by using chemical crosslinking. Within the scope of the study, three-dimensional tissue scaffolds are produced and the cell cultured performed under standard culture conditions.*

Keywords: *Hydrogels, alginate, gelatine, chitosan, bioprinting*

1. INTRODUCTION

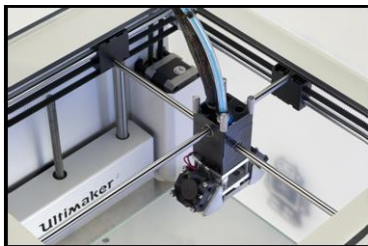
There are intensive studies on the development of injectable polymers for tissue repair or tissue regeneration. The main advantage of injectable biomaterials is their ability to fill different tissue defects that occur. Other advantages are ease of use, insertion into the tissue with a minimal surgical procedure, creating an interface for the development of cells, and the ability to carry a bioactive agent (the end that have form a strong bond with living tissue) on itself (1). In the use of injectable biomaterials that can polymerize in the environment, it is necessary to take into account some properties that other biomaterials do not have (2). Different methods are used to ensure the solidification of the polymer, the most important of which is to ensure the solidification of the tissue in the desired time by using chemical crosslinking (3). In the literature, there are many different hydrogel development studies such

as alginate, chitosan, gelatin, hyaluronic acid (4). In terms of skin tissue engineering, 3D bioprinting technique has the potential to be used in burn treatments and injuries, especially in the military field (5). Within the scope of the study, three-dimensional tissue scaffolds were produced and cultured under standard cell culture conditions. Hydrogels with cells were bioprinted with a three-dimensional bioprinter and their viability was measured.

2. METHOD

2.1. Mechanical Modification

Working with certain parameters, Ultimaker 2 has been used in prototype production, 3D printing and production technologies. A 3D printer device that can move in X, Y and Z planes and used in polymer printing technology has been modified.



The old nozzle and motor system of the Ultimaker 2 printer is shown in figure 1. With the modifications of the mechanical parts, the nozzle structure was removed from the structure, and a nozzle that could provide automatic pipette tip-sized flow was used. These structures are shown in figures 2 and 3.



The pipe system in the serum infusion set was used for the pipeline integrated into the nozzle structure in the modified system. The modification of the sterile infusion set was made in a sterile cabinet. An example of the infusion set used is shown in figure 4.

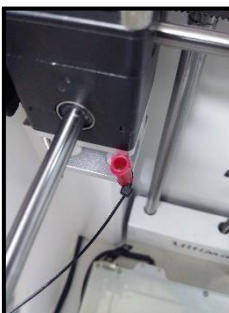


Figure 1. Ultimaker 2 nozzle system (6)

Figure 2. Lateral view of the integrated nozzle structure (6)

Figure 3. Vertical view of the integrated nozzle structure



Figure 4. Infusion Set

For bioprinting, the “New Era Pump” System was used as a pump for bioprinting in the nozzle structure of the Material (Figure 5).



Figure 5. NE-300 Pump System (7)

After the modifications made on the device, the device was made capable of bioprinting.

2.2. Gel Studies

It was prepared by dissolving the alginate into bottles with distilled water at a concentration of 1%, 2% and 3% (8). It was sterilized by autoclaving at 121°C for 15 minutes. The CaCl₂ solution used for crosslinking was passed through filters with a diameter of 0.20 µm and was developed into a ready-made one. Gelatin was prepared by dissolving it into bottles with distilled water at a concentration of 2% and 3% (9). It was sterilized by autoclaving at 121°C for 15 minutes. Since the cross-linking was done with temperature, it was kept at +4°C to see gelation. Chitosan was prepared by dissolving it into bottles with distilled water at a concentration of 1% and 2%. It was sterilized by autoclaving at 121°C for 15 minutes. Since cross-linking is done with acetic acid, acetic acid solution was prepared as 1% and 2% in order to see gelation (10). It was sterilized by passing through 0.2 µm filters. After sterilization, acetic acid solution was added to the Chitosan solution and left for 1 night to dissolve and gel in a magnetic stirrer.

2.3. Cell Culture

Keratinocytes from epidermis layer, that is the upper layer of skin tissue, were used. Human keratinocyte cell line (HS2) that had been characterized before were suspended with in different hydrogels and their mixtures to obtain the most suitable hydrogel for bioprinting (11). Bioprinted skin tissues were tested by MTT assay for viability analysis; and hematoxylin- eosin staining was performed for determination of cell distribution and morphology 7 days after the beginning of the culture.

2.4. Bioprinting

The created biomaterials were taken into a 10 ml syringe and placed in the NE-300 pump and set to 70 ml/min. In the optimization study, it was observed that 30 ml/min and 60 ml/min tests were made for the working speed of the pump and it was not suitable for the printing speed. It has been observed that the “box” drawn for 70 ml/min printing is suitable for the drawing and the optimum printing speed has been reached. Each cellular hydrogel structure structure was collected one by one into the syringe system for printing and printed. Cultivation times for the analyzes to be made 7 days. 24-well plate was used for bioprinting analyzes.

3. Results

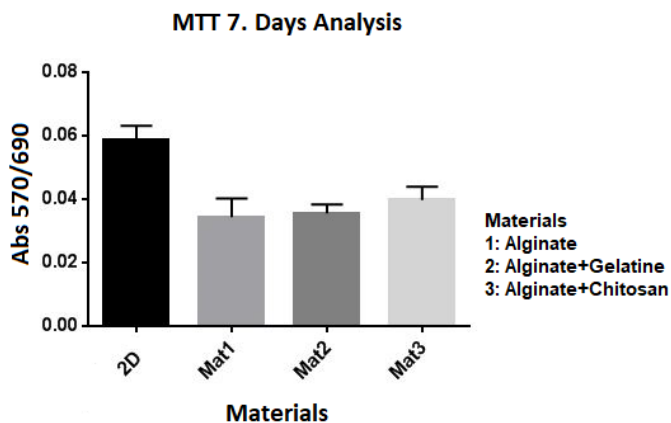


Figure 6. MTT analysis of the control group and materials at 7. Days

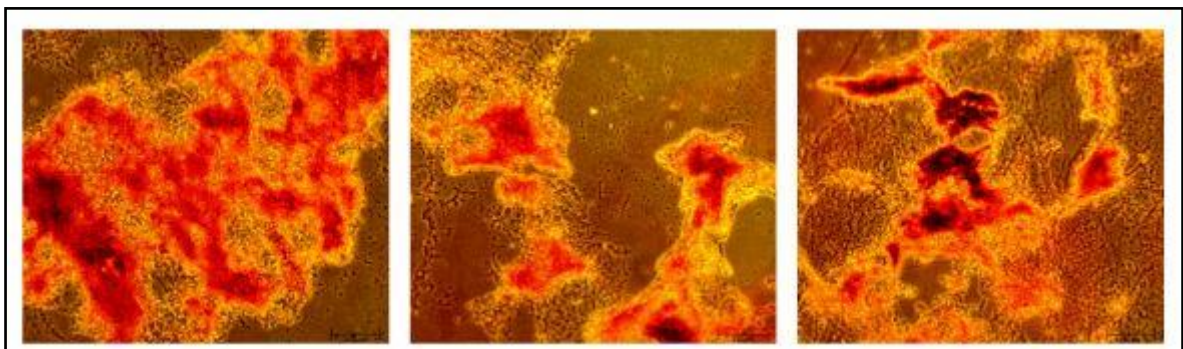


Figure 7. Day 7 H&E staining images with 10x ocular caps (A: Alginate, B: Alginate + Gelatine, C: Alginate + Chitosan)

4. Discussion and Conclusion

It has been observed that the obtained tissue scaffolds have 3D porous structures for cell attachment. It has been observed that the materials used are suitable for freezing sectioning. According to the obtained MTT results, cell viability was close to the viability of the 2D culture. MTT results are an indication that the cells maintain their vitality by adhering to the hydrogel structure. According to the results obtained, the hydrogel that was determined as the best in terms of cell viability among the three hydrogels used was the Alginate-Chitosan hydrogel. The results of cell viability depend on the reaction of the cells in the hydrogel structure with MTT. The good performance of the reaction increases the possibility of correct results. Good performance of this reaction depends on good permeability of the hydrogel structures, exact reaction time, cell densities seeded in the hydrogel, and complete solubility of formazan. It was determined that the sections obtained as a result of hematoxylin&eosin staining were suitable for cell adhesion. In the images obtained as a result of the sections, the porous structures of the hydrogels are in a structure that will provide an opportunity for cell attachment and growth. In order for the obtained modified device to be serial in the bioprinting process, its integrated structure rather than a separate pump and nozzle system from the device will facilitate its production and bioprinting process. Sterilization is an important parameter in the use, dyeing and analysis of products obtained as a result of bioprinting. Depending on sterilization, viability results and cell analysis obtained as a result of staining are affected. For this reason, bioprinting should take place within the best sterilization protocols as possible. Different dyeing methods can be tried in order to prevent the problems in the dyeing process. Depending on the hydrogel and cell characterization, staining should be performed.

5. References

1. Sivashanmugam, A., Kumar, R. A., Priya, M. V., Nair, S. V., & Jayakumar, R. (2015). An overview of injectable polymeric hydrogels for tissue engineering. *European Polymer Journal*, 72, 543-565.
2. Baroli, B. (2006). Photopolymerization of biomaterials: issues and potentialities in drug delivery, tissue engineering, and cell encapsulation applications. *Journal of Chemical Technology & Biotechnology: International Research in Process, Environmental & Clean Technology*, 81(4), 491-499.
3. Daniele, M. A., Boyd, D. A., Adams, A. A., & Ligler, F. S. (2015). Microfluidic strategies for design and assembly of microfibers and nanofibers with tissue engineering and regenerative medicine applications. *Advanced healthcare materials*, 4(1), 11-28.
4. Prasathkumar, M. and Sadhasivam, S. (2021). Chitosan/Hyaluronic acid/Alginate and an assorted polymers loaded with honey, plant, and marine compounds for progressive wound healing—Know-how. *International Journal of Biological Macromolecules*, 186, 656-685.
5. Betz, J. F., Ho, V. B. and Gaston, J. D. (2020). 3D Bioprinting and its application to military medicine. *Military Medicine*, 185(9-10), e1510-e1519.

6. Dine, A., Bentley, E., PoulmarcK, L. A., Dini, D., Forte, A. E. and Tan, Z. (2021). A dual nozzle 3D printing system for super soft composite hydrogels. *HardwareX*, 9, e00176.
7. Gasperini, L., Maniglio, D., Motta, A. and Migliaresi, C. (2015). An electrohydrodynamic bioprinter for alginate hydrogels containing living cells. *Tissue engineering part C: Methods*, 21(2), 123-132.
8. Axpe, E. and Oyen, M. L. (2016). Applications of alginate-based bioinks in 3D bioprinting. *International journal of molecular sciences*, 17(12), 1976.
9. He, H., Li, D., Lin, Z., Peng, L., Yang, J., Wu, M. and Ruan, C. (2020). Temperature-programmable and enzymatically solidifiable gelatin-based bioinks enable facile extrusion bioprinting. *Biofabrication*, 12(4), 045003.
10. Hussain, M., Devi, R. R. and Maji, T. K. (2012). Controlled release of urea from chitosan microspheres prepared by emulsification and cross-linking method. *Iranian Polymer Journal*, 21(8), 473-479.
11. Brandner, J. M., Kief, S., Grund, C., Rendl, M., Houdek, P., Kuhn, C. and Moll, I. (2002). Organization and formation of the tight junction system in human epidermis and cultured keratinocytes. *European journal of cell biology*, 81(5), 253-263.



**BIOINK DESIGN, BIOPRINTING OF 3D BONE MODEL, AND IN VITRO
ANALYSIS**

**Özgün Selim GERMİYAN¹, Umut Doğu SEÇKİN², Aylin ŞENDEMİR³, Yiğit
UYANIKGİL⁴**

¹ Ege University, Health Sciences Institute, Stem Cell Department
ozgungermiyan@gmail.com

² Ege University, Graduate School of Natural and Applied Sciences, Department of Bioengineering

³ Ege University, Engineering Faculty, Department of Bioengineering

⁴ Ege University, Faculty of Medicine, Department of Histology & Embryology

Özet: *Vücudumuzdaki diğer birçok hücre tipi gibi Kemik hücreleri de tek tabakalı hücrelerdir ve hayatlarının devamı için mekanik destek sağlamak için bir ECM'ye ihtiyaç duyarlar. Kemik dokusu karmaşık, organize ve mineralize bir bağ dokusu olmasına rağmen, kemik kollajen bazlı yapılar, hidroksiapatit kristalleri ve osteoblastlar, osteositler ve osteoklastlardan oluşan yüksek bir yapısal hiyerarşiye sahiptir. Diatomlar (Bacillariophyceae); pektin, silika (SiO₂) ve lipidlerden oluşan ve frustül adı verilen duvara sahip bir deniz mikroalg sınıfıdır. Frustül yapısında bulunan silika miktarı diatom tipine göre %36 ile %95 arasında değişmektedir. Boyutları 2 ila 500 mikron arasında değişir. Bioglass, yapay kemik dokusunun mekanik özelliklerini iyileştirmenin yanı sıra kemik rejenerasyonu için kullanılır [1-4]. Bu çalışmada diatomlar aljinat ile karıştırılarak kompozit doku iskelesi oluşturulmuş ve aljinat hidrojel, aljinat/hidroksiapatit kompoziti ile oluşturulan doku iskeleleri ile sadece kemik rejenerasyonuna etkisi incelenmiştir. Bu amaçla önce literatür taraması yapılmış ve diatomların sitotoksik etkisinin olup olmadığı MTT analizi ile incelenmiş, ardından duvar yapılarındaki silika incelenmiş ve bu amaçla FTIR analizi ve SEM kullanılmıştır. Hidroksiapatit ve diatomlar için ideal konsantrasyon %3 w/v olarak belirlenmiştir. Daha sonra kültürlenmiş ve kompozit ve hidrojel yapılar halinde çoğaltılan SAOS-2 hücreleri eklenir, bioink elde edilir ve 3-D bioprinting yapılır ve kültürlenir. Kültivasyondan sonra, kemikleşme analizi için von Kossa ve Alizarin red-S boyaması yapıldı.*

Anahtar Kelimeler: Aljinat, hidroksiapatit, diatom, kemik doku mühendisliği, 3B-biyobaskı

Abstract: *Like many other cell types in our body, Bone cells are monolayer cells and need an ECM to provide them with mechanical support for the continuation of their lives. Although bone tissue is a complex, organized, and mineralized connective tissue, bone has a high structural hierarchy consisting of collagen-based structures, hydroxyapatite crystals and osteoblasts, osteocytes, and osteoclasts. Diatoms (Bacillariophyceae); are a class of marine*

microalgae, which have a wall (called frustules) consisting of pectin, silica (SiO₂), and lipids. The amount of silica present in the frustule structure varies between 36% and 95% depending on the type of diatom. Their size varies from 2 to 500 microns. Bioglass is used for bone regeneration as well as to improve the mechanical properties of artificial bone tissue [1-4]. In this study, diatoms were mixed with alginate and a composite tissue scaffolding was formed and only the effect on bone regeneration was examined with tissue scaffolds formed by alginate hydrogel, alginate/hydroxyapatite composite. For this purpose, first, a literature review was conducted and whether the diatoms have a cytotoxic effect was examined by MTT analysis, then the silica in the wall structures was examined and FTIR analysis and SEM were used for this purpose. The ideal concentration for hydroxyapatite and diatoms is determined as 3% w/v. Then, SAOS-2 cells that are cultured and multiplied into composite and hydrogel structures are added, bioink is obtained, and 3-D bioprinting is performed and cultured. After cultivation, von Kossa and Alizarin red-S staining was performed for ossification analysis.

Keywords: *Alginate, hydroxyapatite, diatom, bone tissue engineering, 3D-bioprinting*

1. INTRODUCTION

Tissue engineering is the repair of biological tissues by cells planted on synthetic or non-synthetic materials and by systemic or local regulators attached to them. The main purpose of tissue engineering is to create and use artificial tissues and organs produced in 3-D with advanced technology instead of tissues and organs that have lost their function or are too damaged to fulfill their functions. Tissues obtained by tissue engineering should respond to physical, chemical, and biological stimuli with adaptation such as natural tissues in vivo [5-7].

3-D printing is defined as the printing of a three-dimensional model as a material and produced with a 3-D printer, unlike traditional processing and production methods. A 3-D printer can be considered a type of industrial robot that produces computer-controlled three-dimensional material output. In the use of 3-D printers, parameters such as temperature, the viscosity of the polymer used and printing flow rate, sheet height are available [8,9].

The 3-D printing technique made using living structures and biomaterials that do not have any toxic effect on these living structures is called "3-D bioprinting". With 3-dimensional bioprinting, there are studies on the production of many tissues and organs today. 3D-Bioprinting aims to produce personalized organs and tissues and to minimize organ or tissue rejection because of complications that may occur after transplantation [10].

Different methods are used to ensure the solidification of the printing material and the most important of these is to ensure that the tissue solidifies in the desired time by using chemical cross-linking. The final step is to culture the created tissue under standard cell culture conditions. Within the scope of this project, 3 different types of bioprinting materials (polymer / composite content) were used and combined with cells [11].

2. METHODS

2.1 Modification of 3D-Printer as a 3D-Bioprinter

The device type used for printing in the study is “Rep-Rap 3-D printer” and it is a 3D printing device that can move in X, Y and Z planes and is frequently used in polymer printing technology. This device prints by extrusion of the molten polymer from the nozzle after the polymer is melted at high temperature in the chamber for prototype production (melting temperature varies depending on the polymer type). This system, which works with the melt method, is not suitable for bioprinting. High temperatures cause both the deterioration of polymer/composite structures and the death of cells. For this reason, mechanical modifications have been made on the device that will allow printing without the need for heating for bioprinting. After the modifications, mouse femur models were printed (Figure-1) [12].

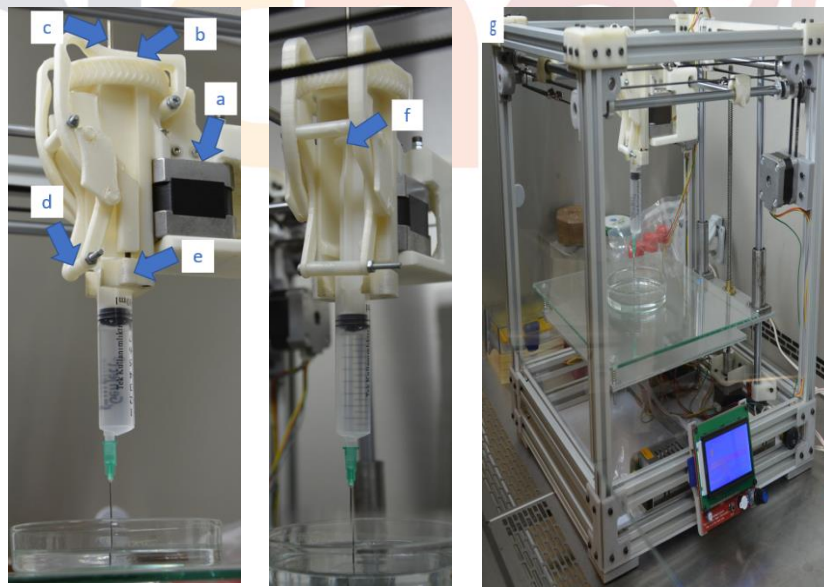


Figure-1: a) NEMA-17 stepper motor used to turn the wheel b) Wheel for the drive shaft c) Shaft d, e) Locking mechanism for the wide syringe f) Shaft pushing the piston down g) 3D bioprinter during printing.

2.2 Designing of 3D Bone Model

The first step in printing the mouse femur model aimed in the study is to create a computer model to determine the exact dimensions of the printed model and to print it. For this purpose,

the femur model was drawn in 2D with Autodesk AutoCAD 2017 program and in 3D with Microsoft 3D Builder v14.1.1302.0 program (Figure-2). The next step is to synthesize the ink (tissue culture containing polymer/material) to be used for tissue printing [13].

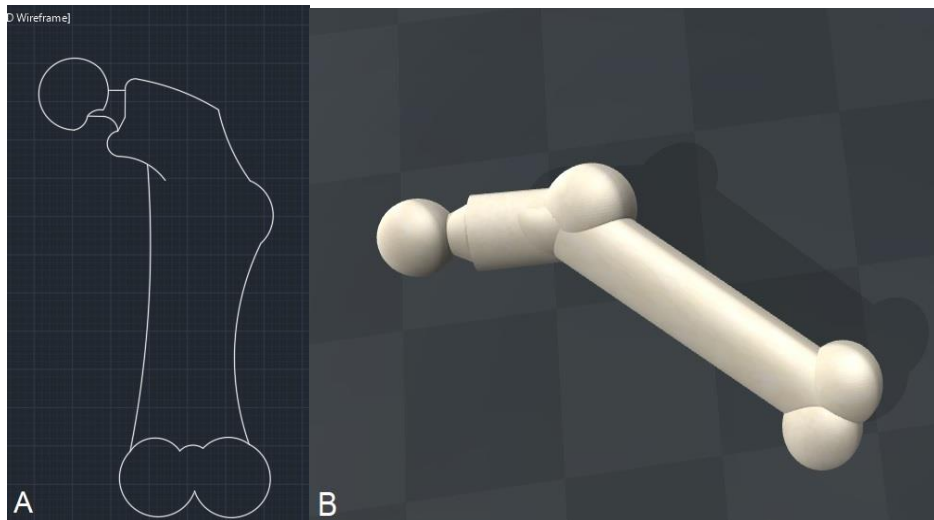


Figure-2: (A) 2-Dimensional mouse femur model, (B) 3-Dimensional mouse femur model

2.3 Cell Culture

In this study, SAOS-2 Osteosarcoma cell line, which is in the stocks of Ege Biomaterials and 3D Biointerphase Laboratory, was used. Cultivation was carried out in McCoy's 5A (%10FBS, %1 L-glutamine, %1 gentamycin) medium at 37°C with 5% CO₂.

2.4 Material Characterization

After the necessary modification in the printer and the completion of the mouse femur model, 10 mL small scale washing solutions were prepared with 10% w/v concentration of NaOCl, acetone, distilled water and methanol in order to remove the green pigments of the diatoms. After the washing process, the lightening of the colors was observed qualitatively the most in the methanol solution. FTIR analysis was performed to examine whether the qualitative result obtained was significant or not. During the washing process, it was observed that the diatoms were disintegrated while they were being discolored, and after each washing process, the samples were prepared and photographed by examining them with SEM without coating.

In order to determine whether diatoms, which have never been used in bone tissue engineering studies, have a cytotoxic effect, MTT analysis was performed in comparison with Hydroxyapatite [14-16].

After the preliminary studies, a literature review was carried out to determine the ideal alginate, diatom and hydroxyapatite concentrations used for bone tissue engineering and it

was determined that 2%, 3% and 4% w/v concentrations for alginate and 3% w/v concentrations for hydroxyapatite and diatom were determined. After obtaining the necessary literature information, viscosity measurement was performed to determine the suitability of the material for bioprinting.

3. RESULTS

3.1 FTIR analysis of diatoms obtained as a result of washings

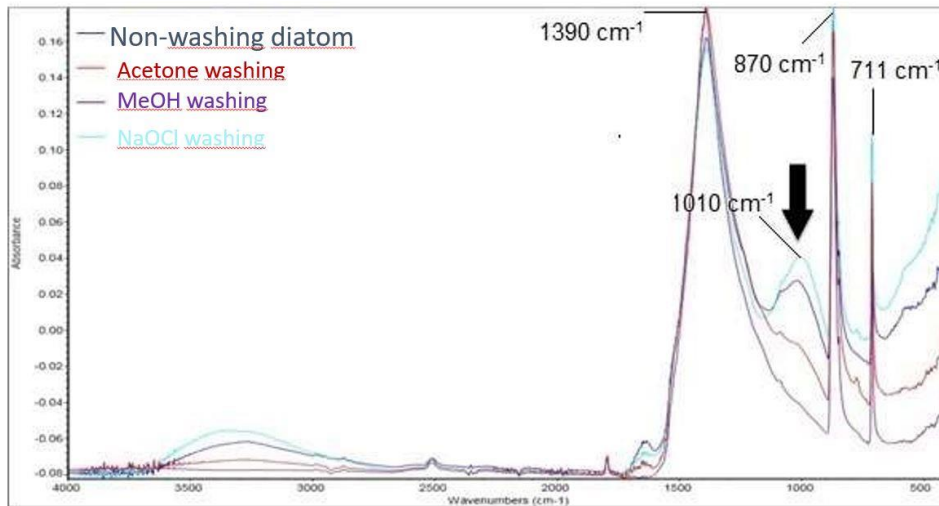


Figure-3: FTIR Graph

As seen in the graph, there are peak values between 1500 cm⁻¹ and 400 cm⁻¹. These peak values and the data they express are as follows; 1390 cm⁻¹ represents CH₃-Si bond, 870 cm⁻¹ Si-C bond, and 711 cm⁻¹ represents Si-O-Si bond

3.2 Diatom SEM Images

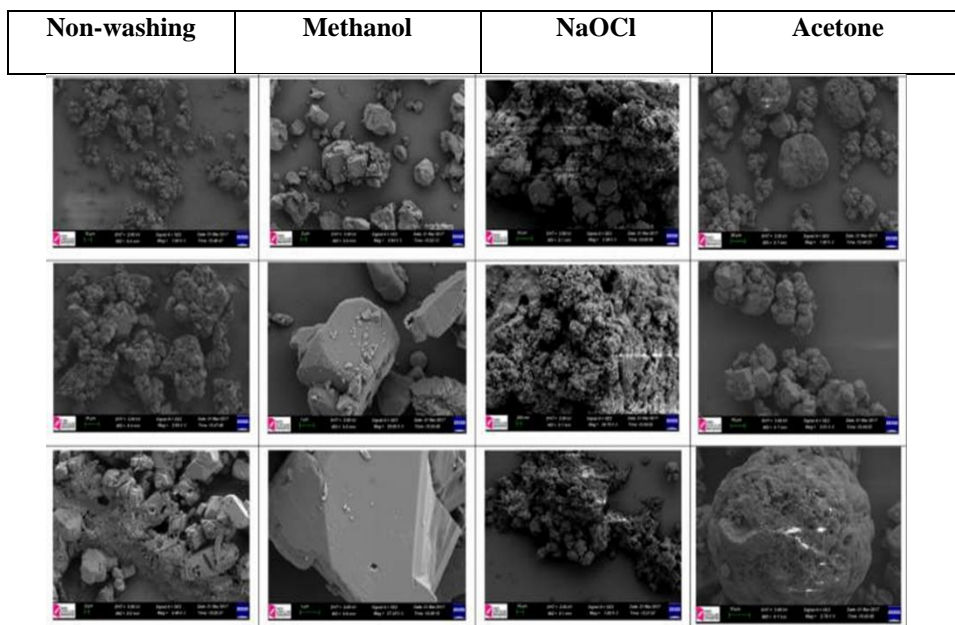


Figure-4: SEM photographs of diatoms were obtained as a result of different washing methods. Scale bar lengths in the images from top to bottom; For non-washing Diatoms; 10µm, 10µm, 2µm, For Diatoms washed with Methanol: 2µm, 1µm, 1µm, For Diatoms washed with NaOCl: 10µm, 0.2µm, 10µm, For Diatoms washed with Acetone: 20µm, 10µm, 10µm

3.3 Viscosity Values of Hydrogels and Composites

The viscosity values of the materials were measured from 10 rpm to 250 rpm. During the measurement, the speed was increased by 20 rpm every 10 seconds and the highest viscosity value was obtained with 4% alginate and the lowest viscosity value with 2% alginate. The ideal viscosity value was obtained with 3% alginate. It was observed that the diatom additive reduced the viscosity very slightly, but this was an acceptable (2% reduction) reduction (Figure-5).

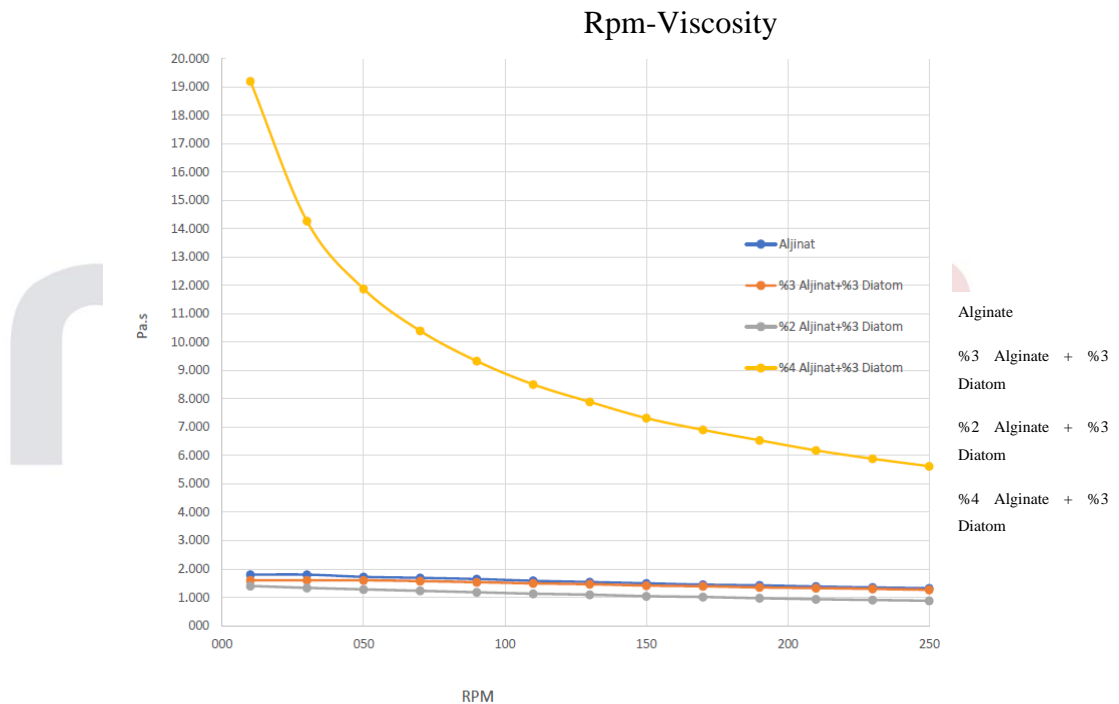


Figure-5: Rpm-Viscosity Graph

3.4 Investigation of the cytotoxic effect of diatoms and hydroxyapatite

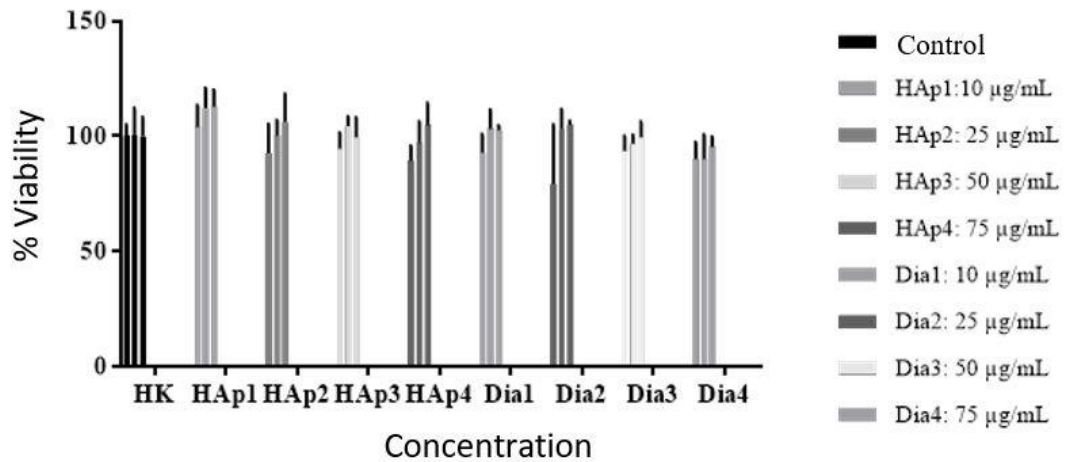


Figure-6: MTT analysis for Diatom & Hap

As a result of the MTT analysis performed to examine the cytotoxic effect of diatoms, it was observed that diatoms given to the cells at different doses did not have a cytotoxic effect.

3.5 3D-Bioprinting

The bioprinting process is carried out by taking the material into a nozzle/syringe and printing it, as shown in the Figure. After the bioprinting process, the products cross-linked with CaCl_2 were printed on 6 well plates and the media were added on them (Figure).



Figure-7: Bioprinted scaffolds

3.6 MTT analysis

MTT 7th day

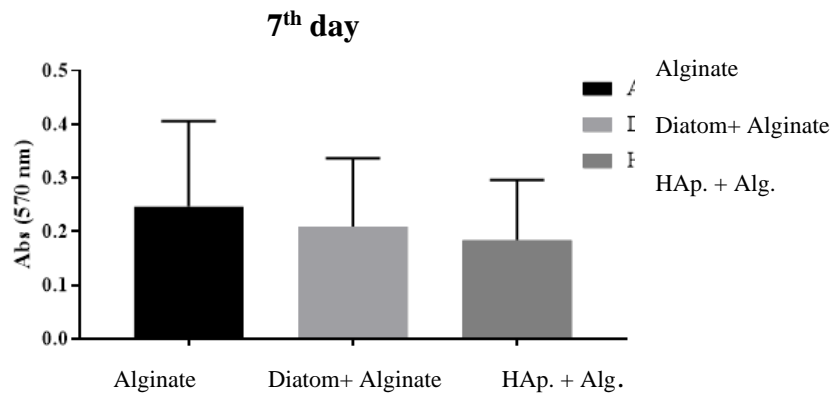


Figure-8: MTT results on day 7th

When the graph in the figure is examined, no significant difference was observed in terms of cell viability at the end of the 7-day incubation period of SAOS-2 cells cultivated in Alginate, Alginate/Diatom and Alginate/Hydroxyapatite scaffolds (Figure-8).

MTT 14th day

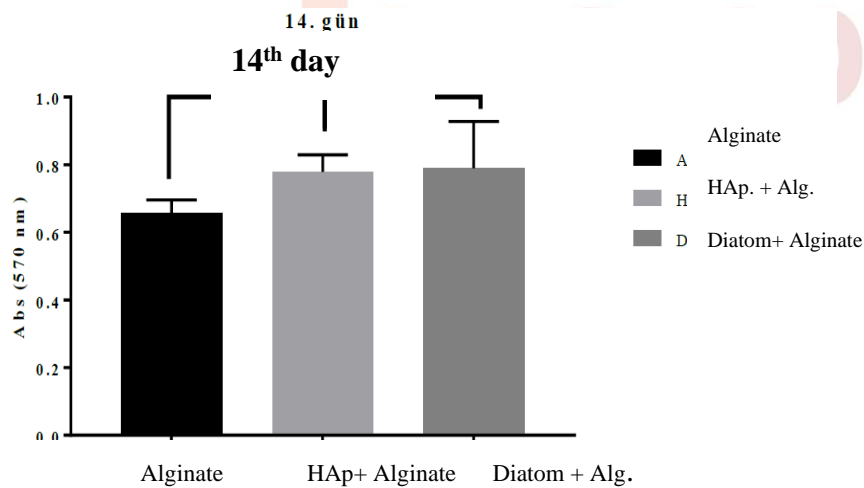


Figure-9: MTT results on day 14th

From this graph, it can be concluded that alginate/diatom and alginate/hydroxyapatite have a similar positive effect on viability and increase the number of cells statistically significantly ($p < 0.0001$) compared to the scaffold using only alginate. (Figure-9.).

3.7 Alizarin red-S Staining

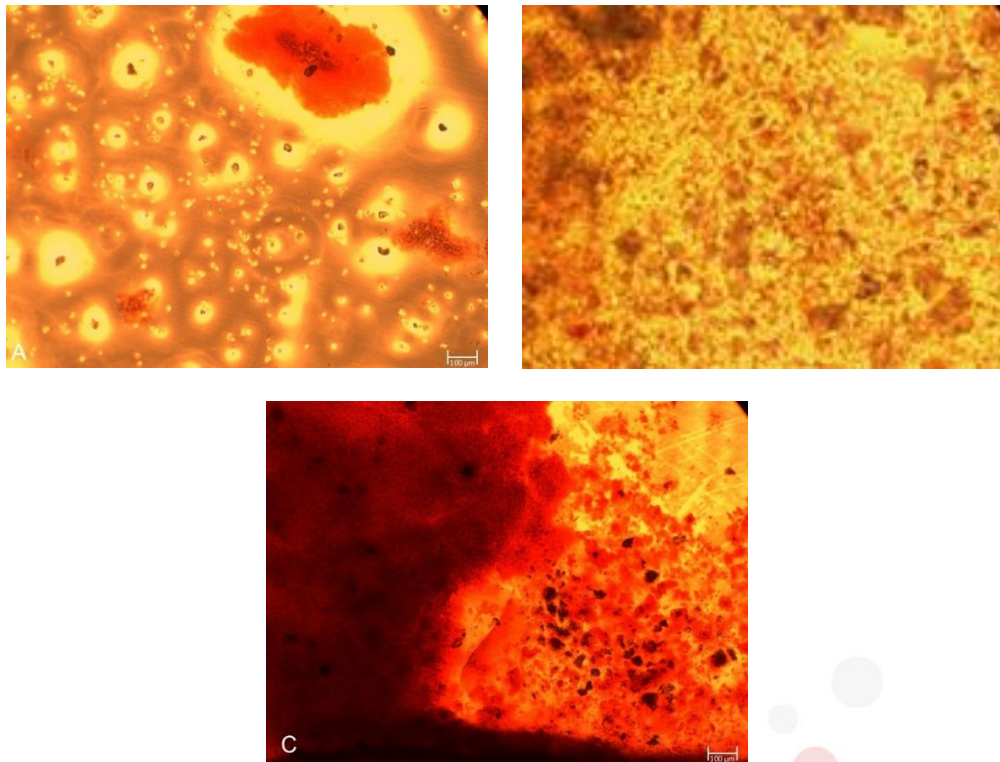


Figure-10: 3-Dimensional scaffolds stained with Alizarin Red-S (A: Alginat/Diatome, B: Alginat, C: Alginat/Hydroxyapatite) (20x)

3.8 von Kossa Staining

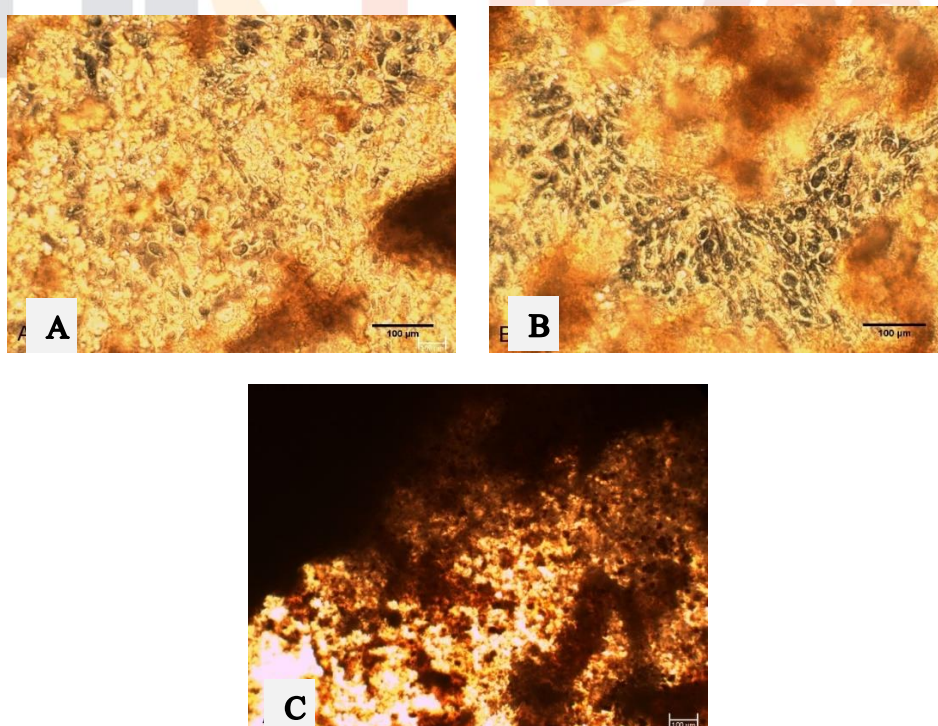


Figure-11: Von Kossa stained 3-Dimensional scaffolds (A: Alginate, B: Alginate/Diatome, C: Alginate/Hydroxyapatite)
(20x)

4. DISCUSSION

According to the obtained MTT results, the diatoms that were depigmented and cleaned with the method used did not show any toxic effects for SaOS2 cells. MTT results are an indication that the cells maintain their vitality by adhering to the hydrogel structure. According to the results obtained, the material determined as the best in terms of cell viability among the three hydrogels used is Alginate/Diatome composite. This is a direct proof that diatom is a promising material for use in bone tissue engineering studies.

As a result of MTT analysis, von Kossa and Alizarin red-S staining, it has been proven that diatoms positively affect ossification and that the determined 3% w/v diatom and 3% w/v alginate concentrations are ideal concentrations in bone tissue engineering studies in terms of both printability and substance diffusion.

5. REFERENCES

- [1] Nassif, N., Livage, J., "From diatoms to silica-based biohybrids", *Chemical Society Reviews*, 40(2):849-59, 2011.
- [2] Özbey, G., Atabey, N. "Diatomit Hakkında Bazı Bilgiler" II. National Chemical Symposium, 493-502, 1985, Ankara
- [3] Hench, L., L., "The Story of Bioglass", *Journal of Material Science: Material of Medicine*, 17:967-978, 2006.
- [4] Qizhi Z., C., Thompson, I., D., Boccaccini, A., R., "45S5 Bioglass-Derived Glass-Ceramic Scaffolds for Bone Tissue Engineering" *Biomaterials* V:27, I: 11, P: 2414-2425, 2006.
- [5] Ölçek-Buzkırın, B., "Veri Zarflama Analizi İle Türkiye'de Organ Nakli Merkezlerinin Performans Kıyaslaması," Akdeniz Üniversitesi Sosyal Bilimler Enstitüsü Ekonometri Ana Bilim Dalı Yüksek Lisans Tezi, 2012.
- [6] Şenköylü, A., Korkusuz, F., "Kıkırdak Onarımında Doku Mühendisliği Uygulamaları", *TOTBİD (Türk Ortopedi ve Travmatoloji Birliği Derneği) Dergisi* Cilt: 3 Sayı: 3-4, 2004.
- [7] Yılıgör-Huri, P., Hasırcı, N., Hasırcı, V., "Kemik Doku Mühendisliği", *Arşiv*, 19, 206, 2010.
- [8] Aydın, L., Küçük, S., Kenar, H., "Doku ve Organ Biyo Yazdırma Amaçlı 3B Biyo Yazıcı Tasarımı ve Geliştirilmesi", *Tıbbi Cihaz Tasarımı 3, Tıp Teknolojileri Ulusal Kongresi 2. Gün*, 16/10/ 2015.
- [9] B., Derby "Printing and prototyping of tissues and scaffolds." *Science* 338.6109: 921-926, 2012.
- [10] Murphy, S. V., Atala, A., "3D Bioprinting of Tissues and Organs". 32(8), 773-785, *Nature Biotechnology*, 2014.
- [11] Mironov, V., "Organ printing: Computer-aided Jet-based 3D Tissue Engineering." *TRENDS in Biotechnology* 21.4: 157-161, 2003.
- [12] <http://marlinfw.org/>
- [13] <http://www.indiana.edu/~ensiweb/lessons/BornToRun.html>
- [14] Berridge M., V., Tan A., S., "Characterization of the Cellular Reduction of 3-(4,5-dimethylthiazol-2-yl)-2,5-diphenyltetrazolium bromide (MTT): Subcellular Localization, substrate dependence, and involvement of mitochondrial electron transport in MTT reduction", *Arch Biochem Biophys*, 303(2):474-82, 1993.
- [15] Mosmann T. "Rapid colorimetric assay for cellular growth and survival: application to proliferation and cytotoxicity assays". *Journal of Immunological Methods*, 65:55-63, 1983.
- [16] Arber, D. A., Orazi, A., Hasserjian, R., Thiele, J., Borowitz, M. J., Le Beau, M. M., Vardiman, J. W. "The 2016 revision to the World Health Organization (WHO) classification of myeloid neoplasms and acute leukemia". *Blood, blood.*, 2016.

**ASPALATHUS LİNERAİS (ROOİBOS) EKSTRAKTININ SIÇAN TESTİS
DOKUSUNDA AKUT DÖNEMDE MELAMİNİN OLUŞTURDUĞU HASAR
ÜZERİNE KORUYUCU ETKİSİNİN İNCELENMESİ**

Selen AKYOL BAHÇECİ¹ Müge SARICAOĞLU²

*İzmir Kâtip Çelebi Üniversitesi Tıp Fakültesi, Histoloji ve Embriyoloji Ana Bilim Dalı, İZMİR, TÜRKİYE,
selenbahceci@gmail.com, mugesaricaoglu@hotmail.com*

Özet: Çalışmamızda, melaminin testiste akut toksisite sonucu, neden olduğu histopatolojik değişikliklere rooibosun iyileştirici etkisinin incelenmesi amaçlanmıştır. 18 adet Wistar-Albino erkek sıçan her grupta 6 hayvan olmak üzere; kontrol, melamin ve Melamin+Rooibos gruplarına ayrıldı. 31 gün süren deney sonrası alınan testis dokularında H&E, PAS, Masson Trikrom, immunohistokimyasal olarak Okludin, Klauidin ve TUNNEL boyamaları yapıldı. Melamin ve Melamin + Rooibos gruplarına 3 gün tek doz oral gavaj ile 140 mg/kg melamin verilmiştir, sonrasında melamin grubuna 28 gün boyunca SF, Melamin+Rooibos grubuna 28 gün 200 mg/kg Rooibos uygulanmıştır. Kontrol grubuna 3 gün oral gavaj, 28 gün I.P olacak şekilde sadece SF uygulanmıştır. Tüm deney gruplarındaki sıçanlar deneyin 31. gününde ketamin/ksilazin anestezisi altında dekapite edilmiş ve testisleri alınmıştır. Kontrol grubunda normal tubulus seminiferus kontortus morfolojisi gözlemlendi. Melamin grubunda tubulus seminiferus kontortus çapı ve alanında azalma, spermatogenik seri hücrelerde dejenerasyon, lümende azalmış spermatozoalar, seminifer epitel bazal membranında PAS+ likte azalma, interstisyel alanda ödem, açılma ve vasküler konjesyonda artmalar görüldü. Okludin ve klauidin boyamalarda diğer gruplardan daha az immün reaktivite pozitifliği vardı. TUNEL immünhistokimyasında ise büyük oranda artış mevcuttu. Rooibosun uygulandığı grupta olası antioksidan etkileri ile melamin kaynaklı oluşan histopatolojik hasarı ve apoptotik hücrelerde ışık mikroskopik düzeyde azalma izlendi. Sonuç olarak, çalışmamızda melamin maruziyeti testis dokusunda hasar oluşturdu ve infertilite tehlikesini arttırdığı, testiste oksidatif stresi indüklediği ve oksidan-antioksidan denge üzerine olumsuz etkisi olduğunu gözlemledik. Bu hasarın tedavisinde Rooibosun iyileştirici etkisinin olduğunu tespit ettik.

Anahtar Kelimeler: Melamin, Rooibos, Testis, Toksisite

Abstract: In our study, it was aimed to examine the curative effect of rooibos on the histopathological changes caused by melamine as a result of acute toxicity in testis. 18 Wistar-Albino male rats, 6 animals in each group; were divided into control, melamine and Melamine+Rooibos groups. H&E, PAS, Masson Trichrome, and immunohistochemically Occludin, Klauidin and TUNNEL stainings were performed on testicular tissues taken after

the 31-day experiment. Melamine and Melamine + Rooibos groups were given 140 mg/kg melamine by oral gavage as a single dose for 3 days, then SF was applied to the melamine group for 28 days, and 200 mg/kg Rooibos was administered to the Melamine+Rooibos group for 28 days. Only SF was applied to the control group, with oral gavage for 3 days and I.P for 28 days. Rats in all experimental groups were decapitated under ketamine/xylazine anesthesia on the 31st day of the experiment and their testicles were removed. Normal tubulus seminiferus contourus morphology was observed in the control group. In the melamine group, decrease in tubulus seminiferus contourus diameter and area, degeneration in spermatogenic series cells, decreased spermatozoa in the lumen, decrease in PAS+ in the seminiferous epithelial basement membrane, edema in the interstitial area, dilation and increased vascular congestion were observed. Occludin and claudin stainings had less immunoreactivity positivity than the other groups. On the other hand, there was a large increase in TUNEL immunohistochemistry. In the group in which rooibos was applied, possible antioxidant effects and histopathological damage caused by melamine and a decrease in apoptotic cells at the light microscopic level were observed.

In conclusion, in our study, we observed that melamine exposure caused damage to the testicular tissue and increased the danger of infertility, induced oxidative stress in the testis and had a negative effect on the oxidant-antioxidant balance. We found that Rooibos has a healing effect in the treatment of this damage.

Keywords: Melamine, Rooibos, Testis, Toxicity

GİRİŞ

Melamin ; plastik, kaplama, tutkal ve alev geciktiricilerin üretiminde yaygın olarak kullanılan kanserojen etkiye de sahip endüstriyel kimyasaldır. ABD'de de evcil hayvanların yiyeceklerine melamin ilavesi yapılarak protein kitlesinin artışı hedeflenmiştir. Ancak bu hayvanlarda melaminin toksik etki de yapabileceğini gösteren bir çalışma yapılmamıştır. Dünya Sağlık Örgütü'nün 2008 yılında; Çin'de melaminin suyla seyreltilmesinden sonra bebek mamalarına ve sütlere katılarak, görünür protein kitlesinin arttırmak için ham bileşenlere eklendiği bildirilmiştir. Bunun sonucunda melaminli süt tozu yiyen 6 bebek hayatını kaybederken, 300 bin çocukta da çeşitli şikâyetler görülmüştür. Ölen bebeklerin böbrek biyopsilerinde, tubulusların içinde kristallerin varlığı kanıtlanmıştır. Rahatsızlanan çocukların annelerinin ifadelerinde özellikle idrar yaparken çılgık çılgığa ağladıkları belirtilmiştir.

Testis fonksiyonunu etkileyen ve testiste sperm yapımını bozan her türlü durum infertilite nedenidir. Testis enfeksiyonları ve travmaları, testise yönelik cerrahi girişimler, Kriptorşidizm, yüksek ısı ve toksik maddeye maruz kalma (radyoterapi/kemoterapi/kurşun-akü-cıva sanayi v.b), insektisitler bu duruma sebebiyet verebilmektedirler. Melaminin akut toksisitesi, esasen böbreklerde lokalize olmakla beraber son yıllarda yapılan çalışmalarla sıçanlarda dişi ve erkek üreme sistemi üzerinde de toksik bir etkisinin mevcut olduğu gösterilmiştir. Testis üzerinde yapılan çalışmalarda artan melamin dozu, oksidatif stres yolu ve apoptozu indükleyerek, hücrelerin apoptotik oranlarını arttırdığını, tubulus seminiferus kontortusların çaplarında değişikliğe ve morfolojisinde farklılıklara neden olduğu bildirilmiştir. Bunlar; tubulus seminiferus kontortus yapısının bozulmasına, nekrotik germ hücrelerinin sayıca artmasına, sperm miktarlarının azalmasına ve anormal görünümlü sperm varlığı dâhil olmak üzere çeşitli anormalliklere sebebiyet vermiştir. Yine farklı oranlarda melamin takviyesi uygulanan hayvan deneyi gruplarında; tubulus seminiferus kontortuslarda spermatojenik hücrelerin sitoplazmasında yer yer foliküler dejenerasyonlar, bazal membranda kalınlaşma ve lümende düzensizlik görülmüştür. Erkek domuzlarda melamin maruziyeti, kan-testis bariyer bütünlüğünü tahrip ederek testis toksisitesine yol açmıştır.

Güney Afrika'da, birçok şifalı bitki onlarca yıldır bitki çayı olarak tüketilmiştir. Rooibos, Güney Afrika'da çok çeşitli formları bulunan bir bitki türüdür. Çok sık olarak, bu bitkiden hazırlanan şarap, bira ve çay gibi içecekler hem kültürel olarak hem de beslenme veya tıbbi amaçlar için de tüketilmektedir. Rooibos çayının, antioksidan, antimutagenik, antialerjik, vazodilatör ve dermatolojik etkileri üzerine tıbbi özellikleriyle ilişkili birçok çalışma yapılmıştır. Lawal ve arkadaşları; rooibos ekstraktının dizel egzoz partiküllerinden kaynaklı kardiyovasküler toksisiteye karşı koruyucu potansiyelini göstermişlerdir. Awoniyi ve arkadaşları, sulu rooibos ekstraktlarının antioksidan savunma mekanizmalarını arttırdığını ve testis dokusunda oksidatif stres hasarına karşı koruyucu etkisi olduğunu göstermişlerdir. Testis dokusu içinde bulunan Sertoli hücreleri, spermatogenez için gereklidir. Sertoli hücreleri, germ hücrelerine doğrudan temas yoluyla yapısal ve nutrisyonel destek sağlar ayrıca tubulus seminiferus kontortusların içindeki mikroçevreyi kontrol ederek spermilerin ilerlemesini kolaylaştırmaktadır. Bitişik Sertoli hücreleri arasında bazolateral bölgede sıkı bağlantı noktaları bulunur ve bu bağlantılar kan-testis bariyerini oluşturmaktadır. Kan-testis bariyeri, testisleri otoantijenik germ hücrelerini immünolojik olarak koruyan ve maddelerin intratübüler sıvıya girişini kontrol eden ayrıcalıklı bariyerdir. Bu bariyerin geçirgenliği periferik endotelial hücrelerden 50-100 kat daha azdır, germ hücre mayozunun tamamlanması

ve spermiogenez için gerekmektedir. Kan-testis bariyerinin bütünlüğü ayrıca genetik, toksik madde maruziyeti, iltihaplanma da dâhil çeşitli hastalıklardan etkilenebilmektedir ve bu durum infertilite ile sonuçlanabilmektedir. Son yıllarda yapılan çalışmalarla, Sertoli hücrelerinin üreme toksisitesi için potansiyel hedef olabileceği gösterilmiştir.

Gow A. Ve arkadaşları yapmış oldukları bir çalışmada, Oligodendrosit spesifik protein (OSP) / Klaudin-11'i, Merkezi sinir sistemi miyelinizasyonunda görev alan ve testiste bilinmeyen fonksiyonlu bir transmembran proteini olarak tanımlamışlardır. OSP olmayan farelerde hem nörolojik hem de üreme eksikliği belirtileri gösterilmiştir. MSS'de sinir iletiminin yavaşlaması, arka bacak zayıflığı, erkek sıçanlarda infertilite dikkat çekmiştir. Elde edilen sonuçlar, OSP'nin paralel dizili sıkı bağlantılar aracısı olduğu ve bu proteinin sıkı bağlantılardaki diğer zar proteinlerinden farklı olduğunu göstermiştir. Bu yeni sonuçlar, Klaudin ailesinin, spermatogenez ve normal MSS fonksiyonu için gerekli olan sıkı bağlantıların parasellüler fiziksel bariyerini oluşturmadaki rolünün doğrudan kanıtıdır.

Kan-testis bariyerinde bulunan sıkı bağlantılarında protein ekspresyon seviyeleri ve testislerde mitojenle aktive olan protein kinaz yolunun protein seviyeleri ölçülmüştür. Melaminin doza bağımlı olarak serum testosteron düzeylerini düşürdüğünü, testis ve epididimde histopatolojik değişikliklere neden olduğu gösterilmiştir. Kan-testis bariyerindeki proteinlerin anormal değişiklikleri bariyerin geçirgenliğinin artmasıyla sonuçlanmıştır. Erkek domuzlarda, melaminin ayrıca ZO-1, okludin, N-kadherin ve connexin-43 protein seviyelerini düşürdüğü, buna paralel olarak p-Erk, p-JNK ve p-p38 protein seviyelerini arttırdığı bildirilmiştir. Bu bulguların sonucunda; melaminin kan-testis bariyerinde, birleşme proteinlerinin ifadelerinin down regülasyonunu göstermekte, melamin maruziyeti kan-testis bariyeri bütünlüğünü tahrip ederek erkek domuzlarda testis toksisitesine yol açtığı gösterilmiştir. (Lu ve ark. 2009)

Literatür incelemesinde melaminin sıçan testislerinde oluşturduğu harabiyet üzerine, rooibos'un iyileştirici etkisinin araştırıldığı ile ilgili herhangi bir çalışmaya rastlamadık. Biz bu çalışmamızda; rooibos ekstraktının takviye olarak kullanılmasıyla, melaminin akut dönemde testis dokusu üzerinde yaptığı harabiyetin iyileştirici etkilerinin hem histopatolojik olarak hem de erkek infertilitesinin önemli nedenlerinden biri olan kan-testis bariyeri sıkı bağlantı proteinlerinden Klaudin ve Okludin'in immünohistokimyasal olarak değerlendirilmesini amaçladık.

YÖNTEM

8 haftalık, 18 adet Wistar-albino sıçanlar kontrol (K), melamin (M), melamin+ rooibos (M+R) gruplarına ayrıldı. Melamin 3 gün oral gavaj-Rooibos 28 gün IP olarak uygulandı. Ketamin anestezisi altında çıkarılan testis dokusu formaldehit ve bouinde fikse edilerek rutin histolojik doku takip edildi. Kesitler 5µm kalınlığında alınarak H&E, Masson, PAS, IHC, TUNEL boyamalar yapıldı.

BULGULAR

Denek Vücut Ağırlıkları Ölçümleri

	Gruplar			Test İstatistikleri	
	Kontrol n=6	Melamin n=6	M+R n=6	Test değeri	P değeri
Vücut Ağırlığı (gr) $\bar{x} \pm ss$	261,5±7,9	119,3±7,9	402,5±4,3	F= 2463,5	<0,001

Denek Testis Ağırlıkları Ölçümleri

	Gruplar			Test İstatistikleri	
	Kontrol n=6	Melamin n=6	M+R n=6	Test değeri	P değeri
Testis Ağırlığı (gr) $\bar{x} \pm ss$	2,9±0,6	2,1±0,4	3,44±0, 4	F= 9,8	0,002

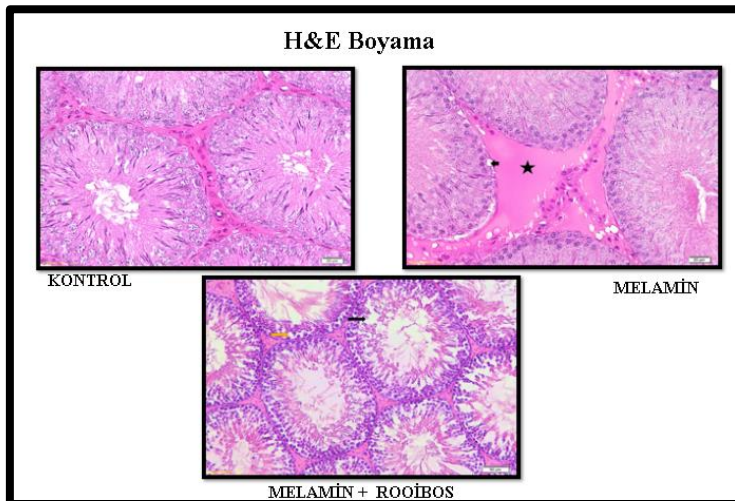
Tubulus Seminiferus Kontortus Çap Ölçümleri

Gruplar	N	Mean±S. Sapma
KONTROL	10	271,33±57,1
MELAMİN	10	192,0 ± 16,4
ROOİBOS	10	360,6 ± 98,5

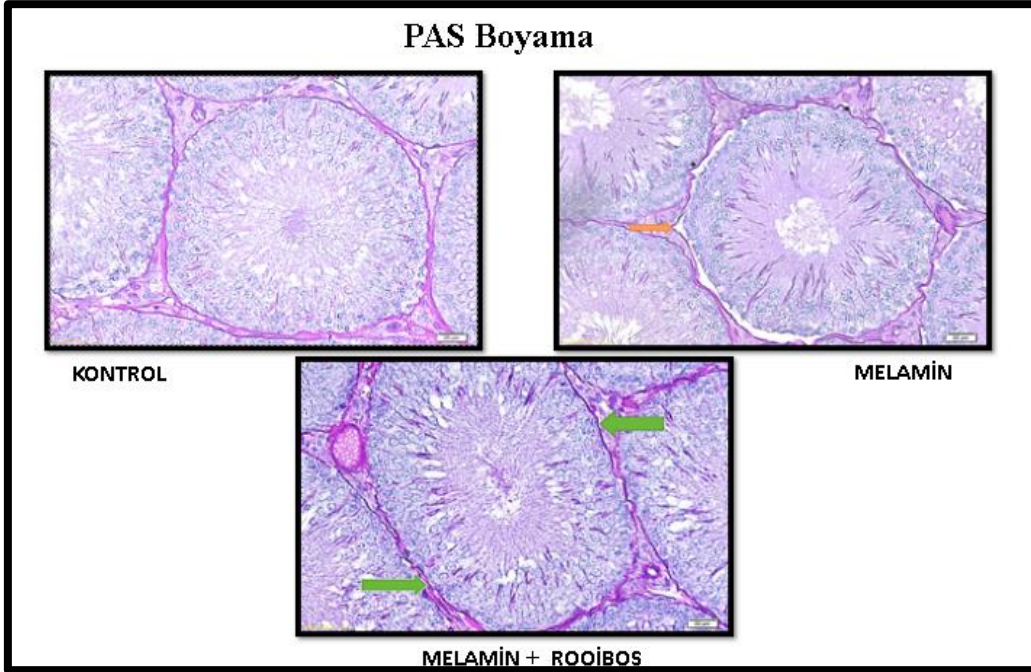
Tubulus Seminiferus Kontortus Alan Ölçümleri

Gruplar	N	Mean±S. Sapma
KONTROL	10	42193,6±2212,7
MELAMİN	10	32675,2 ± 5575,4
ROOİBOS	10	56114,8 ± 11090,0

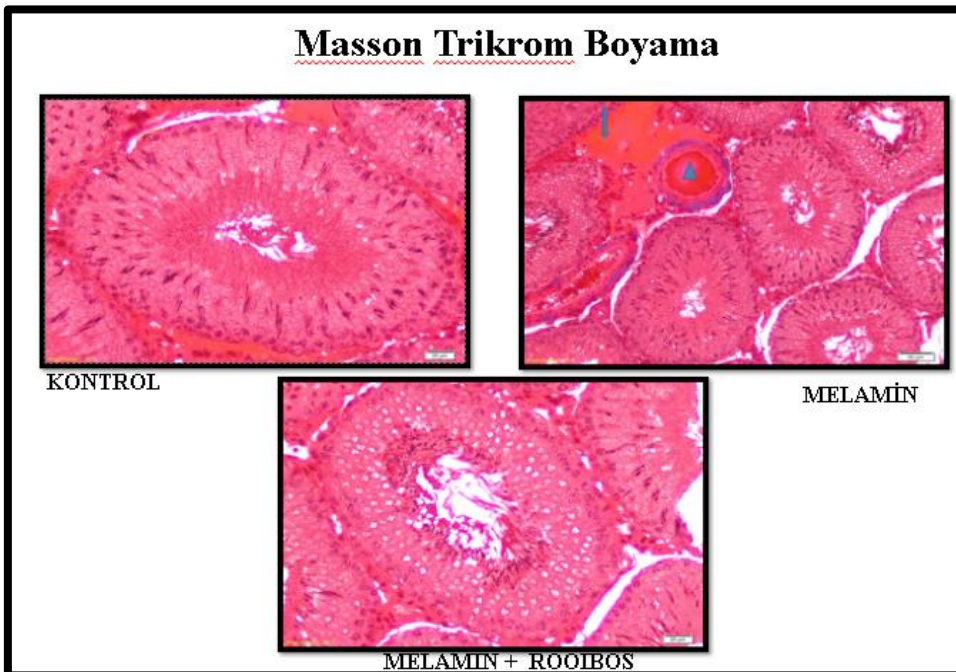
Biz bu çalışmamızda melaminin spermatogenetik seri hücrelerinin prolifasyonunu azalttığı, seminiferus tubulus kontortusların hem çapında hem alanında azalmaya neden olduğu ayrıca deney sonrası vücut ağırlıklarında ve testis ağırlıklarında azalmaya neden olduğu buna karşın apopitozu ise arttırdığını tespit ettik.



Resim 1: Tubulus seminiferus kontortusların Hematoksilin-Eozin boyama görüntüleri. İntersitsiyel alanda ödem (★), Seminifer tübül duvarında ödem (↔) gözlemlendi. Germinal epitelde açılmalar (→), vakuolizasyon gibi (→) bulgularda fark edilir şekilde azalma gözlemlendi.

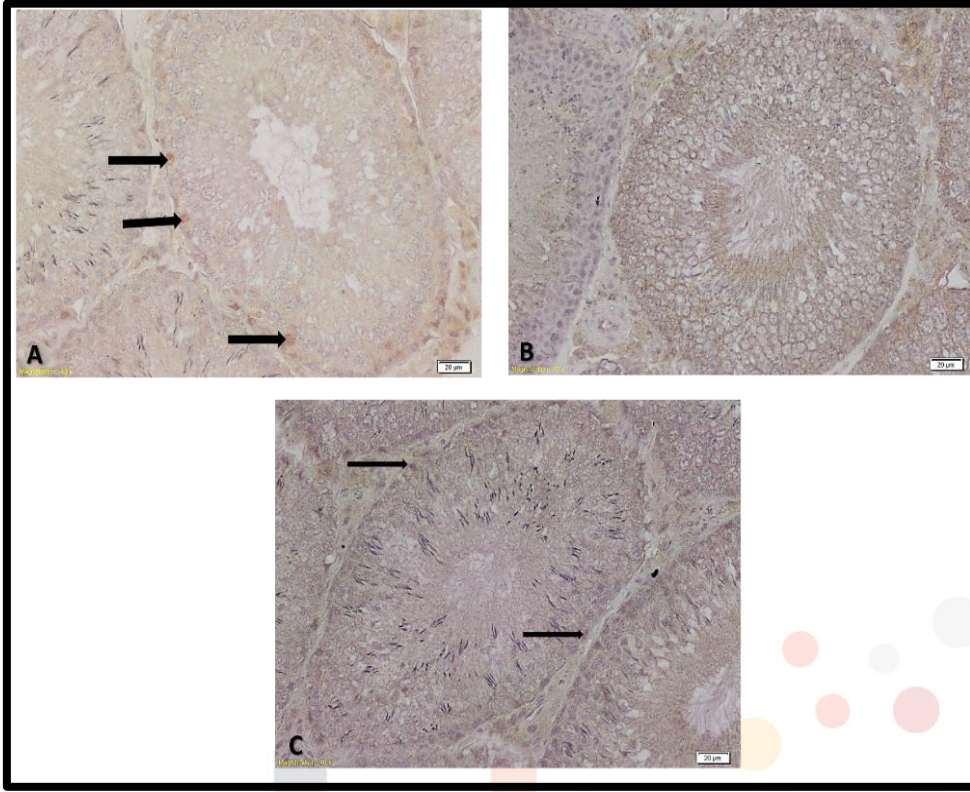


Resim 2: Tubulus seminiferus kontortusların Periyodik asit Schif boyama görüntüleri. Bazal membranda kopma (→) ve ondülasyonlar () gözlemlendi. Bazal membran bütünlüğü (→) gözlemlendi.*

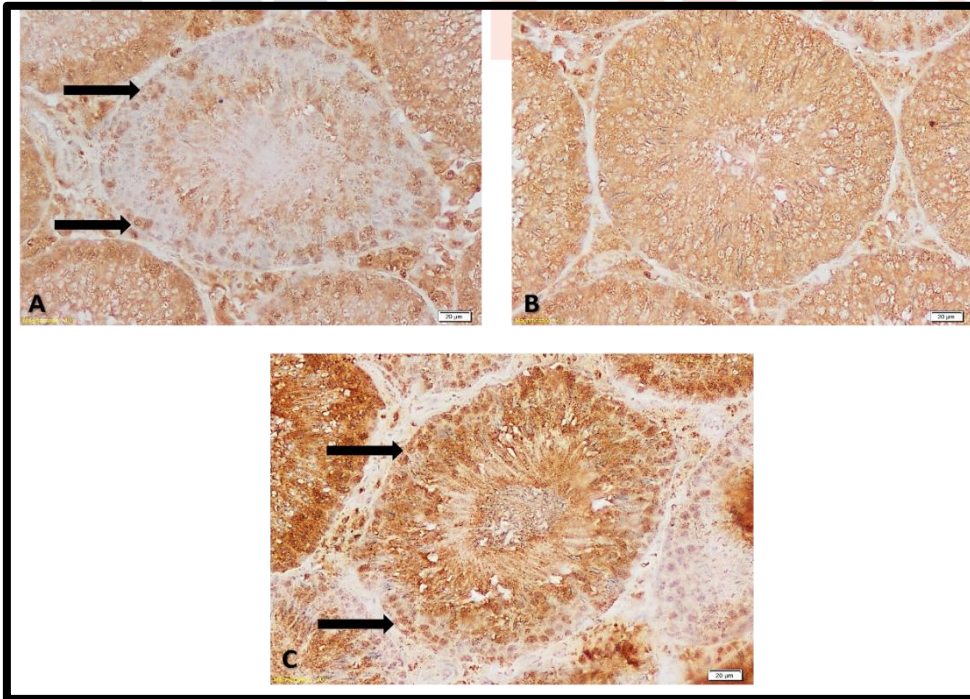


Resim 3: Tubulus seminiferus kontortusların Masson Trikrom boyama görüntüleri.

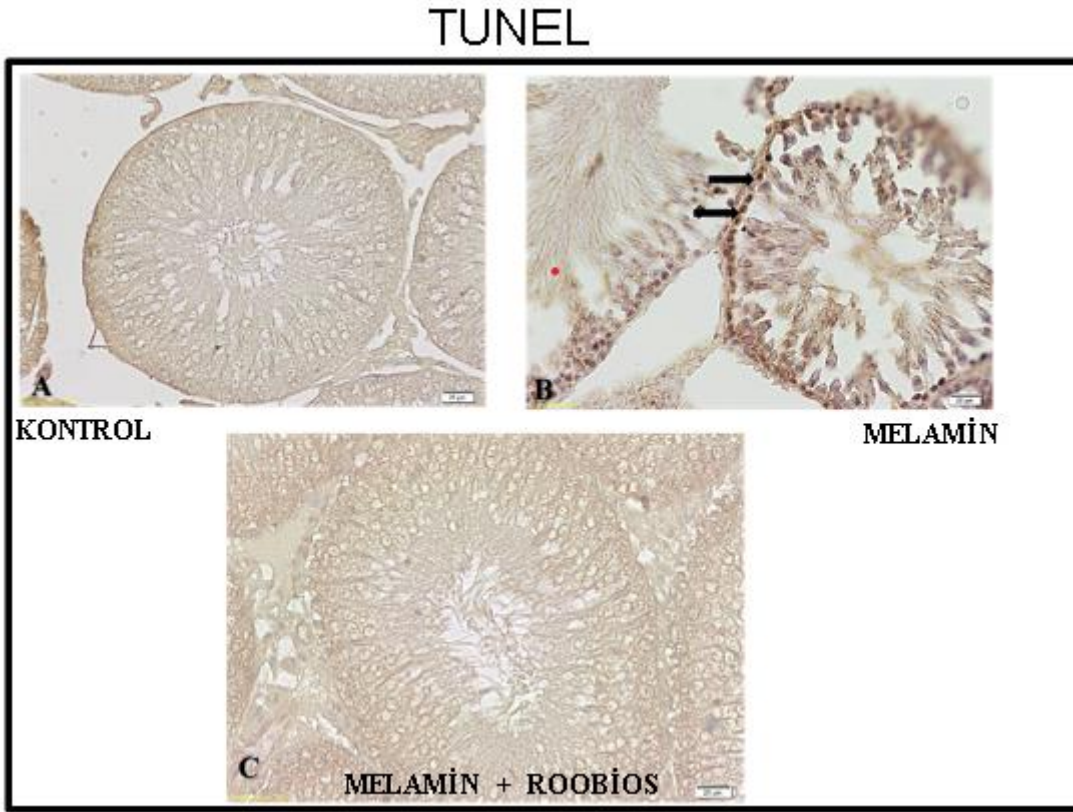
İntersitsiyel alanda ödem (↓), ve vasküler konjesyon (▲) gözlemlendi.



Resim 4: Tubulus seminiferus kontortusların IHC- Okludin immünreaktivitesi boyama görüntüleri. A-Kontrol Grubu, B-Melamin Grubu, C- Melamin +Rooibos Grubu.



Resim 5: Tubulus seminiferus kontortusların IHC- Klaudin immünreaktivitesi boyama görüntüleri. A-Kontrol Grubu, B-Melamin Grubu, C- Melamin +Rooibos Grubu.



Resim 6: Tubulus seminiferus kontortusların Tunnel görüntüleri.

Kontrol grubu ile kıyaslandığında melamin grubunda seminifer tübül çapında ve alanında azalma, rooibos grubunda ise artış istatistiksel olarak ($p < 0.05$) anlamlı bulundu.

Kontrol grubunun H&E boyamasında; seminifer tübüller incelendiğinde spermatogenik seri hücrelerin ve Sertoli hücrelerinin normal görünümde olduğu görüldü. Tübüllerin bazal membranının intakt olduğu, peritubular miyoid hücrelerin, interstisyel bağ doku alanındaki yapıların ve Leydig hücrelerinin normal histolojik görüntüde olduğu gözlemlendi. Melamin grubunda regresif seminifer tübüllere rastlandı. Seminifer tübüllerin lümeninde spermatogenik hücre döküntüleri görüldü. Spermatogenik seri hücrelerinde yer yer vakuolizasyon ve ayrışmalar görüldü. Rooibos grubundaki testislerin histolojik görüntüleri kontrol grubuna benzerdi. Spermatogenik hücreler normale yakın, lümeninde spermatozoalarında varlığı görüntülendi.

Kontrol grubunun PAS boyalı kesitleri incelendiğinde; spermatogenik seri hücreler içerisinde sperm akrozomlarının ve seminifer tubullerin düzgün, kesintisiz PAS (+) bir bazal membranla çevrelendiği görüldü. Melamin grubunda, bazal membranlarında PAS pozitifliğin zayıf

olduđu ve yer yer kesintiye uğradığı görüldü. İnterstisyel alanda Leydig hücrelerinde dejenerasyon ve ödem izlendi. Rooibos grubunda kontrol grubuna benzer şekilde seminifer tubullerin normale yakın morfolojik bulgusu ile vasküler konjesyonda ve bazal membrandaki ayrışmada iyileşme olduđu gözlemlendi.

Kontrol grubu Masson Trikrom boyalı kesitler incelendiğinde, bağ doku kapsülü olan tunika albuginea ve yoğun dizilimli kollajen lifler gözlemlendi. Melamin grubunda ise, kapsülde ayrılmalar, dejeneratif ve nekrotik seminifer tubuller izlendi. Rooibos grubunda, melamin grubuna nazaran interstisyel doku alanındaki hasar ve ödemde azalma görüldü. Tübüler atrofide azalma olup, kontrol grubuyla benzer özellikler bulundu.

Kontrol grubu ve rooibos grubuna ait testis dokularında bulunan seminifer tübüllerdeki hücrelerde çok az sayıda TUNEL pozitif işaretlenmiş hücelere rastlandı. Melamin grubunda ise seminifer tubullerdeki TUNEL pozitif hücelerin sayısında artış olduđu gözlemlendi.

Hücreler arası sıkı bağlantı proteinleri olan okludin, klaudinin immunohistokimyasal incelemelerinde kontrol ve M+R grubunda sertoli hücrelerinde ekspresyonun güçlü olduđu gözlemlendi, ancak melamin grubunda kan testis bariyerinin bozulmasına bağlı olarak okludin, klaudinin ekspresyonun azaldığı tespit edildi.

TARTIŞMA-SONUÇ:

Testiküler toksisiteden sorumlu kritik faktörler arasında hormonal, çevresel, davranışsal ve beslenme dengesizlikleri yer almaktadır (Sharpe ve Franks, 2002). Melamin, günlük ürünlerde yaygın kullanımı ve kimyasal madde toksisitesine de sebep olan bir kimyasaldır. İnsanlarda ve hayvanlarda melaminin akut ve kronik maruziyetine ilişkin veriler daha çok nefrotoksisiteye dayalıdır ancak diğer organlardaki etkileriyle ilgili az veri bulunmaktadır (Skinner ve ark., 2010). Kimyasal kaynaklı toksisitenin ortadan kaldırılması ya da azaltılması amacıyla bitki özütlerinden yararlanıldığı gösterilmiştir. Bu amaçla rooibosun flavonoid içeriği ve antioksidan aktivitelerini araştıran çok çeşitli çalışmalar yapılmıştır

Duan ve arkadaşlarının ICR türü farelerde yapmış olduđu çalışmada, Melamin 2, 10, 50 gr/kg dozlarında ve 28 gün boyunca uygulama sonucunda; MA10 grubunda hafif lezyonlar, MA50 grubunda ise en fazla hasar görülmüştür. Morfolojik olarak seminifer tübül yapısının bozulması, nekrotik germ hücrelerinin ve sperm anormalliklerinin artması, sperm sayısının azalması gibi çeşitli anormallikler görülmüştür, sonuç olarak MA'nın testislere zarar verebileceğini bildirmişlerdir. MA50 grubunda hasarın daha fazla olduđu bu çalışmada

uygulanan ilaç dozunun bizim çalışmamızdakinden az olmasına rağmen süre olarak daha fazla maruz bırakılması nedeniyle bizim çalışmamızın morfolojik bulguları ile uyumluydu.

Chang ve arkadaşlarının farelerde tek başına melaminin ve melamin-siyanürik asit karışımının akut testis toksisitesini ilk kez göstermiş olduğu Kunming cinsinde yapmış olan çalışmada melamin (MA, 30, 140 veya 700 mg/kg/gün), melamin ve siyanürik asit karışımı (MC, her biri 15, 70 veya 350 mg/kg/ gün) uygulanmıştır. Uygulamalar sonrasında 1 ve 5 günde son dozdan sonra ötenazi yapılmıştır. Melamin maruziyetinden sonra, histopatolojik olarak, tüm dozlarda Melamin uygulamaları, kanalların lümeninde tamamen spermatoza yokluğu, piknotik ve nekrotik germ hücresi kütlelerinde artış görülmüştür. Transmission elektron mikroskopik incelemelerde ise tek başına melamine maruz kalma, peritübüler doku yapısında doza bağlı hasara neden olduğu ve testis toksisitesine neden olabileceği rapor edilmiştir. Histopatolojik bulgular bizim çalışmamızla korelasyonluydu.

Ling ve arkadaşlarının domuzlarda yapmış olduğu başka bir deneysel çalışmada, melamin uygulanan grupların testislerinde belirgin Sertoli hücre vakuolasyonu, germ hücrelerinin pul pul dökülmesi ve çok çekirdekli dev hücreler görüldüğünü bildirmişlerdir. Chang ve Ling'in çalışmasında bildirilen çok çekirdekli dev hücreleri, bizim çalışmamızın melamin grubunda mevcut değildi ancak bunun doza bağlı olabileceğini ve ayrıca siyanürik asitin de kümülatif etkisinin de olabileceğini bize düşündürdü. Buna karşın, seminiferus tubulus kontortus lümenlerinde spermatoza yokluğu, piknotik ve nekrotik germ hücresi kütlelerinde artışı gibi bizim çalışmamızın histopatolojik bulguları ile benzerlik göstermekteydi.

Crissman ve arkadaşları, Melamin'in sıçan testislerinde hasara neden olduğunu gösterdikleri başka bir çalışmada, seminiferus tubulus kontortuslarda yapısal değişiklikler, bazal membranın fokal olarak yer yer ayrılmaları bildirmişlerdir. Benzer şekilde bizim çalışmamızda da literatürdeki bu bulgulara paralel olarak melamin grubundaki PAS kesitlerinde, seminiferus tubulus kontortus bazal membranlarında zayıf PAS pozitiflik ve yer yer kesintili yapıda olduğu görüldü.

Chang ve arkadaşlarının yapmış olduğu TM4 hücre hattındaki melamin toksisitesini in vitro olarak değerlendiren ilk çalışmada yapılan melamin maruziyetinin konsantrasyona bağlı bir şekilde TM4 hücrelerinde ultrastrüktürel hasara neden olduğu, Sertoli hücrelerinde tight junction ve hücre iskeleti protein ekspresyonunun bozulmasına neden olduğu gösterilmiştir. MA'ya maruz bırakılan Sertoli hücre kültürlerinde hem N-cadherin hem de okludin ekspresyonunun down regülasyonu gözlenmiştir. Bu down regülasyonlar, melaminin kan-

testis bariyerinin bozulmasından sorumlu olabileceğini ve bu nedenle, çalışma sonunda Sertoli hücrelerinin melamin kaynaklı erkek üreme toksisitesi için önemli bir hücresel hedef olabileceği bildirilmiştir.

Ling ve arkadaşlarının süttten kesilmiş erkek domuz yavrularında yapmış olduğu bir çalışmada, 10 hafta boyunca 0, 100, 300 ve 1000 mg/kg melamin konsantrasyonlarına maruz bırakılmıştır ve 1, 7 ve 14. günlerde ötenazi yapılmıştır. Melaminin doza bağlı olarak serum testosteron düzeylerini düşürdüğünü, testis ve epididimde belirgin histopatolojik lezyonlara neden olduğu belirtilmiştir. Bu histopatolojik değişikliklerin Kan-testis bariyerinde hasarlanma sonucu artan geçirgenliğinden olduğu ile kanıtlanmıştır. Bu çalışmada, kan-testis bariyerindeki hasarlanmaya bağlı olarak ZO-1, Occludin, N-cadherin ve connexin-43 protein ekspresyonlarında azalma olduğu bildirilmiştir. Bizim çalışmamızda da kan-testis bariyerindeki tight junction bağlantısında bulunan Kludin ve Okcludin proteinlerinin bütünlüğünün korunup korunmadığı araştırıldı. Ve literatürle uyumlu bir şekilde immünohistokimyasal boyamalarımız sonucunda tight junction proteinleri olan Occludin-kludin kontrol ve rooibos grubunda net görüntülenirken, melamin grubunda melaminin toksik etkisine bağlı olarak kan-testis bariyerinin zarar görmesiyle bu proteinlerin ekspresyonlarında azalma gözlenmiştir. Bizim çalışmamızda melaminin etkisiyle bozulan kan-testis bariyeri bütünlüğünün Rooibosun iyileştirdiği gözlemlendi.

Huang ve arkadaşlarının Kunming farelerinde yapmış olduğu 5 gün süren çalışmada normal salin negatif kontrol grubu (0,1 mL/10 g vücut ağırlığı), düşük doz (400 mg/kg) melamin grubu, orta doz (800 mg/kg) melamin grubu ve yüksek doz (ve 1600 mg/kg) melamin grupları oluşturulmuştur. Apoptozla ilişkili proteinlerin immünohistokimyasal boyamalarında Bcl-2'nin ekspresyonu önemli ölçüde azalmışken, Bax ve kaspaz-3'ün ifadeleri önemli ölçüde arttığı gösterilmiştir. Ve sonuç olarak melaminin, oksidatif stres yolu ve hücre apoptozunu indükleyerek farelerin üreme sistemine zarar verdiğini bildirmişlerdir. Bizim çalışmamızın sonucunda, melaminin sebep olduğu apoptotik etkilerin, Rooibosun anti-apoptotik etkisinden dolayı iyileştirdiğini düşündük.

Çalışmamızda, Melaminin seminifer tubul bütünlüğünü ve kan testis bariyerini bozduğu, Rooibosun bu dejenerasyonları iyileştirici etki gösterilerek toksisiteye bağlı infertiliteyi iyileştirmede katkı sağladığı düşünüldü.

KAYNAKÇA

- Lawal et al., 2019. A.O. Lawal, D.M. Oluyede, M.O. Adebimpe, L.T. Olumegbon, O.O. Awolaja, O.O. Elekofehinti, O.O. Crown. The cardiovascular protective effects of rooibos (*Aspalathus linearis*) extract on diesel exhaust particles induced inflammation and oxidative stress involve NF-kappaB- and Nrf2-dependent pathways modulation. *Heliyon*, 5 (3) (2019), p. e01426
- D.O. Awoniyi, Y.G. Aboua, J. Marnewick, N. Brooks. The effects of Rooibos (*Aspalathus linearis*), Green tea (*Camellia sinensis*) and commercial Rooibos and Green tea supplements on epididymal sperm in oxidative stress-induced rats. *Phytother. Res*, 26 (2012), pp. 1231-1239
- Gow, A. et al. CNS myelin and Sertoli cell tight junction strands are absent in OSP/claudin-11 null mice. *Cell* 99, 649– 659 (1999). Generation of mice lacking one claudin gene, confirming the importance of claudin and tight junctions at the level of the whole organism.
- C.L. ling, L. Zheng, L. Delong, Z. Liang, W.Z. Wang, Y.Q. Du, H. Yong, Z.X. Min, T. Dewen
- Melamine causes testicular toxicity by destroying blood-testis barrier in piglets
- *Toxicol. Lett. Oct.*, 15 (296) (2018), pp. 114-124, 10.1016/j.toxlet.2018.07.019
- S. Yuksel, B. Erginel, I. Bingul et al., “The effect of hydrogen sulfide on ischemia/reperfusion injury in an experimental testicular torsion model,” *Journal of Pediatric Urology*, vol. 18, no. 1, pp. 16.e1–16.e7, 2022.
- Skinner, C.G., Thomas, J.D. and Osterloh, J.D. (2010). Melamine Toxicity. *J. Med. Toxicol.* 6(1):50–55.
- M. Sharma, R. Manoharlal, N. Puri, R. Prasad. Antifungal curcumin induces reactive oxygen species and triggers an early apoptosis but prevents hyphae development by targeting the global repressor TUP1 in *Candida albicans*. *Biosci. Rep.*, 30 (6) (2010), pp. 391-404
- Sharpe RM, Franks S (2002) Environment, lifestyle and infertility-an intergenerational issue. *Nat Cell Biol* 4: 33-40.
- Skinner CG, Thomas JD, Osterloh JD. 2010. Melamine toxicity. *J Med Toxicol* 6: 50– 5.
- X. Duan, X.-X. Dai, T. Wang, H.-L. Liu, S.-C. Sun. Melamine negatively affects oocyte architecture, oocyte development and fertility in mice. *Hum. Rep.*, 30 (7) (2015), pp. 1643-1652
- L. Chang, R. She, L. Ma, H. You, F. Hu, T. Wang, X. Ding, Z. Guo, M.H. Soomro. Acute testicular toxicity induced by melamine alone or a mixture of melamine and cyanuric acid in mice. *Reprod. Toxicol.*, 46 (2014), pp. 1-11
- C.L. ling, L. Zheng, L. Delong, Z. Liang, W.Z. Wang, Y.Q. Du, H. Yong, Z.X. Min, T. Dewen. Melamine causes testicular toxicity by destroying blood-testis barrier in piglets. *Toxicol. Lett. Oct.*, 15 (296) (2018), pp. 114-124, 10.1016/j.toxlet.2018.07.019
- L. Chang, J. Wang, R. She, L. Ma, Q. Wu. In vitro toxicity evaluation of melamine on mouse TM4 Sertoli cells. *Environ. Toxicol. Pharmacol.*, 50 (2017), pp. 111-118
- Huang J, Yang G, Xia F, Zhang S (2018). Reproductive toxicity of melamine against male mice and the related mechanism. *Toxicol. Mech. Methods*. 28: 345-352

YENİ TASARLANMIŞ PORÖZ TİTANYUM DENTAL İMPLANTLARIN OSTEOİNTEGRASYON VE KEMİK OLUŞUMUNA ETKİSİNİN ARAŞTIRILMASI

Cem TAZE¹, M. Ercüment ÖNDER¹, Özge BOYACIOĞLU^{2,3}, Petek KORKUSUZ⁴,
Umut TEKİN¹, Özkan ÖZGÜL¹

¹ Kırıkkale Üniversitesi, Diş Hekimliği Fakültesi, Ağız, Diş ve Çene Cerrahisi Anabilim Dalı, 71450, Yahşihan, Kırıkkale, Türkiye, e-posta: ercumentonder@kku.edu.tr

² Hacettepe Üniversitesi, Fen Bilimleri Enstitüsü, Biyomühendislik Anabilim Dalı, Beytepe, 06800, Ankara, Türkiye, e-posta: ozge.boyacioglu@hacettepe.edu.tr

³ Atılım Üniversitesi, Tıp Fakültesi, Tıbbi Biyokimya Anabilim Dalı, Gölbaşı, 06830, Ankara, Türkiye

⁴ Hacettepe Üniversitesi, Tıp Fakültesi, Histoloji ve Embriyoloji Anabilim Dalı, Sıhhiye, 06100, Ankara, Türkiye, e-posta: petek@hacettepe.edu.tr

Özet: Diş kayıplarında kemik rejenerasyonu ile tedavinin sağlanmasında dental implantların üretilmesi ve kullanılması oldukça önemlidir. Konvansiyonel implantlara göre daha hızlı yeni kemik oluşumunun gerçekleşmesi amacıyla Titanyum (Ti) implantların yüzeylerine çeşitli modifikasyonlar uygulanmaktadır. Bu doğrultuda grubumuzca tasarlanan, sanal ve gerçek ortam biyomekanik testleri önceden tamamlanmış özgün poröz Ti dental implantların kemik ile temas eden yüzeylerinde konvansiyonel implanta göre güçlü osteointegrasyon ile yeni kemik oluşumuna etkisi in vivo hayvan modelinde değerlendirilebilirse, yeni poröz implant ülkemizde ekonomik olarak seri üretilebilir, katma değeri yüksek bir ürün olarak değerlendirilebilir. Proje kapsamında üretilen 2 adet farklı yüzey özelliğine sahip özgün orta üçlüsü gözenekli ve total gözenekli dental implantlar, piyasada halihazırda kullanılan ticari implant ile in vivo koşullarda karşılaştırmalı olarak değerlendirilmiştir. Total gözenekli poröz Ti implant tibiada konvansiyonel implant ile benzer biçimde osteointegrasyonu sağlamıştır. Total gözenekli implant, konvansiyonel implanta göre kolay ve kısa süreli üretimi ve yüksek uyarılma kabiliyeti ile dental ve ortopedik kullanımlarda yaygınlaşabilir.

Anahtar Kelimeler: Dental, Titanyum (Ti) implant, Kemik, Osteointegrasyon

Abstract: Production and use of dental implants are crucial for bone regeneration in tooth loss. Various modifications are applied to the surfaces of Titanium (Ti) implants to achieve faster new bone formation compared to conventional implants. It was assumed that if the effect of original porous Ti dental implants, designed by our group, whose virtual and real environment biomechanical tests have been previously completed, on strong osteointegration and new bone formation in the implant-bone interface could be evaluated in vivo animal

model, the new porous implant might be economically mass-produced in our country. The original dental implants with 2 different surface properties produced within the scope of the project; middle triple porous and total porous dental implants were evaluated in vivo comparing with the commercial implant currently used in the market. Total porous Ti implant provided osteointegration in the tibia similar to the conventional implant. Total porous implant could be frequently used as a dental and orthopedic implant due to its easy and short-term production and high adaptability when compared to conventional implants.

Keywords: Dental, Titanium (Ti) implant, Bone, Osteointegration

1. GİRİŞ

Diş kaybı, diş eti hastalığı, başarısız kök kanal tedavileri veya diş çürümesi sonucu görülen yaygın bir sağlık sorunudur. Eksik ya da sorunlu dişlerin tedavisi ve kemik rejenerasyonu için dental implantların üretilmesi ve kullanılması oldukça önemlidir. Titanyum (Ti) implantların yüksek biyouyumluluk ve korozyon direncine sahip materyaller olduğu ancak sıkı osteointegrasyonun oluşması için tek başına yetersiz kaldığı bilindiğinden (1) implant çevresinde daha hızlı kemik oluşumunun gerçekleştirilmesi için konvansiyonel Ti malzemelerin yüzeylerine çeşitli modifikasyonlar uygulandığı bildirilmektedir (2). Bu çalışmada grubumuzca tasarlanan, sanal ve gerçek ortam biyomekanik testleri önceden tamamlanmış özgün poröz Ti implantların kemik ile temas eden yüzeylerinde konvansiyonel implanta göre güçlü osteointegrasyon ile yeni kemik oluşumuna etkisi *in vivo* hayvan modelinde histomorfometrik analizle değerlendirilebilir, mikro bilgisayarlı tomografi (Mikro-BT) analizi ile karşılaştırmalı olarak verilebilirse, yeni poröz implantın ülkemizde ekonomik olarak seri üretililecek, katma değeri yüksek bir ürün olarak değerlendirilebileceği varsayılmıştır. Bu doğrultuda proje kapsamında üretilen 2 adet farklı yüzey özelliğine sahip özgün orta üçlüsü gözenekli ve total gözenekli dental Ti implantların ve piyasada halihazırda kullanılan ticari implantın *in vivo* koşullarda tavşan modelinde uygulanması ve implant çevresinde yeni kemik oluşum kapasitesinin değerlendirilmesi amaçlanmıştır. Özgün poröz Ti implantların konvansiyonel implanta göre kolay ve kısa süreli üretimi ve yüksek uyarlama kabiliyeti ile dental ve ortopedik kullanımlarda yaygınlaşabileceği öngörülmektedir.

2. YÖNTEM

2.1. Mikro-BT Analizi

28 adet erkek Yeni Zelanda tavşanının tibia kemiğine uygulanan total gözenekli, orta üçlüsü gözenekli ve konvasiyonel implantların çevresinde 8 hafta sonunda oluşan kemik hacmi ve oranı ile toplam kemik yüzey alanı sırasıyla Mikro-BT ve histomorfometrik olarak değerlendirilmiştir.

Hayvan deneyleri tamamlandıktan sonra tibia kemikleri %10'luk tamponlanmış nötral formalin çözeltisi (pH=7) içine alınmıştır. Örneklerde *in vivo* Mikro-BT taraması ve analizi yapmak üzere yüksek çözünürlüklü masaüstü Mikro-BT sistemi (Bruker Skyscan 1275, Kontich, Belçika) kullanılmış, NRecon yazılımı (v1.6.10.4, SkyScan, Kontich, Belçika) ve CTan (v1.16.1.0, SkyScan) ile numuneler görselleştirilmiş ve numunelerin nicel ölçümleri yapılmıştır. Her örnek için kemik hacmi (mm³), kemik hacmi oranı (BV/TV) hesaplanmıştır.

2.2. Histomorfometrik Analiz

Tüm örneklerden poröz dental implantlar kontrollü olarak çıkarılmış ve %10'luk tamponlanmış nötral formalin çözeltisinde (pH=7) tespit edildikten sonra De Castro çözeltisinde (kloral hidrat, nitrik asit, distile su) kontrollü olarak dekalsifiye edilmiştir. Örnekler sabit vakumlu otomatik bir doku takip cihazı ile izlenerek parafine gömülmüştür. İmplant ile komşu tüm örneği içeren beş mikrometre kalınlığındaki seri kesitler Hematoksilen eozin (HE) ve Masson trikrom (MT) ile boyandıktan sonra kemik matriksini sentezleyen osteoblastlar, yeniden modellenmesinden sorumlu rezorptif osteoklastlar ve ekstrasellüler matriks bileşenleri histomorfometrik olarak değerlendirilmiştir (3). Örneklerde implantla temas alanı, bilgisayar ve dijital kamera (Leica DFC7000 T, Westzlar, Almanya) bağlantılı Leica DMB6 B (Westzlar, Almanya) marka ışık mikroskopunda görüntülenmiş ve en küçük büyütmede saklanıp LAS marka (Leica, Westzlar, Almanya) görüntü analiz programı ile kantitatif olarak değerlendirilmiştir (4-6).

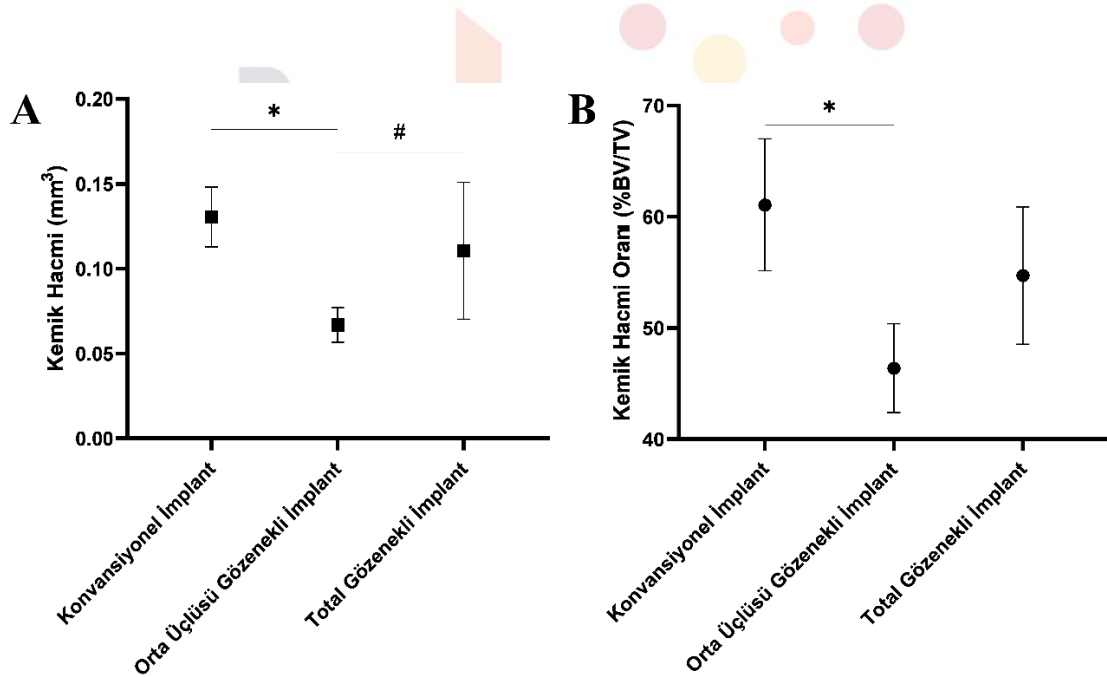
2.3. İstatistiksel Analiz

Analizler için bağımsız değişkenler; gruplar, bağımlı değişkenler; histolojik ve Mikro-BT ölçüm parametreleri olarak belirlenmiştir. Verilerin normal dağılım koşulları ve varyansların homojenliği Shapiro-Wilk testiyle değerlendirilmiştir. Tüm veriler parametrik Tek yönlü

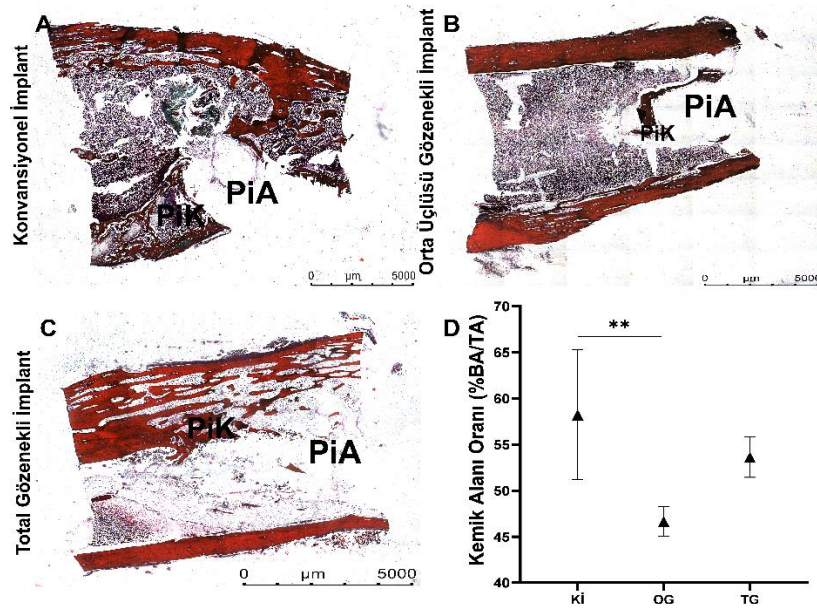
varyans analizi (ANOVA) ve post-hoc Duncan's test ile değerlendirilmiştir. Gruplar arası fark, $p < 0.05$ olduğunda istatistiksel anlamlı kabul edilmiştir.

3. BULGULAR

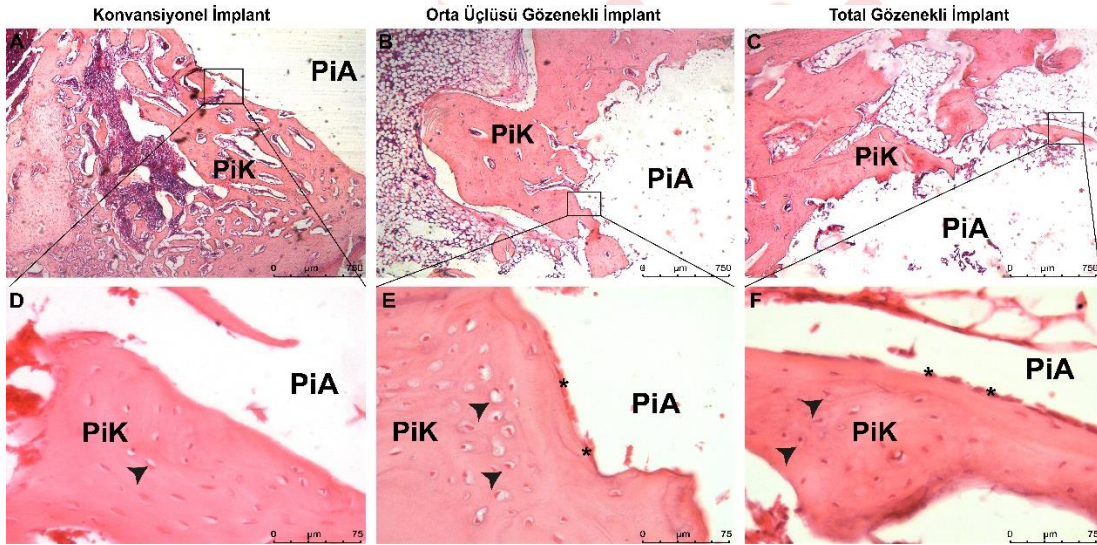
Total gözenekli implant ($p=0.021$) ve konvansiyonel implant ($p=0.034$) uygulanan kemik dokusunun, orta üçlüsü gözenekli implant uygulanan kemik dokusuna göre istatistiksel anlamlı yüksek kemik hacmi içerdiği saptanmıştır (Şekil 1). Total gözenekli ($p=0.016$) ve konvansiyonel implanta ($p=0.008$) ait kemik hacmi oranı orta üçlüsü gözenekli implanta göre istatistiksel anlamlı yüksek saptanmıştır. Tüm gruplarda osteoblastlar ve sement çizgileri ile ayrılan yeni ekstrasellüler matris sentezlemiş osteositler izlenmiştir (Şekil 2-3). Kontrol grubunda yeni oluşan peri-implant kemik yüzey alanının toplam kemik yüzey alanına oranı orta üçlüsü gözenekli implant uygulanan gruba göre istatistiksel anlamlı yüksek bulunmuştur ($p=0.032$). Total gözenekli ile konvansiyonel implant uygulanan grup yeni kemik oluşumunu benzer biçimde tetiklemiştir.



Şekil 1. *in vivo* Mikro-BT ile orta üçlüsü ve total gözenekli ve konvansiyonel implantların kemik dokularında (A) kemik hacmi ve (B) kemik hacmi/toplam hacim (BV/TV) oranına ait ortalama-standart sapma (SS) grafiği gösterilmektedir. (*): Konvansiyonel ve (#): total gözenekli implanta göre $p < 0.05$.



Şekil 2. (A) Konvansiyonel (KI), (B) orta üçlüsü (OG) ve (C) total gözenekli (TG) implant uygulanan gruplara ait mikrograflar ve (D) kemik alanı oranına (BA/TA) ait ortalama-SS grafiği gösterilmektedir. Masson trikrom, 40x. PiA: Peri-implant alan, PiK: Peri-implant kemik. (**): Konvansiyonel implanta göre $p < 0.05$.



Şekil 3. Konvansiyonel (A, D), orta üçlüsü gözenekli (B, E) ve total gözenekli (C, F) implant uygulanan gruplara ait mikrograflar gösterilmektedir. Hematoksilen eozin, A-C 40x; D-F 400x. PiA: Peri-implant alan, PiK: Peri-implant kemik, (*): Osteoblast, siyah ok: Osteosit.

4. TARTIŞMA, SONUÇ

Bu çalışma ile geliştirilen özgün total gözenekli poröz Ti implantın tibiada konvansiyonel implant ile benzer biçimde osteointegrasyonu sağladığı, kolay ve kısa süreli üretimi ve yüksek uyarlama kabiliyeti ile dental ve ortopedik kullanımlarda yaygınlaşabilir.

Bu çalışma 119R008 numaralı TÜBİTAK 1001 projesi kapsamında desteklenmiştir.

5. KAYNAKÇA

1. Zhu, G., G. Wang, and J.J. Li. (2021). Advances in implant surface modifications to improve osseointegration. *Materials Advances*. **2**(21): p. 6901-6927.
2. Hakki, S.S., P. Korkusuz, N. Purali, F. Korkusuz, B.S. Bozkurt, E.E. Hakki, *et al.* (2013). Periodontal ligament cell behavior on different titanium surfaces. *Acta Odontologica Scandinavica*. **71**(3-4): p. 906-916.
3. Trindade, R., T. Albrektsson, S. Galli, Z. Prgomet, P. Tengvall, and A. Wennerberg. (2018). Osseointegration and foreign body reaction: Titanium implants activate the immune system and suppress bone resorption during the first 4 weeks after implantation. *Clin Implant Dent Relat Res*. **20**(1): p. 82-91.
4. Sirin, H.T., I. Vargel, T. Kutsal, P. Korkusuz, and E. Piskin. (2016). Ti implants with nanostructured and HA-coated surfaces for improved osseointegration. *Artificial Cells, Nanomedicine, and Biotechnology*. **44**(3): p. 1023-1030.
5. Tekin, U., H.H. Tuz, E. Onder, O. Ozkaynak, and P. Korkusuz. (2008). Effects of alendronate on rate of distraction in rabbit mandibles. *J Oral Maxillofac Surg*. **66**(10): p. 2042-9.
6. Togral, G., M. Arikan, P. Korkusuz, R.H. Hesar, and M.F. Eksioğlu. (2015). Positive effect of tadalafil, a phosphodiesterase-5 inhibitor, on fracture healing in rat femur. *Eklemler Hastalıkları Cerrahisi*. **26**(3): p. 137-44.



IVF İŞLEMLERİNDE TOPLANAN OOSİTLERDEKİ ANOMALİLERİN TEDAVİ SONUÇLARINA ETKİSİ

**Kübra ÖZUNCA¹, Dilşad ARISOY DEMİR², Cem KORKMAZ³, Tanyeli
GÜNEYLİGİL KAZAZ⁴, Esin MUSLU BAL⁵, Halil OĞUZ⁵**

¹Sağlık Bilimleri Üniversitesi Gülhane Tıp Fakültesi, Histoloji ve Embriyoloji AD, Ankara, TÜRKİYE,
rana94kubra.ozunca@gmail.com

²Gaziantep Üniversitesi Tıp Fakültesi, Histoloji ve Embriyoloji AD, Ankara, TÜRKİYE,
dr.dilsadarisoydemir@gmail.com

³T.C. Sağlık Bakanlığı Gülhane Eğitim ve Araştırma Hastanesi, Tüp Bebek Merkezi Laboratuvar Sorumlusu,
Ankara, TÜRKİYE, cem.korkmaz@sbu.edu.tr

⁴Gaziantep Üniversitesi, Biyoistatistik AD, Gaziantep, TÜRKİYE, tanyeliguneyligil@windowslive.com

⁵T.C. Sağlık Bakanlığı Gülhane Eğitim ve Araştırma Hastanesi, Tüp Bebek Merkezi, Ankara, TÜRKİYE,
esinmuslubal@gmail.com , hllogz14@gmail.com

Özet: Günümüzde IVF tedavilerinde noninvazif olarak embriyo kalitesi belirleme tekniklerine yönelim artmış durumda. Bunların başında ise polarizasyon mikroskobu ile embriyoyu incelemek geliyor. Biz de çalışmamızda embriyo kalitesine etki ettiğini düşündüğümüz sitoplazmik anomalileri polarizasyon mikroskobu ile inceledik ve bu anomalilerin yaş, fertilizasyon oranı, beta hCG pozitifliği gibi faktörlerle ilişkisine baktık. Elde ettiğimiz sonuçlara göre yaş artışı ile beraber fertilizasyon oranı azalmakta, nonfertilize/ölen oosit oranı artmaktadır (Tablo-1). Nonfertilize/ölen oosit yüzdesi 35 yaş ve üzerinde 35 yaş altına göre istatistiksel olarak anlamlı derecede artmıştır ($p=0,027$). Sonuç olarak sınırlı sayıda oosit üstünde çalışma yapılmasına karşın, oosit anomalileri embriyo seçim kriterleri arasında dikkat edilmesi gereken bir konu olarak önemini korumaya devam etmektedir. Oosit anomalisi varlığı ve infertil kadının ileri yaşta (≥ 35) olması fertilizasyon başarısızlığının öngörülmesinde belirleyici olabilir.

Anahtar Kelimeler: Oosit anomalisi, fertilizasyon, IVF

Abstract: Today, the trend towards noninvasive embryo quality determination techniques in IVF treatments has increased. At the beginning of these is to examine the embryo with a polarization microscope. In our study, we examined the cytoplasmic anomalies that we think affect the embryo quality with polarization microscopy and looked at the relationship of these anomalies with factors such as age, fertilization rate, beta hCG positivity. According to the results we obtained, the fertilization rate decreases with increasing age, and the nonfertilized/dead oocyte rate increases (Table-1). The percentage of nonfertilized/dead oocytes was statistically significantly increased at the age of 35 and above compared to those under 35 years of age ($p=0.027$). In conclusion, despite the limited number of studies on

oocytes, oocyte anomalies continue to be an important issue among embryo selection criteria. Presence of oocyte anomaly and advanced age (≥ 35) of the infertile woman may be determinative in the prediction of fertilization failure.

Keywords: Oocyte anomaly, fertilization, IVF

1.GİRİŞ

IVF tedavilerinde son yıllarda noninvazif olarak embriyo kalitesi belirleme tekniklerinde önemli gelişmeler sağlanmıştır. Noninvazif teknikler arasında en sık kullanılan yöntem ise oosit fenotipinin polarize mikroskopla incelenmesidir. Oosit kalitesi, embriyo kalitesinin ve infertilite tedavisindeki başarının önemli bir belirleyicisidir.[1]

IVF laboratuvar uygulamaları sırasında toplanan iyi kalitedeki matür insan oositlerinin açık renkte, hafif granüler bir sitoplazmaya sahip olduğu; küçük bir perivitellin aralık (PVA), berrak, yaklaşık 12 μm kalınlığında zona pellucida (ZP) ve tek bir parçalanmamış polar cisim (PB) içerdiği bilinmektedir. [2] Bununla birlikte, bazı oositler sitoplazmanın şekli, rengi, granülasyon içermesi, PVA'nın genişliği, ZP'nin kalınlığı ve/veya PB'nin durumu bakımından farklılıklar gösterir. Toplanan oositlerin çoğunluğunun (%60 ila %70) bu anormal morfolojik özelliklerden bir veya daha fazlasını sergilediği bildirilmiştir.[3]

Dismorfik oositler genellikle anormal sitoplazmaya (koyu sitoplazma veya sitoplazmik granülasyon), sitoplazmik inklüzyonlara (vakuoller, refraktil cisim veya düz endoplazmik retikulum [SER] kümeleri), anormal oosit şekline (örn. oval), anormal ZP (biparyetal zona), perivitellin aralıkta döküntü, fragmente PB gibi normal dışı özelliklere sahiptirler.[3],[4]



Şekil 1: Fragmente polar cisim.



Şekil 2: PVA'da döküntü

Oositlerin morfolojik anormalliklerinin kaynağı konusunda; yaş ve genetik kusurlar gibi içsel faktörler veya ovaryum stimülasyon protokolü ve/veya aspirasyonun hemen ardından uygulanan işlemler gibi faktörlerin etkili olduğu düşünülmüştür.[5]

Çalışmamızda spesifik morfolojik oosit anormalliklerinin IVF tedavisinin başarısı üzerindeki etkisi fertilizasyon oranı, embriyo kalitesi ve β -hCG pozitifliği açısından retrospektif olarak değerlendirilmiştir.

2.YÖNTEM

Çalışmamızda retrospektif olarak, Ocak 2021'den Aralık 2021'e kadar Gülhane EAH ÜYTE Merkezi'nde infertilite tanısı almış 114 hasta incelenmiştir. Germinal vezikül (GV) yapısındaki oositlerin ve erkek faktörü bulunan infertil hastaların dahil edilmediği, 114 hastadan toplanan 943 oosite PolScope eşliğinde ICSI (*intrasitoplazmik sperm enjeksiyonu*) uygulanmış; intrasitoplazmik (İS) ve ekstrasitoplazmik (ES) oosit anomalileri fertilizasyon oranı, embriyo kalitesi (EK) ve β -hCG sonuçları açısından karşılaştırılmıştır.

3.BULGULAR

Çalışmaya dahil edilen hastalardan toplanan oositlere uygulanan ICSI sonrası %96,18 (907/943) fertilizasyon oranı gözlenmiştir. Yapılan 54 embriyo transferinden 29'u β -hCG pozitifliği ile sonuçlanmış ve kimyasal gebelik oranı %53,70 olarak bulunmuştur.

Araştırmamızdan elde ettiğimiz verilere göre, IVF uygulamalarında intra/ekstrasitoplazmik oosit anomalisi olan gruplar ile fertilizasyon anomalisi ve embriyo kalitesi arasında istatistiksel olarak anlamlı farklılık bulunmamıştır. Oosit anomalilerinin görüldüğü grup ile anomali tespit edilmeyen grup arasında β -hCG pozitifliği, fertilizasyon oranı ve embriyo kalitesi açısından istatistiksel olarak anlamlı bir fark bulunmamasına rağmen; β -hCG pozitifliğinin karşılaştırıldığı gruplarda medyan değerlerinin birbirinden uzaklığı (İS=1,35(0-16,66; ES=11,81(8,5 -25); AY= 76,38(46,15-86,48)) oosit sayısının arttırılması ile istatistiksel olarak anlamlı sonuca ulaşılabileceğini öngörmektedir. Frozen embriyo transferi yapılan grupta taze embriyo transferi yapılan gruba göre β -hCG pozitifliği istatistiksel olarak anlamlı (%62,5-%50, $p=0,001$) şekilde artmıştır(Tablo-2). Ayrıca yaş artışı ile beraber fertilizasyon oranı azalmakta, nonfertilize/ölen oosit oranı artmaktadır(Tablo-1). Nonfertilize/ölen oosit yüzdesi 35 yaş ve üzerinde 35 yaş altına göre istatistiksel olarak anlamlı derecede artmıştır ($p=0,027$).

Sayısal değişkenlerin normal dağılıma uygunluğu Shaphiro Wilk testi ile test edilmiştir. Normal dağılmayan değişkenlerin iki grupta karşılaştırılmasında Mann Whitney U testi, üç grupta karşılaştırılmasında Kruskal Wallis testi kullanılmıştır. Kategorik değişkenler arasındaki ilişkiler Ki-kare testi ile, sayısal değişkenler arasındaki ilişkiler Spearman rank

korelasyon katsayısı ile test edilmiştir. Analizlerde SPSS 22.0 Windows versiyon paket programı kullanılmıştır. $P < 0,05$ anlamlı kabul edilmiştir.

	<35 (n=83) Medyan (%25-%75)	≥ 35 (n=31) Medyan (%25-%75)	P
2 PN	60 (33,33 - 77,77)	40 (20 -66,66)	0,063
1-3 PN	0 (0 -0)	0 (0 -0)	0,082
NONFERTİLİZE/ÖLEN	37,5 (21,05 - 57,14)	60 (33,33 -80)	0,027*

* $p < 0,05$ düzeyinde anlamlı, Mann Whitney U testi

Tablo 1: IVF Uygulamalarında Yaş ile Fertilizasyon Başarısı Arasındaki İlişki.

		TRANSFER			P
		Transfer yapılmayan	Taze transfer	Frozen transfer	
		n(%)	n(%)	n(%)	
B HCG POZİTİFLİĞİ	+ olanlar	0 (0)	15 (50)	15 (62,5)	0,001*
	- olanlar	0 (0)	15 (50)	9 (37,5)	
	Belli olmayanlar	60 (100,0)	0 (0)	0 (0)	

* $p < 0,05$ düzeyinde anlamlı, Ki-kare testi

Tablo-2: IVF Uygulamalarında Transfer Durumu ve β -hCG Pozitifliği Arasındaki İlişki

4.TARTIŞMA

YÜT (yardımcı üreme teknikleri), bireysel döngülerde başarılı tedavi sonuçları ihtimalini tahmin etmeyi zorlaştıran karmaşık bir disiplinler arası alanı temsil eder. Ancak oosit morfolojisi verilerinin eklenmesi, tahminlerin doğruluğunu arttırabilir. Başarılı fertilizasyon ve/veya iyi kalitede embriyo oluşumu açısından spesifik oosit anormalliklerinin prognozunu inceleyen az sayıda çalışma bulunmaktadır.[3] Oosit ve embriyo değerlendirmesi için yenilikçi yöntemler (polarize ışık mikroskobu, embriyo seçimi algoritmalar) rutin uygulamaya dahil edilmeye devam edecek olsa da, basit morfolojik oosit değerlendirmesi önemini korumaya devam etmektedir. Morfolojik değerlendirme, uygulanması kolay ve diğer yöntemlerle birlikte hastalara fayda sağlayabilecek noninvazif bir değerlendirme tekniğidir. Ayrıca hastalara bazı oositlerin neden gelişmediğini veya yüksek kaliteli embriyolara dönüşmediğini açıklamaya yardımcı olabilir.[3]

Çalışmamızda intrasitoplazmik [*koyu sitoplazma veya sitoplazmik granülasyon, sitoplazmik inklüzyonlar (vakuoller, refraktil cisim veya düz endoplazmik retikulum [SER] kümeleri)*] ve ekstrasitoplazmik oosit anormalliklerinin [*anormal ZP (biparyetal zona), perivitellin aralıkta döküntü, fragmante PB*] IVF tedavisinin başarısı üzerindeki etkisini fertilizasyon oranı, embriyo kalitesi ve β -hCG pozitifliği açısından retrospektif olarak değerlendirdik.

Dismorfizmlerin altında yatan nedenlerin belirlenmesi çok önemlidir fakat oosit gelişimi ve maturasyonunun karmaşık doğası göz önüne alındığında bunun belirlenmesi zordur. Bazı dismorfizmlere, hastanın yaşı ve kalıtsal özellikleri gibi endojen faktörler neden olabilirken[6], endometriozis[7], polikistik over sendromu[8], yüksek BMI[9], ekzojen gonadotropinler veya serumdaki anti Müllarian hormon konsantrasyonu[10] gibi faktörler de neden olabilir. Bununla birlikte ovaryan stimülasyon da, foliküllerin sürekli büyümesi ve olgunlaşması nedeniyle bazı dismorfizmlere neden olabilir[11]. Bu dismorfizmler yaşa bağlı artış gösterebilmekle beraber fertilizasyon oranını ve beta-hCG pozitifliğini etkileyebilmektedir.

Araştırmamızdan elde ettiğimiz verilere göre, IVF uygulamalarında intra/ekstrasitoplazmik oosit anomalisi olan gruplar ile fertilizasyon anomalisi ve embriyo kalitesi arasında istatistiksel olarak anlamlı farklılık bulunmaması bu oositlerin normal olarak değerlendirilebileceğini düşündürmekle birlikte, oosit sayısının arttırılması ile istatistiksel olarak anlamlı sonuca ulaşılabilirliğini de öngörmektedir.

Sonuç olarak, morfolojik özelliklerin hiçbiri tek başına insan fertilitesinde güvenilir bir prognostik faktör olarak hizmet etmesede, bazı durumlarda tedavi sonuçlarını açıklamaya yardımcı olabilir.

5.SONUÇ

Frozen embriyo transferi taze embriyo transferine göre kimyasal gebeliğin pozitiflik oranını arttırmıştır. β -hCG pozitifliğinin karşılaştırıldığı gruplarda medyan değerlerinin birbirinden uzaklığı, oosit sayısının artırılması ile istatistiksel olarak anlamlı sonuca ulaşılabileceğini öngörmektedir. Sonuç olarak sınırlı sayıda oosit üstünde çalışma yapılmasına karşın, oosit anomalileri embriyo seçim kriterleri arasında dikkat edilmesi gereken bir konu olarak önemini korumaya devam etmektedir. Oosit anomalisi varlığı ve infertil kadının ileri yaşta (≥ 35) olması fertilizasyon başarısızlığının öngörülmesinde belirleyici olabilir.

6.KAYNAKÇA

- [1] C. Korkmaz, Y. B. Tekin, M. Sakinci, and C. M. Ercan, "Effects of maternal ageing on ICSI outcomes and embryo development in relation to oocytes morphological characteristics of birefringent structures," *Zygote*, vol. 23, no. 4, pp. 550–555, 2015, doi: 10.1017/S0967199414000197.
- [2] L. L. VEECK, "Oocyte Assessment and Biological Performance," *Ann. N. Y. Acad. Sci.*, vol. 541, no. 1, pp. 259–274, 1988, doi: 10.1111/j.1749-6632.1988.tb22263.x.
- [3] E. J. Yu, H. Ahn, J. M. Lee, B. C. Jee, and S. H. Kim, "Fertilization and embryo quality of mature oocytes with specific morphological abnormalities," *Clin. Exp. Reprod. Med.*, vol. 42, no. 4, pp. 156–162, 2015, doi: 10.5653/cerm.2015.42.4.156.
- [4] L. Rienzi, G. Vajta, and F. Ubaldi, "Predictive value of oocyte morphology in human IVF: A systematic review of the literature," *Hum. Reprod. Update*, vol. 17, no. 1, pp. 34–45, 2011, doi: 10.1093/humupd/dmq029.
- [5] R. D. C. S. Figueira, D. P. De Almeida Ferreira Braga, L. Semião-Francisco, C. Madaschi, A. Iaconelli, and E. Borges, "Metaphase II human oocyte morphology: Contributing factors and effects on fertilization potential and embryo developmental ability in ICSI cycles," *Fertil. Steril.*, vol. 94, no. 3, pp. 1115–1117, 2010, doi: 10.1016/j.fertnstert.2009.11.039.
- [6] D. Nikiforov, M. L. Grøndahl, J. Hreinsson, and C. Y. Andersen, "Human Oocyte Morphology and Outcomes of Infertility Treatment: a Systematic Review," *Reprod. Sci.*, no. 0123456789, 2021, doi: 10.1007/s43032-021-00723-y.
- [7] E. Borges, D. P. A. F. Braga, A. S. Setti, L. S. Vingris, R. C. S. Figueira, and A. Iaconelli, "Endometriosis affects oocyte morphology in intracytoplasmic sperm injection cycles," *J. Bras. Reprod. Assist.*, vol. 19, no. 4, pp. 235–240, 2015, doi: 10.5935/1518-0557.20150046.
- [8] A. Allahveisi, E. Yousefian, M. J. Rezaie, and B. Nikkhoo, "Comparison Of Morphometric And Morphology Oocytes After In Vitro Maturation Between Healthy Women And Patients With Polycystic Ovarian Syndrome," *Gen. Endocrinol. Acta Endocrinol.*, vol. XV, no. 3, pp. 295–300, 2019, doi: 10.4183/aeb.2019.295.
- [9] R. Depalo *et al.*, "Oocyte morphological abnormalities in overweight women undergoing in vitro fertilization cycles," *Gynecol. Endocrinol.*, vol. 27, no. 11, pp. 880–884, 2011, doi: 10.3109/09513590.2011.569600.
- [10] E. Borges, D. P. A. F. Braga, A. Setti, R. de C. Figueira, and A. Iaconelli, "The predictive value of serum concentrations of anti-Müllerian hormone for oocyte quality, fertilization, and implantation," *J. Bras. Reprod. Assist.*, vol. 21, no. 3, pp. 176–182, 2017, doi: 10.5935/1518-0557.20170035.
- [11] B. Balaban and B. Urman, "Effect of oocyte morphology on embryo development and implantation," *Reprod. Biomed. Online*, vol. 12, no. 5, pp. 608–615, 2006, doi: 10.1016/S1472-6483(10)61187-X.

**KEMİK TÜMÖRLERİNDE KANNABİNOİDLERİN RESEPTÖR ARACILI
ANTİPROLİFERATİF VE APOPTOTİK ETKİLERİNİN ARAŞTIRILMASI****Başak Işıl ZORBA¹, Özge BOYACIOĞLU^{1,2}, Petek KORKUSUZ³**

¹ Hacettepe Üniversitesi Fen Bilimleri Enstitüsü, Biyomühendislik Anabilim Dalı, Ankara, Türkiye, e-posta: basakisiluyanik@gmail.com

² Atılım Üniversitesi Tıp Fakültesi, Tıbbi Biyokimya Anabilim Dalı, Ankara, Türkiye, e-posta: ozge.boyacioglu@hacettepe.edu.tr

³ Hacettepe Üniversitesi Tıp Fakültesi, Histoloji ve Embriyoloji Anabilim Dalı, Ankara, Türkiye, e-posta: petek@hacettepe.edu.tr

Özet: Primer osteosarkom hızlı metastaz özelliği ile bilinen, çocuklarda ve gençlerde en sık izlenen osteojenik tümördür. Klinikte uygulanan tedavi yöntemlerinin sınırlılıkları ve hastalarda görülen yan etkiler yeni tedavi ajanlarının araştırılması gerekliliğini ortaya koymaktadır. Endokannabinoidler, insan kas-iskelet sisteminde sentezlendiği bilinen, osteoblast, osteoklast ve osteoprogenitör hücrelerde CB1 ve CB2 reseptörleri aracılığıyla kemik yapımı ve yıkımını düzenlediği bildirilmiş lipit yapılı ligandlardır. Kannabinoidlerin osteosarkom hücrelerinde CB2 reseptörleri aracılı hücre çoğalmasını azaltıcı ve apoptozu indükleyici etkileri bildirilmiştir. Antiproliferatif ve apoptotik etkinliği bildirilmiş sentetik spesifik CB2 reseptör agonisti CB65, CB2 reseptörü aracılı olarak osteosarkom hücrelerinde antiproliferatif ve apoptotik etki gösterebilir. Varsayımı test etmek amacıyla in vitro koşullarda MG63 ve Saos-2 osteosarkom hücre hatlarında akım sitometrisi yöntemi ile CB1 ve CB2 reseptörlerinin varlığı gösterilmiştir. Buna göre MG63 ve Saos-2 hatlarında yüksek oranda CB2 immün işaretlenme saptanmıştır. MG63 ve Saos-2 hatlarında CB65'in WST-1 yöntemi ile belirlenen 10^{-12} – 10^{-8} M antiproliferatif etkili doz penceresine göre gerçek zamanlı proliferasyon analizinde MG63 için 1.11×10^{-11} M ve Saos-2 için 4.95×10^{-11} M ED50 hesaplanmıştır. CB65'in osteosarkom hatlarındaki proliferasyonu azaltıcı etkisi CB2 antagonisti AM630 ile bloke olmuştur. Terapötik dozda CB65, akım sitometrisi yöntemi ile MG63 hücrelerinde 48. saatte %7.31 ve Saos-2 hücrelerinde 24. saatte %19.06 oranında geç apoptozu indüklemiştir. Bu çalışma ile ilk kez sentetik spesifik CB2 agonisti CB65'in osteosarkom hücre hatlarındaki gerçek zamanlı antiproliferatif ve apoptotik etkisi ortaya konarak in vitro koşullardaki terapötik penceresi belirlenmiştir. Yağ yapılı kannabinoid agonisti CB65 etkili dozda uzun süreli salımının sağlanması ve in vivo koşullarda validasyonu sonrası kliniğe aktarılabilecek bir tedavi seçeneği olabilir.

Anahtar Kelimeler: osteosarkom, kannabinoid, CB2 reseptörü, CB65, ilaç

Abstract: Primary osteosarcoma is the most common osteogenic tumor in children and adolescents, known with its rapid metastasis. Limitations of the treatment approaches applied in the clinic and the serious side effects reveal the necessity of investigating novel treatment agents. Endocannabinoids are lipid-structured ligands synthesized in human musculoskeletal system and regulate bone formation and resorption through CB1/CB2 receptors in osteoblasts, osteoclasts and osteoprogenitor cells. Cannabinoids reduce proliferation and induce apoptosis in osteosarcoma cells through CB2 receptors. Synthetic specific CB2 receptor agonist CB65 may exert CB2 receptor-mediated antiproliferative and apoptotic effects on osteosarcoma cells. To test the hypothesis, the presence of intracellular and membrane CB1 and CB2 receptors was demonstrated by flow cytometry in human MG63 and Saos-2 osteosarcoma cell lines in vitro. Accordingly, high CB2 immunolabeling was detected in MG63 and Saos-2 lines. 10^{-12} – 10^{-8} M antiproliferative dose window of CB65 by WST-1, ED50 of 1.11×10^{-11} M for MG63 and 4.95×10^{-11} M for Saos-2 cells were calculated by real-time proliferation analysis and the antiproliferative effect was inhibited by CB2 antagonist AM630. CB65 application at its therapeutic dose induced late apoptosis of 7.31% in MG63 cells at 48 hours and 19.06% in Saos-2 cells at 24 hours by flow cytometry. In this study, the real-time antiproliferative and apoptotic effect of CB65 in osteosarcoma cells was revealed for the first time, and the therapeutic window in vitro was determined. CB65 may be a treatment option that can be transferred to the clinic after long-term release at an effective dose and in vivo validation.

Keywords: osteosarcoma, cannabinoid, CB2 receptor, CB65, drug

1. GİRİŞ

Kemik tümörleri çocuklarda görülme sıklığı (1), yüksek metastaz oranına (2) bağlı olarak artış gösteren önemli bir kanserdir. Çocuklarda ve gençlerde primer osteosarkom en sık izlenen osteojenik tümör olarak bilinmektedir (3). Klinikte osteosarkom için cerrahi tedavi, radyoterapi ve kemoterapinin sınırlılıkları ve hedefli ajanların uygulandığı hastalarda görülen sistemik yan etkiler tedavi sürecini güçleştirmektedir (4). Hâlihazırda kullanılan ajanların sınırlı etkileri, yeni ilaç adaylarının araştırılması gerekliliğini ortaya koymaktadır (4). Kannabinoidler, doğada ekzojen olarak *Cannabis* türü bitkilerde (5, 6), endojen olarak insanlarda (7) ve laboratuvar koşullarında sentetik formları (8) üretilen aktif lipit yapılı ligandlardır. Kannabinoid sistemi bileşenlerinin kemik hücrelerinde yaygın olarak dağılım gösterdiği bilinmektedir (9, 10). Kemiğe ait osteoblast, osteoklast ve kemiğin öncül

hücrelerinde klasik kannabinoid 2 (CB2) reseptörünün klasik kannabinoid 1 (CB1) reseptörüne göre daha yüksek oranda sentezlendiği bildirilmiştir (9, 11, 12). Kannabinoidlerin osteosarkom hücrelerinde CB2 veya Transient reseptör potansiyeli vanilloid tipi-1 (TRPV1) reseptörleri aracılı proliferasyon (1), invazyonu (1, 13) ve hücre göçünü azalttığı (1, 13) ve apoptozu indüklediği (1, 13) bildirilmiştir. Literatürde çeşitli kannabinoidlerin osteosarkom hücrelerindeki etkilerine ilişkin çalışmalar bulunsa dahi CB2 reseptörü aracılı proliferasyonu azaltıcı (1) ve apoptozu indükleyici (1, 13) etki mekanizmasına ilişkin bilgiler sınırlı olarak bildirilmiştir. Yarı ömrü kısa olan yağ yapılı kannabinoidlerin uzun süreli ve kontrollü salımı için lipit bazlı ilaç taşıma sistemleri ile osteosarkom hücrelerinin hedeflenmesine ilişkin çalışmalar oldukça sınırlıdır (14). Varsayımımıza göre, sentetik spesifik CB2 reseptör agonisti CB65'in osteosarkom hücre hatlarındaki etkili dozu tespit edilebilir, proliferasyonu azaltıcı ve apoptozu indükleyici etkisi ortaya konabilirse bu ajan, osteosarkom için küratif ilaç adayı olabilir.

2. YÖNTEM

2.1. Hücre Kültürü

Kannabinoid reseptörlerini bulundurdukları bilinen Saos-2 ve MG63 insan osteosarkom hücre hatları ve pozitif kontrol grubu olarak kullanılan A549 KHDAK hücre hattı optimal kültür koşullarında ekspansiyon edilmiştir. Saos-2 hücreleri McCoy's 5A; MG63 ve A549 hücreleri *Dulbecco's Modified Eagle Medium High Glucose* (DMEM HG) besiyeri ile beslenmiştir. Bazal besiyerleri DMEM HG ve McCoy's 5A için %10 FBS, %2 L-glutamin ve %1 penisilin-streptomisin ile hazır hale getirilmiştir.

2.2. Osteosarkom Hücre Hatlarında Reseptör Varlığının Akım Sitometrisi Yöntemiyle Değerlendirilmesi

MG63 ve Saos-2 osteosarkom hücre hatlarında CB1 ve CB2 reseptör varlığı akım sitometrisi yöntemi ile değerlendirilmiştir. 7×10^5 hücre/100 μ l hücre süspansiyonunun %3 paraformaldehit (PFA) ile inkübasyonundan sonra hücreler PBS ile +4 °C 500g'de 5 dakika santrifüj edilmiştir. Kannabinoid reseptörleri hücre içi ve hücre zarında bulduklarından (15-17) akım sitometrisi ile hücre içi ve zarında immün işaretleme yapılmıştır. Hücre içi CB1 ve CB2 kannabinoid düzeyi için hücre içi örneklerine %0.2 Tween-20 uygulanmıştır. Anti-insan CB1 (ab3558, Abcam, Birleşik Krallık) ve anti-insan CB2 (ab3561, Abcam, Birleşik Krallık) primer antikoları örneklerle eklenerek +4 °C'de 1 saat inkübasyona bırakılmıştır.

İnkübasyonun ardından hücreler PBS ile yıkanarak Goat Anti-Rabbit IgG sekonder antikor (ab7086, Abcam, Birleşik Krallık) ile +4 °C’de 30 dakika karanlıkta inkübe edilmiştir. Hücreler PBS içinde 12x75 ml’lik falkon tüplerine alınmış ve akım sitometrisi cihazında (Novocyt 2000R Flow Cytometer System, Agilent, ABD) analiz edilmiştir.

2.3. Osteosarkom Hücre Hatlarında CB65’in Hücre Çoğalmasına Etkisinin

Değerlendirilmesi

Hücreler 5×10^3 hücre/kuyu olacak şekilde 96 kuyucuklu kültür plaklarına ekilmiştir. Konfluense ulaşan hücrelerdeki besiyeri uzaklaştırılmış ve 10^{-12} – 10^{-6} M CB65 hücrelere uygulanmıştır. Hücrelere sırası ile 1, 2 ve 3. günlerde *Water Soluble Tetrazolium-1* (WST-1) ajanı (11644807001, Roche Applied System, İsviçre) eklenmiş, plakalar 4 saat inkübasyona bırakılmıştır. İnkübasyonun ardından hücrelerin proliferasyon düzeyleri VersaMax Microplate Reader (Molecular Device, ABD) mikropilaka okuyucu ile belirlenmiştir. Tüm gruplarda proliferasyon düzeyi en fazla azalan gün/günler saptanmış ve CB2 agonisti CB65’in etkili doz aralığı saptanmıştır.

2.4. Osteosarkom Hücre Hatlarında CB65’in Proliferasyonu Azaltıcı ED50’sinin Gerçek Zamanlı Olarak Değerlendirilmesi

Hücreler her bir kuyucuğa 7×10^3 hücre/200 µl hücre süspansiyonu gelecek tabanı impedansı kaydeden altın mikroelektrotlarla kaplı 96 kuyucuklu hücre plakalarına ekilmiştir. Hücre plakası xCELLigence (RTCA, Roche Applied System, İsviçre) cihazına yerleştirilmiştir. Gerçek zamanlı olarak hücrelerin tabana yaptıkları basının impedansına ait veriler 15 dakikada bir “hücre indeksi” olarak kaydedilmiş ve hücre indeksi 1.0’ı geçtikten sonra WST-1 analizinin sonuçlarına göre 10^{-12} – 10^{-8} M CB65 hücrelere uygulanmıştır. Ek olarak CB2 reseptörü aracılı etkinin izlenmesi amacıyla sentetik spesifik CB2 antagonisti AM630 (1120, Tocris, Birleşik Krallık), 1×10^{-8} M, 2×10^{-8} M ve 5×10^{-8} M dozlarda hücrelere uygulanmıştır.

2.5. Osteosarkom Hücre Hatlarında CB65’in Apoptotik Etkisinin Değerlendirilmesi

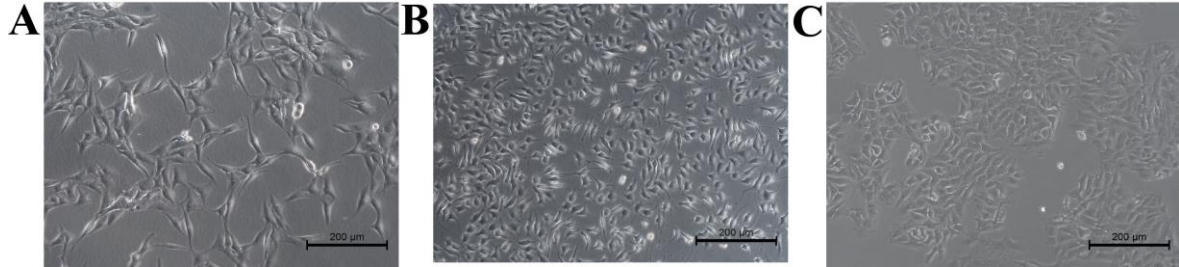
Hücrelerdeki apoptotik etki düzeyi *Annexin-V/Propidium Iodide (FITC Annexin Apoptosis Detection Kit I, 556547 – BD Pharmingen, ABD)* işaretlemesi yapılarak akım sitometrisi ile değerlendirilmiştir. Hücreler 6 kuyucuklu kültür kabına ekilmiş ve konfluense ulaştıklarında ED50’de CB65 hücrelere uygulanmıştır. MG63 hücreleri 48, Saos-2 hücreleri 24 saat inkübasyonun ardından hücreler kültür plağından kaldırılmıştır. Santrifüjlenen hücrelerden

süpernatant uzaklaştırılmış ve hücreler PBS ile yıkanmıştır. Hücrelere 1X *Binding Buffer* eklenmiş ve ardından 5 µl Annexin V ve 5 µl PI eklendikten sonra 15 dakika oda ısısında karanlıkta inkübe edilmiştir. İnkübasyon sonrası 400 µl 1X *Binding Buffer* eklenmiş ve akım sitometri (Novocyt 2000R Flow Cytometer System, Agilent, ABD) cihazında analiz edilmiştir. Gruplar arasında erken ve geç apoptotik hücre düzeyi canlı hücre düzeyiyle karşılaştırılmıştır.

3. BULGULAR

3.1. Hücre Kültürü

MG63 insan osteosarkom hücreleri kültür plağında oval-iğsi biçimli, çok kutuplu, uzantılı görünüm vermiştir (Şekil 1.A). Saos-2 insan osteosarkom hücreleri homojen boyutlu, poligonal biçimli, uzantılı hücreler olarak izlenmiştir (Şekil 1.B). İnsan küçük hücreli dışı akciğer kanseri A549 hücreleri heterojen büyüklükte, poligonal biçimli, epitel kökenli adenokarsinom hücreleri olarak saptanmıştır (Şekil 1.C). Saos-2 ve MG63 hücreleri için pasaj 20-25 ve A549 için pasaj 15-20 olacak şekilde kültüre edilerek sonraki iş paketlerinde kullanılmak üzere çoğaltılmıştır.

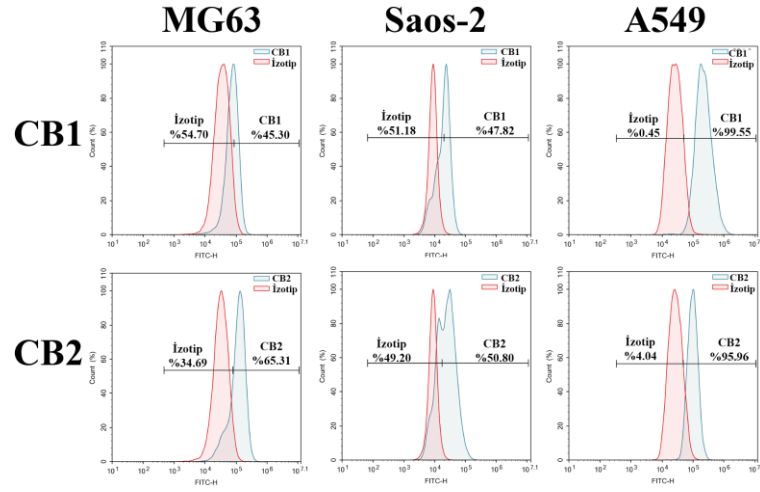


Şekil 1. Kültür plaklarına tutunmuş (A) oval, iğsi MG63, (B) sık yerleşimli oval Saos-2 ve (C) polimorfik A549 hücre hatlarının mikrografları gösterilmiştir (x100).

3.2. MG63 ve Saos-2 Hücre Hatları Akım Sitometrisi Yöntemiyle CB1 Reseptörlerini Düşük CB2 Reseptörlerini Yüksek Bulundurmaktadır

MG63 hücrelerinde hücre içi ortalama CB1 ve CB2 reseptör işaretlenme oranları sırasıyla %45.30±7.42 ve %65.31±12.85 (Şekil 2) olarak ölçülmüştür. Saos-2 hücrelerinde hücre içi CB1 ve CB2 reseptör işaretlenme oranlarına ait ortalama değerler sırasıyla %47.82±6.05 ve %50.80±16.33 (Şekil 2) saptanmıştır. A549 hücrelerinde hücre içi ortalama CB1 ve CB2 reseptör işaretlenme oranları %99.55±0.14 ve %95.96±1.97 (Şekil 2) saptanmıştır. MG63 ve

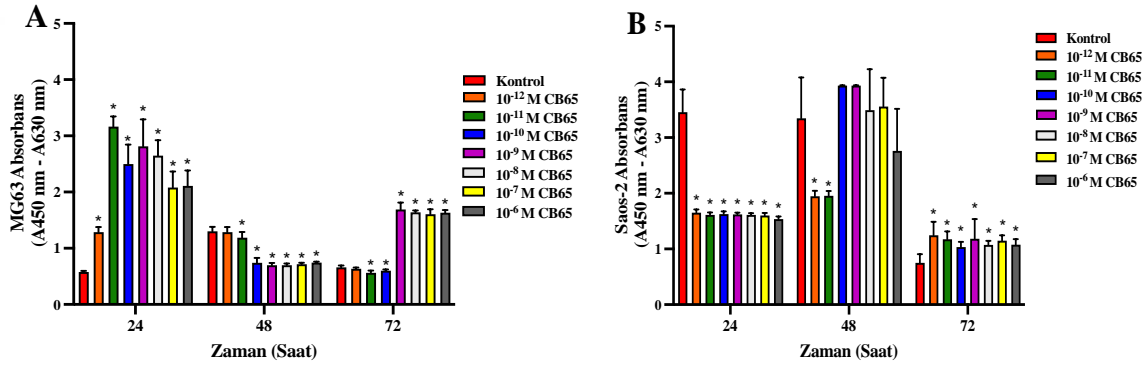
Saos-2 hatlarında CB1 ve CB2 reseptörlerine ait hücre içindeki ölçüm değerleri pozitif kontrol A549 ile karşılaştırıldığında daha düşük saptanmıştır ($p<0.05$).



Şekil 2. MG63, Saos-2 ve A549 hücre hatlarında akım sitometrisi yöntemi ile tayin edilen hücre içi CB1 ve CB2 reseptör immün işaretlenme düzeyleri temsili histogram grafikleri ile gösterilmiştir.

3.3. CB2 Reseptörünü En Yüksek Seviyede Bulunduran MG63 ve Saos-2 Hücrelerinde Sentetik Spesifik CB2 Agonisti CB65 Hücre Çoğalmasını Azaltmaktadır

Birinci günde CB65, uygulandığı 10^{-12} – 10^{-6} M doz aralığında MG63 hücrelerinin proliferasyonunu kontrole göre arttırmıştır ($p<0.05$). Hücrelerin proliferasyon hızı uygulanan dozlar ile farklılık göstermemiştir. İkinci günde CB65 10^{-11} – 10^{-6} M doz aralığında uygulandığında MG63 hücrelerinin proliferasyonu kontrole göre azalmıştır ($p<0.05$). CB65'in 10^{-12} M dozda uygulanması 2. günde kontrole göre MG63 hücrelerinin büyüme hızını değiştirmemiştir. CB65 üçüncü günde 10^{-11} – 10^{-10} M dozlarda uygulandığında kontrole göre proliferasyon hızını azaltmış ($p<0.05$), 10^{-9} – 10^{-6} M doz aralığında uygulandığında hücre çoğalmasını kontrole göre arttırıcı yönde etki göstermiştir (Şekil 3.A). Birinci günde CB65, uygulandığı 10^{-12} – 10^{-6} M doz aralığında Saos-2 hücre proliferasyonunu kontrole göre azaltmıştır ($p<0.05$). Hücrelerin proliferasyon hızı uygulanan dozlar ile farklılık göstermemiştir. İkinci günde CB65 10^{-12} – 10^{-11} M dozlarda uygulandığında hücre proliferasyonu kontrole göre azalmış ($p<0.05$), 10^{-10} – 10^{-6} M dozlarda uygulandığında proliferasyonunu kontrole göre arttırmıştır ($p<0.05$). CB65 üçüncü günde 10^{-12} – 10^{-6} M doz aralığında uygulandığında kontrole göre proliferasyon hızını arttırmıştır (Şekil 3.B).

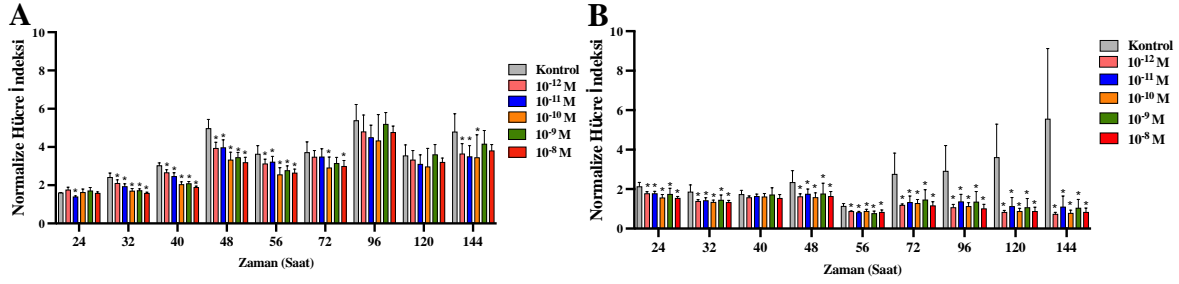


Şekil 3. CB65'in (A) MG63 ve (B) Saos-2 hücre hattının proliferasyonuna etkisi WST-1 ile saptanmıştır. 10^{-12} – 10^{-6} M dozda CB65 uygulanan MG63 hücrelerinin 24, 48 ve 72. saatlerdeki verileri kontrol grubuyla karşılaştırmalı olarak bar grafiğinde gösterilmiştir. 10^{-11} ve 10^{-10} M CB65 uygulamasının 24. saatte proliferatif, 48 ve 72. saatte antiproliferatif etkisi gözlenmiştir (n=6). (*): Kontrolle göre $p < 0.05$.

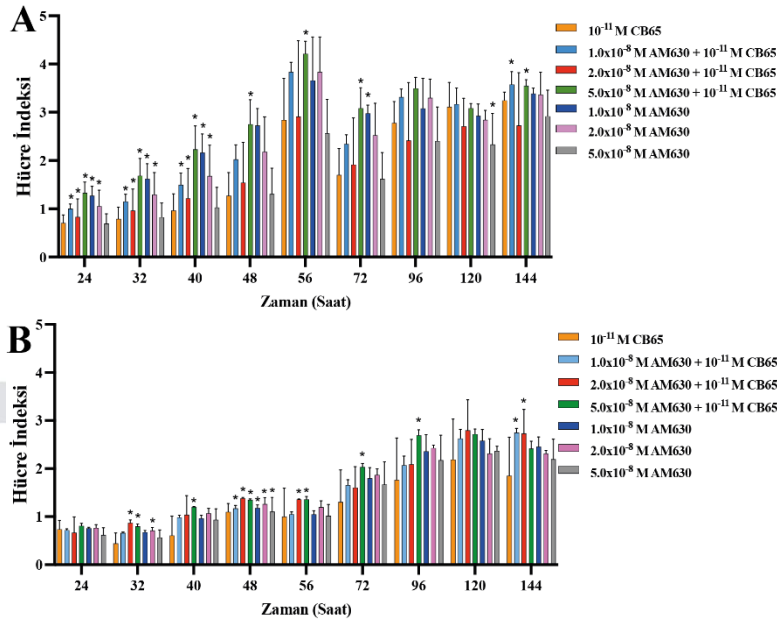
3.4. Osteosarkom Hücrelerinde CB65'in Gerçek Zamanlı Spesifik Yarı Maksimum Antiproliferatif Etki Penceresi MG63 Hattı için 48. Saatte 1.11×10^{-11} M ve Saos-2 Hattı için 24. Saatte 4.95×10^{-11} M Olarak Saptanmıştır. Spesifik Etki CB2 Reseptör Antagonisti ile Bloke Olmuştur

Sentetik spesifik CB2 agonisti CB65, WST analizi ile belirlenen etkili doz aralığında uygulandığında MG63 hücrelerinin proliferasyonunda 24. saatten itibaren azalmaya neden olmuştur (Şekil 4.A). 10^{-12} – 10^{-8} M CB65 uygulanan MG63 hücrelerinin proliferasyonu 32. saatten itibaren 144. saate kadar kontrole göre istatistiksel anlamlı azalmıştır (Şekil 4.A, $p < 0.05$). CB65'in MG63 hücrelerindeki antiproliferatif ED50 değeri 46. saatte 1.11×10^{-11} M olarak hesaplanmıştır. Belirlenen doz aralığında CB65 uygulandıktan sonra Saos-2 hücrelerinin proliferasyonunda 24. saatten itibaren azalmaya neden olmuştur (Şekil 4.B). 10^{-11} M CB65 uygulanan Saos-2 hücrelerinin proliferasyonu 24. saatten itibaren 144. saate kadar kontrole göre istatistiksel anlamlı azalmıştır (Şekil 4.B, $p < 0.05$). 10^{-11} M CB65, Saos-2 hücreleri için en etkili antiproliferatif doz olarak değerlendirilmiştir. CB65'in Saos-2 hücrelerindeki 20. Saatte ED50 değeri 4.95×10^{-11} M olarak hesaplanmıştır. Spesifik CB2 reseptör antagonisti AM630, CB65 ile beraber uygulandığında 5×10^{-8} M dozda, CB65'in MG63 hücrelerindeki antiproliferatif etkisini terapötik pencereyi kapsayan 24. saatten 144. saate kadar inhibe etmiştir (Şekil 5.A). AM630, CB65 ile beraber uygulandığında 1×10^{-8} M ve 2×10^{-8} M dozlarda CB65'in MG63 hücrelerindeki antiproliferatif etkisini terapötik pencerenin içindeki 24. saatten 40. saate kadar inhibe etmiş, etki 40. saatten itibaren sonlanmıştır. Spesifik CB2 reseptör antagonisti AM630, CB65 ile beraber uygulandığı tüm dozlarda (1×10^{-8}

10^{-8} M, 2×10^{-8} M 5×10^{-8} M) CB65'in Saos-2 hücrelerindeki antiproliferatif etkisini terapötik pencereyi kapsayan 32. saatten 144. saate kadar inhibe etmiştir (Şekil 5.B).



Şekil 4. CB65'in (A) MG63 ve (B) Saos-2 osteosarkom hücre hattındaki antiproliferatif etkisi gerçek zamanlı ve impedans temelli olarak saptanmıştır (n=5). Zamana karşı normalize hücre indeksini her doz için gösteren bar grafiğinde, CB65 10⁻¹¹ M dozda hücre çoğalmasını 24-144. saatlerde kontrole göre azaltmıştır. (*): Kontrole göre p<0.05.

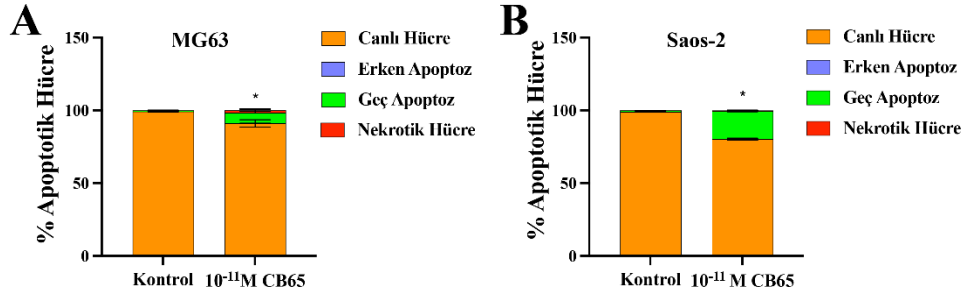


Şekil 5. CB65'in (A) MG63 ve (B) Saos-2 osteosarkom hücre hattındaki antiproliferatif etkisi gerçek zamanlı ve impedans temelli olarak saptanmıştır (n=5). Zamana karşı hücre indeksini her doz için gösteren bar grafiğinde, CB65 10⁻¹¹ M dozda hücre çoğalmasını 24-144. saatlerde kontrole göre azaltmıştır. (*): Kontrole göre p<0.05.

3.5. Sentetik Spesifik Kannabinoid CB2 Agonisti CB65 Akım Sitometrisi ile MG63 ve Saos-2 Osteosarkom Hücre Hatlarında Geç Apoptozu %7.31 ve %19.06 Oranında Arttırmaktadır

CB65'in 1.11×10^{-11} M dozda 48. saatte MG63 hattında (Şekil 4.11.A ve Şekil 4.12.A) *Annexin-PI* ile işaretli geç apoptotik hücre sayısını düşük oranda ancak kontrole göre anlamlı olarak arttırdığı saptanmıştır (p<0.05). CB65 4.95×10^{-11} M dozda 24. saatte Saos-2 hattında (Şekil 4.11.B ve Şekil 4.12.B) benzer şekilde *Annexin-PI* işaretli geç apoptotik hücre sayısını düşük oranda ancak kontrole göre anlamlı olarak arttırdığı saptanmıştır (p<0.05). CB65

uygulanması MG63 ve Saos-2 hatlarında uygulamanın yapıldığı zaman aralığında *Annexin* ile işaretli erken apoptotik ve *PI* ile işaretli nekrotik hücre oranlarını etkilememiştir.



Şekil 6. Bar grafiklerde CB65 (A) MG63 hücre hattında 1.11×10^{-11} M dozda 48. saatte (B) Saos-2 hücre hattında 4.95×10^{-11} M dozda 24. saatte geç apoptozu kontrole göre artırmaktadır. CB65 uygulandığı saat aralığında hücrelerde erken apoptozu neden olmamakta, nekrotik hücre sayısını değiştirmemektedir (n=3). (*): Kontrole göre $p < 0.05$.

4. TARTIŞMA, SONUÇ

Sentetik spesifik CB2 agonisti CB65'in, CB2 reseptörünü yüksek seviyede bulundurduğu bilinen MG63 ve Saos-2 hücre hatlarında farklı oranlarda CB1 ve CB2 reseptörleri saptanmış ve CB2 reseptör oranı CB1 reseptör oranına göre daha yüksek seviyede bulunmuştur. Kannabinoid 2 reseptörü eksprese eden MG63 ve Saos-2 hücre hatlarında WST-1 yöntemi ile, sentetik spesifik CB2 agonisti CB65 proliferasyonu azaltıcı etki göstermiştir. Gerçek zamanlı proliferasyon analizi ile sentetik spesifik CB2 agonisti CB65, MG63 hücrelerinde 1.11×10^{-11} M dozda 48. saatte, Saos-2 hücrelerinde 4.95×10^{-11} M dozda 24. saatte proliferasyonu azaltıcı ve apoptozu indükleyici etki göstermiştir.

Bu proje Hacettepe Üniversitesi Bilimsel Araştırma Projeleri Koordinasyon Birimi tarafından (TYL-2021-15357) desteklenmiştir.

5. KAYNAKÇA

1. Punzo, F., C. Tortora, D. Di Pinto, I. Manzo, G. Bellini, F. Casale, *et al.* (2017). Anti-proliferative, pro-apoptotic and anti-invasive effect of EC/EV system in human osteosarcoma. *Oncotarget*. **8**(33): p. 54459-54471.
2. Lindsey, B.A., J.E. Markel, and E.S. Kleinerman. (2017). Osteosarcoma Overview. *Rheumatol Ther*. **4**(1): p. 25-43.
3. Society, T.A.C. *Key Statistics About Bone Cancer*. 2020.
4. Niu, F., S. Zhao, C.-Y. Xu, H. Sha, G.-B. Bi, L. Chen, *et al.* (2015). Potentiation of the antitumor activity of adriamycin against osteosarcoma by cannabinoid WIN-55,212-2. *Oncology letters*. **10**(4): p. 2415-2421.
5. Abrams, D.I. and M. Guzman. (2015). Cannabis in cancer care. *Clin Pharmacol Ther*. **97**(6): p. 575-86.
6. Bogdanović, V., J. Mrdjanović, and I. Borišev. (2017). A review of the therapeutic antitumor potential of cannabinoids. *The Journal of Alternative and Complementary Medicine*. **23**(11): p. 831-836.
7. Dzierżanowski, T. (2019). Prospects for the use of cannabinoids in oncology and palliative care practice: a review of the evidence. *Cancers*. **11**(2): p. 129.

8. Hinz, B. and R. Ramer. (2019). Anti-tumour actions of cannabinoids. *British journal of pharmacology*. **176**(10): p. 1384-1394.
9. Fitzcharles, M.-A. and W. Häuser. (2016). Cannabinoids in the management of musculoskeletal or rheumatic diseases. *Current rheumatology reports*. **18**(12): p. 1-9.
10. Moreno, E., M. Cavic, A. Krivokuca, V. Casadó, and E. Canela. (2019). The endocannabinoid system as a target in cancer diseases: are we there yet? *Frontiers in pharmacology*. **10**: p. 339.
11. Apostu, D., O. Lucaciu, A. Mester, H. Benea, D. Oltean-Dan, F. Onisor, *et al.* (2019). Cannabinoids and bone regeneration. *Drug Metab Rev*. **51**(1): p. 65-75.
12. Zimmer, A. (2016). A collaboration investigating endocannabinoid signalling in brain and bone. *Journal of basic and clinical physiology and pharmacology*. **27**(3): p. 229-235.
13. Punzo, F., C. Tortora, D. Di Pinto, E. Pota, M. Argenziano, A. Di Paola, *et al.* (2018). Bortezomib and endocannabinoid/endovanilloid system: a synergism in osteosarcoma. *Pharmacol Res*. **137**: p. 25-33.
14. Bellini, G., D. Di Pinto, C. Tortora, I. Manzo, F. Punzo, F. Casale, *et al.* (2017). The Role of Mifamurtide in Chemotherapy-induced Osteoporosis of Children with Osteosarcoma. *Curr Cancer Drug Targets*. **17**(7): p. 650-656.
15. Rodríguez-Rodríguez, I., J. Kalafut, A. Czerwonka, and A. Rivero-Müller. (2020). A novel bioassay for quantification of surface Cannabinoid receptor 1 expression. *Scientific Reports*. **10**(1): p. 18191.
16. Agudelo, M., A. Yndart, M. Morrison, G. Figueroa, K. Muñoz, T. Samikkannu, *et al.* (2013). Differential expression and functional role of cannabinoid genes in alcohol users. *Drug Alcohol Depend*. **133**(2): p. 789-93.
17. Garofano, F. and I.G.H. Schmidt-Wolf. (2020). High Expression of Cannabinoid Receptor 2 on Cytokine-Induced Killer Cells and Multiple Myeloma Cells. *Int J Mol Sci*. **21**(11).



**EVALUATION OF SEMEN PARAMETERS AND SPERM MORPHOLOGY IN
INDIVIDUALS WITH DIFFERENT BODY MASS INDEX (BMI)****Khadeejah Sead Mohammed ABRAHEEM¹, Esra OZKOCER², Duygu DAYANIR³,
Mesut ÖKTEM⁴, Candan ÖZOĞUL⁵**

¹ Gazi University, Faculty of Medicine Department of Histology and Embryology, Ankara, Turkey, and Omar Al-mukhtar university, Faculty of Medicine Department of Histology and Embryology, Albide, Libya, mg303035@gmail.com.

² Gazi University, Faculty of Medicine Department of Histology and Embryology, Ankara, Turkey, sesavari@gmail.com.

³ Gazi University, Faculty of Medicine Department of Histology and Embryology, Ankara, Turkey, duygudayanir@yahoo.com.tr.

⁴ Gazi University, Faculty of Medicine Department of Obstetrics and Gynecology, Ankara, Turkey, mesutoktem@gmail.com.

⁵ Kyrenia University, Department of Histology and Embryology, Kyrenia, Cyprus, ozogulcandan@gmail.com.

Abstract: Infertility is defined as the inability of couples to achieve pregnancy despite having unprotected and regular sexual intercourse for at least 1 year. A pregnancy may only be accomplished via the use of assisted reproductive technologies by couples who are suffering from infertility, which affects about 15% of the population. This study aimed to understand the relationship between BMI and semen parameters of male subjects evaluated in an infertility clinic. In our study, a total of 60 infertile men were divided into three groups as BMI, normal weight (18.5-24.99 kg/m²), overweight (25-29.99 kg/m²) and obese (>30.0) kg/m². Semen parameters (volume, concentration, total semen count, morphology and motility) were compared between the three BMI groups. In the obese group, semen volume, total concentration, total motility, and motility at different rates were shown to be reduced. This study clarified the link between obesity and sperm quality, morphology, chromatin structure, DNA integrity, and antioxidant/oxidant balance. Therefore, increased body mass index BMI can negatively affect normal sperm.

Keywords: Infertility, body mass index, Obesity, TAS, TOS.

Özet: İnfertilite, çiftlerin en az 1 yıl boyunca korunmasız ve düzenli cinsel ilişkiye girmesine rağmen gebelik elde edememesi olarak tanımlanmaktadır (WHO, 2010). Toplumun yaklaşık %15'inde görülen kısırlık sorunundan şikayet eden çiftlerde yardımcı üreme tekniklerine bağlı olarak gebelik ancak bu şekilde sağlanabilir. Bu çalışma, infertilite kliniğinde değerlendirilen erkek deneklerin BMI ile semen parametreleri arasındaki ilişkiyi anlamayı amaçlamıştır. Çalışmamızda, toplam 60 infertil erkek, çalışma popülasyonu BMI, normal kilolu (18,5-24,99 kg/m²), fazla kilolu (25- 29.99 kg/m²) ve obez (>30,0) olmak üzere üç gruba ayrıldı. kg/m²). Semen parametreleri (hacim, konsantrasyon, toplam semen sayısı, morfoloji ve motilite) üç

BMI grubu arasında karşılaştırıldı. Obez grupta normal gruba göre semen hacmi, toplam konsantrasyon, toplam motilite ve motilitenin farklı oranlarda azaldığı belirlendi. Ancak, bu azalmalar tüm parametreler için istatistiksel olarak anlamlı değildi. Bu çalışma, obezite ile sperm kalitesi, morfolojisi, kromatin yapısı, DNA bütünlüğü ve antioksidan/oksidan dengesi arasındaki bağlantıyı netleştirdi. Bu nedenle artan vücut kitle indeksi BMI normal spermi olumsuz etkileyebilir.

Anahtar Kelimeler: *İnfertilite, vücut kitle indeksi, Obezite, TAS, TOS.*

1.INTRODUCTION

The World Health Organization (WHO) (1) defines an infertile couple as a sexually active couple that is unable to conceive naturally within one year of sexual activity. Infertility affects around 15% of all couples. Male infertility affects 50% of couples unable to conceive. Male infertility is caused by a variety of factors, including urogenital system defects, both congenital and acquired, certain malignancies, sperm-duct blockages, urogenital system infections, and the use of certain medications. Among the other possible reasons include testicular injuries and varicocele. Genetic anomalies. On the other side, idiopathic male infertility is a condition in which the reason of male infertility cannot be diagnosed in 30% to 40% of cases (2). The body mass index (BMI), a simple and affordable metric, is a widely accepted criterion for defining obesity. BMI is calculated by dividing a person's total weight (in kilograms) by the square of their height (in meters) (kg/m^2) (3). A BMI that is outside the normal range has been linked to a variety of disorders (4). Today, various models have been used to study the association between obesity and reproductive biology. For instance, a drop in blastocyst development and a decrease in live birth rates were observed in couples with weight issues who sought assisted reproductive procedures and were documented in the literature (5). Numerous research have also examined the detrimental consequences of obesity on the male reproductive system (6, 7). Scientific data overwhelmingly supports the function of oxidative stress (OS) as a causative factor in a variety of clinical diseases (8). The implications of the anomalies in OS levels, which have known systemic consequences, are likewise parallel to the microenvironment of the reproductive system. Increased OS levels in female and/or male persons can cause disease in a variety of processes, ranging from zygote formation through pregnancy continuation (9). Moderate levels of reactive oxygen species (ROS) in the male reproductive system had no detrimental effect on sperm capacitation, acrosome response, or motility activation. However, an increase in the burden of oxidative stress and/or a decrease in antioxidant defense produce pathogenic effects and are a

significant cause of infertility (10). Numerous studies have established a link between increased oxidative stress in the ejaculate and increased BMI. According to some, increased oxidative stress alters the shape of sperm and results in DNA breakage (11). It has been shown that DNA damage produced by elevated seminal oxidative stress levels in sperm impairs natural conception and also lowers pregnancy rates attained through assisted reproductive procedures (12). Infertile males with a BMI of 18.5-24.9 kg/m², overweight infertile men with a BMI of 25.0-29.9 kg/m², and obese infertile men with a BMI of >30 kg/m² were included in this study. Semen samples were analyzed and compared for sperm morphology, oxidative stress parameters, DNA fragmentation, a marker of cell death, sperm nucleus morphology, and general semen parameters.

2.MATERIALS AND METHODS

Permission was granted for the thesis by Gazi University Clinical Research Ethics Committee decision 364 dated 14.05.2018.

Between July 2018 and July 2020, semen samples will be collected from couples who applied to the Gazi University Medical Faculty Assisted Reproductive Treatment Center (ÜYTEM) and male patients diagnosed with male-borne infertility. Each patient signed a paper indicating that he had given his informed consent. The sample group for this study consisted of 60 infertile Turkish men ranging in age from 22 to 54 years. Each patient's medical and infertile history was documented. Volunteer Inclusion Criteria:

- Between the ages of 22 and 54 (13). Volunteers Exclusion Criteria (13-14).
 - Smoking, Alcohol use
 - Regular sauna use
 - Diagnosis of diabetes Mellitus, hypothyroidism, hypertension, chronic kidney-liver disease, asthma, epilepsy, atherosclerosis, orchidectomy, steroid use, hypogonadism in need of medical treatment, thromboembolism diagnosis, testicular cancer, chronic inflammatory bowel disease.
 - Having a history of cerebrovascular disease
 - Detection of bacterial contamination in semen
 - Diagnosed azoospermia ($\sim 1 \times 10^6$ ml⁻¹ sperm concentration) each patient's weight and height with a professional calibrated device were measured. BMI was calculated by dividing the weight to height squared. Patients were stratified according to their BMI into three groups. The evaluation process included a total of 60 patients with infertility symptoms.
 - 20 normal (BMI 18.5-24.9 kg/m²).
 - 20 overweight (25.0-29.9 kg/m²).
 - 20 (BMI \geq 30 kg/m²) obese men were eligible for the study (15).
- Semen specimens were collected and examined for the following:

2.1.Experiment 1: Semen Analysis

Masturbation was used to gather sperm samples following a suggested 3-5 days of abstinence. Following collection, specimens were allowed to liquefy for 30 minutes at room temperature before being used for analysis. On microscopic examination, the number of sperm and the percentage of motility and morphology were determined objectively in accordance with World Health Organization (WHO) recommendations (1).

To evaluate sperm morphology, ten liters of semen were placed on slides. By extracting the semen with the aid of another clean slide, a thin smear of semen was generated. A 4% paraformaldehyde solution was used to repair the air dried stain. Following fixation, the smear was rinsed with distilled water for 10 minutes and dyed with spermic dye (LOT: FP12S05, FertilPro) (16) according to the manufacturer's directions:

2.2.Experiment 2: Chromatin Maturation Assessment

For the acidic aniline blue staining, 10 l of liquefied sperm were spread. For thirty minutes at room temperature, air-dried smears were fixed with 4% paraformaldehyde. Following fixing, the smears were rinsed for five minutes with distilled water. For 5 minutes, stained with a 2% acetic acid, 5% anilin blue (Ph= 3,5) solution (B8563 LOT: SLBQ9814V, Sigma). The extra dya from the previous day is removed by washing with tap water and then air drying. Under a light microscope, 200 sperms were examined at 1000x magnification using immersion oil. Two independent researchers used DM 4000 Leica Germany imaging analysis equipment to classify spermatozoa according to their aniline blue staining characteristics: completely stained (++), partially stained (+ -), and unstaining sperms (-) (17).

2.3.Experiment 3: TUNEL Test for DNA Fragmentation

TUNEL, one of the most frequently used methods for detecting DNA fragmentation, is a therapeutically relevant diagnostic with a high sensitivity and specificity. The TUNEL test is used to determine the amount of fluorescently labeled dUTP present in single and double strand DNA fragments. This reaction is mediated by terminal nucleotidyl transferase (TdT), an enzyme that is not affected by mold. In this thesis, Millipore's ApopTag with peroxidase In Situ Apoptosis Detection kit (S7101) was employed.

All these operations were carried out with the DM 4000 Leica Germany visual analysis system available in our department, 200 sperms were evaluated as sperm positive or negative for TUNEL.

2.4.Experiment 4: TAS/TOS Analysis

Semen 700G was centrifuged for 10 minutes. After the supernatant part was separated it was stored at -20 c in Eppendorf tubes (1-1.5 ml).

TAS (REL Assay Diagnostics, LOT: EL18091A) and TOS (REL Assay Diagnostics, LOT: MT181050) levels were measured calorimetrically using the commercial kit. During the experiment, it was applied as stated in the kit contents. Color change was determined using a SHIMADZU UV-1601 spectrophotometer.

2.5.Statistical Methods

Graphs and the Shapiro-Wilk test were used to determine if continuous variables conformed to the normal distribution. The variables were described using the mean, standard deviation, median, minimum, and maximum values.

ANOVA was used to compare the variables that comprised the parametric test assumptions. When a difference in the ANOVA result was discovered, the Bonferroni post-hoc test was used to determine the source of the difference.

To compare skewed data (nonparametric) variables, the Kruskal-Wallis test was used. When a difference was discovered, post-hoc pairwise comparisons using the Mann-Whitney test with Bonferroni correction were used to determine which group was different.

IBM SPSS Statistics 21 was used for statistical analysis and calculations (IBM Corp, NA, USA). In statistical analysis, the p0.05 value was used to indicate a statistically significant difference.

3.RESULTS

3.1.General Sperm Parameter Findings

Although a decrease was observed in semen volume values in the obese group, the Kruskal-Wallis test result was not statistically significant between all groups (p=0.347).

Regarding to the concentration values The Kruskal-Wallis test result was not statistically significant between all groups (p=0.468).

Although a decrease was observed in total concentration values in the obese group, the Kruskal-Wallis test result was not statistically significant between all groups (p=0.515).

There was no statistical significance among all groups in Total motility values with the result of the Kruskal-Wallis test (p = 0.591).

No statistical significance was found among all groups in The motility sperm count of 4% with the result of the Kruskal-Wallis test ($p = 0.703$).

There was no statistically significant difference between all groups in 3% motility sperm count in the result of the Kruskal-Wallis test ($p = 0.520$).

The Kruskal-Wallis test result was not statistically significant in The 2% motility sperm count between all groups ($p=0.409$).

Table 1. Descriptive data on general sperm parameters and sperm morphology parameters

General Sperm Parameters					Sperm Morphology Parameters				
		Groups					Groups		
		Normal	overweight	Obese			Normal	overweight	Obese
Semen volume (ml)	Mean	3,1	3,2	2,5	Normal shape (%)	Mean	27,20	16,25	15,30
	Standard Deviation	1,4	1,4	0,9		Standard Deviation	13,30	5,61	5,97
	Median	2,8	3,0	3,0		Median	29,50	18,00	15,50
	Minimum	1,5	1,5	1,0		Minimum	5,00	6,00	3,00
	Maximum	6,0	6,0	4,0		Maximum	51,00	24,00	22,00
Concentration (million/ml)	Mean	30	24	31	Total anomaly shape (%)	Mean	72,80	83,90	84,80
	Standard Deviation	24	25	29		Standard Deviation	13,30	5,93	6,07
	Median	26	17	24		Median	70,50	82,00	84,50
	Minimum	3	0	1		Minimum	49,00	76,00	78,00
	Maximum	85	95	88		Maximum	95,00	97,00	97,00
Total concentration (%)	Mean	79	80	76	Head anomaly (%)	Mean	10,15	9,40	11,35
	Standard Deviation	53	111	71		Standard Deviation	5,51	6,18	6,06
	Median	66	51	75		Median	8,50	7,50	12,00
	Minimum	7	0	3		Minimum	0,00	1,00	2,00
	Maximum	200	475	264		Maximum	20,00	20,00	22,00
Total motility (%)	Mean	62	56	60	Neck anomaly (%)	Mean	9,60	10,45	11,85
	Standard Deviation	16	23	18		Standard Deviation	6,05	6,76	4,52
	Median	61	60	60		Median	9,50	9,00	12,00
	Minimum	10	0	0		Minimum	2,00	2,00	5,00
	Maximum	84	90	85		Maximum	26,00	27,00	20,00
Motility %4 (%)	Mean	4	4	2	Tail anomaly (%)	Mean	5,05	4,85	8,20
	Standard Deviation	7	7	5		Standard Deviation	4,19	4,04	5,84
	Median	0	0	0		Median	4,50	4,50	7,50
	Minimum	0	0	0		Minimum	0,00	0,00	0,00
	Maximum	26	21	20		Maximum	15,00	17,00	20,00
Motility %3 (%)	Mean	48	43	47	Head and neck anomaly (%)	Mean	19,55	24,20	21,10
	Standard Deviation	13	19	17		Standard Deviation	8,20	10,14	7,86
	Median	50	45	50		Median	20,00	24,00	21,50
	Minimum	10	0	0		Minimum	9,00	7,00	8,00
	Maximum	68	80	77		Maximum	40,00	43,00	36,00
Motility %2 (%)	Mean	10	9	11	Head and tail anomaly (%)	Mean	0,10	0,50	0,10
	Standard Deviation	5	5	5		Standard Deviation	0,31	1,28	0,45
	Median	10	10	10		Median	0,00	0,00	0,00
	Minimum	0	0	0		Minimum	0,00	0,00	0,00
	Maximum	20	21	20		Maximum	1,00	5,00	2,00
					Head, neck and tail anomaly (%)	Mean	28,35	34,50	32,20
						Standard Deviation	11,88	10,16	15,68
						Median	25,00	36,00	30,00
						Minimum	15,00	16,00	11,00
						Maximum	63,00	49,00	65,00

3.2.Sperm Morphology Findings

When the groups were compared in terms of total sperm count with anomaly, the Kruskal-Wallis test result was statistically significant between all groups ($p=0.004$). Although there was no statistical difference between the overweight and obese groups ($p=1,000$); The percentage of sperm with abnormal morphology was higher in the overweight and obese groups compared to the normal group. This difference was statistically significant according to the Mann Whitney U test with Bonferoni correction ($p= 0.021$; 0.006 , respectively).

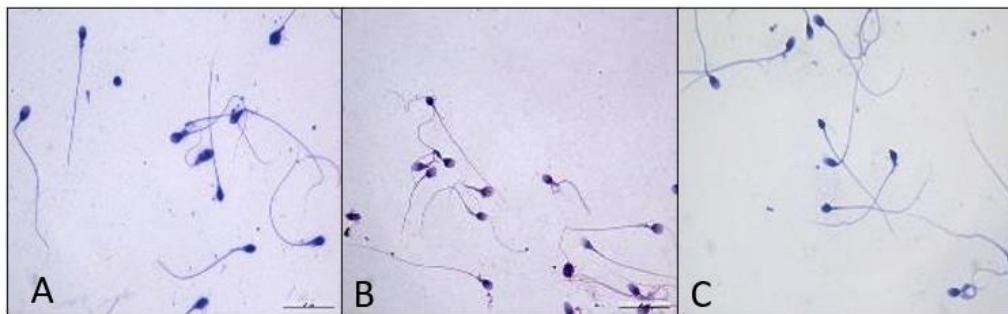


Figure 1. A view of sperm samples obtained from normal (a), overweight (b) and obese (c) men. X1000 spermac

3.3. Chromatin Condensation Findings

Sperm chromatin condensation were evaluated by aniline blue. Mainly, sperm with unstained nuclei were evaluated as mature sperm, while sperm with blue stained nuclei were evaluated as immature sperm.

When the groups were compared in terms of the number of aniline blue stained sperm, the ANOVA test result was statistically significant between all groups ($p=0.005$). Though there was no statistically significant difference between the overweight and obese groups ($p=1,000$); In the overweight and obese groups, the percentage of dyed sperm increased compared to the normal group. This increase was statistically significant compared to the post hoc test with Bonferoni correction (Respectively, $p= 0.011$; 0.015).

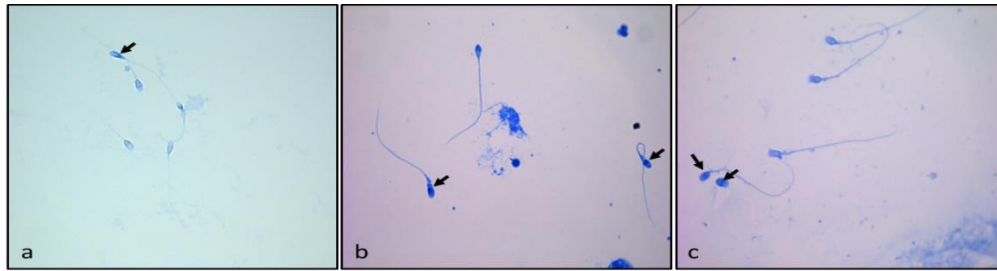


Figure 2. Representative view of aniline blue stained sperm samples of the groups (normal (a), overweight (b) and obese (c)). Arrow: aniline blue dyed sperm nuclei, X1000, Aniline blue

Table 2. Descriptive data of aniline blue staining and TUNEL analysis

Aniline Blue Staining					TUNEL analysis				
		Groups					Groups		
		Normal	overweight	Obese			Normal	overweight	Obese
Aniline blue stained cell (%)	Mean	47,45	62,65	62,05	TUNEL positive cells (%)	Mean	21	52	54
	Standard Deviation	20,02	16,11	9,52		Standard Deviation	18	13	34
	Median	48,50	67,50	63,00		Median	18	56	63
	Minimum	12,00	27,00	40,00		Minimum	0	23	3
	Maximum	93,00	80,00	75,00		Maximum	54	71	100

3.4. TUNEL Findings

When the groups were compared in terms of TUNEL positive sperm count, the Kruskal-Wallis test result was statistically significant between all groups ($p < 0.001$). Although there was no statistical difference between the overweight and obese groups ($p = 1,000$); TUNEL positive sperm percentage increased in the overweight and obese groups compared to the normal group. This increase was statistically significant according to the Bonferoni-corrected Mann Whitney U test ($p < 0.001$; < 0.001 , respectively).

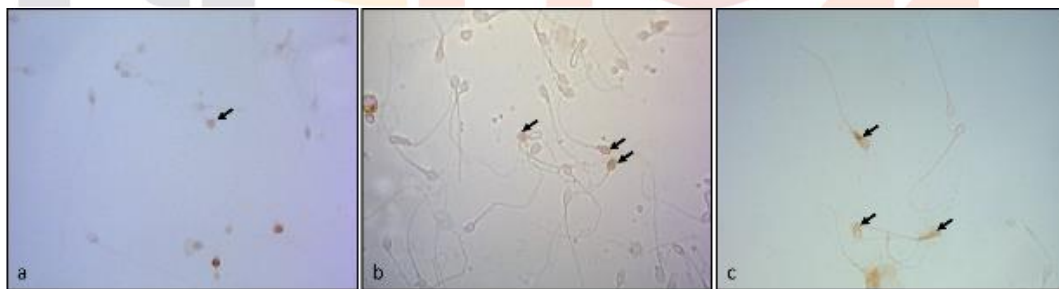


Figure 3. Representative view of TUNEL positive sperms of the groups (normal (a), overweight (b) and obese (c)). Arrow: TUNEL positive sperm, X1000

3.5. Evaluations for TAS and TOS Parameters

3.5.1. TAS values

When the obtained TAS results were evaluated statistically by Kruskal Wallis test, no significant difference was found. Pairwise comparison of groups was applied with Mann Whitney test. When the obtained results were evaluated statistically, no significant difference

was found between Normal and Overweighted groups ($p=0.824$) even TAS values were higher at Normal group. The statistically evaluation of results obtained from Normal and Obese groups also showed no significant difference ($p=0.448$) even TAS values were higher at Normal group. Similarly obtained results of Overweighted and Obese groups were evaluated statistically, again no significant difference was found between groups ($p=0.706$), even TAS values were higher at Overweighted group.

Table 3. Descriptive statistical values obtained from biochemical values of TAS and TOS parameter

		TAS				
		Mean	Standard Deviation	Median	Minimum	Maximum
Groups	normal	1,40	,33	1,50	,65	1,79
	overweight	1,37	,34	1,38	,69	1,81
	obese	1,34	,31	1,35	,67	1,82
		TOS				
		Mean	Standard Deviation	Median	Minimum	Maximum
Groups	normal	18,11	11,96	15,64	4,89	58,94
	overweight	19,22	15,22	14,89	2,77	73,40
	obese	21,68	23,79	11,70	4,89	98,51

3.5.2.TOS values

When the obtained TOS results were evaluated statistically by Kruskal Wallis test, no significant difference was found ($p=0.308$). Pairwise comparison of groups was applied with Mann Whitney test. When the obtained results were evaluated statistically, no significant difference was found between Normal and Overweighted groups ($p=0.937$), even TOS values were higher at Overweighted group. The statistically evaluation of results obtained from Normal and Obese groups also showed no significant difference ($p=0.136$) even TOS values were higher at Obese group. Similarly obtained results of Overweighted and Obese groups were evaluated statistically, again no significant difference was found between groups ($p=0.273$) even TOS values were higher at Obese group.

4.DISCUSSION

Male infertility can be caused by a variety of causes, but it accounts for approximately 40% of all cases of infertility (20). Male infertility can be caused by a variety of causes, including the presence of anti-sperm antibodies, aberrant sperm production, hormonal imbalances,

obstruction of sperm ducts owing to testicular trauma or varicocele, anatomical abnormalities, and even certain medications. As a result, several variables that could influence the semen characteristics associated with BMI were deleted. Additionally, the most recent study overlooked some characteristics, such as smoking, varicocele, hormone changes, and other factors that affect fertility. In 2008, the World Health Organization (WHO) estimated that more than 1.4 billion individuals were overweight or obese (21). When it comes to sperm parameters, research has been inconsistent. The WHO published the semen parameters, which have been utilized in several studies. Additionally, the findings obtained about the effect of obesity on sperm parameters varied (13).

It is still difficult to diagnose spermatozoon malfunction using normal semen analysis, because the spermatozoon is a very particular cell that exhibits a wide array of biological characteristics in order to fertilize (23). Males are assumed to have abnormal sperm parameters as an indicator of reproductive issues. Nonetheless, up to 30% of men with normal sperm characteristics (normozoospermic) are diagnosed with UMI, as the cause of infertility remains unknown (22,24,25). Idiopathic infertility has proven to be a difficult condition for andrologists, with no significant treatment success reported.

This has resulted in the development of increased sperm function and seminal fluid quality assessments, such as oxidative stress and sperm DNA fragmentation (SDF), which can aid in the diagnosis, treatment, and prediction of male fertility outcomes (26, 27, 28). There were no significant variations in the traditional seminal parameters between the three groups evaluated in this investigation. Numerous studies have concluded the same thing as this one, with males being infertile despite having normal sperm parameters (23).

According to a WHO surveillance research, a greater BMI is associated with decreased sperm quality, which affects the volume, concentration, and motility of the sperm (29, 30). The study also examined men who were pregnant with their partners' sperm counts and discovered that obese men's total sperm counts were considerably lower than those of non-obese men (mean 231106 vs. 324106, respectively), despite the fact that sperm parameters were same (31).

Our research examined sperm metrics such as sperm volume, sperm concentration, total sperm concentration, and various sperm motility percentages. In compared to the normal weight group, obese persons exhibited significantly lower levels of semen volume, total

concentration, total motility, and 3% and 4% motility, respectively. However, none of these declines were statistically significant.

Furthermore, Mah and Wittert (32) discovered that obese men had a lower sperm concentration and total sperm count than lean men, despite the fact that motility associated with morphology is unaltered by obesity. In this retrospective study, it was discovered that overweight and obese infertile men had a higher prevalence of oligozoospermia and a lower progressive motile sperm concentration than men of normal weight (33). Overweight and obese men have a decreased sperm volume, which is associated with an increase in the percentage of degenerated spermatozoa, which is associated with an increase in sperm DNA fragmentation (34).

In comparison, multivariate study has demonstrated a negative link between progressive motility, BMI, motility, and neutral alphaglucosidase levels, which have been reported as an epididymal functional marker (35,36). In comparison, other human populations have demonstrated that such a link does not exist (2). Macdonald et al. have published a meta-analysis demonstrating that there is no association between BMI and other seminal factors. There was no statistically significant relationship between (BMI) and sperm concentration, motility, volume of ejaculate, or shape and size of sperm. Similarly, Aghamohammadi and Shahidi (37) found no effect of obesity on sperm concentration, motility, or morphology. Additionally, the most recent study confirms earlier published findings, since no statistical link between the three groups was discovered (33).

Due to the lack of objective measurement criteria, it is possible to contest the appraisal of sperm morphology, as it is still subject to the observer's subjective influences. Male sperm morphology has been demonstrated to be statistically significant indicators of body mass index (BMI). According to small-sample studies, weight loss improves sperm quality, especially sperm count, which is associated with appropriate sperm morphology (38). According to studies, abnormal sperm morphology and (BMI) continue to have a strong positive correlation (39).

The sperm morphology of the participants in the groups were examined in this research. In the normal group, there were 27.20 ± 13.30 percent of sperm with normal morphology; in the overweight and obese groups, it was 16.25 ± 5.61 percent and 15.30 ± 5.97 percent, respectively. For the overweight and obese groups, the total sperm count with abnormalities was $72.8 \pm 13.30\%$, $83.9 \pm 5.93\%$, and $84.8 \pm 6.07\%$, respectively.

Although the classifications of overweight and obesity are statistically indistinguishable. Men who were overweight or obese had a higher proportion of improperly shaped sperm than men who were normal weight. This difference was statistically significant.

Additionally, as noted in, aging has been associated with significant decreases in sperm volume, motility, morphology, and count (40, 41). Additionally, it has been demonstrated that aging and obesity have a detrimental effect on sperm chromatin, which is associated with DNA integrity (42). According to studies, male aging has resulted in an increase in genomic instability within sperm DNA. This instability manifests itself in a variety of ways, including epigenetic modifications and DNA fragmentation, as well as gene mutations and other chromosomal abnormalities (39,43).

For example, as indicated in numerous research publications on the impact of aging and obesity on metabolic imbalances, higher cell disintegration processes and shorter lifespans are associated with genetic instability and disruption of homeostatic pathways (44).

As stated in (45), the integrity of sperm chromatin has a similar effect on reproductive outcomes, provided that father obesity alters the molecular components of motile spermatozoa. As a result, as indicated in (46), sperm chromatin integrity may be deleterious to embryo morphology, which is associated with blastocyst formation. Additionally, as seen in the study, it may result in embryo implantation failure or a high rate of spontaneous abortions (47). As discovered by RAAD, Georges et al., paternal obesity as measured by (BMI and WC) is related with changes in the molecular composition of the motile sperm-enriched fraction and preimplantation embryo morphokinetics (48). When sperm is injected intracytoplasmically (ICSI), the quality of the growing embryo is equally critical (49). When only "abnormal-sperm embryos" are available, injecting individual, aberrant sperm cells may reduce both fertilization and implantation rates (50).

Aniline blue was used to examine sperm chromatin condensation in our investigation. Mature sperm were considered to have unstained nuclei, whereas immature sperm had blue stained nuclei. However, despite the lack of a statistically significant difference between the obese and overweight groups ($p=1,000$), the proportion of colored sperm was higher in the latter two than in the normal group.

Nuclear chromatin condenses during the final stages of spermiogenesis and epididymal transport. One of the most noticeable changes is the replacement of histone lysine-rich proteins with arginine-rich protamine. Simultaneously, bisulfidic connections between

cysteine residues are formed. Nuclear chromatin is densely packed to protect it from damage caused by both natural and chemical processes. There could be an increased rate of DNA fragmentation as a result of irregularities in the condensation of sperm chromatin (48). According to, oxidative stress, abnormal chromatin packing, and incomplete apoptosis are all possible causes of DNA fragmentation (49). Similar to the oxidation of the DNA base guanosine, excessive generation of (ROS) may result in an increase in DNA damage, either indirectly through the creation of byproducts of lipid degradation or directly through direct interaction with the DNA strand. As indicated in the paper, this results in non-specific single- and double-strand breaks (50).

Chavarro et al. (6) discovered that sperm with severe DNA damage were more prevalent in the obese men's group than in the normal weight men's group. According to Kort et al. (51), an increase in (BMI) was associated with an increase in the DNA fragmentation index of the sperm chromatin structure assay. Males who were obese had a higher DNA fragmentation index, which was connected with an increased risk of diabetes development (27 percent and 25.8 percent, respectively). Men who are overweight or obese are more likely to have sperm with DNA damage than men who are normal weight.

The following are the TUNEL results from our investigation, which are in line with previous findings. There was a TUNEL positive sperm count of $21\% \pm 18\%$ in the normal group, $52\% \pm 13\%$ of overweight men, and $54\% \pm 35\%$ of obese men, respectively. although no statistically significant difference between overweight and obese groups.

Overweight and obese males exhibited a significantly higher proportion of TUNEL positive sperm than the normal group.

Additionally, research from throughout the world indicates that infertile men have a larger concentration of free oxygen radicals than fertile men (45). Similarly, Sharma et al. (52) discovered that normozoospermic infertile men with lower TAS levels had higher TOS levels, whereas Shiva et al. (53) discovered that azoospermic males with lower oxidative stress levels possessed superior antioxidant capacities (45,46). While the normal group had significantly higher TAS levels than the overweight group, the researchers discovered no statistically significant difference between the two groups ($p = 0.824$). Although the TAS of the normal group was bigger than that of the obese group ($p = 0.448$), there was no statistically significant difference.

While the overweight group had higher TAS levels than the obese group ($p = 0.706$), this difference was not statistically significant ($p = 0.706$). Even though the overweight group had higher (TOS) values, when the normal and overweight populations were compared, statistically significant differences between the groups ($p = 0.937$) were seen. When (TOS) values for normal and obese patients were compared ($p = 0.136$), despite the fact that obese subjects had considerably higher (TOS) values. Although obese people had higher (TOS) values ($p = 0.273$), there was no statistical difference in (TOS) values between the overweight and obese categories. Because this was a small-scale experiment, it is likely that the negative trend discovered between (BMI) and sperm oxidative stress would have been statistically significant had the sample size been larger (47). Additionally, it was demonstrated that the DNA in human sperm remained firmly packed.

When comparing the Normal and Overweighted groups, no statistically significant differences could be identified. In fact, TAS values were higher at Normal group. The statistically evaluation of results obtained from Normal and Obese groups also showed no significant difference. Also, TAS values were higher at Normal group. Similarly obtained results of Overweighted and Obese groups were evaluated statistically, again no significant difference was found between groups, even TAS values were higher at overweighted group.

Even though TOS values were greater in the Overweighted group, there was no statistically significant difference between the two groups. The statistically evaluation of results obtained from Normal and Obese groups also showed no significant difference, even TOS values were higher at Obese group. Similarly obtained results of Overweighted and Obese groups were evaluated statistically, again no significant difference was found between groups, even TOS values were higher at Obese group.

5.CONCLUSION

According to this research, general sperm parameters were compared and investigated when sperm samples were acquired from normal weight, overweight, and obese individuals. Gaining weight was demonstrated to affect both the quantity of sperm in the body and the rate at which the sperm travelled through the ducts. In the research, which assessed sperm morphology, the proportion of aberrant sperm increased considerably in the overweight and obese categories compared to the normal group. By analyzing the aniline blue staining of sperm nuclear morphologies, we discovered that the overweight and obese groups had a greater number of immature sperm than the normal weight group. Additionally, this study

discovered an increase in the frequency of sperm with DNA breakage in the overweight and obese groups compared to the normal group. TAS and TOS studies used to determine the antioxidant/oxidant connection in cells revealed that the antioxidant level declined as body weight increased; nevertheless, the oxidant level increased.

With increasing BMI, sperm parameters declined, sperm morphology deteriorated, the number of immature sperm rose, and the number of sperm with DNA fragmentation increased. Additionally, antioxidant levels fell and oxidant levels increased. This study showed a link between obesity and sperm quality, chromatin structure, DNA integrity, and antioxidant/oxidant balance. As a result, an elevated BMI may have an effect on a male partner's ability to produce healthy sperm.

REFERENCES

1. Organization, W.H., *WHO laboratory manual for the examination and processing of human semen*. 2010.
2. Aggerholm, A. S., Thulstrup, A. M., Toft, G., Ramlau-Hansen, C. H., and Bonde, J. P. (2008). Is overweight a risk factor for reduced semen quality and altered serum sex hormone profile?. *Fertility and sterility*, 90(3), 619-626.
3. Calamusa, G., Amodio, E., Costantino, C., Di Pasquale, M., Gelsomino, V., Morici, M., and Vitale, F. (2012). Body mass index and factors associated with overweight and obesity: a cross-sectional in a small city of Western Sicily (Italy). *Italian Journal of Public Health*, 9(3).
4. Janssen, I., Katzmarzyk, P. T., and Ross, R. (2002). Body mass index, waist circumference, and health risk: evidence in support of current National Institutes of Health guidelines. *Archives of internal medicine*, 162(18), 2074-2079.
5. Chung, F. (2016). Morbidly obese patients: a clinical challenge. *Current Opinion in Anesthesiology*, 29(1), 101-102.
6. Chavarro, J. E., Toth, T. L., Wright, D. L., Meeker, J. D., and Hauser, R. (2010). Body mass index in relation to semen quality, sperm DNA integrity, and serum reproductive hormone levels among men attending an infertility clinic. *Fertility and sterility*, 93(7), 2222-2231.
7. Eisenberg, M. L., Kim, S., Chen, Z., Sundaram, R., Schisterman, E. F., and Buck Louis, G. M. (2014). The relationship between male BMI and waist circumference on semen quality: data from the LIFE study. *Human reproduction*, 29(2), 193-200.
8. Cabler, S., Agarwal, A., Flint, M., and Du Plessis, S. S. (2010). Obesity: modern man's fertility nemesis. *Asian journal of andrology*, 12(4), 480.
9. Tunc, O., Bakos, H. W., and Tremellen, K. (2011). Impact of body mass index on seminal oxidative stress. *Andrologia*, 43(2), 121-128.
10. Yeung, C. H., Cooper, T. G., De Geyter, M., De Geyter, C., Rolf, C., Kamischke, A., and Nieschlag, E. (1998). Studies on the origin of redox enzymes in seminal plasma and their relationship with results of in-vitro fertilization. *Molecular human reproduction*, 4(9), 835-839.
11. Riaz, M., Mahmood, Z., Shahid, M., Saeed, M. U. Q., Tahir, I. M., Shah, S. A., and El-Ghorab, A. (2016). Impact of reactive oxygen species on antioxidant capacity of male reproductive system. *International journal of immunopathology and pharmacology*, 29(3), 421-425.
12. Jensen, T. K., Andersson, A. M., Jørgensen, N., Andersen, A. G., Carlsen, E., and Skakkebaek, N. E. (2004). Body mass index in relation to semen quality and reproductive hormones among 1,558 Danish men. *Fertility and sterility*, 82(4), 863-870.
13. Engin-Ustun, Y., Yilmaz, N., Akgun, N., Aktulay, A., Tuzluoğlu, A. D., and Bakırarar, B. (2018). Body mass index effects Kruger's criteria in infertile men. *International journal of fertility and sterility*, 11(4), 258.
14. Alsaikhan, B., Alrabeeah, K., Delouya, G., and Zini, A. (2016). Epidemiology of varicocele. *Asian journal of andrology*, 18(2), 179.
15. Internet: WHO – World Health organization (2016). Fact sheet: Obesity and overweight. URL: <http://www.who.int/mediacentre/factsheets/fs/>, Last Access: 18.01.2022
16. Chan, P. J., Corselli, J. U., Jacobson, J. D., Patton, W. C., and King, A. (1999). Sperm stain analysis of human sperm acrosomes. *Fertility and sterility*, 72(1), 124-128.
17. Torabi, F., Binduraim, A., and Miller, D. (2017). Sedimentation properties in density gradients correspond with levels of sperm DNA fragmentation, chromatin compaction and binding affinity to hyaluronic acid. *Reproductive BioMedicine Online*, 34(3), 298-311.
18. Zhang, L. H., Qiu, Y., Wang, K. H., Wang, Q., Tao, G., and Wang, L. G. (2010). Measurement of sperm DNA fragmentation using bright-field microscopy: comparison between sperm chromatin dispersion test and terminal uridine nick-end labeling assay. *Fertility and sterility*, 94(3), 1027-1032.

19. Laokirkkiat, P., Jareemit, N., Thanaboonyawat, I., Smith, H., and Sriam, S. (2019). Correlation between the Hypoosmotic SwellingT and DNA Fragmentation Assessed by the TUNEL Assay in Asthenozoospermia. *Siriraj Medical Journal*, 71(1), 8-13.
20. Kumar, N., and Singh, A. K. (2015). Trends of male factor infertility, an important cause of infertility: A review of literature. *Journal of human reproductive sciences*, 8(4), 191.
21. Calamusa, G., Amodio, E., Costantino, C., Di Pasquale, M., Gelsomino, V., Morici, M., and Vitale, F. (2012). Body mass index and factors associated with overweight and obesity: a crosssectional in a small city of Western Sicily (Italy). *Italian Journal of Public Health*, 9(3).
22. Panner Selvam, M. K., Agarwal, A., Pushparaj, P. N., Baskaran, S., and Bendou, H. (2019). Sperm proteome analysis and identification of fertility-associated biomarkers in unexplained male infertility. *Genes*, 10(7), 522.
23. Sidhu, R. S., Hallak, J., Sharma, R. K., Thomas, A. J., and Agarwal, A. (1998). Relationship between creatine kinase levels and clinical diagnosis of infertility. *Journal of assisted reproduction and genetics*, 15(4), 188-192.
24. Hamada, A., Esteves, S. C., and Agarwal, A. (2011). Unexplained male infertility: potential causes and management. *Human Andrology*, 1(1), 2-16.
25. Wallach, E. E., and Moghissi, K. S. (1983). Unexplained infertility. *Fertility and Sterility*, 39(1), 5-21
26. World Health Organisation. (1999). WHO laboratory manual for the examination of human semen and sperm-cervical mucus interaction. Cambridge university press.
27. Esteves, S. C., Sharma, R. K., Gosálvez, J., and Agarwal, A. (2014). A translational medicine appraisal of specialized andrology testing in unexplained male infertility. *International urology and nephrology*, 46(6), 1037-1052.
28. Panner Selvam, M. K., Ambar, R. F., Agarwal, A., and Henkel, R. (2020). Etiologies of sperm DNA damage and its impact on male infertility. *Andrologia*, e13706.
29. Hammiche, F., Laven, J. S., Twigt, J. M., Boellaard, W. P., Steegers, E. A., and Steegers-Theunissen, R. P. (2012). Body mass index and central adiposity are associated with sperm quality in men of subfertile couples. *Human reproduction*, 27(8), 2365-2372.
30. Thomsen, L., Humaidan, P., Bungum, L., and Bungum, M. (2014). The impact of male overweight on semen quality and outcome of assisted reproduction. *Asian journal of andrology*, 16(5), 749.
31. Kay, V., and Da Silva, S. M. (2020). Male obesity—impact on semen quality. In *Obesity and Gynecology* (pp. 119-126). Elsevier.
32. Mah, P. M., and Wittert, G. A. (2010). Obesity and testicular function. *Molecular and cellular endocrinology*, 316(2), 180-186.
33. Hammoud, A. O., Wilde, N., Gibson, M., Parks, A., Carrell, D. T., and Meikle, A. W. (2008). Male obesity and alteration in sperm parameters. *Fertility and sterility*, 90(6), 2222-2225.
34. Bounartzi, T., Dafopoulos, K., Anifandis, G., Messini, C. I., Koutsonikou, C., Kouris, S., and Messinis, I. E. (2016). Pregnancy prediction by free sperm DNA and sperm DNA fragmentation in semen specimens of IVF/ICSI-ET patients. *Human Fertility*, 19(1), 56-62.
35. Martini, A. C., Tissera, A., Estofán, D., Molina, R. I., Mangeaud, A., de Cuneo, M. F., and Ruiz, R. D. (2010). Overweight and seminal quality: a study of 794 patients. *Fertility and sterility*, 94(5), 1739-1743.
36. MacDonald, A., Herbison, G. P., Showell, M., and Farquhar, C. M. (2010). The impact of body mass index on semen parameters and reproductive hormones in human males: a systematic review with meta-analysis. *Human reproduction update*, 16(3), 293-311.
37. Aghamohammadi, A., and Shahidi, M. (2011). Male body mass index and sperm parameters. *GINECO RO*, 7(2), 92-93.
38. Loutradi, K. E., Tarlatzis, B. C., Goulis, D. G., Zepiridis, L., Pagou, T., Chatziioannou, E., and Bontis, I. (2006). The effects of sperm quality on embryo development after intracytoplasmic sperm injection. *Journal of assisted reproduction and genetics*, 23(2), 69-74.
39. Wang, Z., Liu, X., Xu, J., Yang, Q., Niu, W., Dai, S., and Guo, Y. (2020). Paternal age, body mass index, and semen volume are associated with chromosomal aberrations-related miscarriages in couples that underwent treatment by assisted reproductive technology. *Aging (Albany NY)*, 12(9), 8459.
40. Hellstrom, W. J., Overstreet, J. W., Sikka, S. C., Denne, J., Ahuja, S., Hoover, A. M., ... and Whitaker, J. S. (2006). Semen and sperm reference ranges for men 45 years of age and older. *Journal of andrology*, 27(3), 421-428.
41. Kidd, S. A., Eskenazi, B., and Wyrobek, A. J. (2001). Effects of male age on semen quality and fertility: a review of the literature. *Fertility and sterility*, 75(2), 237-248.
42. Das, M., Al-Hathal, N., San-Gabriel, M., Phillips, S., Kadoch, I. J., Bissonnette, F., and Zini, A. (2013). High prevalence of isolated sperm DNA damage in infertile men with advanced paternal age. *Journal of assisted reproduction and genetics*, 30(6), 843-848.
43. Brahem, S., Mehdi, M., Elghezal, H., and Saad, A. (2011). The effects of male aging on semen quality, sperm DNA fragmentation and chromosomal abnormalities in an infertile population. *Journal of assisted reproduction and genetics*, 28(5), 425-432.
44. Ahima, R. S. (2009). Connecting obesity, aging and diabetes. *Nature medicine*, 15(9), 996-997.
45. Evenson, D., and Wixon, R. (2006). Meta-analysis of sperm DNA fragmentation using the sperm chromatin structure assay. *Reproductive biomedicine online*, 12(4), 466-472.
46. Virant-Klun, I., Tomazevic, T., and Meden-Vrtovec, H. (2002). Sperm single-stranded DNA, detected by acridine orange staining, reduces fertilization and quality of ICSI-derived embryos. *Journal of assisted reproduction and genetics*, 19(7), 319-328.
47. Denomme, M. M., McCallie, B. R., Parks, J. C., Schoolcraft, W. B., and Katz-Jaffe, M. G. (2017). Alterations in the sperm histone-retained epigenome are associated with unexplained male factor infertility and poor blastocyst development in donor oocyte IVF cycles. *Human reproduction*, 32(12), 2443-2455.

48. Rathke, C., Baarends, W. M., Awe, S., & Renkawitz-Pohl, R. (2014). Chromatin dynamics during spermiogenesis. *Biochimica et Biophysica Acta (BBA)-Gene Regulatory Mechanisms*, 1839(3), 155-168.
49. Loutradi, K. E., Tarlatzis, B. C., Goulis, D. G., Zepiridis, L., Pagou, T., Chatziioannou, E., and Bontis, I. (2006). The effects of sperm quality on embryo development after intracytoplasmic sperm injection. *Journal of assisted reproduction and genetics*, 23(2), 69-74.
50. De Vos, A., Van De Velde, H., Joris, H., Verheyen, G., Devroey, P., and Van Steirteghem, A. (2003). Influence of individual sperm morphology on fertilization, embryo morphology, and pregnancy outcome of intracytoplasmic sperm injection. *Fertility and Sterility*, 79(1), 42-48.
51. Kort, H. I., Massey, J. B., Elsner, C. W., Mitchell-Leef, D., Shapiro, D. B., Witt, M. A., and Roudebush, W. E. (2006). Impact of body mass index values on sperm quantity and quality. *Journal of andrology*, 27(3), 450-452.
52. Sharma, R. K., Pasqualotto, F. F., Nelson, D. R., Thomas Jr, A. J., & Agarwal, A. (1999). The reactive oxygen species—total antioxidant capacity score is a new measure of oxidative stress to predict male infertility. *Human reproduction*, 14(11), 2801-2807.
53. Shiva, M., Gautam, A. K., Verma, Y., Shivgotra, V., Doshi, H., & Kumar, S. (2011). Association between sperm quality, oxidative stress, and seminal antioxidant activity. *Clinical biochemistry*, 44(4), 319-324.



PHOENIXIN-14 IMMUNOREACTIVITY IN RAT KIDNEY TISSUE**Engin ESEN¹, Tuba PARLAK AK^{2*}**

¹Munzur Üniversitesi, Lisansüstü Eğitim Enstitüsü, Biyoteknoloji ABD, Tunceli, TÜRKİYE,
engin_esen21@hotmail.com

^{2*}Munzur Üniversitesi, Sağlık Bilimleri Fakültesi, Beslenme ve Diyetetik Bölümü, Tunceli, TÜRKİYE,
tubaparlakak@gmail.com

Abstract: *Phoenixin (Pnx), a novel endogenous neuropeptide, has been suggested to have diverse biological effects in many organs. This study was performed to study the investigation of immunoreactive distribution of Pnx-14 in the kidney tissues of male rats. Six adult Sprague-Dawley male rats, 3-4 months old, were used in the study. Immunohistochemical staining procedure was applied according to the avidin-biotin-peroxidase complex method. The amount of staining in the sections was done using light microscopy to give an immunoreactive histoscore (H-score) determined by scanning different areas of kidney tissue. Pnx-14 immunoreactivity was detected significantly increased in kidney sections compared to negative control sections ($p<0.05$). When compared with the negative control sections, it was observed that Pnx-14 immunoreactivity intensified especially in the tubules of kidney tissue. It was concluded that neuropeptide Pnx-14 participates in the regulation of various homeostatic functions by its potent immunoreactivity in the kidney and could potentially be an important regulator of renal physiology.*

Keywords: *Phoenixin-14, immunohistochemistry, kidney, rat*

1. INTRODUCTION

The diverse biological effects of neuropeptides are of wide interest to researchers. Different identification strategies allow the discovery of novel peptides, including identification from biological activities, receptor or genomic approaches (1). Phoenixin (Pnx), a novel endogenous neuropeptide, mainly exists as two active isoforms, phoenixin-14 (Pnx-14) and phoenixin-20 (Pnx-20) (2). Pnx is a highly conserved peptide across different species including human, rat, mouse, porcine, and canine (3). Although it has not yet been ten years since then, many studies have shown that Pnx exerts a variety of biological effects (1). Interestingly, Pnx immunoreactivity was detected in various peripheral tissues, including heart, thymus, stomach, and spleen, with the highest expression in hypothalamus in rats (4). This study was performed to study the investigation of immunoreactive distribution of Pnx-14 in the kidney tissues of male rats.

2. MATERIALS AND METHODS

Six adult Sprague-Dawley male rats, 3-4 months old, were used in the study. The rats were obtained from Firat University Experimental Research Center (FUDAM) and were housed in standard laboratory conditions (40-60% humidity, 24±3 °C temperature, 12 hours light: 12 hours dark cycle) during the study. The rats were provided with feed and water ad libitum. The procedures applied on rats were carried out with the approval of the Ethics Committee (Protocol No: 2019/145) approved by the Firat University Animal Experiments Local Ethics Committee. After the rats were decapitated, laparotomy procedures were performed quickly and kidney tissues were removed. Tissue samples were fixed in 10% buffered neutral formalin solution for 24-30 hours. Immunohistochemical staining procedure was applied according to the avidin-biotin-peroxidase complex method. Rabbit polyclonal Phoenixin-14 amide antibody (1:300, H-079-01, Phoenix Pharmaceuticals, Inc., Burlingame, CA 94010, USA) was administered as the primary antibody. UltraVision Detection System (Cat. No. TP-015-HA, Anti-polyvalent, HRP/AEC, Thermo Fisher Scientific Co., USA) was used for the other steps according to the instructions of the supplied company. Staining was completed using 3-amino-9-ethylcarbazole (AEC) chromogen. Sections were counterstained with Mayer's hematoxylin and covered with medium. In addition, sections were prepared for negative control evaluation. The amount of staining in the sections was done using light microscopy to give an immunoreactive histoscore (H-score) determined by scanning different areas of kidney tissue. SPSS 21.00 software package was used for statistical analyses. H-score evaluations are given as the mean ± standard deviation (SD).

3. RESULTS

The mean H-score of Pnx-14 in kidney tissue were illustrated in Table 1. Pnx-14 immunoreactivity was detected significantly increased in kidney sections compared to negative control sections ($p < 0.05$). When compared with the negative control sections (Figure 1), it was observed that Pnx-14 immunoreactivity intensified especially in the tubules of kidney tissue (Figure 2).

Table 1. Histoscore of Pnx-14 immunoreactivity in rat kidney tissues.

Kidney Tubules	Histoscore
Negative control	0.0±0.0
Pnx-14 positive	2.52±0.37 ^a

^a mean ± standard deviation (SD) (p<0.05).

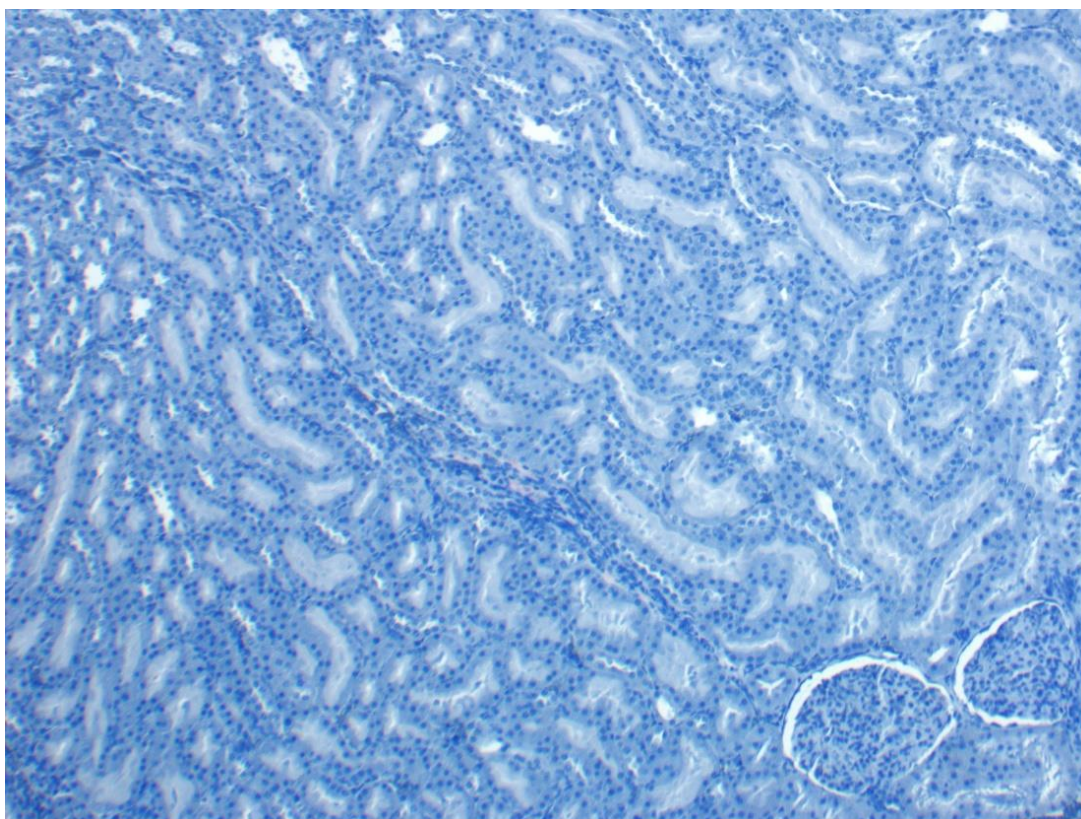


Figure 1. Negative control of rat kidney tissue (IHC, Mayer's haematoxylin counterstain, Magnification x100).

4. CONCLUSION

Our results demonstrated that Pnx-14 immunoreactivity in kidney tubules. It was concluded that neuropeptide Pnx-14 participates in the regulation of various homeostatic functions by its potent immunoreactivity in the kidney and could potentially be an important regulator of renal physiology.

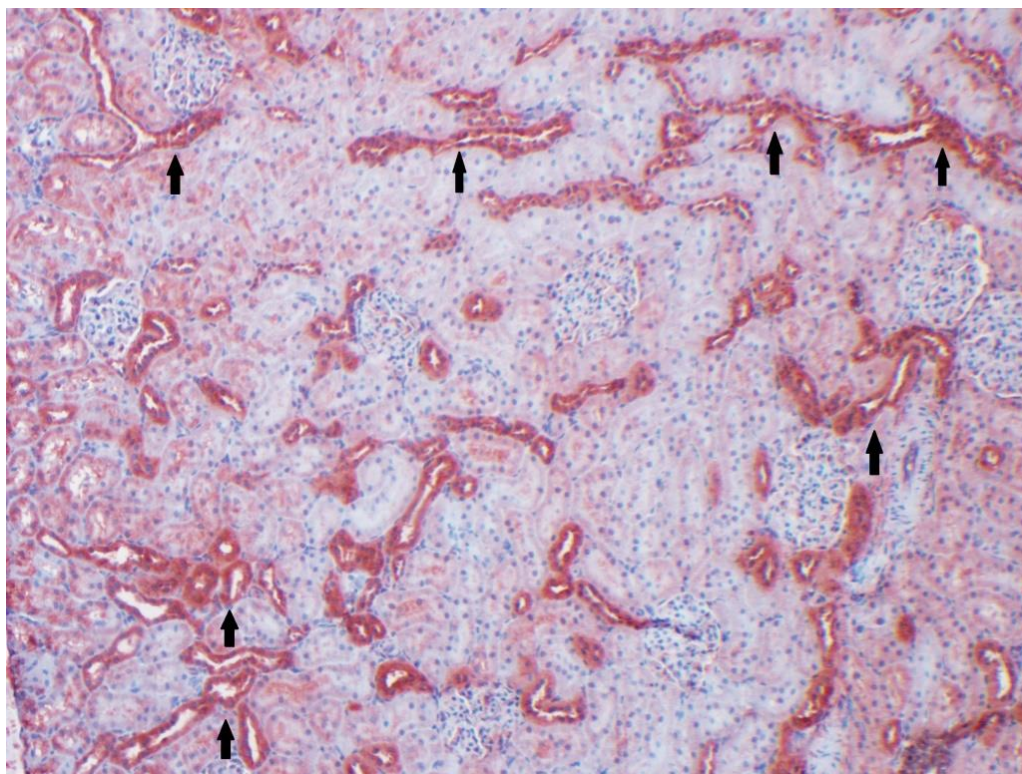


Figure 2. Immunoreactivity of Pnx-14 (arrows) in rat kidney tissue (IHC, Mayer's haematoxylin counterstain, Magnification x100).

5. REFERENCES

1. Billert, M., Rak, A., Nowak, K.W., Skrzypski, M. (2020). Phoenixin: more than reproductive peptide. *Int J Mol Sci*, 21, 8378.
2. Pałasz, A., Janas-Kozik, M., Borrow, A., Arias-Carrión, O., Worthington, J.J. (2018). The potential role of the novel hypothalamic neuropeptides nesfatin-1, phoenixin, spexin and kisspeptin in the pathogenesis of anxiety and anorexia nervosa. *Neurochem Int*, 113, 120-136.
3. Rajeswari, J.J., Unniappan, S. (2020). Phoenixin-20 stimulates mRNAs encoding hypothalamo-pituitary-gonadal hormones, is pro-vitellogenic, and promotes oocyte maturation in zebrafish. *Sci Rep*, 10, 6264.
4. Jiang, J.H., He, Z., Peng, Y.L., Jin, W.D., Mu, J., Xue, H.X., Wang, Z., Chang, M., Wang, R. (2015). Effects of Phoenixin-14 on anxiolytic-like behavior in mice. *Behav Brain Res*, 286, 39-48.

THREE-DIMENSIONAL MODELLING OF HASSALL'S CORPUSCLES

**Pınar AYRAN FİDAN¹, Berat Mert AKTAŞ², Selin YILDIZ², Beril BÜKE GÜLEÇ²,
Atahan ÖZDOĞAN², Delal DEMİR²**

1: Baskent University Faculty of Medicine, Department of Histology and Embryology, Ankara, Türkiye,
pinarfidan@baskent.edu.tr

2: Students from Baskent University Faculty of Medicine, Ankara, Türkiye, beratmert-191@hotmail.com,
selin.yildiz@live.com, berilgulec@hotmail.com, atahanozdogan@gmail.com, demirdelal@gmail.com

Abstract: *Thymus is the primary lymphoid organ and thymic epithelial cells carry out critical functions for T-cell development. Hassall's corpuscles composed of type VI thymic epithelial cells are the unique structures of thymus. In the past, Hassall's corpuscles were thought to be having no significant function because of their degenerating components. However in recent studies it is shown that Hassall's corpuscles represent functionally active components of thymic microenvironment regulating the differentiation of T lymphocytes. So, we aimed to investigate 3D structure of Hassall's corpuscles to obtain further evidence on their structural organization and function. Thymuses of two healthy adult, female, Sprague-Dawley rats were used. Plastic blocks were prepared and semi-thin serial sections of 200 nanometers thick were taken. Toluidine blue stained sections were examined in light microscope and digital images were obtained. Digital images were transformed into 3D images by using TanTuna 3D-Başkent Measuring and Modelling Programme (TT3D-BMMP) developed in our laboratory. It was observed that many Hassall's corpuscles were interconnected to each other in serial sections. Because of the difficulties to obtain thousands of serial section to reconstitute entire medulla of thymuses we examined different 3D reconstructed compartments of medulla and we observed interconnected Hassall's corpuscles in all samples. As Hassall's corpuscles do not represent inert structures, they possibly play a critical role in the elimination of T lymphocytes following their differentiation, selection and maturation processes. The structural confluency of these unique structures may have a significant role in their function which remains to be further elucidated.*

Keywords: *Hassall's Corpuscles, Three-dimensional modelling, Thymus, TT3D-BMMP*

1. Introduction

The thymus is the primary lymphoid organ for T cell development and thymic epithelial cells carry out critical functions for T-cell development. Connective tissue capsule surrounds the organ and sends septa to the parenchyma dividing the organ into incomplete lobules. The

thymus is composed of two compartments: independent cortex and a shared medulla. Cortex stains much darker than medulla because of the predominant population of maturing T lymphocytes. There are also macrophages and thymic epithelial cells in this compartment. Medulla stains paler histologically because of the predominance of thymic epithelial cells which also houses positively selected lymphocytes. A unique structure 'Hassall's corpuscles' is also present in the medulla. T cell development and selection takes place in the spaces between thymic epithelial cells forming a special microenvironment for this critical process. Hassall's corpuscles composed of tightly packed flattened type VI thymic epithelial cells which form concentric lamellae (1-3). In general, Hassall's corpuscles were believed to be having no significant function due to the presence of degenerating components like cellular debris. However, recent studies showed that epithelial cells in Hassall's corpuscles secrete some cytokines, growth factors and chemokines (4-10). So they provide Hassall's corpuscles are functionally active and may play a critical role in T lymphocyte differentiation. Although the development of the thymus and formation of Hassall's corpuscles were examined previously, functional importance of Hassall's corpuscles have not been validated yet (11-13). We aimed to investigate the 3D structure of Hassall's corpuscles to obtain further evidence on their function.

2. Materials and Methods

This study was approved by Baskent University Ethical Committee for Experimental Research on Animals (Project no: DA 19/05) and supported by Baskent University Research Fund. Thymuses of two healthy adult, female, Sprague-Dawley rats were used. Plastic blocks were prepared and semi-thin serial sections of 200 nanometers thick were taken. Toluidine blue stained sections were examined by LEICA DM3000 light microscope and digital images were obtained by using LEICA DFC500 camera (which is attached to LEICA DM3000) with LAS (Leica Application Suite) software. Prior to segmentation process the digital images were aligned in Adobe Photoshop CS4 program. The aligned digital images were transformed into 3D images by using TT3D-BMMP developed by Prof. Dr. Erhan Kızıltan (Head of Biophysics Department at Başkent University Faculty of Medicine) and Prof. Dr. Attila Dağdeviren (Head of Histology and Embryology Department at Başkent University Faculty of Medicine) (14). TT3D-BMMP is used for segmentation, and it has both manual and automatic (semi-automatic) options aiming to increase accuracy when needed. After

segmentation process, another freeware (Gmsh) is used for 3D reconstruction and imaging using these segmentation products.

3. Results

In thymus serial sections, cortex-medulla was easily distinguished. Numerous sections of Hassall's corpuscles were observed in the medulla. It was observed that many Hassall's corpuscles were interconnected to each other in serial sections which were used to create 3D reconstructed samples. Because of the difficulties to obtain thousands of serial sections to reconstitute entire medulla of thymuses we examined different 3D reconstructed compartments of medulla and we observed interconnected Hassall's corpuscles in all samples (Figure 1, 2).

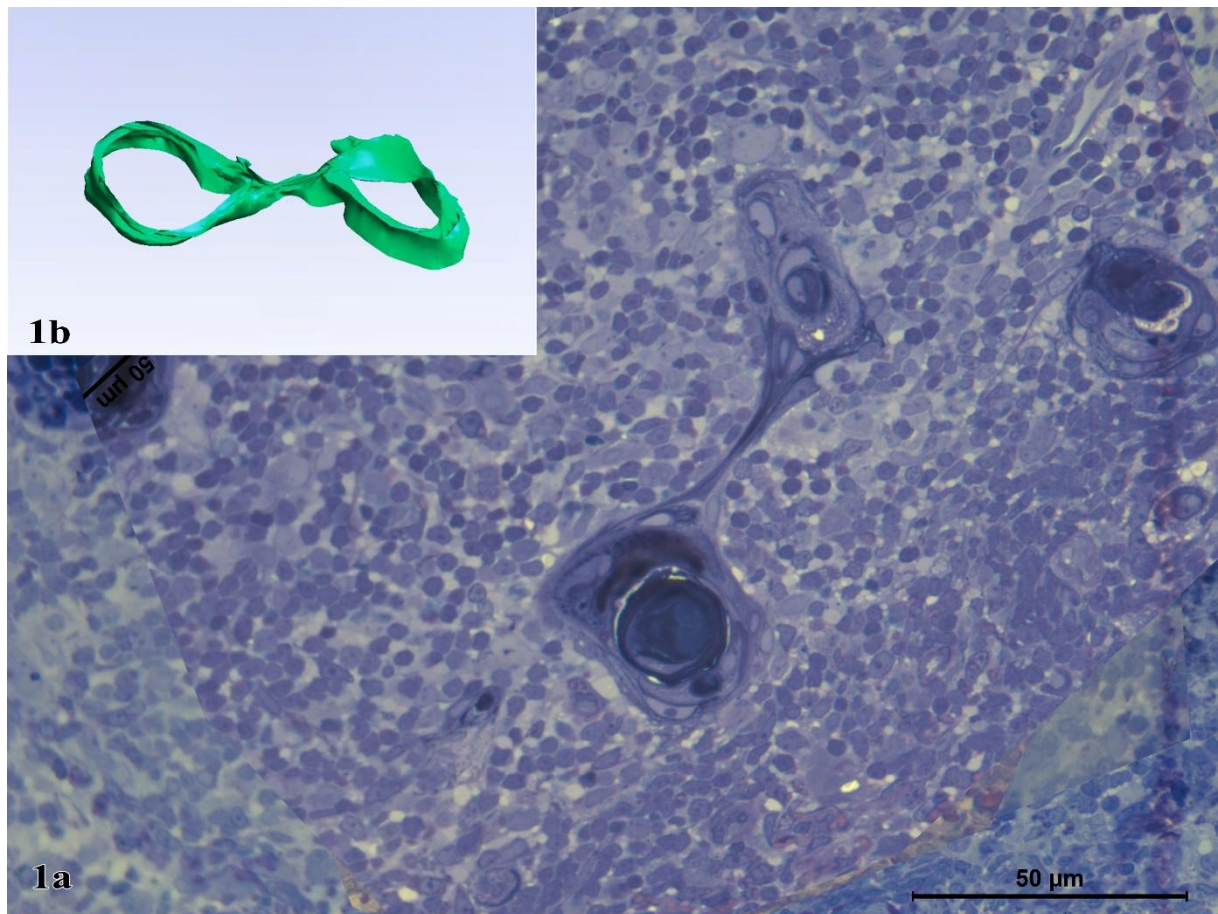


Figure 1: 1a) One of the serial sections of Hassall's corpuscles. (Toluidin blue, X40) **1b)** 3D image of the selected area by using the TT3D-BMMP.

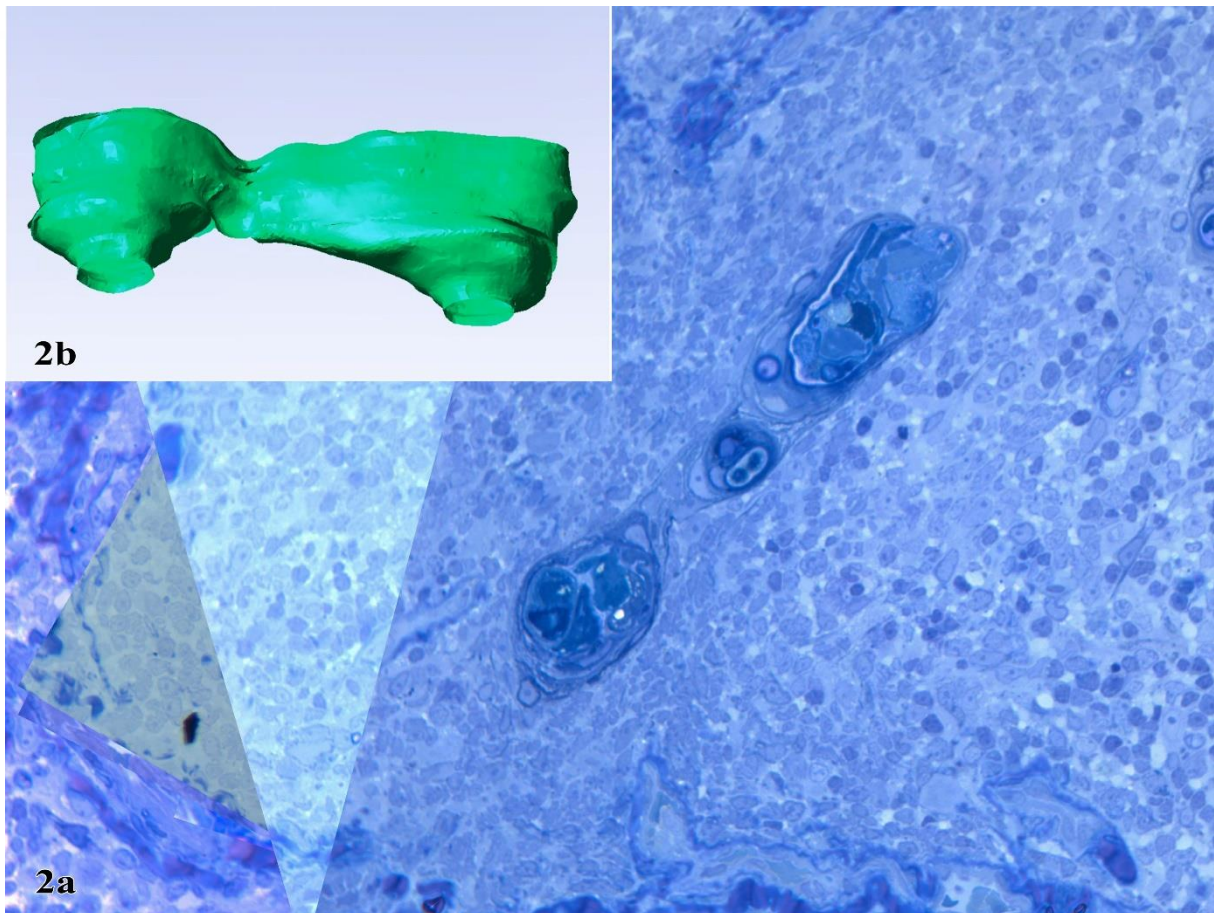


Figure 2: 2a) One of the serial sections of Hassall's corpuscles. (Toluidin blue, X40) 2b) 3D image of the selected area by using the TT3D-BMMP.

4. Discussion and Conclusion

There is only one study in the literature stating that Hassall's corpuscles are connected to each other. This study is actually examining the first formation period of the Hassall's corpuscles in the embryo, and they shared their observations in the following periods (11). Our findings are parallel to this study. Although the existence of Hassall's corpuscles has been known for over 150 years, its function is not yet fully understood. In recent studies, it has been suggested that they participate in the physiological activities of the thymus.

In our study, it was observed that Hassall's corpuscles were confluent both during the examination of serial sections under the light microscope and with the 3D program. The structural confluency of these unique structures may have a significant role in their function which remains to be further elucidated. The software, TT3D-BMMP is a comprehensive and freely available application for academic purpose. The software can be obtained directly from the Dr. Kızıltan (erhankiziltan@gmail.com). The most significant advantage of the presented

software is the availability of Dr. Kızıltan to modify and improve it according to specific needs of the end users comments.

5. References

1. Kierszenbaum, A.L., Tres, L.L. (2012). *Histology and cell biology, An introduction to pathology*. Third edition, Philadelphia, Elsevier Saunders.
2. Ross, M.H., Pawlina, W., (2011). *Histology a text and atlas*. 6th edition, Baltimore, Wolters Kluwer.
3. Anderson, G., Jenkinson, E. J. & Rodewald, H. R. (2009). A roadmap for thymic epithelial cell development. *European Journal of Immunology*, 39, 1694-1699.
4. Bodey, B., Siegel, S. E. & Kaiser, H. E. (2000). Novel insights into the function of the thymic Hassall's bodies. *In Vivo*, 14, 407-418.
5. Mikusova, R., Mest'anova, V., Polak, S. & Varga, I. (2017). What do we know about the structure of human thymic Hassall's corpuscles? A histochemical, immunohistochemical, and electron microscopic study. *Annals of Anatomy-Anatomischer Anzeiger*, 211, 140-148.
6. Sahni, S.S., Gupta, R., Gupta, T. & Aggarwal, A. (2017). Immunohistochemical Assessment of Hassall's Corpuscles in Human Foetal Thymuses. *Faseb Journal*, 31, 1.
7. Nishio, H., Matsui, K., Tsuji, H., Tamura, A., Suzuki, K. (2001). Immunolocalization of the mitogen-activated protein kinase signalling pathway in Hassall's corpuscles of the human thymus. *Acta Histochem.* 103,89-98.
8. Raica, M., Cimpean, AM., Encica, S., Motoc, A. (2006). Lymphocyte-rich Hassall bodies in the normal human thymus. *Ann. Anat.* 187, 175-177.
9. Watanabe, N., Wang, Y.H., Lee, H.K., Ito, T., Wang, Y.H., Cao, W., Liu, Y.J. (2005). Hassall's corpuscles instruct dendritic cells to induce CD4+CD25+ regulatory T cells in the human thymus. *Nature* 436, 1181-1185.
10. Zaitseva, M., Kawamura, T., Loomis, R., Goldstein, H., Blauvelt, A., Goldina, H. (2002). Stromal-derived factor 1 expression in the human thymus. *J. Immunol.* 168, 2609-2617.
11. Asghar, A., Yunus, S.M. & Faruqi, N.A. (2012). Histogenesis And Morphogenesis Of Hassall's Corpuscles In Human Fetuses: A Light Microscopic Study. *Journal of the Anatomical Society of India*, 61, 163-165.
12. Dubey, A., Jethani, S. L. & Singh, D. (2014). Estimation of gestational age from histogenesis of the thymus in human fetuses. *Journal of the Anatomical Society of India*, 63, 25-29.
13. Krishnamurthy, J.V., Devi, V.S. & Reddy, J.V. (2015). Developmental histology of human foetal thymuses at different gestational ages. *Journal of Evolution of Medical and Dental Sciences-Jemds*, 4, 6944-6953.
14. Kiziltan, E., Dağdeviren, A. (2020). Three-dimensional reconstruction of anatomical structures: interactive software providing patient specific solutions. *Türkiye Klinikleri J Med Sci.* 40(1):10-8. DOI:10.5336/medsci.2019-70940.

**THE ROLE OF CYTOKINES IN THE EFFECT OF CHRONOLOGICAL AGE ON
OVARIAN RESERVE; COMPARISON OF CYTOKINE CONCENTRATIONS IN
FOLLICULAR FLUID AND OVARIAN RESERVES IN IVF CYCLES OF WOMEN
OVER AND UNDER 35 YEARS OF AGE**

Filiz YILMAZ¹, Ercan AYAZ², Cihan TOGRUL³

¹Hitit University Erol Olçok Training and Research Hospital, IVF Center, Corum, Turkey,
drfilizyilmaz@gmail.com

²Hitit University Faculty of Medicine, Department of Histology and Embryology, Corum, Turkey,
ercanayaz21@hotmail.com

³Hitit University Faculty of Medicine, Department of Obstetrics and Gynecology, Corum, Turkey,
cihantogrul@hitit.edu.tr

Abstract:

Introduction: Fertility declines with chronological age, but there are not many studies on the molecular mechanism involved in this process. When aging and age-related diseases are examined, it has been shown that cytokines have an irregular distribution. We aimed to investigate the role of cytokines in ovarian reserve, which decreases with aging. We evaluated the role of cytokines in ovarian reserve adequacy by evaluating ovarian reserve-related cytokines in the young patient group.

Materyal Metod: This prospective randomized study was performed with follicle fluids. 86 patients included in the study were divided into 2 groups as under 35 years old and over 35 years old. Each group was divided into 2 subgroups as those with poor and normal ovarian reserve. Concentrations of IL-17F, IL-21, INF-alpha2 cytokines were measured by ELISA analysis. Correlation between patients' reproductive hormones, AMH, AFC, fertilization rates and cytokine concentrations were evaluated.

Results: We showed that IL-17F, IL-21 and INF-alpha2 levels in the follicular fluid change with aging. In addition, IL-17F level was found to be lower in patients with low ovarian reserve, regardless of age. We found that this decrease correlated with AMH and AFC ($p < 0.05$).

Conclusion: These findings suggest that IL-17F decrease in follicular fluid may adversely affect ovarian reserve, regardless of age. By interfering with the cytokine IL-17F, which we have shown in our study to have a role in the pathogenesis of poor ovarian reserve, a new treatment method can be developed and may provide an idea for diagnostic tests.

Keywords: Follicular fluid, cytokine, aging, ovarian reserve.

1.INTRODUCTION

Failure to achieve pregnancy despite regular unprotected sexual intercourse for 12 months is defined as infertility. Roughly 15% of married couples are affected by infertility. Hence, the interest in assisted reproductive techniques continues to increase and develop today. Ovarian reserve is the most significant prognostic factor in achieving pregnancy in IVF cycles. Patients with low ovarian reserve make up the majority of the group with poor response to ovarian stimulation in IVF cycles, with high cycle cancellation and low pregnancy rates. The most up-to-date criteria used to describe a low ovarian response to ovarian stimulation are the ESHRE Bologna criteria. According to these criteria, it was stated that advanced maternal age (>40 years) or any risk factor for poor ovarian response (chemotherapy, radiotherapy, etc.), previous episodes of poor ovarian response to ovarian stimulation, or the presence of at least two of the criteria for abnormality in ovarian reserve tests (antral follicle count <5-7 and/or AMH <1.2ng/mL) may define poor ovarian response for the patient.

One of the most important parameters to be considered in assisted reproductive therapy applications at all ages are ovarian reserve. The term ovarian reserve signifies the size and quality of the ovarian follicle pool, and various sonographic and hormonal markers are utilized for quantification. Some of the markers used to evaluate ovarian reserve are as follows: clinical factors, age, basal blood tests, FSH, LH, estradiol, progesterone, inhibin B, AMH, ultrasound tests, antral follicle count (AFC) and ovarian volume.

The total number of oocytes a woman has is genetically determined and this number gradually decreases throughout her life. Thus, a woman's chronological age is a straightforward way to learn about her ovarian reserve. Although ovarian age is often parallel to chronological age, it is not adequate on its own to evaluate ovarian reserve since it represents a physiological process.

Serum FSH and E2 levels quantified by blood analysis in the early follicular stage of the menstrual cycle (3rd of the cycle) give clues about the ovarian reserve. Another reliable marker used to determine ovarian reserve is the serum AMH level. AMH, also known as MIF, is a homodimeric glycoprotein that is a member of the TGF- β family, including inhibin and activin glycoproteins. AMH is secreted by granulosa cells of preantral and early antral follicles. This secretion continues until the follicles become responsive to FSH (6-8 mm). Yet, it is not secreted in 8 mm or larger follicles, theca cells, and atretic follicles. AMH, which

plays a role in the preservation of the primordial follicle pool, also reduces the FSH sensitivity of preantral and antral follicles, thus inhibiting excessive follicle development and playing a key role in folliculogenesis.

Ovarian reserve contains follicles and granulosa cells as well as oocytes. Granulosa cells are the cells that not only provide physical support to the oocyte but also play a crucial role in the regulation and nutrition of the oocyte. Moreover, the oocyte plays a considerable role in the survival and differentiation of granulosa cells. Studies have argued that the primary causes of the poor oocyte, embryo quality, and low implantation rates are at the molecular level. Follicular fluid is a biological window reflecting the hormonal and metabolic changes that occur in the microenvironment of the mature oocyte before ovulation. Parameters obtained from this fluid have been used to determine fertilization, embryo cleavage, embryo morphology, and pregnancy rates in IVF.

With the recent in vitro culture, IVF, and in vitro maturation studies, it has become important not only the quality of the oocyte but also the healthy granulosa cells that support it, in selecting the best oocyte that will form the embryo. When the literature is reviewed, it is noticed that studies investigating human granulosa cells in IVF cycles are increasing. Follicular fluid is the environment in which the oocyte resides during oogenesis and is important in oocyte development. This fluid is made up of plasma and secretion formed by oocyte and granulosa-theca cells. Follicular fluid is aspirated together with the oocyte during the OPU process. Hence, with the analysis of follicular fluid, the molecular relationship of the oocyte and surrounding cells can also be evaluated.

These are peptide or glycoprotein substances synthesized by stimulated lymphocytes, monocytes, macrophages, and some other somatic cells in order to increase the activities of cells involved in the immune/inflammatory response. It has been documented that the cells of the immune system and related cytokines affect neuroendocrine events in the reproductive system, ovarian functions, placenta, and embryo development. Lymphocytes and macrophages in the female reproductive system secrete cytokines that impact embryo and trophoblast development. Concentrations of some cytokines are remarkably higher in follicular fluid than in peripheral blood.

When aging and age-related diseases (such as Alzheimer's, hypertension, and heart failure) are examined, it has been revealed that cytokines have an uneven distribution. For instance, it has been shown that IL-8 levels are considerably higher in the brain in Alzheimer's disease

and the IL-8 level changes in relation to the correlation of TNF alpha level with cardiac pathologies in the elderly and the age of the infertile patient.

Our aim in the study is to investigate the role of cytokines in the effect of chronological age on ovarian reserve. Thus, we compared ovarian reserves with cytokine concentrations in follicular fluid in IVF cycles of women aged above and below 35 years.

2.MATERIAL METHOD

Experimental Design

This prospective randomized study was conducted with follicle fluids obtained from patients who underwent OPU during the ICSI/ET cycle at the IVF Center of Hitit University Erol Olçok Training and Research Hospital in 2021. The study was started following the approval of the University Ethics Committee (Approval code:283/01.07.2020). Written and verbal consent was obtained from all patients participating in the study before the procedure.

Primary or secondary infertile patients between the ages of 22 and 44 who were decided to undergo ICSI/ET due to various infertility reasons (male factor, female factor, unexplained infertility) were included in the study. The patients to be included in the study were divided into 2 main groups under 35 years old and over 35 years old. Each group was divided into 2 subgroups those with low and normal ovarian reserve. Hence, 4 groups were formed.

Patients with bilateral antral follicle count <7 in the early follicular phase or with FSH >10 mIU/ml or AMH value <1.1ng/dl on the 3rd day of the menstrual cycle and with a previous history of poor ovarian response (canceled cycle or less than 4 oocytes retrieved) were considered to be patients with low ovarian reserve.

Exclusion criteria; Patients with a BMI >30 kg/m², metabolic endocrine disorders such as hypothyroidism/hyperthyroidism, a history of previous ovarian surgery, and a baseline FSH level of >15 mIU/ml were excluded from the study. In the study, when OPU was performed, follicular fluids were taken by aspirating. Follicular fluids and oocytes contaminated with rinsing fluid and blood were not included in the study. After the oocyte was removed, the follicle fluid was placed in separate sterile, apyrogenic, polypropylene conical bottom 15 ml tubes using a sterile pipette. Materials were stored at -80°C until the day of analysis.

Quantification Of Cytokine Level

Follicular fluid samples were analyzed in the Ankara Atlas Biotechnology laboratory. Analysis of cytokines, INF alpha2, IL-21, and IL-17F concentrations were evaluated by ELISA analysis.

Statistical Analysis

It was conducted via IBM SPSS 25.0 (IBM Corp., Armonk, NY, USA) software. Whether the variables fit the normal distribution or not was analyzed with the Kolmogorov-Smirnov Test. The difference between the groups was determined by Student's t-test for normally distributed variables, and by Mann Whitney U-test for non-normally distributed variables. Pearson correlation analysis was also conducted to compare cytokine levels with age, AMH, LH, FSH, E2, AFC, oocyte count, and PN count. The results were considered significant at $p < 0.05$.

3.RESULTS

Patients

The characteristic features of 86 patients are presented in Figure 1. When we compared the 2 main groups, age distribution, AMH and FSH levels, AFC, number of oocytes picked up and PN was found to be significant ($p < 0.05$) (Figure-2A). No significant difference was found between the two groups, in terms of LH and E2 levels. Our findings showed that AMH, FSH, AFC, number of oocytes retrieved, and PN count changed with aging. Besides, LH and E2 levels were not affected by aging.

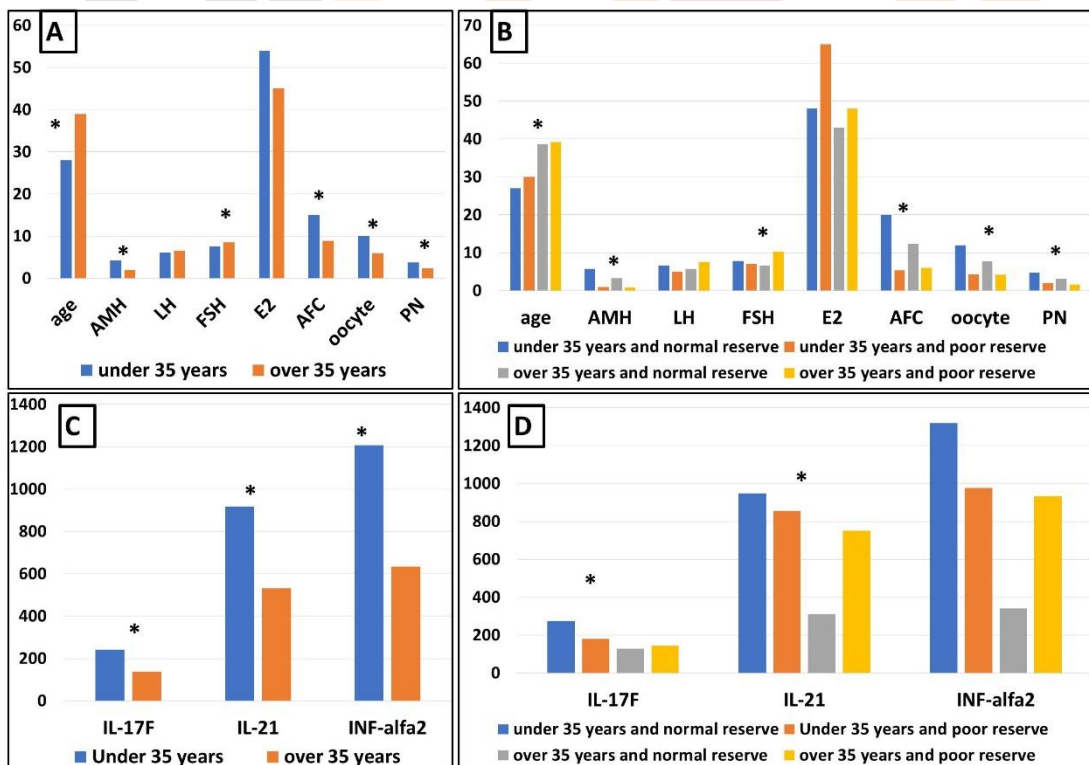
Figure-1: Characteristics of the patients

	n	Age	AMH	LH	FSH	E2	AFC	Oocyte	PN
Under 35 years	52	28,6± 0,4	4,2± 0,6	6,1± 0,4	7,6± 1,0	54,2± 5,0	15,3± 1,3	10,0± 0,9	3,8± 0,5
Under 35 years And normal over reserve	35	27,0± 0,4	5,8± 0,7	6,6± 0,5	7,8± 1,5	48,5± 4,5	20,1± 1,4	12,6± 1,1	4,7± 0,7
Under 35 years And poor over reserve	17	30,0± 0,7	0,9± 0,1	5,0± 0,5	7,1± 0,5	65,8± 11,9	5,4± 0,4	4,3± 0,6	2,0± 0,4
Over 35 years	34	38,9± 0,4	2,0± 0,3	6,6± 0,5	8,5± 0,5	45,6± 2,6	8,9± 0,9	6,0± 0,7	2,4± 0,5
Over 35 years and normal over reserve	17	38,6± 0,6	3,3± 0,6	5,7± 0,6	6,7± 0,4	43,0± 3,0	12,3± 1,5	7,7± 1,2	3,1± 0,8
Over 35 years and poor over reserve	17	39,2± 0,6	0,8± 0,1	7,6± 0,8	10,3± 0,8	48,2± 4,2	6,0± 0,4	4,2± 0,6	1,6± 0,4

On the other hand, when we compared the 4 subgroups, age distribution, AMH and FSH levels, and AFC, the number of collected oocytes and PN were found to be significant ($p < 0.05$) (Figure-2B). No significant difference was found between the two groups, in terms of LH and E2 levels.

In the pairwise comparisons between subgroups, the most striking findings were stated respectively: 1. age distribution, there was no significant difference between the patient groups over 35 years of age (normal ovarian reserve and decreased ovarian reserve groups). We interpreted this finding as age has no impact on ovarian reserve in patients over 35 years of age. 2. AMH levels did not differ significantly between patients younger than 35 years of age and with decreased ovarian reserve and patients over 35 years of age and patients with decreased ovarian reserve. This data suggested that the AMH level gives clues about ovarian reserve, regardless of age. 3. FSH value; there was no significant difference between the patient groups under the age of 35, whereas a significant difference was found between the patient groups over the age of 35 ($p < 0.05$). We interpreted this data as FSH level could not be used to show ovarian reserve in women under 35 years of age, whereas we can have information about ovarian reserve with FSH level in women over 35 years of age. 4. LH and E2 hormone levels were not associated with age or ovarian reserve.

Figure-2: A-B: Comparison between characteristic features of 86 patients, C-D: Comparison between cytokine concentrations of patients.



Cytokine Concentration

The values in the follicular fluid of the patient group under 35 years of age were as follows: INF alpha2:1207.6±162.6, IL17F:243.5±24.4, IL-21:917.3±112.6 and in the over-35 patient group mean values were as follows: INF alpha2:635.7±158.6, IL17F:137.2 ±21.9, IL-21:531.2 ±107.2.

When we compared the two main groups, INF alpha2, IL-17F, and IL-21 levels were found to be significant ($p<0.05$) (Figure-2C). This data indicates that the levels of these cytokines in the follicular fluid change with aging.

When we compared the four subgroups, a significant difference was found between IL-17F and IL-21 levels ($p<0.05$) (Figure-2D). However, no significant difference was found in INF-alpha2 levels.

In the pairwise comparisons between subgroups, the most remarkable findings were as follows: 1. IL-17F level was found to be significantly different among the patient groups below the age of 35 (normal ovarian reserve and decreased ovarian reserve groups) ($p<0.05$). Yet, no significant difference was observed between the patient groups over 35 years of age (normal ovarian reserve and decreased ovarian reserve groups). This data suggests that the IL-17F level may play a role in the reduction of ovarian reserve in women under 35 years of age and that it has no impact on ovarian reserve in the patient group over 35 years of age. 2. IL-21 and IL-17F levels were found to be significantly different between the groups of patients under 35 and over 35 years of age with normal ovarian reserve ($p<0.05$). However, no significant difference was not observed between patients with decreased ovarian reserve and patients with normal ovarian reserve. This data implies that IL-21 and IL-17F levels were associated with age but had no impact on ovarian reserve.

Correlation Analysis

IL-17F has been found to be positive correlated with age, AMH, AFC, IL-21, and INF-alpha2 ($p<0.00$). Besides, it has been revealed that IL-21 is positive correlated with age, while IL-17F is correlated with INF-alpha2 ($p<0.00$). While there was a correlation between INF-alpha2 and age, a correlation was found between E2 and IL-17F and INF-alpha2 ($p<0.00$). The strong correlation between the three cytokines indicates that they affect each other's secretion levels. Moreover, three cytokines were also found to be correlated with age. This data shows that aging affects IL-17F, IL-21, and INF-alpha2 secretion. The most

remarkable data was that among cytokines only IL-17F levels correlated with AMH and AFC. This data suggests that IL-17F may play a role in poor ovarian reserve.

4.DISCUSSION

Patients with low ovarian reserve are the most difficult patient group in IVF treatment cycles. The number of oocytes affects the success of treatment. Especially in the elderly patient group, the success rate is even lower (1). In order to increase the success of IVF treatment in patients with low ovarian reserve, it is necessary to conduct research on treatment protocols and pathogenesis. In this study, the level of cytokine in the follicular fluid was measured and compared in patients with normal ovarian reserve regardless of age and with those with low ovarian reserve.

Cytokines are thought to regulate monthly ovarian processes, including promoting ovarian follicular growth, activation required for leukocyte infiltration and ovulation, and tissue remodeling during luteinization and luteolysis. Cytokines predicted to be associated with infertility were investigated (2). For example, Beth et al. showed that IL-8 level in the follicular fluid of infertile patients was associated with follicle diameter (3). Huan et al. showed that IL-1alpha and IL-1beta cytokine levels are higher in the follicular fluid of infertile patients diagnosed with primary ovarian failure (4). Yu liang et al. investigated the effect of endometrioma cystectomy on 16 different cytokine levels in the follicular fluid and suggested that cytokine levels may be related to IVF treatment success (5). In our study, we analyzed previously unexplored cytokines and showed that IL-17F may be associated with ovarian reserve.

According to the literature, there are irregularities in the level of cytokines with aging, which causes age-related diseases by affecting the immune system or inflammation. For example, some pro-inflammatory cytokines are thought to be dysregulated in relation to aging and age-related diseases. IL-17, Elderly people (age ≥ 65) showed a reduced frequency of IL-17-producing cells in the memory subset of CD4⁺ T cells compared to healthy young people, IL-17 promotes inflammation and is associated with RA, systemic lupus erythematosus, inflammatory bowel disease, and psoriasis. It is overexpressed in many autoimmune diseases.

According to the literature, there are irregularities in the level of cytokines with aging, which causes age-related diseases by affecting the immune system or inflammation. For example, some pro-inflammatory cytokines are thought to be dysregulated in relation to aging and age-related diseases. IL-17, elderly people (age ≥ 65) showed a reduced frequency of IL-17-

producing cells in the memory subset of CD4⁺ T cells compared to healthy young people, IL-17 promotes inflammation and is associated with RA, systemic lupus erythematosus, inflammatory bowel disease, and psoriasis. It is overexpressed in many autoimmune diseases (6). IL-21 is vital in the formation of T follicular helper (Tfh) cells. The absence of T follicular helper (Tfh) cells causes unregulated systemic inflammation. Therefore, the role of IL-21 in the weakened immune system with aging has been the subject of research (7). Daniel et al. investigated the role of IL-21 in the treatment of HIV infection in the elderly and showed that by increasing the level of IL-21, recovery could be accelerated (8). Similarly, studies have shown that the expression of interferon varieties changes with aging (9).

Based on this information, we investigated the role of cytokines in the pathogenesis of ovarian reserve, which decreases with aging. Fernanda et al. investigated lipidomic and metabolomic pathways in ovarian aging. They noted that there were differences in 15 different lipid levels in the follicle fluid (10). Xing Zhang et al., on the other hand, performed a metabolomics profile analysis of the effects of aging in the follicle fluid in order to have information about the pathophysiology (11). We found that the 3 cytokines we selected were age-related, but only IL-17F had an effect on the ovarian reserve.

Conclusion

In summary, cytokines appear to play a crucial role in ovarian aging, and further analysis and validation of potential cytokine biomarkers may facilitate IVF improvement in the future.

5. REFERENCES

1. Jirge P. R. (2016). Poor ovarian reserve. *Journal of human reproductive sciences*, 9(2), 63–69. <https://doi.org/10.4103/0974-1208.183514>.
2. Piccinni, M. P., Vicenti, R., Logiodice, F., Fabbri, R., Kullolli, O., Pallecchi, M., Paradisi, R., Danza, G., Macciocca, M., Lombardelli, L., & Seracchioli, R. (2021). Description of the Follicular Fluid Cytokine and Hormone Profiles in Human Physiological Natural Cycles. *The Journal of clinical endocrinology and metabolism*, 106(2), e721–e738. <https://doi.org/10.1210/clinem/dgaa880>.
3. Malizia, B. A., Wook, Y. S., Penzias, A. S., & Usheva, A. (2010). The human ovarian follicular fluid level of interleukin-8 is associated with follicular size and patient age. *Fertility and sterility*, 93(2), 537–543. <https://doi.org/10.1016/j.fertnstert.2008.11.033>.
4. Yang, H., Pang, H., & Miao, C. (2018). Ovarian IL-1 α and IL-1 β levels are associated with primary ovarian insufficiency. *International journal of clinical and experimental pathology*, 11(9), 4711–4717.
5. Liang, Y., Yang, X., Lan, Y., Lei, L., Li, Y., & Wang, S. (2019). Effect of Endometrioma cystectomy on cytokines of follicular fluid and IVF outcomes. *Journal of ovarian research*, 12(1), 98. <https://doi.org/10.1186/s13048-019-0572-7>
6. Rea, I. M., Gibson, D. S., McGilligan, V., McNerlan, S. E., Alexander, H. D., & Ross, O. A. (2018). Age and Age-Related Diseases: Role of Inflammation Triggers and Cytokines. *Frontiers in immunology*, 9, 586. <https://doi.org/10.3389/fimmu.2018.00586>.

7. Almanan, M., Raynor, J., Ogunsulire, I., Malyshkina, A., Mukherjee, S., Hummel, S. A., Ingram, J. T., Saini, A., Xie, M. M., Alenghat, T., Way, S. S., Deepe, G. S., Jr, Divanovic, S., Singh, H., Miraldi, E., Zajac, A. J., Dent, A. L., Hölscher, C., Chougnat, C., & Hildeman, D. A. (2020). IL-10-producing Tfh cells accumulate with age and link inflammation with age-related immune suppression. *Science advances*, 6(31), eabb0806. <https://doi.org/10.1126/sciadv.abb0806>.
8. Kvistad, D., Pallikkuth, S., Sirupangi, T., Pahwa, R., Kizhner, A., Petrovas, C., Villinger, F., & Pahwa, S. (2021). IL-21 enhances influenza vaccine responses in aged macaques with suppressed SIV infection. *JCI insight*, 6(20), e150888. <https://doi.org/10.1172/jci.insight.150888>.
9. Benayoun, B. A., Pollina, E. A., Singh, P. P., Mahmoudi, S., Harel, I., Casey, K. M., Dulken, B. W., Kundaje, A., & Brunet, A. (2019). Remodeling of epigenome and transcriptome landscapes with aging in mice reveals widespread induction of inflammatory responses. *Genome research*, 29(4), 697–709. <https://doi.org/10.1101/gr.240093.118>.
10. Cordeiro, F. B., Montani, D. A., Pilau, E. J., Gozzo, F. C., Fraietta, R., & Turco, E. (2018). Ovarian environment aging: follicular fluid lipidomic and related metabolic pathways. *Journal of assisted reproduction and genetics*, 35(8), 1385–1393. <https://doi.org/10.1007/s10815-018-1259-5>.
11. Zhang, X. X., Yu, Y., Sun, Z. G., Song, J. Y., & Wang, A. J. (2018). Metabolomic Analysis Of Human Follicular Fluid: Potential Follicular Fluid Markers Of Reproductive Aging. *JPMA. The Journal of the Pakistan Medical Association*, 68(12), 1769–1781.



INVESTIGATION OF WOUND HEALING POTENTIALS OF PINE BARK EXTRACTS AND DEVELOPMENT OF GEL FORMULATION

Melis DEMİRÖZER¹, Canberk TOMRUK², Derya ERIŞİK², Fatih KARABEY³, Timur
KÖSE⁴, Yiğit UYANIKGİL², Emel Öykü ÇETİN UYANIKGİL¹

1 Ege University Faculty of Pharmacy, Department of Pharmaceutical Technology, Department of Biopharmaceutics and Pharmacokinetics, İzmir, TURKEY, melisdemirozer@hotmail.com, emel.oyku.cetin@ege.edu.tr

2 Ege University, Faculty of Medicine, Department of Histology and Embryology, İzmir, TURKEY canberktomruk@hotmail.com, derya_erisik@hotmail.com, yigituyanikgil@gmail.com

3 Parkim Group Perfectionist Solutions by Creative Minds R&D Center, Informatics Valley, 41455, Dilovası, Gebze/Kocaeli, TURKEY, fatihkarabey@gmail.com

4 Ege University Faculty of Medicine, Department of Biostatistics and Medical Informatics, İzmir, TURKEY, timur.kose@ege.edu.tr

Abstract: Wound is deterioration of tissues that make up skin or mucosa and disruption of normal skin structure as a result of physical or chemical damage. Wound healing is a process consists of biochemical and cellular events leading to repair of damaged tissues. Extracts of *Pinus brutia*, *Pinus sylvestris* and *Pinus pinea* barks were used for cytotoxic and wound healing studies. Wound healing results were evaluated statistically. *Pinus brutia* bark extract containing Carbopol[®] 940 gel formulations were prepared and *in vitro* characterization studies were done. In conclusion, developed and evaluated *Pinus Brutia* extract containing gel formulation significantly accelerated wound healing and has a promising effect.

Keywords: Wound healing, Carbopol[®] 940 gel, Pine bark extract

INTRODUCTION

Wound healing is a process consists of biochemical and cellular events leading to repair of damaged tissues (1). The wound healing process can be divided into three phases: inflammatory phase; proliferative phase; and maturational phase.

Pine (*Pinus L.*) is the important genus of the family of Pinaceae. *Pinus brutia*, *P. nigra*, *P. sylvestris*, *P. pinea* and *P. halepensis* are found in Turkey. Various parts of *Pinus* species have been used for rheumatism or as anti-inflammatory, antioxidant and antiseptic. Terpenoids, steroids, procyanidins and flavonoids are the ingredients of *Pinus* extracts. Turpentine has been known to have a long history of healing mostly as topical counter irritants for the treatment of rheumatic disorders and muscle pain (2). Pine bark extracts are a rich source of natural polyphenols with potential beneficial antioxidant properties. Typical phenolic compounds present in pine bark are (+)-catechin, (-)-epicatechin, dihydroquercetin (3).

Pycnogenol[®] is commercially available pine bark extract, which is a standardised extract of French maritime pine bark (*Pinus maritima*), and probably the most studied phenolic tree extract containing proanthocyanidins (4). Hydrogels are used for the treatment of skin wounds. Carbopol is widely used as a main component of drug delivery gel systems (5). This study aims to determine wound healing activity of pine bark extracts and developing a gel formulation.

MATERIALS & METHODS

Cytotoxicity Test

The type of cells used in the cytotoxicity test is BJ and its source is Human Foreskin Fibroblast (Monolayer). Each pine bark extract in 6 different concentrations (25 µg/ mL, 50 µg/ mL, 100 µg/ mL, 200 µg/ mL, 400 µg/ mL, and 800 µg/ mL) on the cells planted at a concentration of 1×10^5 cells/ mL on 96-well microplates. Cytotoxic effects at the end of 48 hours (5% CO₂ at 95 %C and 95% humidity) were evaluated by MTT test by reading the absorbances in the spectrophotometer (570 nm). As a result of measurements with spectrophotometer, calculations were made with the determined values and cytotoxicity values were calculated for pine bark extracts to affect the viability of the cells (6).

In Vitro Wound Healing Study

The wound healing effect of pine bark extracts were studied with in vitro wound healing cell culture model on BJ (Human Foreskin Fibroblast, monolayer) cells. A sterile yellow (100µL) pipette tip was used to make a straight scratch on the monolayer of cells, stimulating a wound. The cells were treated with 6 concentrations (1 µg/mL, 5 µg/mL, 10 µg/mL, 20 µg/mL, 40 µg/mL ve 80 µg/mL) of pine bark extracts and incubated at 37°C in 5% CO₂ and 95% humidity. Untreated cells were used as positive control (7,8). The Olympus IX-71 inverted microscope and Olympus DP 72 camera were used to observe the wound healing test. The images were taken at 4x magnification with an inverted light microscop at 0 and 24 hours. Measurements were made on images using the Image Pro Express program. Wound healing results were evaluated statistically.

Formulation studies of Carbopol 940[®] Gel

Preformulation studies were done (F1-F8). F7 and F8 were selected for further studies. *Pinus brutia* bark extract containing 0.5% and 1% Carbopol® 940 gel formulations (respectively F7, F8) were prepared. Physical appearance, homogeneity and color properties of the formulations were evaluated at room temperature. Viscosity and pH measurements and rheology analysis were conducted for characterization of the gel formulations. *In vitro* dissolution study of the formulations was performed by using dialysis bag method and drug release kinetics were calculated.

RESULTS

Based on the data obtained from the cytotoxicity test, non-cytotoxic dose ranges were determined for the extracts, in the wound healing test for each pine extract. It was decided to apply 6 different concentrations. After the *in vitro* wound model application of each pine type, distances were analyzed using inverted microscopy. When the values of the control group and the 0th and 24th hours of each dose are evaluated within themselves, $p = 0.007$ for the control group, $p = 0.003$ for the dose of 1 $\mu\text{g}/\text{mL}$, $p = 0.008$ for the dose of 10 $\mu\text{g}/\text{mL}$, and 40 $\mu\text{g}/\text{mL}$ and 80 $\mu\text{g}/\text{mL}$ (Figure 1).

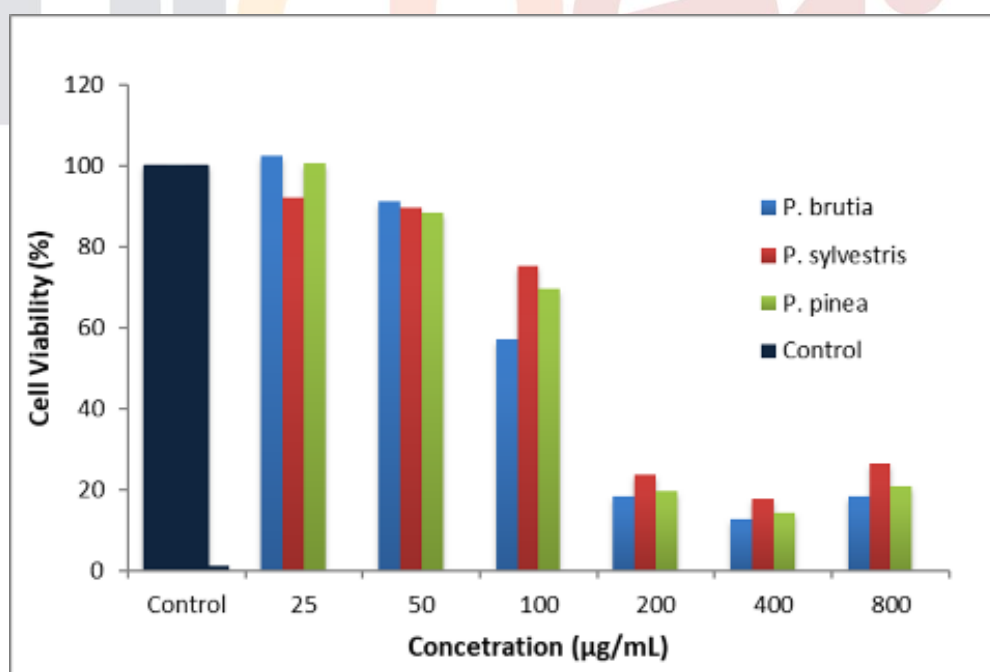


Figure 1. Cell viability against different concentrations of *Pinus brutia*, *Pinus sylvestris* and *Pinus pinea* extracts.

It was found statistically significant for doses ($p < 0.001$). It was decided to prepare the gel formulations and to use *Pinus brutia* extract at a concentration of 20 $\mu\text{g}/\text{mL}$ in the next steps. It was found that *in vitro* dissolution rate was decreased when the Carbopol[®] 940 concentration was increased (Figure 2).

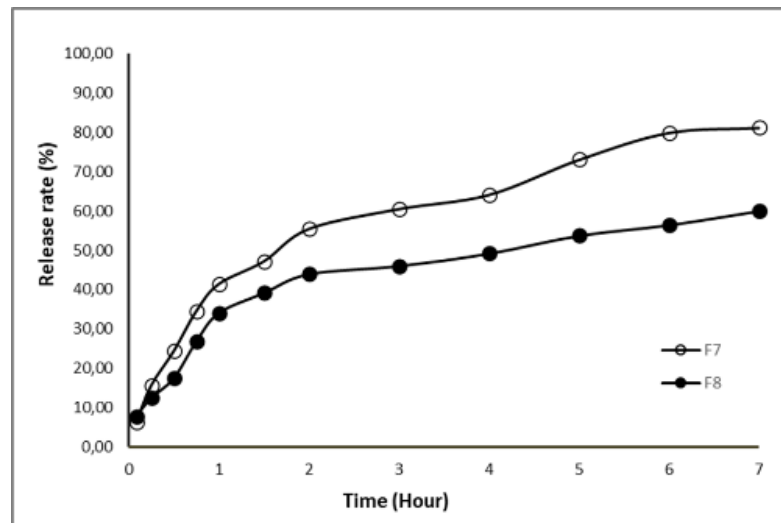


Figure 2. Release %- time graphic of F7 and F8 formulations.

Rheological properties gel formulations were fitted to non-Newtonian plastic flow curves. The formulations showed viscoplastic flow behaviour. The viscosity of gel formulations was increased when the Carbopol[®] 940 concentration was increased (Figure 3).

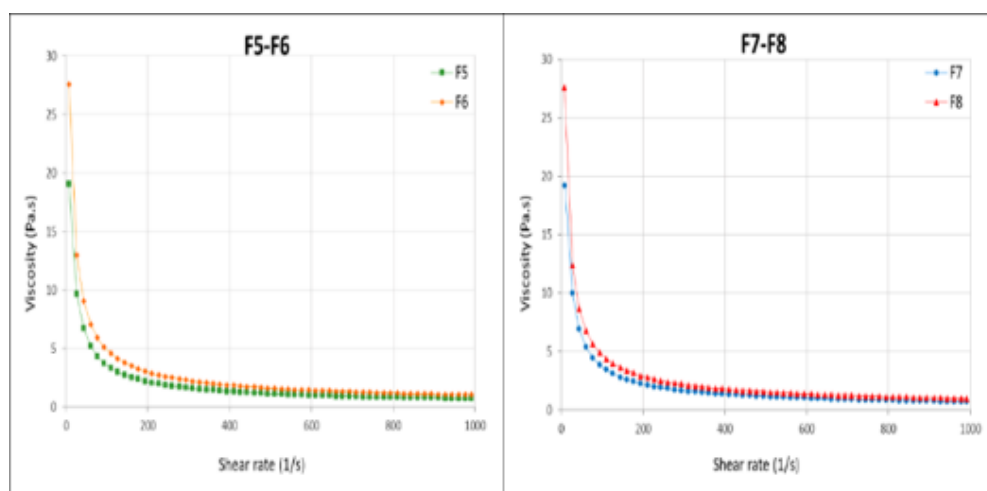


Figure 3. Shear rate vs viscosity graphs of F5- F6 and F7- F8 formulations.

DISCUSSION AND CONCLUSION

Formulations prepared from plants have been widely used for the treatment of wounds and burns. In this study the wound healing effect of pine bark extracts were evaluated. According to the results wound healing activity of *Pinus Brutia* extract was found to be significantly higher than the other extracts. In conclusion *Pinus Brutia* extract containing gel formulation can be used for wound healing.

REFERENCES

1. C. D. O. Gonzalez, Z. D. A. Andrade, T. F. Costa, and A. R. A. P. Medrado. (2016). "Wound healing -A literature review," *An. Bras. Dermatol.*, 91(5), 614–620.
2. Ç. Kizilarlan and E. Sevg. (2013). "Ethnobotanical uses of genus *Pinus* L. (Pinaceae) in Turkey," *Indian J. Tradit. Knowl.*, 12(2), 209–220.
3. S. Ku, J. P. Jang, and S. P. Mun, (2007). "Exploitation of polyphenol-rich pine barks for potent antioxidant activity," *J. Wood Sci.*, 53(6), 524–528.
4. E. O. Cetin, O. Yesil-Celiktas, T. Cavusoglu, E. Demirel-Sezer, O. Akdemir, and Y. Uyanikgil, (2013) "Incision wound healing activity of pine bark extract containing topical formulations: A study with histopathological and biochemical analyses in albino rats," *Pharmazie*, 68(1), 75-80
5. Hayati, S. M. Ghamsari, A. Tavassoli, and M. Azizzadeh. (2016). "Carbomer 940 Hydrogel Enhances Capillary Blood Flow and Tissue Viability in a Skin Burn Wound," *Iran. J. Vet. Surg.*, 11(1), 29–36.
6. Mosmann T, (1983) "Rapid Colorimetric Assay for Cellular Growth and Survival: Application to Proliferation and Cytotoxicity Assays," *J. Immunological Methods*, (65), 55–63.
7. C. C. Liang, A. Y. Park, and J. L. Guan. (2007) "In vitro scratch assay: A convenient and inexpensive method for analysis of cell migration in vitro," *Nat. Protoc.*, 2(2), 329–333.
8. S. Martinotti and E. Ranzato. (2020) "Scratch wound healing assay," *Methods Mol. Biol.*, 2109, 225–229.

**ALLOGENEIC BONE MARROW MESENCHYMAL STEM CELL-DERIVED
EXOSOMES AMELIORATE HYPOXIC ACUTE TUBULAR INJURY IN HUMAN
PROXIMAL TUBULE-ON-A-CHIP WITHIN A PRECISE TREATMENT WINDOW**

**Sefa Burak Cam¹, Eda Çiftci Dede², Nazlıhan Gürbüz², Gözde İmren³,
Ekim Zihni Taşkıran³, Bülent Altun⁴, Petek Korkusuz¹**

¹ Hacettepe University, Faculty of Medicine, Dept. of Histology and Embryology, Ankara, Turkey.

² Hacettepe University, Graduate School of Science and Engineering, Department of Bioengineering,
Ankara, Turkey

³ Hacettepe University, Faculty of Medicine, Dept. of Medical Genetics, Ankara, Turkey

⁴ Hacettepe University, Faculty of Medicine, Dept. of Nephrology, Ankara, Turkey

Correspondence: sefacam@hacettepe.edu.tr

Mesenchymal stem cells (MSCs) and MSC exosomes (MSC-Exos) are promising therapeutic possibilities for ischemic acute kidney injury (AKI)¹, but their safety and efficacy are still debatable on proximal tubules (PT) at the cellular level. Recently microfluidic kidney-on-a-chip systems present smart platforms mimicking tubular microphysiopathological environment to assess theragnostic tools before translation to clinics. A gravity-driven membrane-less microfluidic-based 3D culture platform may reproduce acute hypoxic PT injury and real-time assess the therapeutic potency of human bone marrow-derived MSC exosomes (hBMMSC-Exos) as cellular therapeutics.

We aimed to isolate, characterize and quantitatively analyze the efficacy of hBMMSC-Exos with a real-time proliferation assay (RTCA) and assess the potency in terms of tubular epithelial permeability, epithelial polarity, expression of injury-specific genes and proliferation on the novel microfluidic acute hypoxic PT injury platform (Figure 1).

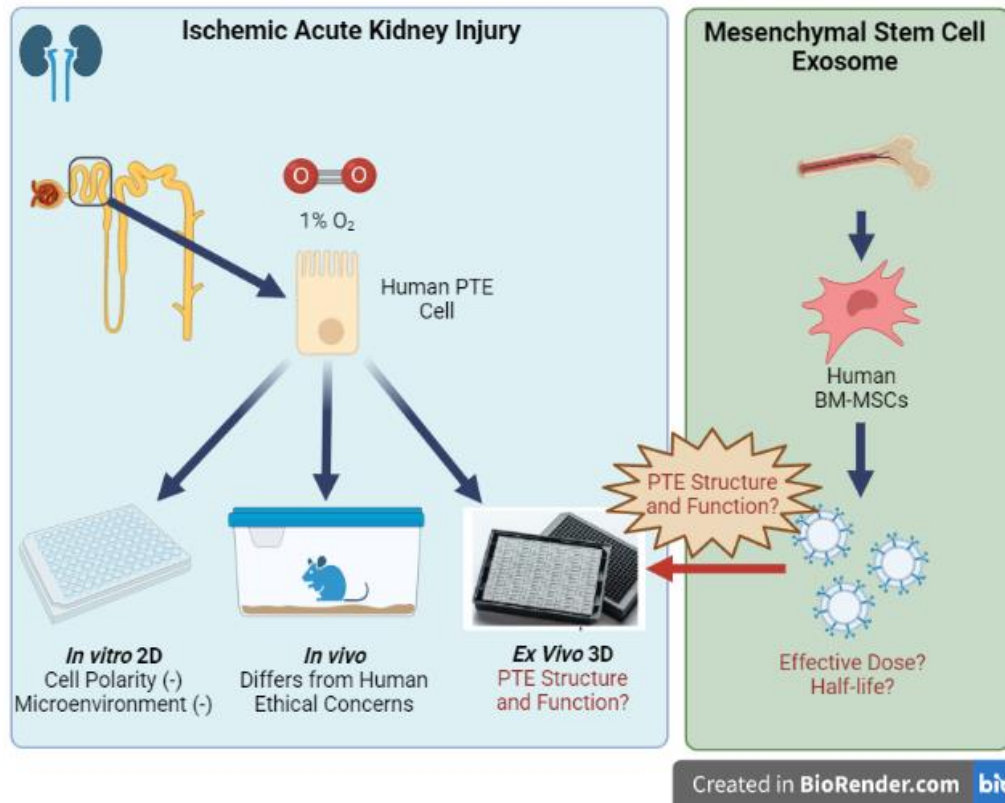


Figure 1. The purpose of the study.

Our study was designed as a randomized observational study with the control group to test our hypothesis (Figure 2)

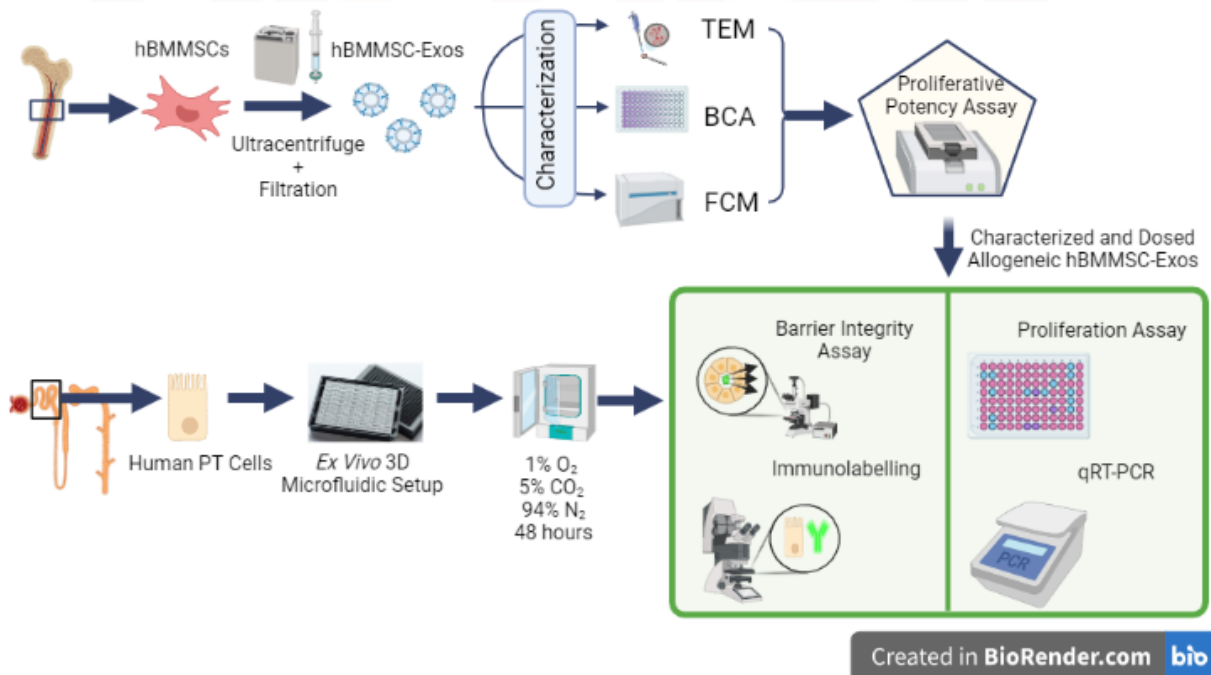


Figure 2. The study design and workflow.

hBMMSC-Exos were isolated and characterized. RTCA determined the effective dose and treatment window for acute hypoxic PT injury. 2-lane 3D gravity-driven microfluidic platform was set to mimic PT *in vitro*. ZO-1, acetylated α -tubulin immunolabelling, permeability index assessed structural; cell proliferation by WST-1, BNIP3, HO-1, HIF1A1 expression by qRT-PCR measured functional integrity of PT.

hBMMSC-Exos were characterized in terms of protein concentration, morphology and surface markers (Figure 3).

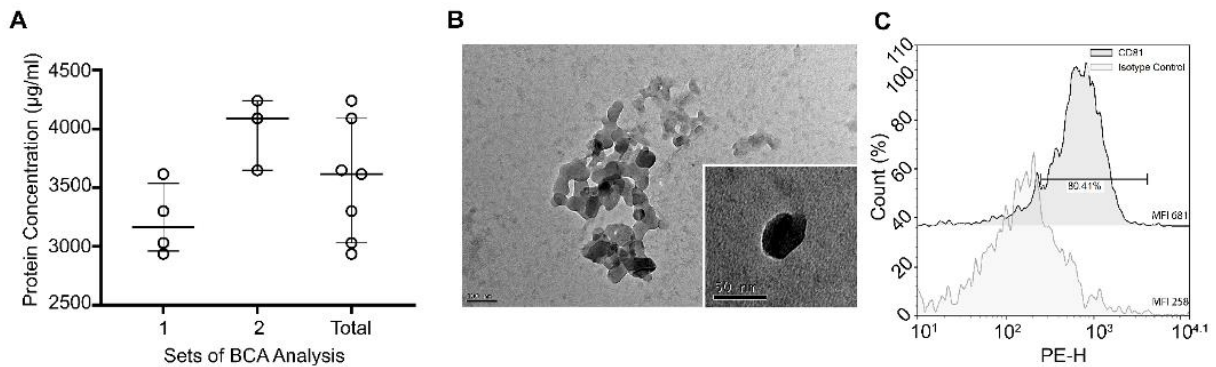


Figure 3. hBMMSC-Exo characterization data.

hBMMSC-Exos induced PT proliferation with ED50 of 172,582 $\mu\text{g/ml}$ at 26th hour (Figure 4).

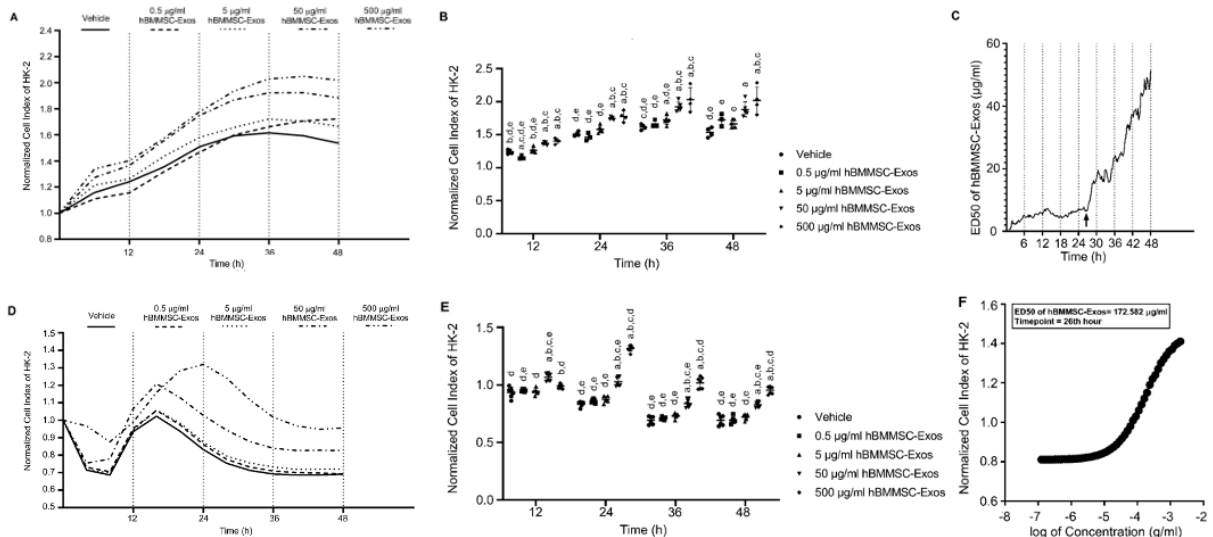


Figure 4. Proliferative potency assay.

Hypoxia significantly decreased ZO-1, increased permeability index, decreased cell proliferation rate, increased BNIP3, HO-1 and decreased HIF1A1 on 24-48 hours in the microfluidic platform.

hBMMSC-Exos reinforced polarity by 1.72-fold increase in ZO-1 ($p=0.0121$, Figure 5)

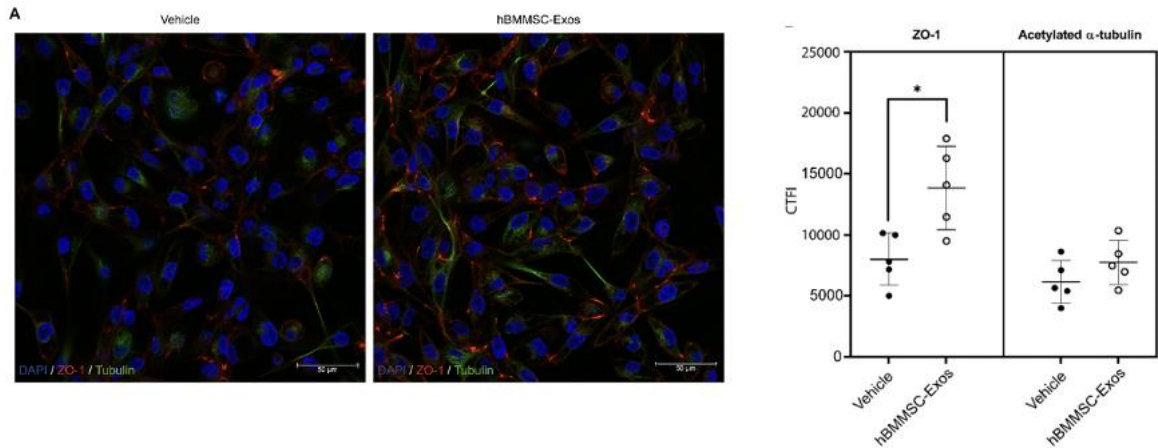


Figure 5. Immunofluorescent labelling of ZO-1 and acetylated α -tubulin.

hBMMSC-Exos restored epithelial permeability by 20/45-fold against 20/155 kDa dextran ($p=0.0004$ and $p<0.0001$, respectively, Figure 6).

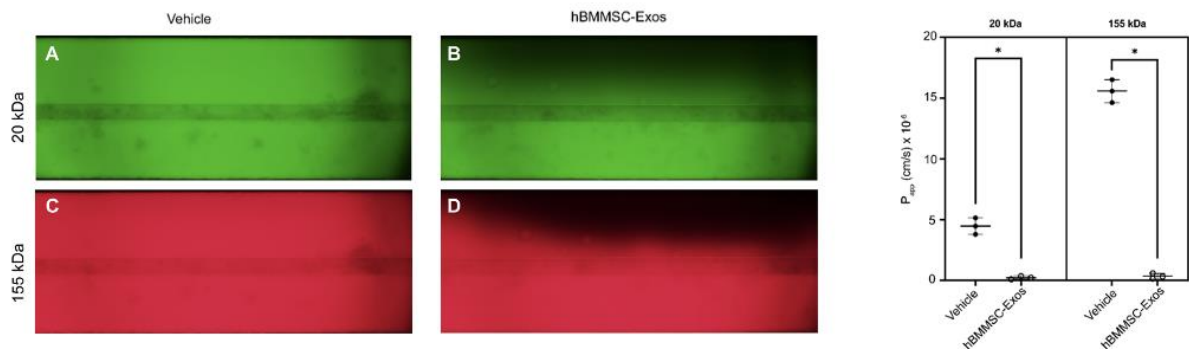


Figure 6. Barrier integrity assay.

hBMMSC-Exos increased epithelial proliferation 3-fold ($p<0.0001$) and decreased BNIP3 expression by 0.62-fold compared to control (Figure 7).

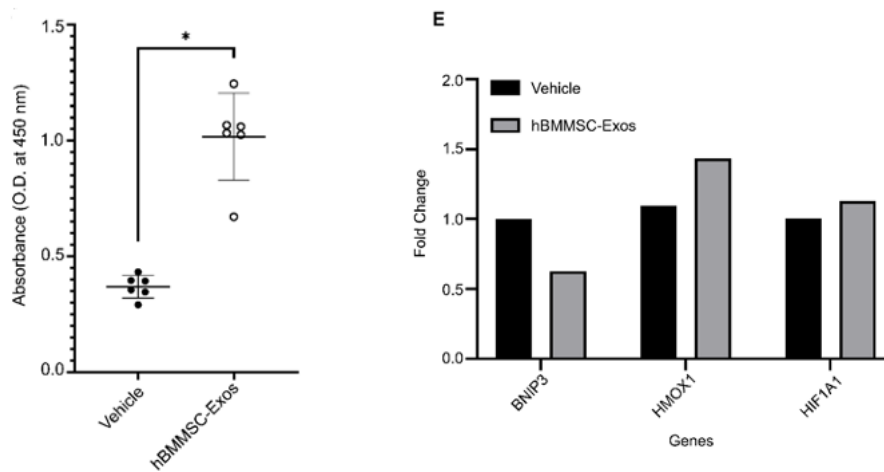


Figure 7. Cell proliferation assay and qRT-PCR.

The real-time potency assay and 3D gravity-driven microfluidic acute hypoxic PT injury platform precisely demonstrated therapeutic performance window of allogeneic hBMMSC-Exos on ischemic AKI providing molecular, structural and functional cellular data. The novel standardized, non-invasive 2-step system validates cell-based personalized theragnostic tools in a real-time physiological microenvironment prior to safe and efficient clinical usage in nephrology.

This work is funded by Hacettepe University Scientific Research Projects Coordination Unit (TSA-2020-18383).

Keywords

AKI, Proximal Tubule, Exosome, Microfluidic, Kidney-on-a-chip

References

1. B. Altun et al.; American Journal of Nephrology 35(6) (2012) 531-539.

